EUROPEAN UNION
European Structural and Investment Funds
Operational Programme Research,
Development and Education

MINISTRY OF EDUCATION,
YOUTH AND SPORTS

Integrated photonics

Štefan Višňovský

2020

Content

Chapter 1

Introduction

Present requirements on the information volume, speed of transfer and performance can only be satisfied at carrier frequencies in the optical range. Integrated and fiber photonics is focused on the realization of compact, high capacity communication systems for generation, treatment, transfer and detection of information at optical frequencies. This requires the solution of numerous physical and technological problems. The integration of optoelectronic elements has become a necessity. Without the optical element integration, the power requirements in present computer networks would increase to an unacceptable level.[1]

The optical signal propagation in optical circuits and devices is achieved by waveguiding. The use of laser in optical communications was enabled by the realization of low loss optical fiber waveguides. These connect any distant points on the globe at the light velocity. The present monomode optical fiber waveguides employing the carrier wavelengths of 810 nm, 1,3 μm, or 1,55 μm transfer data at the speed of 10 terabits per second (10×10^{12} bit/s). This corresponds to 150 milion telephone calls. Several optical elements were realized in optical fiber waveguides, among them, diffraction gratings, nonlinear elements, amplifiers, oscillators (in the fibers doped by rare earth $4f$ metals, e.g., Er, Yb), etc.

Based on the optical waveguides, important specific important applications employed in physics, chemistry, biology, medicine and technology were developed, i.e., optical thin film and fiber sensors of physical and chemical quantities including mechanical stress and strain, highly sensitive submarine microphones, sensors of electric currents and magnetic fields including magnetometers for femto Tesla (10^{-15} Tesla) range, humidity sensors, chemical pollution sensors, position sensors, i.e., optical fiber gyroscopes (based on the Sagnac effect), etc. The optical fiber waveguides are employed in probing combustion

[1] P. K. Tien, Integrated optics and new wave phenomena in optical waveguides, Rev. Mod. Phys. **49**, 361–455 (1977), T. Tamir, ed. Integrated Optics, Springer Verlag, Berlin 1975, R. G. Hunsperger, Integrated Optics: Theory and Technology, Springer Verlag, Berlin 1982.

chambers, monitoring clinical picture of human organs, mapping furnace temperature, strain in concrete bridge beams, etc.

Unlike metallic conductors, e.g., coaxial cables, dielectric optical waveguides are resistant against electromagnetic noise and wiretapping. The absence of short circuit sparks makes them suitable for the use in fire danger areas, e.g., in airplanes for inner communication systems. Expensive copper in classical communication systems is replaced by widely available silicon oxide, SiO_2 . However, this must be of extremely high purity. The concentration of transition metal atoms must be reduced to 10^{-9} . Another advantages of integrated optical circuits against classical systems consists in miniaturization, improved mechanical and temperature stability, improved reliability and lower cost. Compared to free space microwave and optical communications, the fiber optic cables are vulnerable to earth quakes.

From the physical point of view, the integrated and fiber optoelectronics deals with problems of electromagnetic waves localized in the structures with one or two dimensions of the order of radiation wavelength. The propagation in dielectric waveguides exploits the interference effects and total internal reflection. The analysis starts from Maxwell theory of electromagnetic waves which leads to the solution of vector wave and diffuse equations.

The confinement of electromagnetic waves in waveguides shows formal correspondence with confinement of quantum particles in potential wells. Then, a free particle characterized by continuous energy spectrum corresponds to a (non localized) radiation mode. A particle in a potential well with a discrete energy spectrum corresponds to bound waveguide modes with a discrete spectrum of propagation constant. The formalism of Hermitian matrices displays a certain analogy with the formalism employed in the description of guided modes in dielectric waveguides built on lossless media. A one dimensional (non)symmetrical potential well with a step profile corresponds to a (non)symmetrical planar dielectric waveguide with a step profile of the real index of refraction.[2]

A two dimensional potential well corresponds to a two dimensional dielectric waveguide. The problem of waveguides with a parabolic profile of the index of refraction squared (dielectric permittivity) can be solved using known solutions for potential wells with parabolic profiles, i.e., for those pertinent to a harmonic oscillator,[3]

$$n^2 = n_f^2 \left(1 - x^2/x_0^2\right) ,$$

restricted to a practical range of the real index of refraction, n , i.e., $n > 1$ The analogy

[2] An infinitely deep potential well corresponds to waveguide with infinitely conducting walls made of an ideal metal. Then the wave function is zero beyond the wall and the penetration depth at the waveguide interfaces tends to zero.

[3] H. Kogelnik, Theory of Dielectric Waveguides, in T. Tamir, ed. Integrated Optics, Springer Verlag, Berlin 1975.

can be extended to other profiles, e.g., a profile characterized by a function $1/\left(\cosh^2 x\right) = \mathrm{sech}^2 x$,

$$n^2 = n_s^2 + 2n_s\,\Delta n/\cosh^2(2x/h)$$

(h represents an effective waveguide thickness) or to dielectric structures with the symmetry of circular or elliptical cylinder (optical fibers).

In analogy with the Bloch states in crystals, there are also Bloch states in structures with translation symmetry in one, two or three dimensions. In optics and photonics, the dielectric structures displaying two or three dimensional translation symmetry are known as *photonic crystals*. The physics of dielectric waveguides and the non relativistic quantum physics share approximations in the solutions to analogous problems using perturbation theory, variational calculus, orthonormal series, etc. Analysis of electromagnetic waves in structures of integrated optoelectronics and fiber optics is employed in the design of devices, circuits, and systems and in modeling of their optical response.

Thanks to the progress in technology, optical circuits and devices can be realized with the resolution better than a fraction of radiation wavelength in a medium. Note that the radiation wavelength, λ, in a non absorbing medium characterized by the real index of refraction, n, may be much smaller than the wavelength in a vacuum, λ_{vac}, $\lambda = \lambda_{\text{vac}}/n$. The requirements on the lithography resolution can be appreciated on distributed feedback lasers and lasers with Bragg reflectors which are built on semiconductors with $n \approx 3,6$.

1.1 Circuits and Devices

The circuits of integrated optoelectronics involve planar, channel and fiber waveguides suitable for a undistorted broad band transmission of optical signals, radiation sources (lasers), amplifiers, detectors, couplers, modulators, frequency selective filters, switchers, phase shifters, multiplexors, interferometers, attenuators, non reciprocal devices, etc. The microwave modulation at optical carrier frequency can be realized using electroabsorption in semiconductors (electroabsorption modulated lasers, EML).

1.2 Materials

Dielectrics (the real index of refraction, n, much greater than the extinction coefficient, k, i.e., $n \gg k$) are mostly employed in waveguides for passive transmission at optical frequencies.

Semiconductors, mostly the family III-V (e.g., $\mathrm{Ga}_{1-x}\mathrm{Al}_x\mathrm{As}$, InP), are employed in monolithic integrated optical circuits as lasers, amplifiers, and detectors ($n \approx k$). With the band gap controlled by chemical composition, the semiconductors can perform other functions including modulation and passive waveguiding ($n \gg k$). A special modern area is represented by silicon photonics.[4]

Metals ($n \ll k$) are employed as effective reflectors, modal filters, transmission of plasmons, $n \ll k$ at frequencies below the plasma edge (long range surface plasmons). They can be employed as optically transparent electrodes for thin film electrooptic switches and modulators. A considerable attention is paid to the waves at interfaces between a metal and a dielectrics in the spectral region where the metal (e.g., Au or Ag) displays a real negative permittivity ($n^2 - k^2 < 0\,,\ 2nk \approx 0$).[5] Ferromagnetic metals (Fe, Co, Ni) find use in magnetooptical and nonreciprocal devices.

From the point of view of structure, the materials involve single crystals, polycrystals, polymers or amorphous media. The devices take form of one dimensional planar waveguides, rectangular waveguides, channel waveguides, periodic structures, optical fibers with circular or elliptical cross-sections, optical fibers with structured profiles (photonic crystal fibers).

1.3 Three basic ideas of integrated optoelectronics

The basic ideas of integrated optics involve:
(1)The use of thin film technology for the fabrication of optical elements.
(2) Replacement of diverging Gaussian beams by guided waves in analogy with microwave circuits.
(3) Integration of optical elements on a common substrate in analogy with microelectronics.

1.4 Three main areas of activity

The research in integrated optoelectronics is focused on the following areas.
(1) The first one develops new materials using approaches of quantum physics and physics of condensed matter.
(2) The second one studies electromagnetic wave processes including the wave propagation in periodic nanostructures.
(3) The third one assembles optoelectronic devices into systems (system architecture in optical networking).

At present, the main interest is devoted to optical waves in nanostructures, photonic crystals, plasmon waveguiding, and photonic crystal fibers.

[4] M. J. R. Heck et al., Hybrid Silicon Photonics ...,IEEE J. Sel. Top. Quantum Electron. **17**, 333–346 (2011).

[5] P. Berini, Long range surface plasmon polaritons, Adv. Optics & Photonics **1**, 484-588 (2009).

1.5 Optical fibres

A systematic demand on the volume and speed of data carried with electromagnetic waves requires an increase in carrier frequencies from radio waves and microwaves towards the optical region. The transfer of optical waves, in particular to high distances is performed by optical fibers of circular cross section.[6] The optical fibers technology has developed since sixties of twenty century and starts from extremely high purity silicon oxide. The optimal cross section is controlled by precise doping during fiber pulling. The attenuation in these high technology fibers is much lower than those in optical materials employed in the best optical devices. Long distance optical fiber communications employs wavelengths of 1.3 μm and 1.55 μm corresponding to the attenuation and dispersion minima, respectively. The attenuation is evaluated in decibels as a logarithm of the base 10 evaluated for a ratio of the input optical power, P_{in} , to the output optical power, P_{out} , multiplied the factor of ten,

$$N_{\text{dB}} = 10 \log_{10} \frac{P_{\text{in}}}{P_{\text{out}}} \tag{1.1}$$

The attenuation per 1 km represents the basic optical fiber parameter. In particular, for the attenuation per 1 km in the fiber of the highest quality is as low as,

$$N_{\text{dB/km}} = 0.1\text{dB/km} \tag{1.2}$$

the output power at the 1 km distance becomes

$$\frac{P_{\text{in}}}{P_{\text{out}}} = 10^{0.01} \approx 1.0233 \tag{1.3}$$

e.g. on the 1 km distance

$$P_{\text{out}} \approx 0.977 P_{\text{in}} \tag{1.4}$$

less than 2.3 % of the power is lost.

At the distance of d_{km} km the power attenuation in decibels (dB) becomes

$$N_{\text{dB}} = N_{\text{dB/km}} \times d_{\text{km}} \tag{1.5}$$

The attenuation of 3 dB corresponds to the decrease of the the output power to the half of the input power

$$\begin{aligned} 3\text{dB} &= 10 \log_{10} \frac{P_{\text{in}}}{P_{\text{out}}} \\ 0.30103 = \log_{10} 2 &\approx \log_{10} \frac{P_{\text{in}}}{P_{\text{out}}} \end{aligned}$$

[6] R. Olshansky, Propagation in glass optical waveguides, Rev. Mod. Phys. **51**, 341–367 (1979)

Assuming $N_{\mathrm{dB/km}} = 0.1$ dB, this decrease takes place on the distance of 30 km. At $N_{\mathrm{dB/km}} = 0.1$ dB and $d_{\mathrm{km}} = 50$ km

$$N_{\mathrm{dB}} = 10\log_{10}\frac{P_{\mathrm{in}}}{P_{\mathrm{out}}} = 5 \text{ dB} \tag{1.6}$$

corresponding to a power ratio,

$$\frac{P_{\mathrm{in}}}{P_{\mathrm{out}}} = 10^{0,5} = \sqrt{10} \approx 3.162 \tag{1.7}$$

giving

$$P_{\mathrm{out}} \approx 0.316 P_{\mathrm{in}} \tag{1.8}$$

At the 50 km distance the fiber transfers 31.6 % of the input power. The 50 km distance is chosen as a distance between amplifiers in submarine optical fibers.

Chapter 2

Principle of dielectric waveguides

2.1 Thin film interference

A detailed description of the wave propagation in dielectric structures may be rather complicated. Nevertheless, the basic principle can be explained using elementary considerations on the uniform plane wave interference in a planar one dimensional structure consisting of a thin film sandwiched between a substrate and a cover.[1] The cover occupies the half space above the film characterized by a real index of refraction, n_c. Often, the cover is ambient air with $n_c = 1$. The film is characterized by the real index of refraction n_f , and the substrate characterized by n_s fills the half space below the film.

The problem geometry is chosen as follows. The interface between the cover and the film is situated in the plane $x = 0$ of the Cartesian coordinate system with the positive x axis directed to the cover half space. The interface between the film and substrate is situated in the plane $x = -h$ (Figure 2.1). We assume the existence of two pairs of uniform plane waves linearly polarized with the electric field vectors perpendicular or parallel to the plane of incidence (perpendicular to the unit vector $\hat{\boldsymbol{y}}$ in each of these regions. The waves display the normal components of propagation vectors, $\boldsymbol{k}_l$, of different signs

$$\boldsymbol{k}_l \;=\; n_l \frac{\omega}{c} \left(\hat{\boldsymbol{z}} \sin\theta_l \pm \hat{\boldsymbol{x}} \cos\theta_l \right) , \qquad 0 \le \theta_l < \frac{\pi}{2} \tag{2.1}$$

where $l = c\,, f\,, s$. The plane of incidence which contains $\boldsymbol{k}_l$ is defined by the Cartesian unit vectors $\hat{\boldsymbol{z}}$ and $\hat{\boldsymbol{x}}$, i.e., the plane of incidence normal coincides with $\hat{\boldsymbol{y}}$.

The angles θ_l stand for the angles θ_c , θ_f , and θ_s , between $\boldsymbol{k}_c$, $\boldsymbol{k}_f$, and $\boldsymbol{k}_s$ and the interface normal (here $\hat{\boldsymbol{x}}$), respectively. The angular frequency and the speed of light

[1] D. Marcuse, Light Transmission Optics, Van Nostrand Reinhold Company, New York 1972, H. Kogelnik, Theory of Dielectric Waveguides, in T. Tamir, ed. Integrated Optics, Springer Verlag, Berlin 1975, D. Marcuse, Theory of Dielectric Optical Waveguides, Academic Press, New York and London 1974.

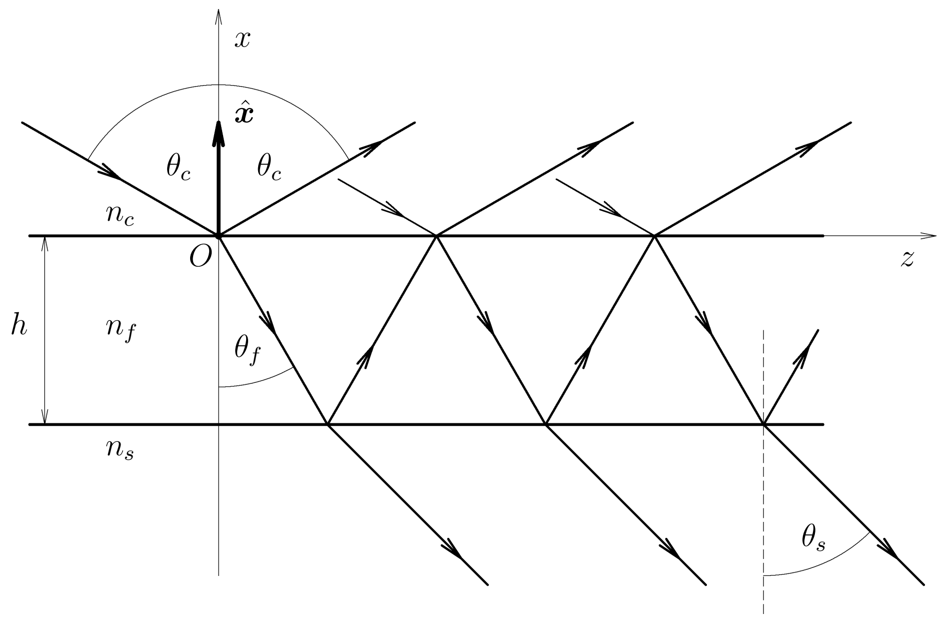

Figure 2.1: Multiple reflections in a dielectric thin film of a thickness, h, characterized by a real index of refraction, n_f, sandwiched between a dielectric cover characterized by a real index of refraction, n_c, and a dielectric substrate characterized by a real index of refraction, n_s. The angles between the propagation vectors and the unit vector $\hat{\boldsymbol{x}}$ perpendicular to the interface planes in the cover, the film and the substrate are denoted as θ_c, θ_f, and θ_s, respectively.

in a vacuum are denoted as ω and c, respectively. These are related with the vacuum wavelength, λ_{vac} by the relation,

$$\frac{2\pi}{\lambda_{\text{vac}}} = \frac{\omega}{c} \tag{2.2}$$

The signs in Eq. (2.1) distinguish the waves with the propagation vector x-components parallel or anti-parallel to $\hat{\boldsymbol{x}}$. All $\boldsymbol{k}_l$ are restricted to the zx plane normal to $\hat{\boldsymbol{y}}$. The magnitudes of propagation vectors, $\boldsymbol{k}_l = n_l \frac{\omega}{c} \left(\hat{\boldsymbol{z}} \sin\theta_l \pm \hat{\boldsymbol{x}} \cos\theta_l \right)$ are given by

$$|\boldsymbol{k}_l| = \frac{\omega}{c} n_l \tag{2.3}$$

Fields of these traveling waves will be taken proportional to an exponential function with an argument imaginary pure

$$\exp\left[\mathrm{j}\left(\omega t - \boldsymbol{k}_l \cdot \boldsymbol{r}\right)\right] = \exp\left[\mathrm{j}\left(\omega t - \frac{\omega}{c} n_l z \sin\theta_l \mp \frac{\omega}{c} n_l x \cos\theta_l\right)\right] \tag{2.4}$$

For example, the electric field of the *incident* wave, E_i, in the cover region, c, with the propagation vector, $\boldsymbol{k}_c^{(\text{in})} = n_c \frac{\omega}{c} \left(\hat{\boldsymbol{z}} \sin\theta_c - \hat{\boldsymbol{x}} \cos\theta_c \right)$, traveling towards the $c-f$ interface is proportional to

$$E_i \propto \exp\left[\mathrm{j}\left(\omega t - \frac{\omega}{c} n_c z \sin\theta_c + \frac{\omega}{c} n_c x \cos\theta_c\right)\right] \tag{2.5}$$

The electric field of the *reflected* wave, E_r, in the cover region, c, with the propagation vector $\boldsymbol{k}_c^{(\text{refl})} = n_c \frac{\omega}{c} (\hat{\boldsymbol{z}} \sin\theta_c + \hat{\boldsymbol{x}} \cos\theta_c)$, i.e. traveling out of the $c - f$ interface is proportional to

$$E_r \quad \propto \quad \exp\left[\mathrm{j}\left(\omega t - \frac{\omega}{c} n_c z \sin\theta_c - \frac{\omega}{c} n_c x \cos\theta_c\right)\right] \tag{2.6}$$

The account of the medium linearity and Snell law

$$n_c \sin\theta_c = n_f \sin\theta_f = n_s \sin\theta_s \tag{2.7}$$

(the conservation of the propagation vector components of the incident, reflected and transmitted waves parallel to the interface plane) gives

$$\exp\left[\mathrm{j}\left(\omega t - \frac{\omega}{c} n_l z \sin\theta_l\right)\right] , \tag{2.8}$$

i.e., an invariant formed by the product of $\sin\theta_l$ and the real index of refraction, n_l for the media $l = c, f, s$.

To simplify the problem, let us assume that the electric field amplitude of the wave traveling from the substrate towards the $s-f$ interface is zero. For the sake of conciseness, we denote the phase increment corresponding to a single traverse across the film as

$$\phi_f \quad = \quad \frac{\omega}{c} n_f h \cos\theta_f \tag{2.9}$$

The phase increment is maximum at the normal incidence where $\theta_f = 0$. The ratio of the total electric field of reflected waves, E_r, to the electric field of the incident wave, E_i, in the cover region c becomes

$$\frac{E_r}{E_i} \quad = \quad r_{cf} + \left(t_{cf}\, \mathrm{e}^{-\mathrm{j}\phi_f}\, r_{fs}\, \mathrm{e}^{-\mathrm{j}\phi_f}\, t_{fc} + t_{cf}\, \mathrm{e}^{-\mathrm{j}\phi_f}\, r_{fs}\, \mathrm{e}^{-\mathrm{j}\phi_f}\, r_{fc}\, \mathrm{e}^{-\mathrm{j}\phi_f}\, r_{fs}\, \mathrm{e}^{-\mathrm{j}\phi_f}\, t_{fc} + \ldots\right) \tag{2.10}$$

where the Fresnel transmission and reflection coefficient for the interface between the entrance medium, c (cover), and the film f are denoted as r_{cf} and t_{cf}, respectively, for the waves incident from the cover region c and as r_{fc} and t_{fc} for the waves incident from the film region, f. In a similar way, we denote the Fresnel transmission and reflection coefficient for the interface between the film, f, and the exit medium (substrate), s, as r_{fs} and t_{fs}, respectively for the waves traveling from the film region, f, towards the interface $s - f$.[2]

[2] The transmission coefficient t_{fs} would be taken into account in the analysis of the waves transmitted to the substrate.

2.1.1 Fresnel equations

Fresnel equations below the critical angle of incidence

The present analysis employs reflection and transmission coefficients at planar interface between linear isotropic and homogeneous (LIH) media. These are given by Fresnel equations for the electric field amplitude ratios of reflected and transmitted waves with respect to that of the incident wave. The Fresnel reflection and transmission coefficients for the planar waves with TE polarization (i.e., with the linearly polarized electric field perpendicular to the plane of incidence) and those with TM polarization (i.e., with the linearly polarized magnetic field perpendicular to the plane of incidence) pertinent to a planar interface between nonmagnetic LIH media 1 and 2 become[3]

$$r_{12}^{(\mathrm{TE})} = \frac{n_1\cos\theta_i - n_2\cos\theta_t}{n_1\cos\theta_i + n_2\cos\theta_t} = \frac{n_1\cos\theta_i - \left(n_2^2 - n_1^2\sin^2\theta_i\right)^{1/2}}{n_1\cos\theta_i + \left(n_2^2 - n_1^2\sin^2\theta_i\right)^{1/2}} \tag{2.11a}$$

$$t_{12}^{(\mathrm{TE})} = 1 + r_{12}^{(\mathrm{TE})} = \frac{2n_1\cos\theta_i}{n_1\cos\theta_i + n_2\cos\theta_t} = \frac{2n_1\cos\theta_i}{n_1\cos\theta_i + \left(n_2^2 - n_1^2\sin^2\theta_i\right)^{1/2}} \tag{2.11b}$$

$$\begin{aligned} r_{12}^{(\mathrm{TM})} &= \frac{n_2\cos\theta_i - n_1\cos\theta_t}{n_2\cos\theta_i + n_1\cos\theta_t} = \frac{n_2^2\cos\theta_i - n_1n_2\cos\theta_t}{n_2^2\cos\theta_i + n_1n_2\cos\theta_t} \\ &= \frac{n_2^2\cos\theta_i - n_1\left(n_2^2 - n_1^2\sin^2\theta_i\right)^{1/2}}{n_2^2\cos\theta_i + n_1\left(n_2^2 - n_1^2\sin^2\theta_i\right)^{1/2}} \end{aligned} \tag{2.11c}$$

$$\begin{aligned} t_{12}^{(\mathrm{TM})} &= \frac{n_1}{n_2}\left(1 + r_{12}^{(\mathrm{TM})}\right) = \frac{2n_1\cos\theta_i}{n_2\cos\theta_i + n_1\cos\theta_t} = \frac{2n_1n_2\cos\theta_i}{n_2^2\cos\theta_i + n_1n_2\cos\theta_t} \\ &= \frac{2n_1n_2\cos\theta_i}{n_2^2\cos\theta_i + n_1\left(n_2^2 - n_1^2\sin^2\theta_i\right)^{1/2}} \end{aligned} \tag{2.11d}$$

where θ_i and θ_t represent the angle of incidence and the angle of refraction, respectively. In the last step, we have eliminated $\cos\theta_t$ using Snell law. The Snell law requires the continuity of the propagation vector components parallel to the interface,

$$\frac{\omega}{c}n_1\sin\theta_i = \frac{\omega}{c}n_2\sin\theta_t \tag{2.12}$$

Then $n_2\cos\theta_t$ or $n_1\cos\theta_t$ in Eqs. (2.11) can be expressed as

$$n_2\cos\theta_t = \left(n_2^2 - n_1^2\sin^2\theta_i\right)^{1/2} \qquad (\mathrm{TE}) \tag{2.13a}$$

$$n_1\cos\theta_t = \frac{n_1}{n_2}\left(n_2^2 - n_1^2\sin^2\theta_i\right)^{1/2} \qquad (\mathrm{TM}) \tag{2.13b}$$

[3] The Fresnel equations in this form remain also valid for an interface of magnetic media which display the same magnetic permeability.

Critical angle of incidence

A wave traveling from a medium of higher index of refraction n_1 and incident to an interface with a medium of lower index of refraction n_2 (i.e., $n_2 < n_1$) at an angle of incidence higher than a certain critical angle is totally reflected. To include the phenomenon of total reflection, the Fresnel formulae (2.11) require a generalization (Section 2.1.1). In particular, at the critical angle of incidence $\theta_i^{(\mathrm{crit})}$ in the medium 1,

$$\boxed{\sin\theta_i^{(\mathrm{crit})} = n_2/n_1 < 1} \tag{2.14}$$

the cosine of the angle of refraction to the medium 2 follows from

$$n_2\cos\theta_t^{(\mathrm{crit})} = \left(n_2^2 - n_1^2\sin^2\theta_i^{(\mathrm{crit})}\right)^{1/2} = 0 = n_2\cos\frac{\pi}{2} \tag{2.15}$$

i.e., at the critical angle of incidence, the angle of refraction, $\theta_t^{(\mathrm{crit})}$, is equal to $\pi/2$,

$$\theta_t^{(\mathrm{crit})} = \frac{\pi}{2}$$

Refracted waves travel parallel to the interface.

The substitutions of Eq. (2.15) into Eqs. (2.11) provide the values at the critical angle of incidence $\theta_i^{(\mathrm{crit})}$ of the reflection and transmission coefficients for waves incident from a medium characterized by an index of refraction, n_1, to the interface with a medium characterized by an index of refraction, $n_2 < n_1$

$$r_{12}^{(\mathrm{TE})}\left(\theta_i^{(\mathrm{crit})}\right) = 1 \tag{2.16a}$$

$$t_{12}^{(\mathrm{TE})}\left(\theta_i^{(\mathrm{crit})}\right) = 2 \tag{2.16b}$$

$$r_{12}^{(\mathrm{TM})}\left(\theta_i^{(\mathrm{crit})}\right) = 1 \tag{2.16c}$$

$$t_{12}^{(\mathrm{TM})}\left(\theta_i^{(\mathrm{crit})}\right) = 2\frac{n_1}{n_2} \tag{2.16d}$$

Reflection above the critical angle of incidence

We wish to find the dependence of phase of reflection coefficient on the angle of incidence above the critical angle of incidence. We consider a planar interface between two LIH media characterized by real indices of refraction n_1 a n_2, at the condition $n_1 > n_2$. The interface is situated in the plane normal to the x axis of a Cartesian coordinate system.

The unit vector $\hat{\boldsymbol{x}}$ normal to the interface plane points from the medium of higher index of refraction, n_1, to the medium of lower index of refraction, n_2. A plane wave from the medium of n_1 impinges at the interface at an angle of incidence, θ_i, greater than the critical angle for total reflection, $\theta_{12}^{(\mathrm{crit})} = \arcsin(n_2/n_1)$, i.e., $\theta_i > \theta_{12}^{(\mathrm{crit})}$. A plane wave defined by its propagation vector

$$\boldsymbol{k}_i = k_1\left(\hat{\boldsymbol{x}}\cos\theta_i + \hat{\boldsymbol{z}}\sin\theta_i\right) = \frac{\omega}{c}n_1\left(\hat{\boldsymbol{x}}\cos\theta_i + \hat{\boldsymbol{z}}\sin\theta_i\right) ,$$

propagates with an incident electric field

$$\begin{aligned} E_i &= E_{0i} \exp\left[\mathrm{j}\left(\omega t - \boldsymbol{k}_i \cdot \boldsymbol{r}\right)\right] \\ &= E_{0i} \exp\left[\mathrm{j}\omega t - \mathrm{j}k_1\left(\hat{\boldsymbol{x}} \cos\theta_i + \hat{\boldsymbol{z}} \sin\theta_i\right) \cdot \left(\hat{\boldsymbol{x}}x + \hat{\boldsymbol{y}}y + \hat{\boldsymbol{z}}z\right)\right] \\ &= E_{0i} \exp\left[\mathrm{j}\omega t - \mathrm{j}k_1\left(x \cos\theta_i + z \sin\theta_i\right)\right] \end{aligned} \tag{2.17a}$$

The incident wave produces a reflected wave defined by a propagation vector

$$\boldsymbol{k}_r = k_1\left(-\hat{\boldsymbol{x}} \cos\theta_i + \hat{\boldsymbol{z}} \sin\theta_i\right) = \frac{\omega}{c} n_1\left(-\hat{\boldsymbol{x}} \cos\theta_i + \hat{\boldsymbol{z}} \sin\theta_i\right)$$

characterized by a reflected electric field

$$\begin{aligned} E_r &= E_{0r} \exp\left[\mathrm{j}\left(\omega t - \boldsymbol{k}_r \cdot \boldsymbol{r}\right)\right] \\ &= E_{0r} \exp\left[\mathrm{j}\omega t - \mathrm{j}k_1\left(-\hat{\boldsymbol{x}} \cos\theta_i + \hat{\boldsymbol{z}} \sin\theta_i\right) \cdot \left(\hat{\boldsymbol{x}}x + \hat{\boldsymbol{y}}y + \hat{\boldsymbol{z}}z\right)\right] \\ &= E_{0r} \exp\left[\mathrm{j}\omega t - \mathrm{j}k_1\left(-x \cos\theta_i + z \sin\theta_i\right)\right] \end{aligned} \tag{2.17b}$$

and a transmitted wave with a propagation vector $\boldsymbol{k}_t = \hat{\boldsymbol{x}}k_{tx} + \hat{\boldsymbol{z}}k_{tz}$ characterized by a transmitted electric field

$$\begin{aligned} E_t &= E_{0t} \exp\left[\mathrm{j}\left(\omega t - \boldsymbol{k}_t \cdot \boldsymbol{r}\right)\right] \\ &= E_{0t} \exp\left[\mathrm{j}\omega t - \mathrm{j}\left(k_{tx}x + k_{tz}z\right)\right] . \end{aligned} \tag{2.17c}$$

The propagation constants of the incident and reflected waves, k_i and k_r are the same, i.e., $k_i = k_r = k_1 = n_1(\omega/c)$, that of the transmitted wave is given by $k_t = k_2 = n_2(\omega/c)$. The propagation vector components parallel to the planar interface at the interface are conserved (Snell law) and amount $\boldsymbol{k}_{iz} = \hat{\boldsymbol{z}}n_1(\omega/c)\sin\theta_i$. The normal component of the incident propagation vector is simply $\boldsymbol{k}_{ix} = \hat{\boldsymbol{x}}n_1(\omega/c)\cos\theta_i$. That of the reflected wave is of opposite orientation, i.e., $\boldsymbol{k}_{rx} = -\hat{\boldsymbol{x}}n_1(\omega/c)\cos\theta_i$. The magnitude of the normal component of the transmitted propagation vector follows from the equation

$$\boldsymbol{k}_{tx}^2 = \boldsymbol{k}_t^2 - \boldsymbol{k}_{tz}^2 = \left(\frac{\omega}{c}\right)^2 \left(n_2^2 - n_1^2 \sin^2\theta_i\right) < \left(\frac{\omega}{c}\right)^2 \left(n_2^2 - n_1^2 \sin^2\theta_{12}^{(\mathrm{crit})}\right) = 0 . \tag{2.18}$$

Above the critical angle, $\theta_i > \theta_{12}^{(\mathrm{crit})}$, the scalar product $\boldsymbol{k}_{tx} \cdot \hat{\boldsymbol{x}} = k_{tx}$ becomes imaginary pure. We get

$$k_{tx} = \pm\mathrm{j}\frac{\omega}{c}\left(n_1^2 \sin^2\theta_i - n_2^2\right)^{1/2} \tag{2.19}$$

where $\left(n_1^2 \sin^2\theta_i - n_2^2\right)^{1/2} \geq 0$. The transmitted wave traveling with the normal component of the propagation vector oriented along positive $\hat{\boldsymbol{x}}$ (with increasing x coordinate), must be exponentially decaying with the increasing x. As a consequence, we have to choose

$$\boldsymbol{k}_{tx} = -\mathrm{j}\hat{\boldsymbol{x}}\frac{\omega}{c}\left(n_1^2\sin^2\theta_i - n_2^2\right)^{1/2} \tag{2.20}$$

to get for the scalar product

$$\boldsymbol{k}_{tx}\cdot\hat{\boldsymbol{x}}x = k_{tx}x = -\mathrm{j}\frac{\omega}{c}\left(n_1^2\sin^2\theta_i - n_2^2\right)^{1/2}x \tag{2.21}$$

In the electromagnetic wave theory of dielectric waveguides, the amplitude of the normal propagation vector component,

$$|k_{tx}| = \frac{\omega}{c}\left(n_1^2\sin^2\theta_i - n_2^2\right)^{1/2} = \frac{2\pi}{\lambda_{\mathrm{vac}}}\left(n_1^2\sin^2\theta_i - n_2^2\right)^{1/2} \tag{2.22}$$

is defined as a transverse attenuation constant, γ. In the chosen configuration, the vectors $\boldsymbol{k}_{tx}$ a $\hat{\boldsymbol{x}}$ (i.e. for the wave propagating in the positive direction of $+\hat{\boldsymbol{x}}$) are parallel with same orientation. Based on these considerations, the transmitted, so called *evanescent*, wave can be characterized by its electric field,

$$E_t = E_{0t}\exp\left[\mathrm{j}\left(\omega t - n_1\frac{\omega}{c}z\sin\theta_i\right)\right]\exp\left[-\frac{\omega}{c}\underbrace{\left(n_1^2\sin^2\theta_i - n_2^2\right)^{1/2}}_{>0}x\right] \tag{2.23}$$

The value $|k_{tx}|^{-1}$ corresponds to the penetration depth of the evanescent wave into the medium with n_2 at the total reflection at the interface of media characterized by $n_1 > n_2$. The penetration depth is denoted as $\delta^{(12)}$

$$\delta^{(12)} = \frac{1}{|k_{tx}|} = \frac{\lambda_{\mathrm{vac}}}{2\pi\left(n_1^2\sin^2\theta_i - n_2^2\right)^{1/2}}. = \frac{1}{\frac{\omega}{c}\left(n_1^2\sin^2\theta_i - n_2^2\right)^{1/2}} \tag{2.24}$$

It is minimal at $\theta_i \to \pi/2$ and goes to the infinity at $\theta_i^{(\mathrm{crit})}$.

Let us list the propagation vectors of these three waves

$$\boldsymbol{k}_i = k_1\left(\hat{\boldsymbol{x}}\cos\theta_i + \hat{\boldsymbol{z}}\sin\theta_i\right) \tag{2.25a}$$

$$\boldsymbol{k}_r = k_1\left(-\hat{\boldsymbol{x}}\cos\theta_i + \hat{\boldsymbol{z}}\sin\theta_i\right) \tag{2.25b}$$

$$\boldsymbol{k}_t = -\mathrm{j}\hat{\boldsymbol{x}}\frac{\omega}{c}\left(n_1^2\sin^2\theta_i - n_2^2\right)^{1/2} + \hat{\boldsymbol{z}}k_1\sin\theta_i \tag{2.25c}$$

and the corresponding scalar product in the exponential factors

$$\boldsymbol{k}_i\cdot\boldsymbol{r} = k_1\left(x\cos\theta_i + z\sin\theta_i\right) \tag{2.26a}$$

$$\boldsymbol{k}_r\cdot\boldsymbol{r} = k_1\left(-x\cos\theta_i + z\sin\theta_i\right) \tag{2.26b}$$

$$\boldsymbol{k}_t\cdot\boldsymbol{r} = -\mathrm{j}x\frac{\omega}{c}\left(n_1^2\sin^2\theta_i - n_2^2\right)^{1/2} + zk_1\sin\theta_i \tag{2.26c}$$

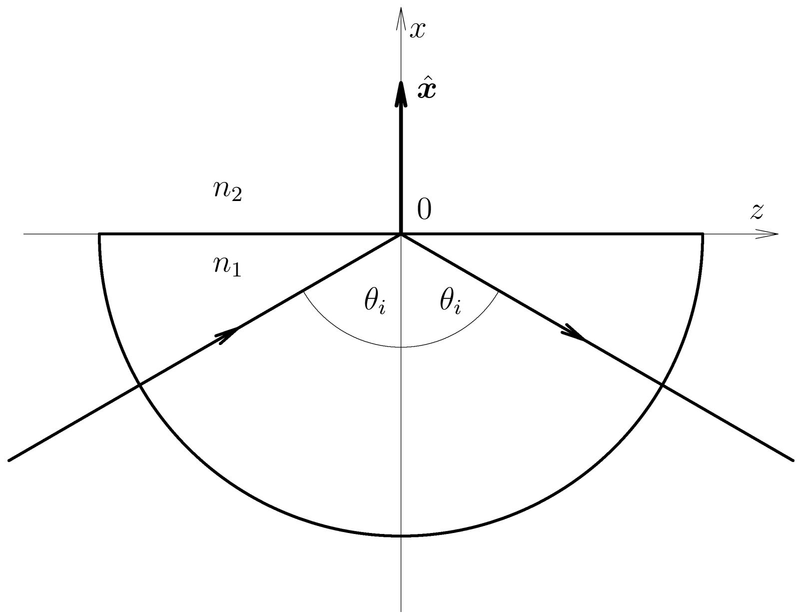

Figure 2.2: Reflection at the upper boundary of the film.

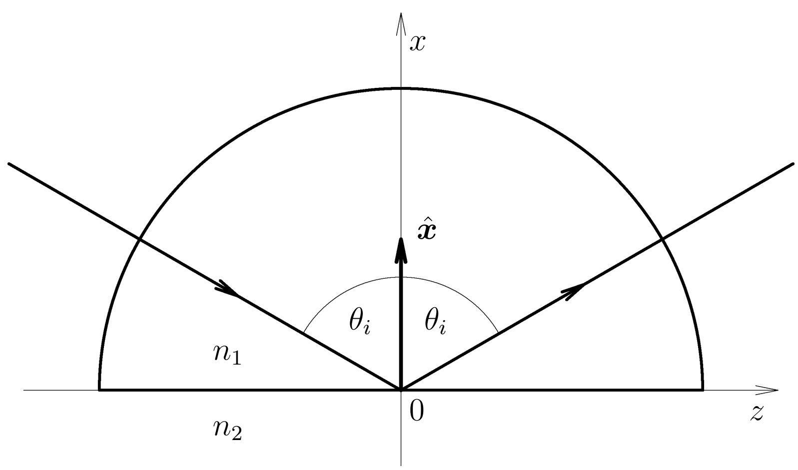

Figure 2.3: Reflection at the lower boundary of the film.

In the analysis of total internal reflections at the upper and lower interface in a film of the refractive index n_1 , sandwiched between media of lower indices of refraction, $n_2 < n_1$ it is useful to consider another configuration, the configuration with an opposite orientation of the propagation vector component normal to the interface. So far, we have analyzed the reflection at the "upper" interface boundary (Figure 2.2). At the"lower" interface boundary (Figure 2.3) in the same coordinate system, the unit vector $\hat{\boldsymbol{x}}$, normal to the interface plane will be of opposite orientation, i.e., $\hat{\boldsymbol{x}}$ will oriented from the medium of a lower index of refraction, n_2 , to the medium of higher index of refraction, $n_1 > n_2$. The propagation vectors from Eqs. (2.25) are transformed to

$$\begin{aligned} \boldsymbol{k}_i &= k_1 \left(-\hat{\boldsymbol{x}} \cos\theta_i + \hat{\boldsymbol{z}} \sin\theta_i\right) && (2.27a) \\ \boldsymbol{k}_r &= k_1 \left(\hat{\boldsymbol{x}} \cos\theta_i + \hat{\boldsymbol{z}} \sin\theta_i\right) && (2.27b) \\ \boldsymbol{k}_t &= \mathrm{j}\hat{\boldsymbol{x}} \frac{\omega}{c} \left(n_1^2 \sin^2\theta_i - n_2^2\right)^{1/2} + \hat{\boldsymbol{z}} k_1 \sin\theta_i && (2.27c) \end{aligned}$$

and the corresponding scalar products in Eqs. (2.26) become

$$\begin{aligned} \boldsymbol{k}_i \cdot \boldsymbol{r} &= k_1 \left(-x \cos\theta_i + z \sin\theta_i\right) && (2.28a) \\ \boldsymbol{k}_r \cdot \boldsymbol{r} &= k_1 \left(x \cos\theta_i + z \sin\theta_i\right) && (2.28b) \\ \boldsymbol{k}_t \cdot \boldsymbol{r} &= \mathrm{j} x \frac{\omega}{c} \left(n_1^2 \sin^2\theta_i - n_2^2\right)^{1/2} + z k_1 \sin\theta_i && (2.28c) \end{aligned}$$

The transmitted evanescent wave, previously expressed by Eq. (2.23), now traveling in the direction of decreasing $x < 0$ should be expressed as

$$E_t = E_{0t} \exp\left[\mathrm{j}\left(\omega t - n_1 \frac{\omega}{c} z \sin\theta_i\right)\right] \exp\left[\frac{\omega}{c} \underbrace{\left(n_1^2 \sin^2\theta_i - n_2^2\right)^{1/2}}_{>0} x\right] \tag{2.29}$$

The two cases may be involved in a single equation using the expression with the absolute value of x , i.e. $|x|$

$$E_t = E_{0t} \exp\left[\mathrm{j}\left(\omega t - n_1 \frac{\omega}{c} z \sin\theta_i\right)\right] \exp\left[-\frac{\omega}{c} \underbrace{\left(n_1^2 \sin^2\theta_i - n_2^2\right)^{1/2}}_{>0} |x|\right] \tag{2.30}$$

2.1.2 Fresnel equations above the critical angle of incidence

At a planar interface of nonmagnetic media (or at a planar interface of media characterized by a common magnetic permeability) of the indices of refraction $n_1 > n_2$ the Fresnel equations for wave reflection above the critical angle assume the form (independent on the choice of a coordinate system for the incident wave and the interface) given by

$$r_{12}^{(\mathrm{TE})} = \frac{n_1 \cos\theta_i + \mathrm{j}\left(n_1^2 \sin^2\theta_i - n_2^2\right)^{1/2}}{n_1 \cos\theta_i - \mathrm{j}\left(n_1^2 \sin^2\theta_i - n_2^2\right)^{1/2}} \tag{2.31a}$$

$$r_{12}^{(\mathrm{TM})} = \frac{n_2^2 \cos\theta_i + \mathrm{j}\, n_1 \left(n_1^2 \sin^2\theta_i - n_2^2\right)^{1/2}}{n_2^2 \cos\theta_i - \mathrm{j}\, n_1 \left(n_1^2 \sin^2\theta_i - n_2^2\right)^{1/2}} \tag{2.31b}$$

where the incident waves traveling to the interface from the medium of higher index of refraction, n_1, at an angle of incidence with respect to the interface normal of $\theta_i > \theta_{12}^{\mathrm{crit}}$. In Eqs. (2.11), we have replaced

$$\left(n_2^2 - n_1^2 \sin^2\theta_i\right)^{1/2} \rightarrow -\mathrm{j}\left(n_1^2 \sin^2\theta_i - n_2^2\right)^{1/2} .$$

From Eqs. (2.31), it is obvious that $\left|r_{12}^{(\mathrm{TE})}\right| = 1$ a $\left|r_{12}^{(\mathrm{TM})}\right| = 1$, corresponding to the *total internal reflection*. We employ the exponential representation

$$r_{12}^{(\mathrm{TE})} = \mathrm{e}^{2\mathrm{j}\phi_{12}^{(\mathrm{TE})}}, \qquad \phi_{12}^{(\mathrm{TE})} = \arctan \frac{\left(n_1^2 \sin^2\theta_i - n_2^2\right)^{1/2}}{n_1 \cos\theta_i} \tag{2.32a}$$

$$r_{12}^{(\mathrm{TM})} = \mathrm{e}^{2\mathrm{j}\phi_{12}^{(\mathrm{TM})}}, \qquad \phi_{12}^{(\mathrm{TM})} = \arctan \frac{n_1^2}{n_2^2}\frac{\left(n_1^2 \sin^2\theta_i - n_2^2\right)^{1/2}}{n_1 \cos\theta_i} \tag{2.32b}$$

The angles $2\phi_{12}^{(\mathrm{TE})}$ and $2\phi_{12}^{(\mathrm{TM})}$ represent phase shifts of the incident planar waves traveling from the medium characterized by n_1 with TE and TM polarization, respectively, at the total reflection at the interface with the medium of a lower index of refraction n_2 ($n_2 < n_1$). The curves of $\phi_{12}^{(\mathrm{TE})}$ and $\phi_{12}^{(\mathrm{TM})}$ dependent on the angle of incidence are illustrated in Figure 2.4. The ratio $n_1/n_2 = 3,6$ corresponds to the interface between a GaAS semiconductor and air. The ratio $n_1/n_2 = 2$ illustrates the situation at the interface between an $\mathrm{LiNbO_3}$ ionic crystal and air. Further, the ratio $n_1/n_2 = 1,4$ corresponds to the interface between a fused quartz (amorphous $\mathrm{SiO_2}$) and air. Finally, the ratio $n_1/n_2 = 1,01$ illustrate the situation at the interface between the core and cladding in optical fibers or at at an interface in semiconductor heterostructures GaAlAs considered for the monolithic integrated optoelectronics ($n_1 = 3,6$ a $n_2 = 3,55$).

2.1.3 Sum of multiple reflection series

The expression in the parentheses in Eq. (2.10) represent geometric series $\sum_{n-1}^{\infty} a_1 q^{n-1}$

$$\frac{E_r}{E_i} = r_{cf} + \left(t_{cf} r_{fs} t_{fc}\,\mathrm{e}^{-2\mathrm{j}\phi_f}\right)\left[1 + \left(r_{fc} r_{fs}\,\mathrm{e}^{-2\mathrm{j}\phi_f}\right) + \left(r_{fc} r_{fs}\,\mathrm{e}^{-2\mathrm{j}\phi_f}\right)^2 + \ldots\right] \tag{2.33}$$

At the condition of convergence, i.e. for $q < 1$, the sum is given by

$$s = \sum_{n=1}^{\infty} a_1 q^{n-1} = \frac{a_1}{1-q}$$

Here

$$a_1 = t_{cf} r_{fs} t_{fc} \mathrm{e}^{-2\mathrm{j}\phi_f}$$
$$q = r_{fc} r_{fs} \mathrm{e}^{-2\mathrm{j}\phi_f}$$

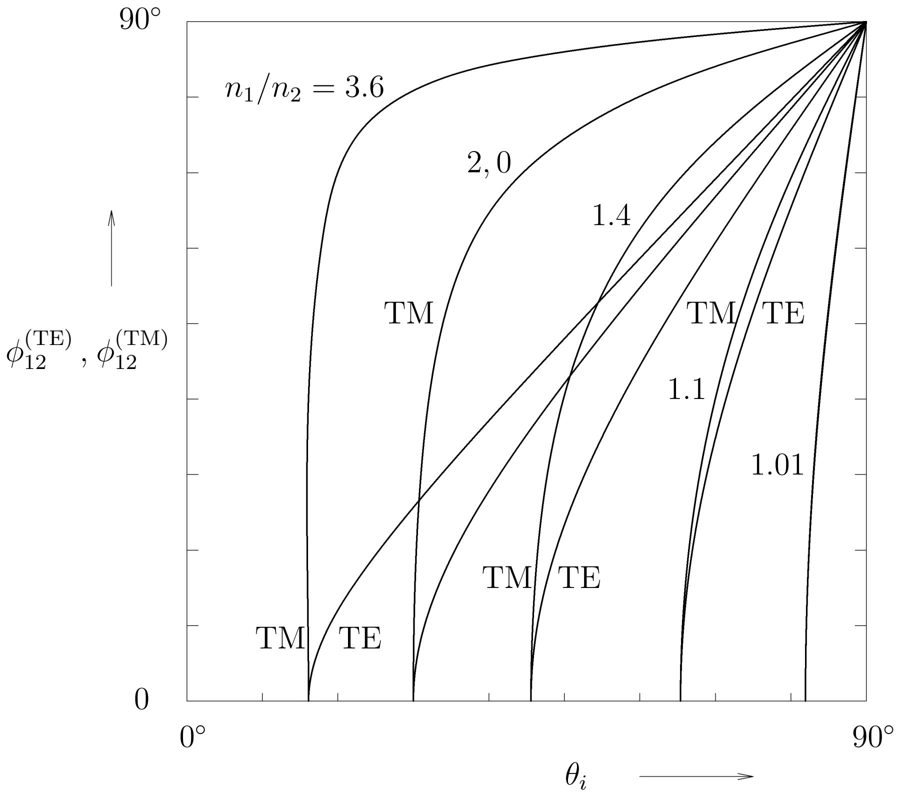

Figure 2.4: Phase half shifts $\phi_{12}^{(\mathrm{TE})}$ and $\phi_{12}^{(\mathrm{TM})}$ above the critical angle of incidence at the internal total reflection as functions of the angle of incidence, θ_i , for several ratios of indices of refraction, n_1/n_2 . At the critical angle, $\mathrm{d}\left[\phi_{12}^{(\mathrm{TE})}\left(\theta_i\right)\right]/\mathrm{d}\theta_i \to \infty$ and $\mathrm{d}\left[\phi_{12}^{(\mathrm{TM})}\left(\theta_i\right)\right]/\mathrm{d}\theta_i \to \infty$. At $\theta_i = 90^\circ$, $\mathrm{d}\left[\phi_{12}^{(\mathrm{TE})}\left(\theta_i\right)\right]/\mathrm{d}\theta_i$ equals $n_1\left(n_1^2 - n_2^2\right)^{-1/2} = \dfrac{\mu_2}{\mu_1}\dfrac{n_1}{\left(n_1^2 - n_2^2\right)^{1/2}}$ and $\mathrm{d}\left[\phi_{12}^{(\mathrm{TM})}\left(\theta_i\right)\right]/\mathrm{d}\theta_i$ equals $n_2^2 n_1^{-1}\left(n_1^2 - n_2^2\right)^{-1/2} = \dfrac{\varepsilon_2}{\varepsilon_1}\dfrac{n_1}{\left(n_1^2 - n_2^2\right)^{1/2}}$.

and according to Eq. (2.9)

$$\phi_f = \frac{\omega}{c} n_f h \cos\theta_f$$

The global reflection coefficient of the planar system cover – film – substrate will be given as a ratio of the electric field amplitude of the reflected wave, E_r , and that of the incident wave, E_i

$$\begin{aligned}\frac{E_r}{E_i} &= r_{cf} + \frac{t_{cf}t_{fc}r_{fs}\mathrm{e}^{-2\mathrm{j}\phi_f}}{1 - r_{fc}r_{fs}\mathrm{e}^{-2\mathrm{j}\phi_f}} \\ &= \frac{r_{cf}\left(1 - r_{fc}r_{fs}\mathrm{e}^{-2\mathrm{j}\phi_f}\right) + t_{cf}t_{fc}r_{fs}\mathrm{e}^{-2\mathrm{j}\phi_f}}{1 - r_{fc}r_{fs}\mathrm{e}^{-2\mathrm{j}\phi_f}} \\ &= \frac{r_{cf} + \left(t_{cf}t_{fc} - r_{cf}r_{fc}\right) r_{fs}\mathrm{e}^{-2\mathrm{j}\phi_f}}{1 - r_{fc}r_{fs}\mathrm{e}^{-2\mathrm{j}\phi_f}}\end{aligned}$$

We account for the following identity which follows e.g., from the Fresnel formulae

$$t_{cf}t_{fc} - r_{cf}r_{fc} = 1\,, \qquad r_{cf} = -r_{fc}$$

Then

$$\frac{E_r}{E_i} = \frac{r_{cf} + r_{fs}\mathrm{e}^{-2\mathrm{j}\phi_f}}{1 - r_{fc}r_{fs}\mathrm{e}^{-2\mathrm{j}\phi_f}} \tag{2.34}$$

where $|r_{cf}| \leq 1$ and $|r_{fs}| \leq 1$.

Alternatively, we could start from the analysis of the wave transmitted into the substrate. The ratio of the transmitted electric field amplitude, E_t, to that of the incident electric field, E_i, would be given by

$$\frac{E_t}{E_i} = \frac{t_{cf}t_{fs}\mathrm{e}^{-\mathrm{j}\phi_f}}{1 - r_{fc}r_{fs}\mathrm{e}^{-2\mathrm{j}\phi_f}} \tag{2.35}$$

For the present purpose, it is relevant that the form of the denominator in Eq. (2.34) and in Eq. (2.35) is the same.

2.2 Guided waves in planar structures

2.2.1 Eigenvalue equation

The eigenvalue equation, i.e., the condition for the guided eigenmodes in planar (i.e., unidimensional, 1D) systems formed by a cover, c, a thin film, f, and a substrate, s, is given by poles of the function $1 - r_{fc}r_{fs}\mathrm{e}^{-2\mathrm{j}\phi_f}$, entering the denominator on the right hand side in Eqs. (2.34) and (2.35),

$$1 - r_{fc}r_{fs}\mathrm{e}^{-2\mathrm{j}\phi_f} = 0 \tag{2.36}$$

It can be satisfied above the higher of the critical angles critical angles $\theta_{fc}^{(\mathrm{crit})}$ and $\theta_{fs}^{(\mathrm{crit})}$ for the total reflection at the f-c or f-s interface, at the conditions $n_c < n_f$ and $n_s < n_f$,

$$\theta_{fc}^{(\mathrm{crit})} = \arcsin\frac{n_c}{n_f}\,, \tag{2.37a}$$

$$\theta_{fs}^{(\mathrm{crit})} = \arcsin \frac{n_s}{n_f}\,. \tag{2.37b}$$

The angle, θ_f, spanned by the propagation vector, in the film, $\boldsymbol{k}_f$, and the interface normal is restricted to the range

$$\theta_f > \theta_{fc}^{(\mathrm{crit})} = \arcsin \frac{n_c}{n_f} \tag{2.38a}$$

or

$$\theta_f > \theta_{fs}^{(\mathrm{crit})} = \arcsin \frac{n_s}{n_f} \tag{2.38b}$$

whichever is narrower. Then $|r_{cf}| = 1$ and $|r_{fs}| = 1$ and the Fresnel reflection coefficients can be expressed in exponential forms as in Eqs. (2.32)

$$\begin{aligned} r_{fc} &= \mathrm{e}^{2\mathrm{j}\phi_{fc}} \\ r_{fs} &= \mathrm{e}^{2\mathrm{j}\phi_{fs}} \end{aligned}$$

The waveguiding condition can be transformed into the form

$$\begin{aligned} \frac{1}{r_{fc}}\frac{1}{r_{fs}}\mathrm{e}^{2\mathrm{j}\phi_f} &= 1 \\ \mathrm{e}^{2\mathrm{j}\phi_f}\mathrm{e}^{-2\mathrm{j}\phi_{fc}}\mathrm{e}^{-2\mathrm{j}\phi_{fs}} &= 1\,. \end{aligned}$$

After the substitution for ϕ_f according to Eq. (2.9), i.e., $\phi_f = \frac{\omega}{c} n_f h \cos\theta_f$, we rewrite the condition as

$$\exp\left[2\mathrm{j}\left(\frac{\omega}{c} n_f h \cos\theta_f - \phi_{fc} - \phi_{fs}\right)\right] = \exp\left(2\mathrm{j}\nu\pi\right)$$

where, in general, $\nu = 0, \pm1, \pm2, \ldots$, i.e., ν is an integer. The comparison of the exponents provides the waveguiding condition in a convenient form

$$\frac{\omega}{c} n_f h \cos\theta_f - \phi_{fc} - \phi_{fs} = \nu\pi\,, \qquad \nu = 0, 1, 2, 3, \ldots \tag{2.39a}$$

restricted, for the sake of simplicity, to non negative ν. Here, the projection $\boldsymbol{k}_f \cdot \hat{\boldsymbol{x}} = \frac{\omega}{c} n_f \cos\theta_f$ represents a transverse component of the propagation vector. In the electromagnetic field theory of guided waves in dielectric structures, this will be defined as transverse propagation constant and denoted by a symbol κ. Waveguiding modes are distinguished by the integer ν.

In terms of the vacuum wavelength, $\lambda_{\mathrm{vac}} = \omega/c$, the eigenvalue equation representing the waveguiding condition assumes the final conventional form

$$\boxed{\frac{2\pi h}{\lambda_{\mathrm{vac}}} n_f \cos\theta_f - \phi_{fc} - \phi_{fs} = \nu\pi\,, \qquad \nu = 0, 1, 2, 3, \ldots} \tag{2.39b}$$

The waveguiding condition is valid for each eigen polarization, i.e., for either TE or TM, separately,

$$\frac{\omega}{c}n_f h\cos\theta_f - \phi_{fc}^{(\mathrm{TE})} - \phi_{fs}^{(\mathrm{TE})} = \nu\pi\,, \qquad \nu = 0,1,2,3,\ldots \tag{2.40a}$$

$$\frac{\omega}{c}n_f h\cos\theta_f - \phi_{fc}^{(\mathrm{TM})} - \phi_{fs}^{(\mathrm{TM})} = \nu\pi\,, \qquad \nu = 0,1,2,3,\ldots \tag{2.40b}$$

The simultaneous waveguiding condition takes the form of product,

$$\left(1 - r_{fc}^{(\mathrm{TE})}r_{fs}^{(\mathrm{TE})}\mathrm{e}^{-2\mathrm{j}\phi_f}\right)\left(1 - r_{fc}^{(\mathrm{TM})}r_{fs}^{(\mathrm{TM})}\mathrm{e}^{-2\mathrm{j}\phi_f}\right) = 0 \tag{2.41}$$

The TE and TM waves satisfying the waveguiding condition are called (eigen) TE *modes* and (eigen) TM *modes*.

2.2.2 Effective guide index

The effective guide index is defined by the relation

$$N = n_f \sin\theta_f \tag{2.42}$$

where n_f and θ_f are the index of refraction in the film and the angle spanned by the propagation vector and the normal to the film interfaces, respectively. We denote the indices of refraction of cover and the substrate as n_c resp. n_s, respectively. The effective guide index is confined to the smaller of the intervals $n_c < N < n_f$ and $n_s < N < n_f$.

In terms of N, the phase half shifts at the total internal reflection given in Eqs. (2.32) become

$$\phi_{fc}^{(\mathrm{TE})} = \arctan\frac{\left(n_f^2\sin^2\theta_f - n_c^2\right)^{1/2}}{n_f\cos\theta_f} = \arctan\left[\left(\frac{N^2-n_c^2}{n_f^2-N^2}\right)^{1/2}\right] \tag{2.43a}$$

$$\phi_{fc}^{(\mathrm{TM})} = \arctan\frac{n_f^2}{n_c^2}\frac{\left(n_f^2\sin^2\theta_f - n_c^2\right)^{1/2}}{n_f\cos\theta_f} = \arctan\left[\frac{n_f^2}{n_c^2}\left(\frac{N^2-n_c^2}{n_f^2-N^2}\right)^{1/2}\right] \tag{2.43b}$$

$$\phi_{fs}^{(\mathrm{TE})} = \arctan\frac{\left(n_f^2\sin^2\theta_f - n_s^2\right)^{1/2}}{n_f\cos\theta_f} = \arctan\left[\left(\frac{N^2-n_s^2}{n_f^2-N^2}\right)^{1/2}\right] \tag{2.43c}$$

$$\phi_{fs}^{(\mathrm{TM})} = \arctan\frac{n_f^2}{n_s^2}\frac{\left(n_f^2\sin^2\theta_f - n_s^2\right)^{1/2}}{n_f\cos\theta_f} = \arctan\left[\frac{n_f^2}{n_s^2}\left(\frac{N^2-n_s^2}{n_f^2-N^2}\right)^{1/2}\right] \tag{2.43d}$$

We denote the film thickness by h and replace $\omega/c = 2\pi/\lambda_{\mathrm{vac}}$. The waveguiding conditions for eigen TE and TM modes given in Eqs. (2.40) can be rearranged. For the TE modes,

$$\frac{2\pi h}{\lambda_{\mathrm{vac}}}\left(n_f^2 - N^2\right)^{1/2} - \arctan\left[\left(\frac{N^2 - n_c^2}{n_f^2 - N^2}\right)^{1/2}\right] - \arctan\left[\left(\frac{N^2 - n_s^2}{n_f^2 - N^2}\right)^{1/2}\right] = \nu\pi \tag{2.44a}$$

and for the TM modes,

$$\begin{aligned} \frac{2\pi h}{\lambda_{\mathrm{vac}}}\left(n_f^2 - N^2\right)^{1/2} - \arctan\left[\left(\frac{n_f}{n_c}\right)^2\left(\frac{N^2 - n_c^2}{n_f^2 - N^2}\right)^{1/2}\right] & \\ - \arctan\left[\left(\frac{n_f}{n_s}\right)^2\left(\frac{N^2 - n_s^2}{n_f^2 - N^2}\right)^{1/2}\right] &= \nu\pi \end{aligned} \tag{2.44b}$$

Using

$$\arctan x + \arctan y = \arctan\frac{x+y}{1-xy}, \tag{2.45}$$

in Eqs. (2.44), we get for TE modes,

$$\begin{aligned} &\arctan\left[\left(\frac{N^2 - n_c^2}{n_f^2 - N^2}\right)^{1/2}\right] + \arctan\left[\left(\frac{N^2 - n_s^2}{n_f^2 - N^2}\right)^{1/2}\right] \\ &= \arctan\frac{\left[\left(\frac{N^2 - n_c^2}{n_f^2 - N^2}\right)^{1/2}\right] + \left[\left(\frac{N^2 - n_s^2}{n_f^2 - N^2}\right)^{1/2}\right]}{1 - \left[\left(\frac{N^2 - n_c^2}{n_f^2 - N^2}\right)^{1/2}\right]\left[\left(\frac{N^2 - n_s^2}{n_f^2 - N^2}\right)^{1/2}\right]} \\ &= \arctan\left\{\frac{\left(n_f^2 - N^2\right)^{1/2}\left[(N^2 - n_s^2)^{1/2} + (N^2 - n_c^2)^{1/2}\right]}{\left(n_f^2 - N^2\right) - (N^2 - n_c^2)^{1/2}(N^2 - n_s^2)^{1/2}}\right\}, \end{aligned} \tag{2.46a}$$

and for the TM modes,

$$
\begin{aligned}
&\arctan\left[\left(\frac{n_f}{n_c}\right)^2\left(\frac{N^2-n_c^2}{n_f^2-N^2}\right)^{1/2}\right]+\arctan\left[\left(\frac{n_f}{n_s}\right)^2\left(\frac{N^2-n_s^2}{n_f^2-N^2}\right)^{1/2}\right] \\
&= \arctan\frac{\left[\left(\frac{n_f}{n_c}\right)^2\left(\frac{N^2-n_c^2}{n_f^2-N^2}\right)^{1/2}\right]+\left[\left(\frac{n_f}{n_s}\right)^2\left(\frac{N^2-n_s^2}{n_f^2-N^2}\right)^{1/2}\right]}{1-\left[\left(\frac{n_f}{n_c}\right)^2\left(\frac{N^2-n_c^2}{n_f^2-N^2}\right)^{1/2}\right]\left[\left(\frac{n_f}{n_s}\right)^2\left(\frac{N^2-n_s^2}{n_f^2-N^2}\right)^{1/2}\right]} \\
&= \arctan\left\{\frac{n_f^2\left(n_f^2-N^2\right)^{1/2}\left[n_c^2\left(N^2-n_s^2\right)^{1/2}+n_s^2\left(N^2-n_c^2\right)^{1/2}\right]}{n_c^2n_s^2\left(n_f^2-N^2\right)-n_f^4\left(N^2-n_c^2\right)^{1/2}\left(N^2-n_s^2\right)^{1/2}}\right\}.
\end{aligned}
\tag{2.46b}
$$

Equations (2.44) can then be expressed for TE modes as,

$$
\frac{2\pi h}{\lambda_{\mathrm{vac}}}\left(n_f^2-N^2\right)^{1/2}-\arctan\left\{\frac{\left(n_f^2-N^2\right)^{1/2}\left[\left(N^2-n_s^2\right)^{1/2}+\left(N^2-n_c^2\right)^{1/2}\right]}{\left(n_f^2-N^2\right)-\left(N^2-n_c^2\right)^{1/2}\left(N^2-n_s^2\right)^{1/2}}\right\} = \nu\pi
\tag{2.47a}
$$

and for the TM modes,

$$
\frac{2\pi h}{\lambda_{\mathrm{vac}}}\left(n_f^2-N^2\right)^{1/2}-\arctan\left\{\frac{\frac{\left(n_f^2-N^2\right)^{1/2}}{n_f^2}\left[\frac{\left(N^2-n_s^2\right)^{1/2}}{n_s^2}+\frac{\left(N^2-n_c^2\right)^{1/2}}{n_c^2}\right]}{\frac{\left(n_f^2-N^2\right)}{n_f^4}-\frac{\left(N^2-n_s^2\right)^{1/2}}{n_s^2}\frac{\left(N^2-n_c^2\right)^{1/2}}{n_c^2}}\right\} = \nu\pi\,.
\tag{2.47b}
$$

2.2.3 Ray model

Alternatively, the waveguiding condition in Eq. (2.39) in three planar (1D) ideally dielectric (i.e., lossless) media, cover – film – substrate system, characterized by real indices of refraction in the cover, n_c, in the film, n_f, and in the substrate, n_s in Eq. (2.39) can be deduced from the considerations on plane waves with defined propagation vectors using so called ray model, The n_c, n_f, and n_s satisfy $n_c < n_f$ and $n_s < n_f$. We shall further assume $n_c < n_s$. The refractive index profile is determined by

$$
n_c \;<\; n_s \;<\; n_f
\tag{2.48}
$$

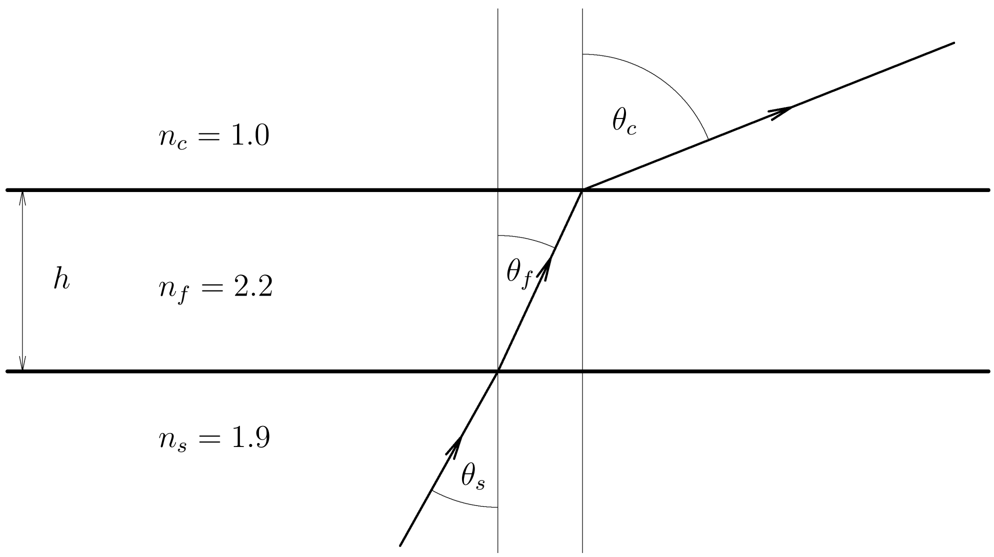

Figure 2.5: Radiation mode at $\theta_f = 25°$. After Herwig Kogelnik, *Theory of Dielectric Waveguides* in Integrated Optics, Editor: Theodor Tamir, Topics in Applied Physics, Vol. 7, Springer Verlag, Berlin, Heidelberg, New York, 1975.

The critical angles for total internal reflection are given by Eqs. (2.37)

$$\theta_{fc}^{(\text{crit})} = \arcsin \frac{n_c}{n_f} \tag{2.49a}$$

$$\theta_{fs}^{(\text{crit})} = \arcsin \frac{n_s}{n_f} \tag{2.49b}$$

We again choose the Cartesian coordinate system with the x axis normal to the interface planes. The c–f interface is situated in the plane $x = 0$ and the interface f–s is situated in the plane $x = -h$ as in Figure 2.1. The cover fills the half space $x > 0$ the film is confined to the region $0 > x > -h$ and the substrate occupies the half space $x < -h$. The propagation vectors of the plane waves with either TE or TM eigen polarizations are confined to the plane of incidence normal to the y axis.

Continuous spectrum of radiation modes

We observe the transmission of a plane wave propagating in the substrate half space towards the interface substrate – film at an angle of incidence, θ_s, spanned by its propagation vector and the interface normal, smaller than the critical angles for total internal reflection,

$$\theta_f < \theta_{fc}^{(\text{crit})} < \theta_{fs}^{(\text{crit})} \tag{2.50}$$

The wave after traversing the substrate – film interface is refracted at an angle $\theta_f < \theta_s$ and leaves the film – cover interface at an angle $\theta_c > \theta_f$. The angular spectrum given by the condition (2.50) is continuous and represents the spectrum of radiation modes. The situation is illustrated in Figure 2.5.

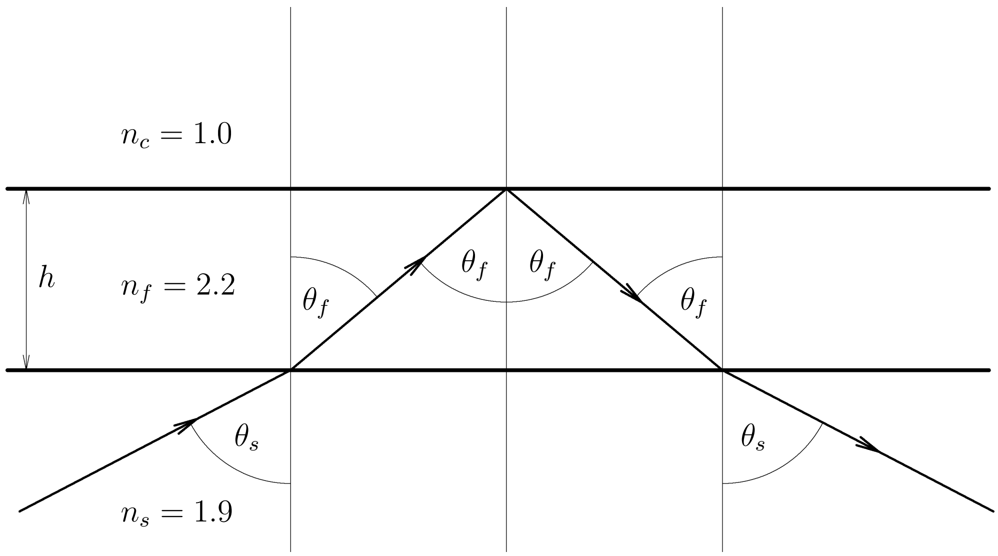

Figure 2.6: Substrate mode, $\theta_f = 50°$. After Herwig Kogelnik, *Theory of Dielectric Waveguides* in Integrated Optics, Editor: Theodor Tamir, Topics in Applied Physics, Vol. 7, Springer Verlag, Berlin, Heidelberg, New York, 1975.

Continuous spectrum of substrate modes

Now we consider a plane wave traveling from the substrate half space to the substrate – film interface and propagating in the film at an angle θ_f smaller than the critical angle at the interface film – substrate but greater than the critical angle at film – cover interface,

$$\theta_{fc}^{(\mathrm{crit})} \;<\; \theta_f \;<\; \theta_{fs}^{(\mathrm{crit})} \tag{2.51}$$

The wave arrives at the substrate – film interface at an angle θ_s and becomes refracted at an angle $\theta_f < \theta_s$. After being totally reflected it returns back to the substrate after passing the film – substrate interface. The angular spectrum of θ_f according to the condition (2.51) is again continuous and defines the spectrum of substrate modes. The situation is illustrated in Figure 2.6.

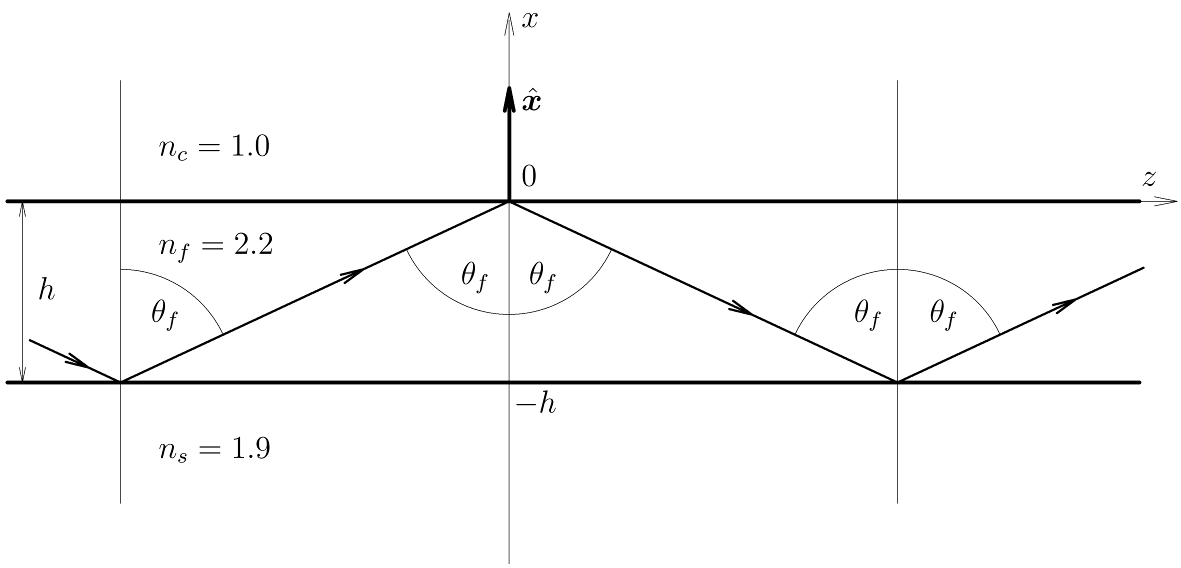

Figure 2.7: Guided mode, $\theta_f = 65°$. After Herwig Kogelnik, *Theory of Dielectric Waveguides* in Integrated Optics, Editor: Theodor Tamir, Topics in Applied Physics, Vol. 7, Springer Verlag, Berlin, Heidelberg, New York, 1975.

Discrete spectrum of guided modes

We now consider the existence of plane waves inside the film characterized by propagation vectors spanning with the interface normal (parallel to the unit vector, $\hat{\boldsymbol{x}}$) an angle θ_f, greater than the critical angles for the total internal reflection at both the film – cover interface and at the film – substrate interface,

$$\theta_{fc}^{(\text{crit})} \; < \; \theta_{fs}^{(\text{crit})} \; < \; \theta_f \tag{2.52}$$

At a fixed value of propagation vector component parallel to the interface planes and to the waveguide axis (chosen along the z axis) of magnitude β, i.e., $\hat{\boldsymbol{z}}\beta = \hat{\boldsymbol{z}} n_f \frac{\omega}{c} \sin\theta_f$, the corresponding propagation vector component normal to the interface planes of the magnitude κ assumes the values $\pm\hat{\boldsymbol{x}}\kappa = \pm\hat{\boldsymbol{x}} n_f \frac{\omega}{c}\cos\theta_f$. Here, β denotes the *longitudinal propagation constant* related to the effective guide index N from Section 2.2.2 by the relation $\beta = (\omega/c)N$. Then κ will denote the *transverse propagation constant*.

In the film, there exist two waves, one traveling to the film – cover interface

$$E^{\uparrow} \;=\; E_0^{\uparrow} \exp\left[\mathrm{j}\left(\omega t - n_f \frac{\omega}{c} z \sin\theta_f - n_f \frac{\omega}{c} x \cos\theta_f\right)\right] \tag{2.53a}$$

and another one traveling to the film substrate interface

$$E^{\downarrow} \;=\; E_0^{\downarrow} \exp\left[\mathrm{j}\left(\omega t - n_f \frac{\omega}{c} z \sin\theta_f + n_f \frac{\omega}{c} x \cos\theta_f\right)\right] \tag{2.53b}$$

At constructive interference, the sum of these waves generates a guided mode infinite along the z axis (Figure 2.7). To find the condition for the guided mode, we have to account not only a phase shift across the film but also abrupt total internal reflection

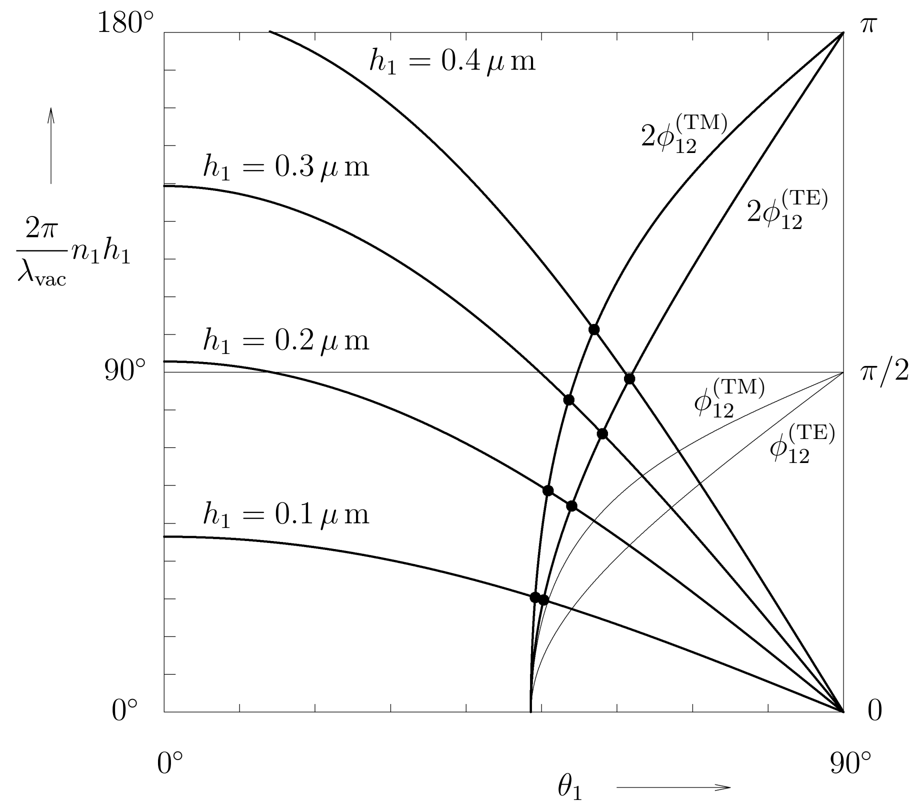

Figure 2.8: Graphical solution to the eigenvalue equation in a symmetric waveguide for the fundamental mode $\nu = 0$ at the wavelength $\lambda_{\mathrm{vac}} = 1.55\,\mu\mathrm{m}$. The film characterized by the index of refraction $n_1 = 2.0$ of the thickness h_1 is sandwiched between media of the index of refraction $n_2 = 1.5$. The horizontal axis represents the internal reflection angle, θ_1, in the film. The solution for θ_1 is given by an intersection of the curve for the phase shift across the film (increasing with the increased film thickness, h_1), and the curve of the thickness independent sum of half phase shifts $\phi_{12}^{(\mathrm{TE})}$ or $\phi_{12}^{(\mathrm{TM})}$ at the lower and upper interfaces.

phase changes at the interfaces. A wave characterized by the electric field, $E^{\uparrow}$, traveling to the interface at $x = 0$ and receiving a phase shift $2\phi_{fc}$ transforms at the total internal reflection into the wave characterized by the electric field $E^{\downarrow}$,

$$E_0^{\uparrow} \exp\left(\mathrm{j}2\phi_{fc}\right) = E_0^{\downarrow} \tag{2.54a}$$

The wave characterized by $E^{\downarrow}$ traveling to the interface $x = -h$ and receiving a phase shift $2\phi_{fs}$ transforms into the wave characterized by $E^{\uparrow}$

$$E_0^{\downarrow} \exp\left[\mathrm{j}\left(-n_f \frac{\omega}{c} h \cos\theta_f\right)\right] \exp\left(\mathrm{j}2\phi_{fs}\right) = E_0^{\uparrow} \exp\left[\mathrm{j}\left(n_f \frac{\omega}{c} h \cos\theta_f\right)\right] \tag{2.54b}$$

An invariant factor $\exp\left[\mathrm{j}\left(\omega t - n_f \frac{\omega}{c} z \sin\theta_f\right)\right]$ on both sides of Eqs. (2.54) was removed.

$$\begin{aligned} \boldsymbol{k}^{\uparrow} &= \hat{\boldsymbol{x}}\, n_f \frac{\omega}{c} \cos\theta_f + \hat{\boldsymbol{z}}\, n_f \frac{\omega}{c} \sin\theta_f & (2.55a) \\ \boldsymbol{k}^{\downarrow} &= -\hat{\boldsymbol{x}}\, n_f \frac{\omega}{c} \cos\theta_f + \hat{\boldsymbol{z}}\, n_f \frac{\omega}{c} \sin\theta_f & (2.55b) \end{aligned}$$

The phase relations between the waves at the interface $x = 0$ and at the interface $x = -h$ expressed in Eqs. (2.54) form a homogeneous equation system,

$$E_0^{\uparrow} \exp\left(\mathrm{j}2\phi_{fc}\right) - E_0^{\downarrow} = 0 \qquad (2.56a)$$

$$E_0^{\uparrow} \exp\left[\mathrm{j}\left(n_f \frac{\omega}{c} h \cos\theta_f\right)\right] - E_0^{\downarrow} \exp\left[\mathrm{j}\left(-n_f \frac{\omega}{c} h \cos\theta_f + 2\phi_{fs}\right)\right] = 0 \qquad (2.56b)$$

The condition for nontrivial solutions to a homogeneous equation system requires the zero determinant of the left hand side. In the present case of the equation system for the amplitudes $E_0^{\uparrow}$ and $E_0^{\downarrow}$ the following determinant must vanish,

$$\begin{vmatrix} \exp\left(\mathrm{j}2\phi_{fc}\right) & -1 \\ \exp\left[\mathrm{j}\left(n_f \frac{\omega}{c} h \cos\theta_f\right)\right] & -\exp\left[\mathrm{j}\left(-n_f \frac{\omega}{c} h \cos\theta_f + 2\phi_{fs}\right)\right] \end{vmatrix} = 0 \qquad (2.57)$$

After computing the determinant, we get

$$-\exp\left[\mathrm{j}\left(-n_f \frac{\omega}{c} h \cos\theta_f + 2\phi_{fc} + 2\phi_{fs}\right)\right] + \exp\left[\mathrm{j}\left(n_f \frac{\omega}{c} h \cos\theta_f\right)\right] = 0$$

We divide the equation by the first term on the left hand side to get

$$\exp\left[\mathrm{j}\left(2n_f \frac{\omega}{c} h \cos\theta_f - 2\phi_{fc} - 2\phi_{fs}\right)\right] = 1$$

The comparison of the exponents leads to the already known eigenvalue equation, Eq. (2.39), which expresses the so called *transverse resonance condition*,

$$\frac{\omega}{c} n_f h \cos\theta_f - \phi_{fc} - \phi_{fs} = \nu\pi\,, \qquad \nu = 0, 1, 2, 3, \ldots \qquad (2.58)$$

The angular spectrum of θ_f consistent with Eq. (2.58) falling into the range (2.52) becomes discrete. It form the spectrum of guided modes. The result is valid separately for the TE and TM eigen polarizations as in Eqs. (2.40).

The eigenvalue equation for guided TE and TM modes was derived in several equivalent forms presented, e.g., in Eqs. (2.40) or (2.44). Its graphical solution is shown in Figures 2.8 through 2.14. Figure 2.8 illustrates the solution to the eigenvalue equation for the fundamental mode $\nu = 0$ in a symmetric planar waveguide. The solutions for modes $\nu > 0$ are shown in Figure 2.9. The solutions for the fundamental TE and TM fundamental modes $\nu = 0$ in an asymmetric planar waveguide are compared in Figure 2.10. Note that the cut-off film thickness is higher for the TM mode than that for the TE mode.

Table 2.1: Guided TE modes of the order ν at the vacuum wavelength $\lambda_{\text{vac}} = 1\,060\,\text{nm}$ in a dielectric planar waveguide consisting of a layer (ZnS) of the index of refraction, $n_f = 2.2899$, and of the thickness, $h = 1\,500\,\text{nm}$, sandwiched between an overlayer (air) of the index of refraction, $n_c = 1.0$ and a substrate (glass) of the index of refraction, $n_s = 1.5040$. The results of the graphical solution to the eigenvalue equation (2.40a) in Figures 2.13 and 2.14 are expressed in terms of the "zig-zag" angle θ_f spanned by the propagation vector and the normal to the interfaces and in terms of the waveguide index, $N = n_f \sin\theta_f$.

ν	0	1	2	3	4
θ_f	82.1°	74.1°	65.7°	56.9°	47.7°
N	2.268	2.202	2.087	1.918	1.694

At the chosen film thickness, $h = 1500\,\text{nm}$, and the vacuum wavelength $\lambda_{\text{vac}} = 1\,060\,\text{nm}$ (Nd:YAG laser) the waveguide allows the propagation of modes in the range $0 \leq \nu \leq 4$. The graphical solutions to eigenvalue equation for $0 \leq \nu \leq 3$ and $1 \leq \nu \leq 4$ along with the cut-off thicknesses are shown in Figures 2.11 and 2.12, respectively. The eigenvalues of the "zig-zag" angles, θ_f, for TE and TM modes of the order $0 \leq \nu \leq 3$ and $1 \leq \nu \leq 4$ at the film thickness $h = 1500\,\text{nm}$ and the vacuum wavelength $\lambda_{\text{vac}} = 1\,060\,\text{nm}$ can be determined from the scales in Figures 2.13 and 2.14, respectively.

The waveguide in Figure 2.11 allows the propagation of the guided TE and TM modes above the cut-off film thickness, $h = 56\,\text{nm}$ and $h = 126\,\text{nm}$, respectively. The waveguide remains a monomode one for the TE and TM modes up to the film thickness, $h = 364$ nm and $h = 432$ nm, respectively. The TE and TM modes of the order $\nu = 2$ become allowed above $h = 670$ nm and $h = 740$ nm, respectively. For example, at an intermediate film thickness, $h = 906$ nm, shown in the Figure 2.11, the waveguide still carries the TE and TM modes $\nu = 0,\ 1,\ 2$, only.

In Figure 2.12, the guided TE and TM modes of the order $\nu = 3$ start above the film thickness, $h = 976\,\text{nm}$ and $h = 1048\,\text{nm}$, respectively. The guided TE and TM modes of the order $\nu = 4$ start above the film thickness, $h = 1280\,\text{nm}$ and $h = 1352\,\text{nm}$, respectively. At $h = 1500\,\text{nm}$ the modes of the order $\nu > 4$ are forbidden. The results of graphical solutions to the eigenvalue equation read from Figures 2.13 and 2.14 are summarized for the TE modes in Table 2.1 and for the TM modes in Table 2.2.

Table 2.2: Guided TM modes of the order ν at the vacuum wavelength $\lambda_{\mathrm{vac}} = 1\,060\,\mathrm{nm}$ in a dielectric planar waveguide consisting of a layer (ZnS) of the index of refraction, $n_f = 2.2899$, and of the thickness, $h = 1\,500\,\mathrm{nm}$, sandwiched between an overlayer (air) of the index of refraction, $n_c = 1.0$ and a substrate (glass) of the index of refraction, $n_s = 1.5040$. The results of the graphical solution to the eigenvalue equation (2.40b) in Figures 2.13 and 2.14 are expressed in terms of the "zig-zag" angle θ_f spanned by the propagation vector and the normal to the interfaces and in terms of the waveguide index, $N = n_f \sin\theta_f$.

ν	0	1	2	3	4
θ_f	81.4°	72.8°	63.7°	54.2°	44.3°
N	2.264	2.187	2.053	1.857	1.599

2.3 Modal dispersion

In a planar waveguide with a step like profile of the index of refraction, the central region (film) is characterized by a uniform real index of refraction. The waves propagate along the film as a sequence of total internal reflections at the film interfaces. The guided waves of the same frequency may travel with different angles with respect to the interface normal (greater than the critical angle for the total internal reflection). Because of the uniform index of refraction in the film region, the waves travel different paths and also different optical paths defined as a product of the geometrical path and the (uniform) index of refraction. The optical paths for the waves traveling with the propagation vectors of different inclinations and different angles of incidence are different. The waves traveling at the angle of incidence close to the critical angle propagate with a nearly maximum number of total reflections per unit length on the waveguide axis (conventionally parallel to the Cartesian z axis) travel the longest path. On the other hand, the waves traveling with the propagation vector close to the waveguide axis (close to the glancing incidence angle) propagate with the shortest path. A fixed point on the waveguide axis is reached by former waves in a longer time interval than by the latter waves. The incident rectangular pulse formed by modes traveling with different velocities becomes distorted in a distant point on the axis. The phenomenon, termed the modal distortion, increases with the traveled distance.

The modal distortion can be corrected by replacing the step like refractive index profile by a convenient graded profile. The best solution is represented by a profile characterized by

$$n^2(x) \;=\; n_s^2 + 2n_s\Delta n\left[\cosh\left(\frac{x}{2h}\right)\right]^{-2} \tag{2.59}$$

i.e., with a profile displaying a graded permittivity component proportional to a square of hyperbolic secant

$$\operatorname{sech} x = (\cosh x)^{-1} \tag{2.60}$$

It is distinguished by an ideal suppression of modal distortion (Figure 2.15).

A strong suppression of modal distortion is already achieved in dielectric waveguides with the central region displaying a permittivity profile proportional to the squared distance from the axis, i.e.,

$$n^2(x) = n_f^2 \left[1 - \left(\frac{x}{2h}\right)^2\right] \tag{2.61}$$

This can be appreciated from the Mc Laurin development[4] of the function

$$\begin{aligned} \operatorname{sech}\left(\frac{x}{2h}\right) &= \left[\cosh\left(\frac{x}{2h}\right)\right]^{-1} \\ &= 1 - \frac{1}{2!}\left(\frac{x}{2h}\right)^2 + \frac{5}{4!}\left(\frac{x}{2h}\right)^4 - \frac{61}{6!}\left(\frac{x}{2h}\right)^6 + \dots \end{aligned} \tag{2.62}$$

With the restriction to first terms of the development[5] of $\left[\operatorname{sech}\left(\frac{x}{2h}\right)\right]^2$

$$\left[\operatorname{sech}\left(\frac{x}{2h}\right)\right]^2 \approx 1 - \left(\frac{x}{2h}\right)^2 \tag{2.63}$$

2.4 Normalized eigenvalue equation

The eigenvalue equation for planar dielectric waveguides for TE modes (2.40a) can be transformed into a normalized form as a function of three parameters, i.e., a normalized frequency-thickness product, $V = V(\omega h)$, a normalized waveguide index, b, and an asymmetry waveguide parameter a.[6] We start from the eigenvalue equation for TE modes (2.44a) in terms of the waveguide index, N,

$$\frac{2\pi h}{\lambda_{\text{vac}}}\left(n_f^2 - N^2\right)^{1/2} - \arctan\left[\left(\frac{N^2 - n_c^2}{n_f^2 - N^2}\right)^{1/2}\right] - \arctan\left[\left(\frac{N^2 - n_s^2}{n_f^2 - N^2}\right)^{1/2}\right] = \nu\pi \tag{2.64}$$

where the effective waveguide index is related to the longitudinal propagation constant, β, by the angle of refraction, θ_f, and the index of refraction in the film, n_f. The film is

[4] $f(x) = f(0) + \frac{x}{1!}f'(0) + \frac{x^2}{2!}f''(0) + \dots + \frac{x^n}{n!}f^{(n)}(0) + \dots$

[5] $\frac{\mathrm{d}\,(\cosh x)^{(2n)}}{\mathrm{d}x} = \cosh x\,,\ \frac{\mathrm{d}\,(\cosh x)^{(2n-1)}}{\mathrm{d}x} = \sinh x\,,\ n = 1, 2, 3, \dots$.

[6] Herwig Kogelnik, *Theory of Dielectric Waveguides* in Integrated Optics, Editor: Theodor Tamir, Topics in Applied Physics, Vol. 7, Springer Verlag, Berlin, Heidelberg, New York, 1975.

sandwiched between the half spaces characterized by the indices of refraction n_c (cover) and n_s (substrate) restricted to $n_f > n_s \geq n_c$,

$$\beta = N\frac{\omega}{c} \tag{2.65a}$$

$$N = n_f \sin\theta_f \tag{2.65b}$$

$$n_s < N < n_f \tag{2.65c}$$

in agreement with Eqs. (2.42) and (2.48). The normalized frequency ω and thickness, h, product, so called V number is defined as

$$V = \frac{\omega h}{c}\left(n_f^2 - n_s^2\right)^{1/2} = \frac{2\pi h}{\lambda_{\text{vac}}}\left(n_f^2 - n_s^2\right)^{1/2}, \quad 0 < V < \infty \tag{2.66a}$$

where λ_{vac} denotes the vacuum wavelength. The normalized waveguide index, b is defined as

$$b = \frac{N^2 - n_s^2}{n_f^2 - n_s^2}, \qquad 0 < b < 1 \tag{2.66b}$$

At $N \to n_s$, normalized waveguide index, $b \to 0$, and the guiding disappears. The asymmetry parameter, a, is defined as

$$a = \frac{n_s^2 - n_c^2}{n_f^2 - n_s^2}, \qquad 0 \leq a < \infty \tag{2.66c}$$

In a symmetric waveguide, where $n_s = n_c$, the asymmetry becomes zero, $a = 0$. We arrange the first term in the eigenvalue equation (2.64)

$$\begin{aligned}
\frac{2\pi h}{\lambda_{\text{vac}}}\left(n_f^2 - N^2\right)^{1/2} &= \frac{2\pi h}{\lambda_{\text{vac}}}\left(n_f^2 - N^2\right)^{1/2}\frac{\left(n_f^2 - n_s^2\right)^{1/2}}{\left(n_f^2 - n_s^2\right)^{1/2}} \\
&= \underbrace{\frac{2\pi h}{\lambda_{\text{vac}}}\left(n_f^2 - n_s^2\right)^{1/2}}_{V}\frac{\left(n_f^2 - N^2\right)^{1/2}}{\left(n_f^2 - n_s^2\right)^{1/2}} \\
&= V\,\frac{\left(n_f^2 - N^2\right)^{1/2}}{\left(n_f^2 - n_s^2\right)^{1/2}} \\
&= V\,\frac{\left[n_f^2 - n_s^2 - \left(N^2 - n_s^2\right)\right]^{1/2}}{\left(n_f^2 - n_s^2\right)^{1/2}} \\
&= V\left[\left(\frac{n_f^2 - n_s^2}{n_f^2 - n_s^2}\right) - \left(\frac{N^2 - n_s^2}{n_f^2 - n_s^2}\right)\right]^{1/2} \\
&= V\left(1 - b\right)^{1/2}
\end{aligned} \tag{2.67a}$$

The second term in the eigenvalue equation (2.64) can be put in the form

$$-\arctan\left[\left(\frac{N^2-n_s^2}{n_f^2-N^2}\right)^{1/2}\right] = -\arctan\left\{\left[\frac{\dfrac{N^2-n_s^2}{n_f^2-n_s^2}}{\dfrac{n_f^2-n_s^2-(N^2-n_s^2)}{n_f^2-n_s^2}}\right]^{1/2}\right\}$$

$$= -\arctan\left\{\left[\frac{\left(\dfrac{N^2-n_s^2}{n_f^2-n_s^2}\right)}{1-\left(\dfrac{N^2-n_s^2}{n_f^2-n_s^2}\right)}\right]^{1/2}\right\}$$

$$= -\arctan\left[\left(\frac{b}{1-b}\right)^{1/2}\right] \tag{2.67b}$$

The third term in the eigenvalue equation (2.64) is transformed to

$$-\arctan\left[\left(\frac{N^2-n_c^2}{n_f^2-N^2}\right)^{1/2}\right] = -\arctan\left\{\left[\frac{\dfrac{N^2-n_s^2+(n_s^2-n_c^2)}{n_f^2-n_s^2}}{\dfrac{n_f^2-n_s^2-(N^2-n_s^2)}{n_f^2-n_s^2}}\right]^{1/2}\right\}$$

$$= -\arctan\left\{\left[\frac{\left(\dfrac{N^2-n_s^2}{n_f^2-n_s^2}\right)+\left(\dfrac{n_s^2-n_c^2}{n_f^2-n_s^2}\right)}{\left(\dfrac{n_f^2-n_s^2}{n_f^2-n_s^2}\right)-\left(\dfrac{N^2-n_s^2}{n_f^2-n_s^2}\right)}\right]^{1/2}\right\}$$

$$= -\arctan\left[\left(\frac{b+a}{1-b}\right)^{1/2}\right] \tag{2.67c}$$

After the substitutions according to Eqs. (2.67), Eq. (2.64) can be transformed into the normalized form

$$V\,(1-b)^{1/2} = \nu\pi + \arctan\left[\left(\frac{b}{1-b}\right)^{1/2}\right] + \arctan\left[\left(\frac{b+a}{1-b}\right)^{1/2}\right] \tag{2.68}$$

The cut-off frequency or thickness follows from $b \to 0$ $(N \to n_s)$. According to Eq. (2.68), the cut-off frequecy/thickness of the fundamental mode, $\nu = 0$, becomes

$$V_0 = \arctan\,(a)^{1/2} \leq \frac{\pi}{2} \approx 1,5708 \tag{2.69}$$

With the help of Eq. (2.66a) we get

$$V_0 = \frac{[\omega h]_0}{c}\left(n_f^2-n_s^2\right)^{1/2} = 2\pi\left[\frac{h}{\lambda_{\mathrm{vac}}}\right]_0\left(n_f^2-n_s^2\right)^{1/2} = \arctan\,(a)^{1/2} \tag{2.70}$$

where V_0, resp. $[\omega h]_0$, and $\left[\dfrac{h}{\lambda_{\text{vac}}}\right]_0$ are the cut-off values of the parameters for the fundamental mode, $\nu = 0$, i.e., the cut-off values of the V-number, cut-off (i.e., the lowest) value of the thickness, h, the cut-off (i.e., the lowest) value of frequency, ω, or the cut-off (i.e., the highest) value of the vacuum wavelength, λ_{vac}. It follows

$$2\pi \left[\frac{h}{\lambda_{\text{vac}}}\right]_0 \left(n_f^2 - n_s^2\right)^{1/2} \;=\; \arctan\left(\frac{n_s^2 - n_c^2}{n_f^2 - n_s^2}\right)^{1/2} \tag{2.71}$$

The cut-off frequency and thickness correspond to $b = 0$ $(N \to n_s)$. For higher mode orders, $\nu > 0$, we get according to Eq. (2.68),

$$V_\nu \;=\; \nu\pi + \arctan(a)^{1/2} \;=\; \nu\pi + V_0 \leq \nu\pi + \frac{\pi}{2}. \tag{2.72}$$

At high orders, $\nu \gg 1$, V_0 becomes negligible,

$$V_\nu \;\approx\; \nu\pi \tag{2.73}$$

The number of allowed waveguide modes increases with the mode frequency and with the film thickness. Consequently, the number of allowed waveguide modes increases with V, according to Eq. (2.66a), at a fixed $\left(n_f^2 - n_s^2\right)$,

$$\nu \;\approx\; \frac{V_\nu}{\pi} \;=\; \left(\frac{2h}{\lambda_{\text{vac}}}\right)_\nu \left(n_f^2 - n_s^2\right)^{1/2} \tag{2.74}$$

Note that V number given by Eq. (2.66a) can be expressed in terms of the ratio of the thickness, h, to the minimum penetration depth at the film - substrate interface, $\delta_{\min}^{(fs)}$. The penetration depth is given by Eq. (2.24). Its minimum occurs at $\theta_f \to \pi/2$),

$$\begin{aligned}\delta_{\min}^{(fs)} \;&=\; \lim_{\theta_f \to \pi/2} \delta^{(fs)} = \lim_{\theta_f \to \pi/2} \frac{\lambda_{\text{vac}}}{2\pi\left(n_f^2 \sin^2\theta_f - n_s^2\right)^{1/2}} \\ &=\; \frac{\lambda_{\text{vac}}}{2\pi\left(n_f^2 - n_s^2\right)^{1/2}}\end{aligned} \tag{2.75}$$

Equation (2.75) provides for V number

$$V \;=\; \frac{2\pi h}{\lambda_{\text{vac}}}\left(n_f^2 - n_s^2\right)^{1/2} = \frac{h}{\delta_{\min}^{(fs)}} \tag{2.76}$$

2.5 Goos – Hänchen shift

So far, we have considered the waveguiding in terms of plane waves characterized by their propagation vector and their phase. We now include the analysis of energy flow using the notion of ray.[7] The orientation of a ray coincides with that of a Poynting vector, $\boldsymbol{S}$, associated with a wave bundle. A ray orientation can be understood as an axis of the corresponding wave bundle. The propagation vector is characterized by the wave phase velocity while the Pointing vector, $\boldsymbol{S}$, is related to the group velocity. For a plane wave in unbound isotropic medium, $\boldsymbol{k}$ and $\boldsymbol{S}$ are parallel with the same orientation. In general, this is not true in anisotropic media and, in certain cases at the interfaces of isotropic media. At total internal reflection at the interface of two dielectrics, $\boldsymbol{k}$ and the mean value of $\langle \boldsymbol{S} \rangle$ are perpendicular to each other and the reflected ray is shifted with respect to the incident ray. The phenomenon is called the Goose – Hänchen shift. Here we consider the Goose – Hänchen shift suffered by waveguide modes at the waveguide interfaces characterized by a guide index N. Here N represent the solution either to the eigenvalue equation (2.44a) for TE modes or that to the eigenvalue equation (2.44b) for TM modes.

2.5.1 Nonmagnetic media

We consider incidence of a ray on the interface of dielectrics characterized by different electric permittivities ($\varepsilon_f \neq \varepsilon_s$) while their magnetic permeabilities are equal ($\mu_f = \mu_s = \mu$) at the angles of incidence θ_f exceeding the critical angle $\theta_f > \theta_f^{(\text{crit})}$ where $\theta_f^{(\text{crit})} = \arcsin(n_s/n_f)$. Then $\dfrac{\varepsilon_f \mu}{\varepsilon_{\text{vac}} \mu_{\text{vac}}} = n_f^2$ and $\dfrac{\varepsilon_s \mu}{\varepsilon_{\text{vac}} \mu_{\text{vac}}} = n_s^2$. For the sake of simplicity, we replace a Gaussian wave bundle by a sum of two plane waves. The orientation of their propagation vectors differs by a small angle (Figure 2.16). The angular difference affects the longitudinal propagation constant $\beta = (\omega/c)N$ and can be expressed as,

$$\Delta\beta = \frac{\omega}{c} n_f \, \Delta(\sin\theta_f) = \frac{\omega}{c} \, \Delta N \tag{2.77}$$

The interface is set to the plane $x = 0$. The electric field of the incident ray, E_i, in the plane $x = 0$ is given by a sum of electric wave fields of unit amplitudes with slightly different propagation vectors with $\beta + \Delta\beta$ and $\beta - \Delta\beta$

$$\begin{aligned} E_i &= \exp[-\mathrm{j}(\beta + \Delta\beta) z] + \exp[-\mathrm{j}(\beta - \Delta\beta) z] \\ &= 2\cos(\Delta\beta\, z) \exp(-\mathrm{j}\beta z) \end{aligned} \tag{2.78}$$

The maximum of E_i is situated at $z = 0$. The difference in angles of incidence will result in different phase shifts at total internal reflection. For TE waves, we have, according to Eq. (2.32a), pertinent to the interface between a film, f, and a substrate, s, a phase half shift

$$\phi_{fs}^{(\text{TE})} = \arctan \frac{\left(n_f^2 \sin^2\theta_f - n_s^2\right)^{1/2}}{n_f \cos\theta_f} \tag{2.79}$$

[7] Herwig Kogelnik, *Theory of Dielectric Waveguides* in Integrated Optics, Editor: Theodor Tamir, Topics in Applied Physics, Vol. 7, Springer Verlag, Berlin, Heidelberg, New York, 1975, p.25.

Equation (2.65) for $\phi_{fs}^{(\mathrm{TE})}$ can be expressed either in terms of β or N

$$\begin{aligned}\phi_{fs}^{(\mathrm{TE})} &= \arctan\left[\frac{\left(N^2-n_s^2\right)^{1/2}}{\left(n_f^2-N^2\right)^{1/2}}\right] = \arctan\left[\frac{\left(\frac{\omega}{c}\right)\left(N^2-n_s^2\right)^{1/2}}{\left(\frac{\omega}{c}\right)\left(n_f^2-N^2\right)^{1/2}}\right] \\ &= \arctan\left\{\left[\frac{\beta^2-\left(\frac{\omega}{c}\right)^2 n_s^2}{\left(\frac{\omega}{c}\right)^2 n_f^2-\beta^2}\right]^{1/2}\right\}\end{aligned} \tag{2.80}$$

A development of $\phi_{fs}^{(\mathrm{TE})}$ into a Taylor series up to the linear term gives

$$\begin{aligned}\phi_{fs}^{(\mathrm{TE})}(\beta\pm\Delta\beta) &= \phi_{fs}^{(\mathrm{TE})}(\beta)\pm\left[\frac{\mathrm{d}}{\mathrm{d}\beta}\phi_{fs}^{(\mathrm{TE})}(\beta)\right]_{\beta}\Delta\beta \\ &= \phi_{fs}^{(\mathrm{TE})}(\beta)\pm\Delta\left[\phi_{fs}^{(\mathrm{TE})}(\beta)\right]\end{aligned} \tag{2.81}$$

The electric field of the totally reflected ray in the interface plane $x=0$, includes the phase shift $2\phi_{fs}^{(\mathrm{TE})}(\beta\pm\Delta\beta)$ of the sum of two plane waves

$$\begin{aligned}E_r &= \exp\left[-\mathrm{j}\left(\beta+\Delta\beta\right)z+\mathrm{j}2\left(\phi_{fs}^{(\mathrm{TE})}+\Delta\phi_{fs}^{(\mathrm{TE})}\right)\right] \\ &+ \exp\left[-\mathrm{j}\left(\beta-\Delta\beta\right)z+\mathrm{j}2\left(\phi_{fs}^{(\mathrm{TE})}-\Delta\phi_{fs}^{(\mathrm{TE})}\right)\right] \\ &= \exp\left[-\mathrm{j}\left(\beta z-2\phi_{fs}^{(\mathrm{TE})}\right)\right] \\ &\quad\times\left\{\exp\left[-\mathrm{j}\left(\Delta\beta z-2\Delta\phi_{fs}^{(\mathrm{TE})}\right)\right]+\exp\left[\mathrm{j}\left(\Delta\beta z-2\Delta\phi_{fs}^{(\mathrm{TE})}\right)\right]\right\} \\ &= 2\exp\left[-\mathrm{j}\left(\beta z-2\phi_{fs}^{(\mathrm{TE})}\right)\right]\cos\left(\Delta\beta z-2\Delta\phi_{fs}^{(\mathrm{TE})}\right)\end{aligned} \tag{2.82}$$

The maximum of E_r is situated at a distance $z_{\max}^{(\mathrm{TE})}$ from the origin on the z axis and remains in the plane $x=0$,

$$\Delta\beta\, z_{\max}^{(\mathrm{TE})}-2\,\Delta\phi_{fs}^{(\mathrm{TE})} = 0 \tag{2.83}$$

We define the distance $z_{\max}^{(\mathrm{TE})}=2z_s^{(\mathrm{TE})}$. From Eq. (2.83) it follows

$$z_{\max}^{(\mathrm{TE})}=2z_s^{(\mathrm{TE})} = \frac{2\Delta\phi_{fs}^{(\mathrm{TE})}}{\Delta\beta}\approx 2\frac{\mathrm{d}}{\mathrm{d}\beta}\phi_{fs}^{(\mathrm{TE})} = 2\frac{c}{\omega}\frac{\mathrm{d}}{\mathrm{d}N}\phi_{fs}^{(\mathrm{TE})} \tag{2.84}$$

After som algebra

$$\begin{aligned}
\frac{\mathrm{d}}{\mathrm{d}N}\phi_{fs}^{(\mathrm{TE})} &= \frac{\mathrm{d}}{\mathrm{d}N}\ \arctan\left[\left(\frac{N^2-n_s^2}{n_f^2-N^2}\right)^{1/2}\right] \\
&= \frac{1}{1+\dfrac{\left(N^2-n_s^2\right)}{\left(n_f^2-N^2\right)}}\frac{1}{2}\left(\frac{n_f^2-N^2}{N^2-n_s^2}\right)^{1/2}\frac{2N\left(n_f^2-N^2\right)+2N\left(N^2-n_s^2\right)}{\left(n_f^2-N^2\right)^2} \\
&= \frac{n_f^2-N^2}{\left(n_f^2-n_s^2\right)}\left(\frac{n_f^2-N^2}{N^2-n_s^2}\right)^{1/2}\frac{N\left(n_f^2-n_s^2\right)}{\left(n_f^2-N^2\right)^2} = \left(\frac{n_f^2-N^2}{N^2-n_s^2}\right)^{1/2}\frac{N}{\left(n_f^2-N^2\right)} \\
&= \frac{N}{\left[\left(N^2-n_s^2\right)\left(n_f^2-N^2\right)\right]^{1/2}} \\
&= \frac{n_f\sin\theta_f}{\left(N^2-n_s^2\right)^{1/2}n_f\cos\theta_f} \\
&= \frac{\tan\theta_f}{\left(N^2-n_s^2\right)^{1/2}}\,,
\end{aligned} \tag{2.85}$$

where,

$$\tan\theta_f = \frac{N}{\left(n_f^2-N^2\right)^{1/2}} \tag{2.86}$$

The half distance between the incident and reflected rays, $z_s^{(\mathrm{TE})}$ in Eq. (2.84) becomes, with the help of Eq. (2.85),

$$\begin{aligned}
z_s^{(\mathrm{TE})} &= \frac{c}{\omega}\frac{\mathrm{d}\phi_{fs}^{(\mathrm{TE})}}{\mathrm{d}N} \\
&= \frac{\tan\theta_f}{\dfrac{\omega}{c}\left(N^2-n_s^2\right)^{1/2}}
\end{aligned} \tag{2.87}$$

An intersection of the axes of incident and reflected rays is found in the depth $x_s^{(\mathrm{TE})}$. For $\tan\theta_f$ we further have,

$$\tan\theta_f = \frac{z_s^{(\mathrm{TE})}}{x_s^{(\mathrm{TE})}}\,, \tag{2.88}$$

i.e.,

$$z_s^{(\mathrm{TE})} = x_s^{(\mathrm{TE})}\tan\theta_f \tag{2.89}$$

The distance, $2z_s^{(\mathrm{TE})}$ between the intersection of the axis of incident ray with the z axis and the intersection of the axis of reflected ray with the z axis is called Goose – Hänchen for TE polarization.

We get, after the elimination of $z_s^{(\mathrm{TE})}$ and $\tan\theta_f$ using Eqs. (2.87) and (2.88),

$$\begin{aligned} x_s^{(\mathrm{TE})} &= \frac{1}{\dfrac{\omega}{c}\left(N^2 - n_s^2\right)^{1/2}} = \frac{1}{\dfrac{\omega}{c}\left(n_f^2 \sin^2\theta_f - n_s^2\right)^{1/2}} \\ &= \frac{\lambda_{\mathrm{vac}}}{2\pi\left(n_f^2 \sin^2\theta_f - n_s^2\right)^{1/2}} \end{aligned} \tag{2.90}$$

which represents the penetration depth into the substrate for TE waves (at the same magnetic permeabilities in the film and in the substrate, $\mu_f = \mu_s$), according to Eq. (2.24).

The Goose – Hänchen shift at the interface between the film and the surrounding (substrate) dielectrics of a lower index of refraction, evaluated as $2z_s$, and the wave penetration into the surrounding dielectrics, x_s, increase with a decreasing difference in indices of refraction, $n_f - n_s$, as demonstrated in Figures 2.16 and 2.17.

2.5.2 Magnetic media

We consider incidence of a ray on the interface of dielectrics characterized by different electric permittivities ($\varepsilon_f \neq \varepsilon_s$) once more, now in a more general case where their magnetic permeabilities are different ($\mu_f \neq \mu_s$) at the angles of incidence θ_f exceeding the critical angle $\theta_f > \theta_f^{(\mathrm{crit})}$ where $\theta_f^{(\mathrm{crit})} = \arcsin(n_s/n_f)$ for $\dfrac{\varepsilon_f\mu_f}{\varepsilon_{\mathrm{vac}}\mu_{\mathrm{vac}}} = n_f^2$ and $\dfrac{\varepsilon_s\mu_s}{\varepsilon_{\mathrm{vac}}\mu_{\mathrm{vac}}} = n_s^2$. For the sake of simplicity, we replace a Gaussian wave bundle by a sum of two plane waves. The orientation of their propagation vectors differs by a small angle (Figure 2.16). As in Eq. (2.77), the angular difference will affect the longitudinal propagation constant $\beta = (\omega/c)N$ and will be expressed as,

$$\Delta\beta = \frac{\omega}{c} n_f\,\Delta(\sin\theta_f) = \frac{\omega}{c}\,\Delta N \tag{2.91}$$

The interface is set to the plane $x = 0$. The electric field of the incident ray, E_i, in the plane $x = 0$ is given by a sum of electric wave fields of unit amplitudes with slightly different propagation vectors with $\beta + \Delta\beta$ and $\beta - \Delta\beta$

$$\begin{aligned} E_i &= \exp\left[-\mathrm{j}\left(\beta + \Delta\beta\right)z\right] + \exp\left[-\mathrm{j}\left(\beta - \Delta\beta\right)z\right] \\ &= 2\cos\left(\Delta\beta z\right)\exp\left(-\mathrm{j}\beta z\right) \end{aligned} \tag{2.92}$$

The maximum of E_i is situated at $z = 0$. The difference in angles of incidence will result in different phase shifts at total internal reflection. For TE waves, we have, according to Eq. (2.32a), pertinent to the interface between a film, f, and a substrate, s, a half phase shift

$$\phi_{fs}^{(\mathrm{TE})} = \arctan\left[\frac{\mu_f}{\mu_s}\frac{\left(n_f^2\sin^2\theta_f - n_s^2\right)^{1/2}}{n_f\cos\theta_f}\right] \tag{2.93}$$

Equation (2.65) for $\phi_{fs}^{(\mathrm{TE})}$ can be expressed either in terms of β or N,

$$\begin{aligned}
\phi_{fs}^{(\mathrm{TE})} &= \arctan\left[\frac{\mu_f}{\mu_s}\frac{\left(N^2-n_s^2\right)^{1/2}}{\left(n_f^2-N^2\right)^{1/2}}\right] = \arctan\left[\frac{\mu_f}{\mu_s}\frac{\left(\frac{\omega}{c}\right)\left(N^2-n_s^2\right)^{1/2}}{\left(\frac{\omega}{c}\right)\left(n_f^2-N^2\right)^{1/2}}\right] \\
&= \arctan\left\{\frac{\mu_f}{\mu_s}\left[\frac{\beta^2-\left(\frac{\omega}{c}\right)^2 n_s^2}{\left(\frac{\omega}{c}\right)^2 n_f^2-\beta^2}\right]^{1/2}\right\}
\end{aligned} \tag{2.94}$$

A development of $\phi_{fs}^{(\mathrm{TE})}$ into a Taylor series up to the linear term gives

$$\begin{aligned}
\phi_{fs}^{(\mathrm{TE})}(\beta\pm\Delta\beta) &= \phi_{fs}^{(\mathrm{TE})}(\beta)\pm\left[\frac{\mathrm{d}}{\mathrm{d}\beta}\phi_{fs}^{(\mathrm{TE})}(\beta)\right]_\beta \Delta\beta \\
&= \phi_{fs}^{(\mathrm{TE})}(\beta)\pm\Delta\left[\phi_{fs}^{(\mathrm{TE})}(\beta)\right]
\end{aligned} \tag{2.95}$$

The electric field of the totally reflected ray in the interface plane $x=0$, includes the phase shift $2\phi_{fs}^{(\mathrm{TE})}(\beta\pm\Delta\beta)$ of the sum of two plane waves. It is of the same form as in Eq. (2.82),

$$\begin{aligned}
E_r &= \exp\left[-\mathrm{j}(\beta+\Delta\beta)z+\mathrm{j}2\left(\phi_{fs}^{(\mathrm{TE})}+\Delta\phi_{fs}^{(\mathrm{TE})}\right)\right] \\
&\quad+\exp\left[-\mathrm{j}(\beta-\Delta\beta)z+\mathrm{j}2\left(\phi_{fs}^{(\mathrm{TE})}-\Delta\phi_{fs}^{(\mathrm{TE})}\right)\right] \\
&= \exp\left[-\mathrm{j}\left(\beta z-2\phi_{fs}^{(\mathrm{TE})}\right)\right] \\
&\quad\times\left\{\exp\left[-\mathrm{j}\left(\Delta\beta z-2\Delta\phi_{fs}^{(\mathrm{TE})}\right)\right]+\exp\left[\mathrm{j}\left(\Delta\beta z-2\Delta\phi_{fs}^{(\mathrm{TE})}\right)\right]\right\} \\
&= 2\exp\left[-\mathrm{j}\left(\beta z-2\phi_{fs}^{(\mathrm{TE})}\right)\right]\cos\left(\Delta\beta z-2\Delta\phi_{fs}^{(\mathrm{TE})}\right).
\end{aligned} \tag{2.96}$$

The maximum of E_r is situated at a distance $z_{\max}^{(\mathrm{TE})}$ from the origin on the z axis and remains in the plane $x=0$,

$$\Delta\beta z-2\Delta\phi_{fs}^{(\mathrm{TE})} = 0 \tag{2.97}$$

We again define the distance $z_{\max}^{(\mathrm{TE})}=2z_s^{(\mathrm{TE})}$. From Eq. (2.97) it follows

$$z_{\max}^{(\mathrm{TE})}=2z_s^{(\mathrm{TE})} = \frac{2\Delta\phi_{fs}^{(\mathrm{TE})}}{\Delta\beta} \approx 2\frac{\mathrm{d}}{\mathrm{d}\beta}\phi_{fs}^{(\mathrm{TE})} = 2\frac{c}{\omega}\frac{\mathrm{d}}{\mathrm{d}N}\phi_{fs}^{(\mathrm{TE})} \tag{2.98}$$

We employ $\beta = N\,(\omega/c)$ and compute

$$
\begin{aligned}
\frac{\mathrm{d}}{\mathrm{d}N}\phi_{fs}^{(\mathrm{TE})} &= \frac{\mathrm{d}}{\mathrm{d}N}\arctan\left[\frac{\mu_f}{\mu_s}\left(\frac{N^2-n_s^2}{n_f^2-N^2}\right)^{1/2}\right] \\
&= \frac{1}{1+\dfrac{\mu_f^2}{\mu_s^2}\dfrac{\left(N^2-n_s^2\right)}{\left(n_f^2-N^2\right)}}\frac{1}{2}\frac{\mu_f}{\mu_s}\left(\frac{n_f^2-N^2}{N^2-n_s^2}\right)^{1/2}\frac{2N\left(n_f^2-N^2\right)+2N\left(N^2-n_s^2\right)}{\left(n_f^2-N^2\right)^2} \\
&= \frac{1}{\dfrac{n_f^2-N^2}{\mu_f^2}+\dfrac{N^2-n_s^2}{\mu_s^2}}\frac{N}{\mu_f\mu_s}\frac{n_f^2-n_s^2}{\left(n_f^2-N^2\right)^{1/2}\left(N^2-n_s^2\right)^{1/2}} \\
&= \frac{\mu_f\mu_s\left(n_f^2-n_s^2\right)}{\mu_s^2\left(n_f^2-N^2\right)+\mu_f^2\left(N^2-n_s^2\right)}\frac{N}{\left[\left(N^2-n_s^2\right)\left(n_f^2-N^2\right)\right]^{1/2}} \\
&= \frac{\mu_f\mu_s\left(n_f^2-n_s^2\right)}{\mu_s^2\left(n_f^2-N^2\right)+\mu_f^2\left(N^2-n_s^2\right)}\frac{n_f\sin\theta_f}{\left(N^2-n_s^2\right)^{1/2}n_f\cos\theta_f} \\
&= \frac{\mu_f\mu_s\left(n_f^2-n_s^2\right)}{\mu_s^2\left(n_f^2-N^2\right)+\mu_f^2\left(N^2-n_s^2\right)}\frac{\tan\theta_f}{\left(N^2-n_s^2\right)^{1/2}}
\end{aligned}
\tag{2.99}
$$

The half distance between the incident and reflected rays, $z_s^{(\mathrm{TE})}$ in Eq. (2.98) becomes, with the help of Eq. (2.99),

$$
\begin{aligned}
z_s^{(\mathrm{TE})} &= \frac{\mu_f\mu_s\left(n_f^2-n_s^2\right)}{\mu_s^2\left(n_f^2-N^2\right)+\mu_f^2\left(N^2-n_s^2\right)}\frac{\tan\theta_f}{\dfrac{\omega}{c}\left(N^2-n_s^2\right)^{1/2}} \\
&= \frac{\lambda_{\mathrm{vac}}}{2\pi}\frac{1}{\mu_f\mu_s}\frac{\left(n_f^2-N^2\right)+\left(N^2-n_s^2\right)}{\dfrac{n_f^2-N^2}{\mu_f^2}+\dfrac{N^2-n_s^2}{\mu_s^2}}\frac{\tan\theta_f}{\left(N^2-n_s^2\right)^{1/2}} \\
&= \frac{\lambda_{\mathrm{vac}}}{2\pi}\frac{1}{\mu_f\mu_s}\frac{\left(n_f^2-N^2\right)+\left(N^2-n_s^2\right)}{\dfrac{n_f^2-N^2}{\mu_f^2}+\dfrac{N^2-n_s^2}{\mu_s^2}}\frac{N}{\left(N^2-n_s^2\right)^{1/2}\left(n_f^2-N^2\right)^{1/2}} \\
&= \frac{\lambda_{\mathrm{vac}}}{2\pi}\frac{\left(n_f^2-N^2\right)+\left(N^2-n_s^2\right)}{\dfrac{\mu_s}{\mu_f}\left(n_f^2-N^2\right)+\dfrac{\mu_f}{\mu_s}\left(N^2-n_s^2\right)}\frac{N}{\left(N^2-n_s^2\right)^{1/2}\left(n_f^2-N^2\right)^{1/2}}
\end{aligned}
\tag{2.100a}
$$

The duality transforms $z_s^{(\mathrm{TE})}$ to $z_s^{(\mathrm{TM})}$,

$$\begin{aligned}
z_s^{(\mathrm{TM})} &= \frac{\varepsilon_f\varepsilon_s\left(n_f^2-n_s^2\right)}{\varepsilon_s^2\left(n_f^2-N^2\right)+\varepsilon_f^2\left(N^2-n_s^2\right)}\frac{\tan\theta_f}{\frac{\omega}{c}\left(N^2-n_s^2\right)^{1/2}} \\
&= \frac{\lambda_{\mathrm{vac}}}{2\pi}\frac{1}{\varepsilon_f\varepsilon_s}\frac{\left(n_f^2-N^2\right)+\left(N^2-n_s^2\right)}{\frac{n_f^2-N^2}{\varepsilon_f^2}+\frac{N^2-n_s^2}{\varepsilon_s^2}}\frac{\tan\theta_f}{\left(N^2-n_s^2\right)^{1/2}} \\
&= \frac{\lambda_{\mathrm{vac}}}{2\pi}\frac{1}{\varepsilon_f\varepsilon_s}\frac{\left(n_f^2-N^2\right)+\left(N^2-n_s^2\right)}{\frac{n_f^2-N^2}{\varepsilon_f^2}+\frac{N^2-n_s^2}{\varepsilon_s^2}}\frac{N}{\left(N^2-n_s^2\right)^{1/2}\left(n_f^2-N^2\right)^{1/2}} \\
&= \frac{\lambda_{\mathrm{vac}}}{2\pi}\frac{\left(n_f^2-N^2\right)+\left(N^2-n_s^2\right)}{\frac{\varepsilon_s}{\varepsilon_f}\left(n_f^2-N^2\right)+\frac{\varepsilon_f}{\varepsilon_s}\left(N^2-n_s^2\right)}\frac{N}{\left(N^2-n_s^2\right)^{1/2}\left(n_f^2-N^2\right)^{1/2}}
\end{aligned} \tag{2.100b}$$

In the special case where the magnetic permeability in the film is the same as in the substrate,[8] i.e., where $\mu_f=\mu_s$, we can take $\varepsilon_f=n_f^2\varepsilon_{\mathrm{vac}}$ and $\varepsilon_s=n_s^2\varepsilon_{\mathrm{vac}}$ to arrive at,

$$\begin{aligned}
z_s^{(\mathrm{TM})} &= \frac{n_f^2n_s^2\left(n_f^2-n_s^2\right)}{n_s^4\left(n_f^2-N^2\right)+n_f^4\left(N^2-n_s^2\right)}\frac{\tan\theta_f}{\frac{\omega}{c}\left(N^2-n_s^2\right)^{1/2}} \\
&= \frac{\lambda_{\mathrm{vac}}}{2\pi}\frac{\frac{1}{n_s^2}-\frac{1}{n_f^2}}{\frac{1}{n_f^2}-\frac{1}{n_s^2}-N^2\left(\frac{1}{n_f^4}-\frac{1}{n_s^4}\right)}\frac{\tan\theta_f}{\left(N^2-n_s^2\right)^{1/2}} \\
&= \frac{\lambda_{\mathrm{vac}}}{2\pi}\frac{\left(\frac{1}{n_s^2}-\frac{1}{n_f^2}\right)}{N^2\left(\frac{1}{n_s^2}-\frac{1}{n_f^2}\right)\left(\frac{1}{n_s^2}+\frac{1}{n_f^2}\right)+\left(\frac{1}{n_f^2}-\frac{1}{n_s^2}\right)}\frac{\tan\theta_f}{\left(N^2-n_s^2\right)^{1/2}} \\
&= \frac{\lambda_{\mathrm{vac}}}{2\pi}\frac{1}{N^2\left(\frac{1}{n_s^2}+\frac{1}{n_f^2}\right)-1}\frac{\tan\theta_f}{\left(N^2-n_s^2\right)^{1/2}}
\end{aligned} \tag{2.101}$$

The axes of the incident and reflected beams intersect in the substrate at the depth, $x_s^{(\mathrm{TE})}$. Alternatively, $\tan\theta_f$ can also be expressed as

$$\tan\theta_f = \frac{z_s^{(\mathrm{TE})}}{x_s^{(\mathrm{TE})}}, \tag{2.102}$$

[8] Herwig Kogelnik, *Theory of Dielectric Waveguides* in Integrated Optics, Editor: Theodor Tamir, Topics in Applied Physics, Vol. 7, Springer Verlag, Berlin, Heidelberg, New York, 1975, p. 27.

i.e.,

$$z_s^{(\mathrm{TE})} = x_s^{(\mathrm{TE})} \tan\theta_f \tag{2.103}$$

As before, the distance, $2z_s^{(\mathrm{TE})}$, spanned by the point of intersection between the incident ray axis and the z axis and the point of intersection between the reflected ray axis and the z axis represents the Goose – Hänchen shift for TE waves. Note that the z axis is restricted to the interface plane between the film and the substrate. The configuration is shown in Figure 2.16. The elimination of $z_s^{(\mathrm{TE})}$ and $\tan\theta_f$ using Eqs. (2.100) and (2.102) provides a more general expression for $x_s^{(\mathrm{TE})}$,

$$x_s^{(\mathrm{TE})} = \frac{\lambda_{\mathrm{vac}}}{2\pi}\frac{1}{\mu_f\mu_s}\frac{\left(n_f^2 - N^2\right) + \left(N^2 - n_s^2\right)}{\dfrac{n_f^2 - N^2}{\mu_f^2} + \dfrac{N^2 - n_s^2}{\mu_s^2}}\frac{1}{\left(N^2 - n_s^2\right)^{1/2}} \tag{2.104a}$$

The expression for the penetration depth, $x_s^{(\mathrm{TM})}$, for TM waves follows from the duality transformation,

$$x_s^{(\mathrm{TM})} = \frac{\lambda_{\mathrm{vac}}}{2\pi}\frac{1}{\varepsilon_f\varepsilon_s}\frac{\left(n_f^2 - N^2\right) + \left(N^2 - n_s^2\right)}{\dfrac{n_f^2 - N^2}{\varepsilon_f^2} + \dfrac{N^2 - n_s^2}{\varepsilon_s^2}}\frac{1}{\left(N^2 - n_s^2\right)^{1/2}} \tag{2.104b}$$

2.6 Effective guide thickness

2.6.1 TE polarization

The modification of Eqs. (2.90) or (2.104a) to the case of the film – cover interface provides,

$$x_c^{(\mathrm{TE})} = \frac{1}{\dfrac{\omega}{c}\left(n_f^2\sin^2\theta_f - n_c^2\right)^{1/2}} = \frac{1}{\dfrac{\omega}{c}\left(N^2 - n_c^2\right)^{1/2}} \tag{2.105}$$

We define *effective guide thickness* for TE waves, shown in Figures 2.18 and 2.19, as the sum of the physical film thickness, h, and both the penetration depths (restricted to TE waves in waveguides with $\mu_f = \mu_s = \mu_c$) given in Eqs. (2.104a) and (2.105),

$$h_{\mathrm{eff}}^{(\mathrm{TE})} = h + x_s^{(\mathrm{TE})} + x_c^{(\mathrm{TE})} \tag{2.106}$$

The Goos–Hänchen shifts on the upper and lower interface between the film and the surrounding media of lower indices of refraction, z_c and z_s, and the penetration depths into the upper (cover) and lower (substrate) media, x_c and x_s increase with decreasing the difference between the index of refraction and that in the upper or lower medium. For TE waveguide modes, the effective guide index, $N = n_f \sin\theta_f$ given Eq. (2.42) and employed in the expressions for $z_s^{(\mathrm{TE})}$ and $x_s^{(\mathrm{TE})}$ ($z_c^{(\mathrm{TE})}$ and $x_c^{(\mathrm{TE})}$) follows from the solution to Eq. (2.44a).[9] We have

$$\tan\theta_f = \frac{z_s^{(\mathrm{TE})}}{x_s^{(\mathrm{TE})}} = \frac{z_c^{(\mathrm{TE})}}{x_c^{(\mathrm{TE})}} \tag{2.107}$$

Normalized effective guide thickness for TE waves is defined as

$$\mathcal{H}^{(\mathrm{TE})} = \frac{\omega}{c} h_{\mathrm{eff}}^{(\mathrm{TE})} \left(n_f^2 - n_s^2\right)^{1/2} \tag{2.108}$$

which should be compared with the definition of the V number in Eq. (2.66a)

$$V = \frac{\omega}{c} h \left(n_f^2 - n_s^2\right)^{1/2} \tag{2.109}$$

Then

$$\frac{\mathcal{H}^{(\mathrm{TE})}}{V} = \frac{h_{\mathrm{eff}}^{(\mathrm{TE})}}{h} \tag{2.110}$$

The substitution into Eq. (2.106) with the help of Eqs. (2.90) and (2.105) and with the account of Eq. (2.108) provides

$$\begin{aligned} h_{\mathrm{eff}}^{(\mathrm{TE})} &= \frac{\mathcal{H}^{(\mathrm{TE})}}{\frac{\omega}{c}\left(n_f^2 - n_s^2\right)^{1/2}} \\ &= h + \frac{1}{\frac{\omega}{c}\left(N^2 - n_s^2\right)^{1/2}} + \frac{1}{\frac{\omega}{c}\left(N^2 - n_c^2\right)^{1/2}} \end{aligned} \tag{2.111}$$

and for $\mathcal{H}^{(\mathrm{TE})}$ we get,

$$\mathcal{H}^{(\mathrm{TE})} = \frac{\omega}{c} h \left(n_f^2 - n_s^2\right)^{1/2} + \frac{\left(n_f^2 - n_s^2\right)^{1/2}}{\left(N^2 - n_s^2\right)^{1/2}} + \frac{\left(n_f^2 - n_s^2\right)^{1/2}}{\left(N^2 - n_c^2\right)^{1/2}} \tag{2.112}$$

With help of Eqs. (2.66), it follows,

$$\mathcal{H}^{(\mathrm{TE})} = V + b^{-1/2} + (b + a)^{-1/2} \tag{2.113}$$

where b represents the solution to Eq. (2.68).

[9] For TM waveguide modes, the effective guide index, $N = n_f \sin\theta_f$ given Eq. (2.42) follow from the solution to Eq. (2.44b).

2.6.2 TM polarization

The modification of Eq. (2.104b) to the case of the film – cover interface provides

$$x_c^{(\mathrm{TM})} = \frac{\lambda_{\mathrm{vac}}}{2\pi}\frac{1}{\varepsilon_f\varepsilon_c}\frac{\left(n_f^2-N^2\right)+\left(N^2-n_c^2\right)}{\dfrac{n_f^2-N^2}{\varepsilon_f^2}+\dfrac{N^2-n_c^2}{\varepsilon_c^2}}\frac{1}{\left(N^2-n_c^2\right)^{1/2}} \tag{2.114}$$

The effective guide thickness is given by the sum of the physical film thickness, h, and the both penetration depths given by Eqs. (2.104b) and (2.114)

$$h_{\mathrm{eff}}^{(\mathrm{TM})} = h + x_s^{(\mathrm{TM})} + x_c^{(\mathrm{TM})} \tag{2.115}$$

The normalized effective guide thickness for TM waves deduced in a similar way as in Eq. (2.108) is given by the expression,

$$\mathcal{H}^{(\mathrm{TM})} = \frac{\omega}{c}h_{\mathrm{eff}}^{(\mathrm{TM})}\left(n_f^2-n_s^2\right)^{1/2} \tag{2.116}$$

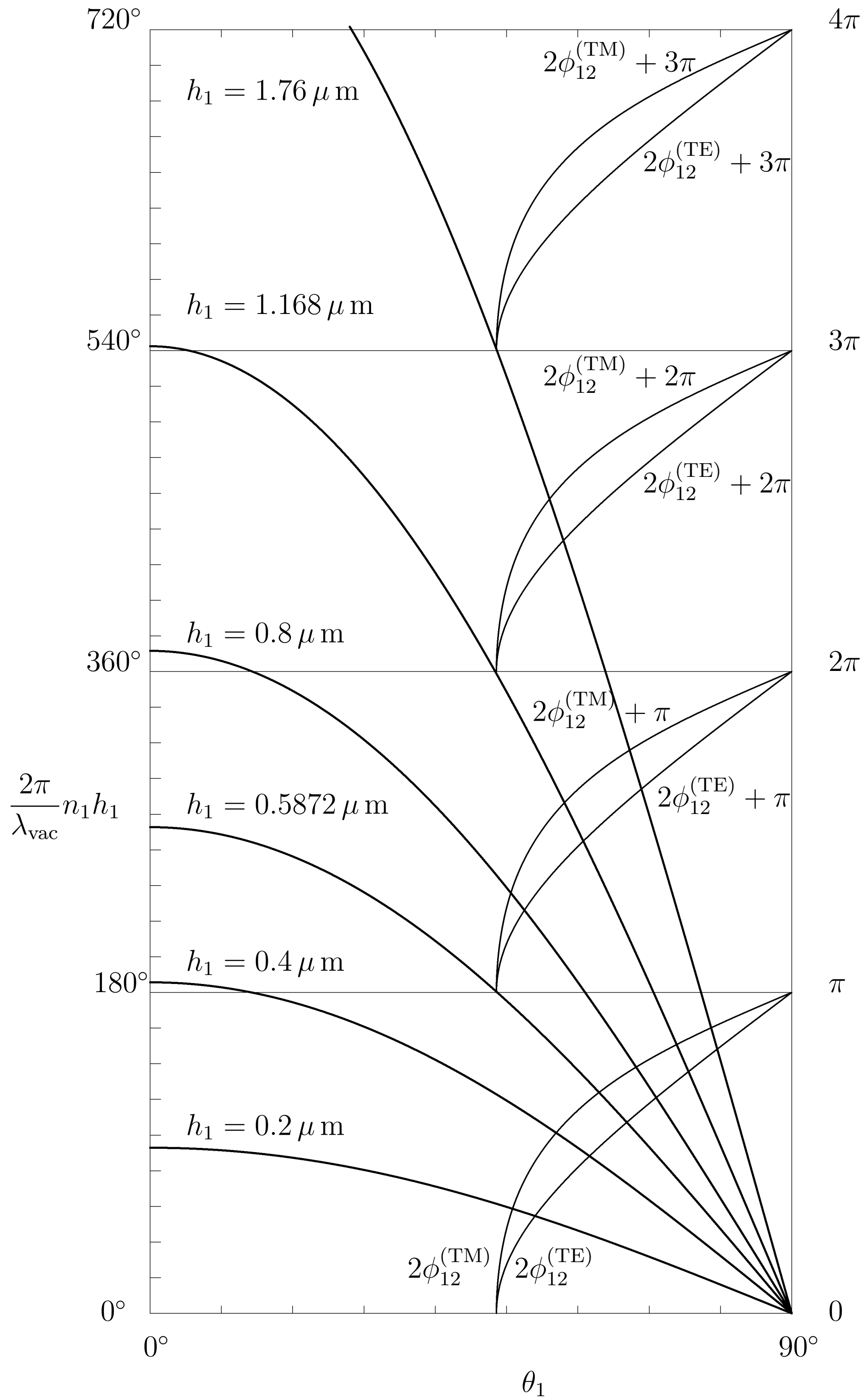

Figure 2.9: Graphical solution to the eigenvalue equation in a symmetric waveguide for mode orders $\nu \geq 0$ at the wavelength $\lambda_{\mathrm{vac}} = 1.55\,\mu$m. The planar film characterized by the thickness, h_1, and the index of refraction, $n_1 = 2.0$, is sandwiched between the same media characterized by the index of refraction, $n_2 = 1.5$. For the thickness range $h_1 \leq 0.587\,\mu$m, the waveguide is monomode, it carries the fundamental mode $\nu = 0$, only. An extension of the thickness range to $h_1 \leq 1.168\,\mu$m, enables propagation of both the fundamental mode, $\nu = 0$ and the mode of the order $\nu = 1$. A further extension to $h_1 \leq 1.76\,\mu$m, allows the propagation of modes of the order $\nu = 0$, $\nu = 1$, and $\nu = 2$. The modes of the order $\nu > 2$ are forbidden.

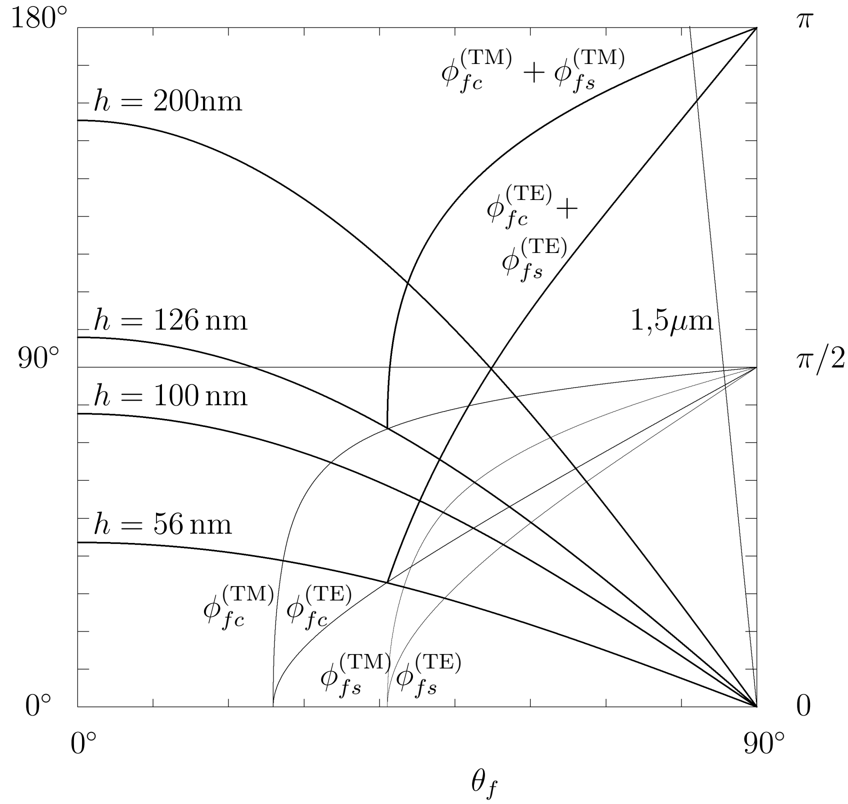

Figure 2.10: Graphical solution to the eigenvalue equation, $2\pi h n_f \cos\theta_f/\lambda_{\text{vac}} = \phi_{fc} + \phi_{fs}$, for the fundamental ($\nu = 0$) TE and TM modes in an asymmetric waveguide at the vacuum wavelength $\lambda_{\text{vac}} = 1\,060\,\text{nm}$. The waveguide consists of a planar layer (ZnS) of the index of refraction $n_f = 2.2899$ and of the thickness, h, sandwiched between the cover (air) of the index of refraction, $n_c = 1.0$, and a substrate (glass) of the index of refraction $n_s = 1.5040$. The waveguide allows the propagation of the guided TE and TM modes above the cut-off thickness, $h = 56\,\text{nm}$ and $h = 126\,\text{nm}$, respectively. After P. K. Tien, *Integrated optics and new wave phenomena in optical waveguides*, Review of Modern Physics, vol. **49**, pp. 361-420, April 1977.

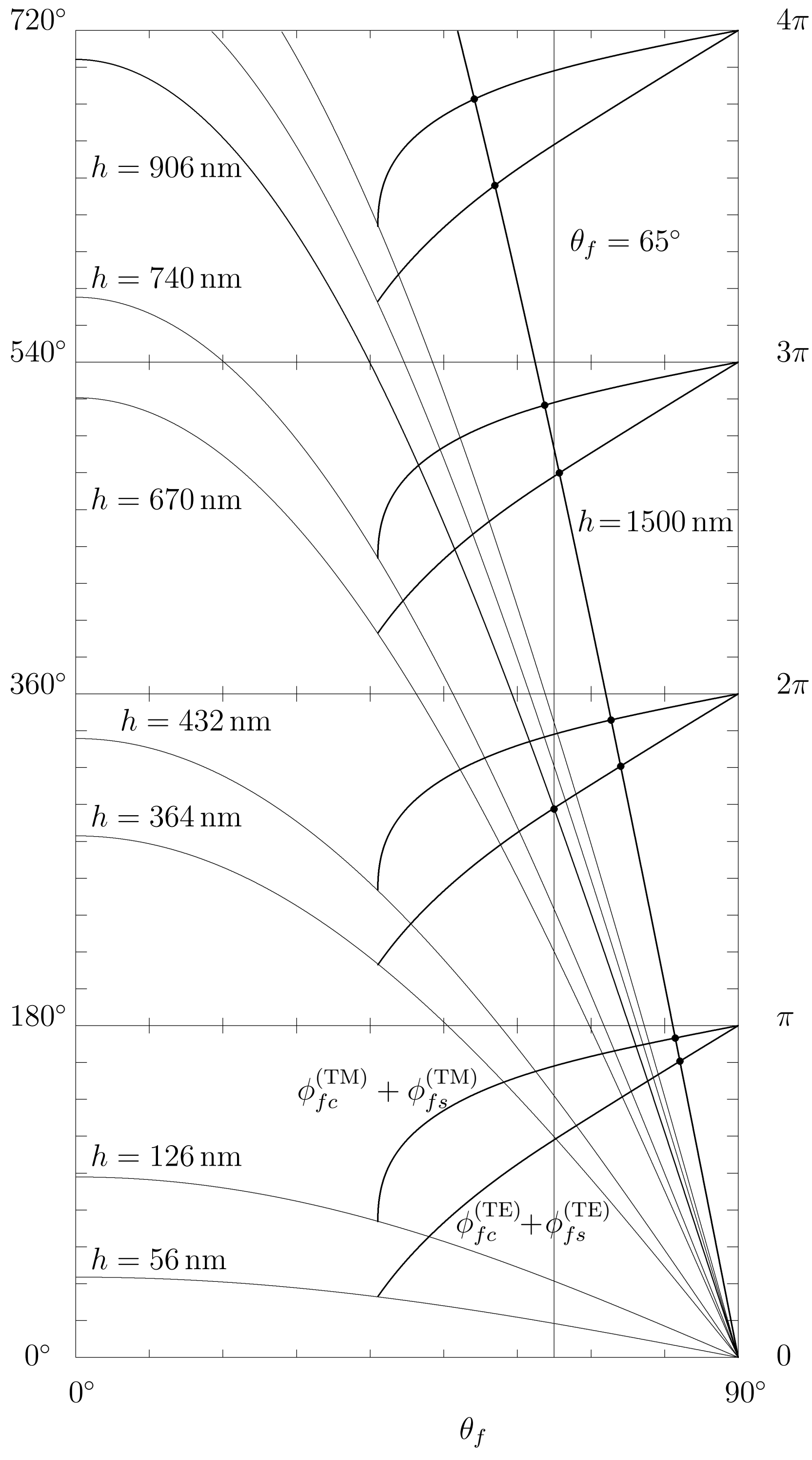

Figure 2.11: Graphical solution to the eigenvalue equation for the TE and TM modes, $\nu = 0, 1, 2, 3$, in an asymmetric waveguide at the vacuum wavelength $\lambda_{\mathrm{vac}} = 1\,060\,\mathrm{nm}$. The waveguide consists of a planar layer (ZnS) of the index of refraction $n_f = 2.2899$ and of the thickness, h, sandwiched between the cover (air) of the index of refraction, $n_c = 1.0$, and a substrate (glass) of the index of refraction $n_s = 1.5040$ for several film thicknesses, h. The vertical line indicates the TE solution for $\nu = 1$ at $\theta_f = 65°$. See Tables 2.1 and 2.2.

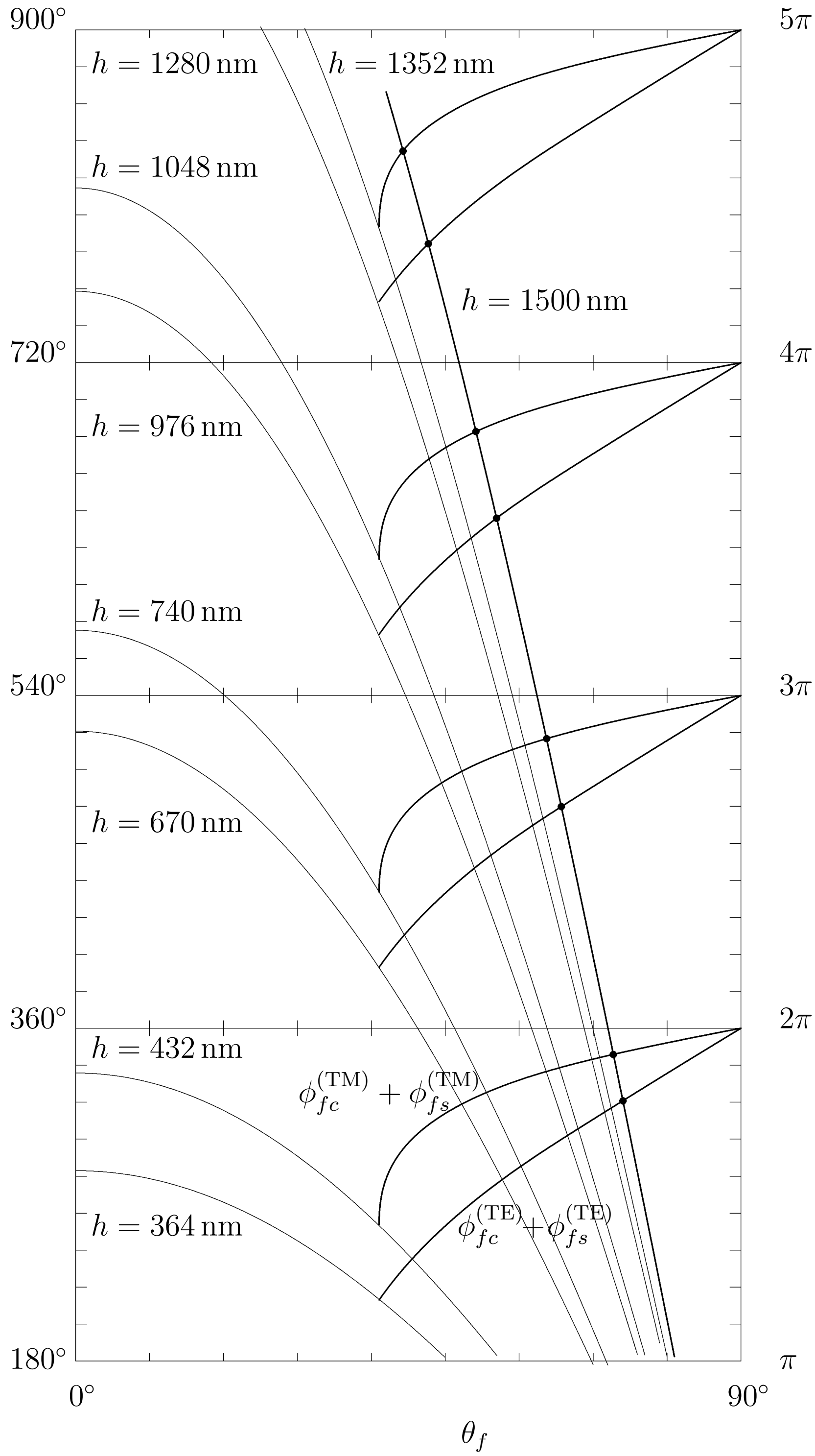

Figure 2.12: Graphical solution to the eigenvalue equation for the TE and TM modes, $\nu = 1, 2, 3, 4$, in an asymmetric waveguide at the vacuum wavelength $\lambda_{\mathrm{vac}} = 1\,060\,\mathrm{nm}$. The waveguide consists of a planar layer (ZnS) of the index of refraction $n_f = 2.2899$ and of the thickness, h, sandwiched between the cover (air) of the index of refraction, $n_c = 1.0$, and a substrate (glass) of the index of refraction $n_s = 1.5040$. See Tables 2.1 and 2.2.

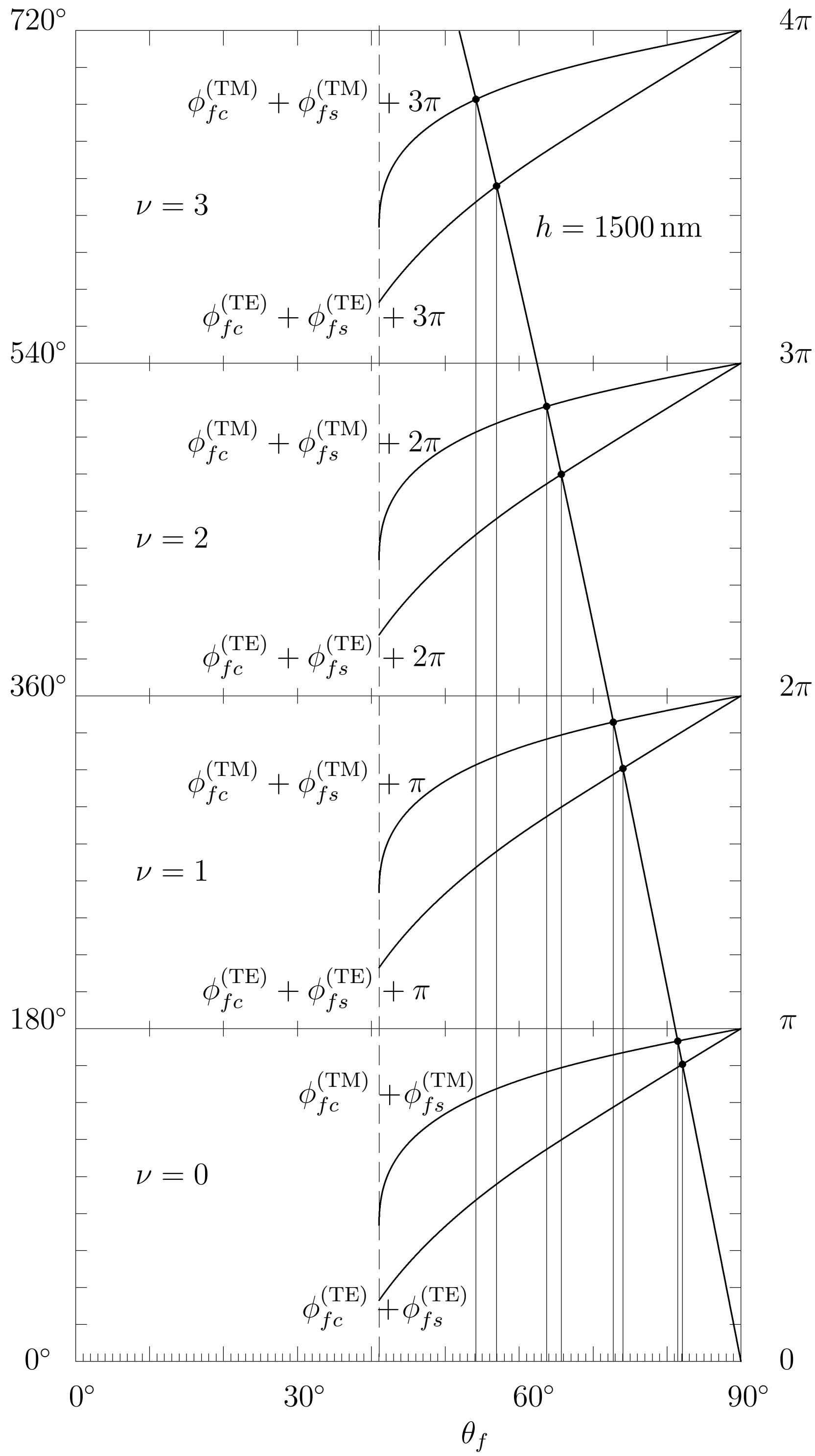

Figure 2.13: Graphical solution to the eigenvalue equation, for the TE and TM modes, $\nu = 0,\,1,\,2,\,3$, in an asymmetric waveguide at $\lambda_{\mathrm{vac}} = 1\,060\,\mathrm{nm}$. The waveguide consists of a film of the index of refraction $n_f = 2.2899$ and of the thickness, $h = 1\,500\,\mathrm{nm}$, sandwiched between a cover ($n_c = 1.0$), and a substrate ($n_s = 1.5040$). The guided TE and TM modes of the order $\nu = 0$ propagate with $\theta_f^{(TE)} = 82.1°$ and $\theta_f^{(TM)} = 81.4°$, those of the order $\nu = 1$ with $\theta_f^{(TE)} = 74.1°$ and $\theta_f^{(TM)} = 72.8°$, those of the order $\nu = 2$ with $\theta_f^{(TE)} = 65.7°$ and $\theta_f^{(TM)} = 63.7°$ and those of the order $\nu = 3$ with $\theta_f^{(TE)} = 56.9°$ and $\theta_f^{(TM)} = 54,2°$, respectively.

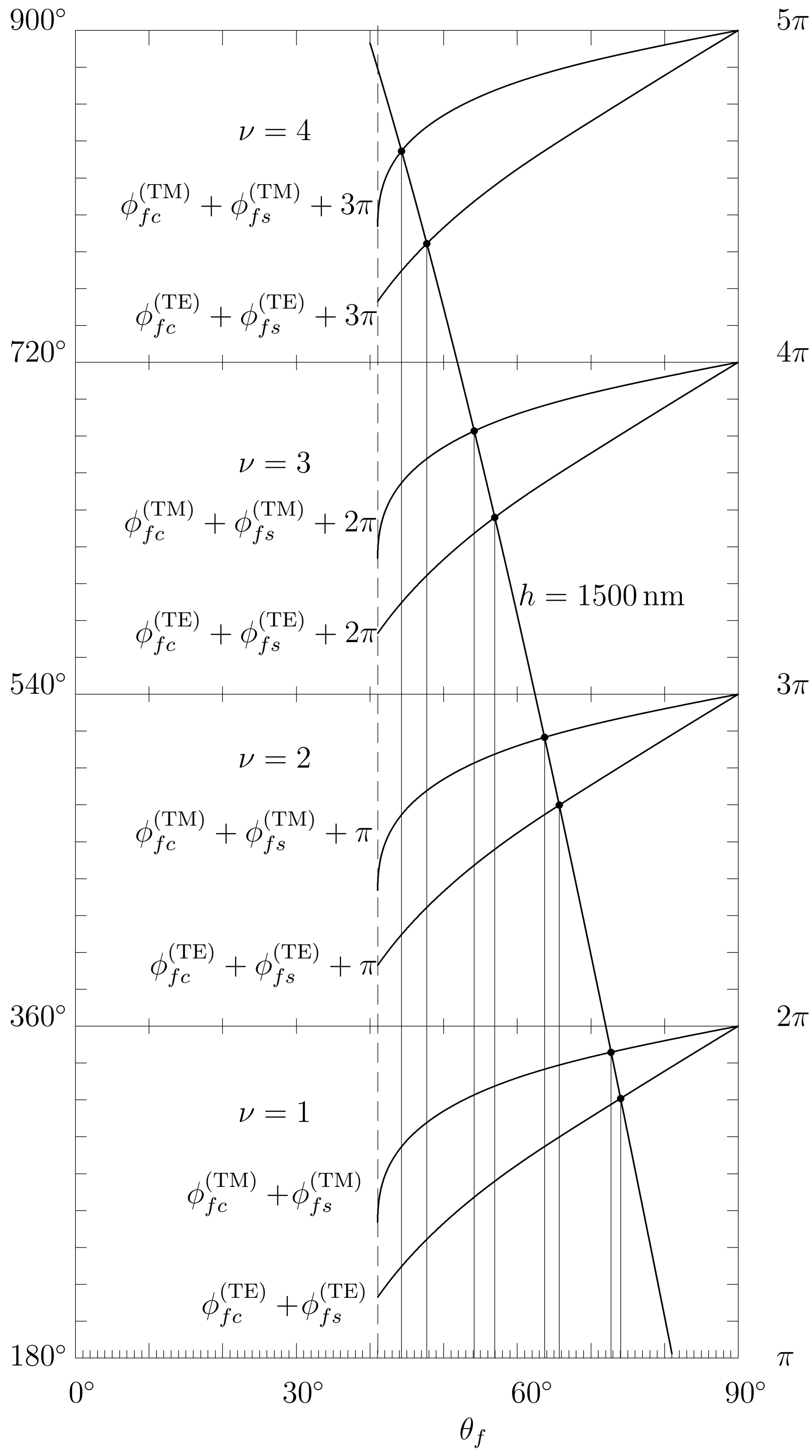

Figure 2.14: Graphical solution to the eigenvalue equation in an asymmetric waveguide at $\lambda_{\text{vac}} = 1060\,\text{nm}$. The waveguide consists of a film ($n_f = 2.2899$) of the thickness, $h = 1\,500\,\text{nm}$, sandwiched between a cover ($n_c = 1.0$), and a substrate ($n_s = 1.5040$). The guided TE and TM modes of the order $\nu = 1$ propagate with $\theta_f^{(\text{TE})} = 74,1°$ and $\theta_f^{(\text{TM})} = 72,8°$, those of the order $\nu = 2$ with $\theta_f^{(\text{TE})} = 65,7°$ and $\theta_f^{(\text{TM})} = 63,7°$, those of the order $\nu = 3$ with $\theta_f^{(\text{TE})} = 56,9°$ and $\theta_f^{(\text{TM})} = 54,2°$ and those of the order $\nu = 4$ with $\theta_f^{(\text{TE})} = 47,7°$ and $\theta_f^{(\text{TM})} = 44,3°$, respectively. See Tables 2.1 and 2.2.

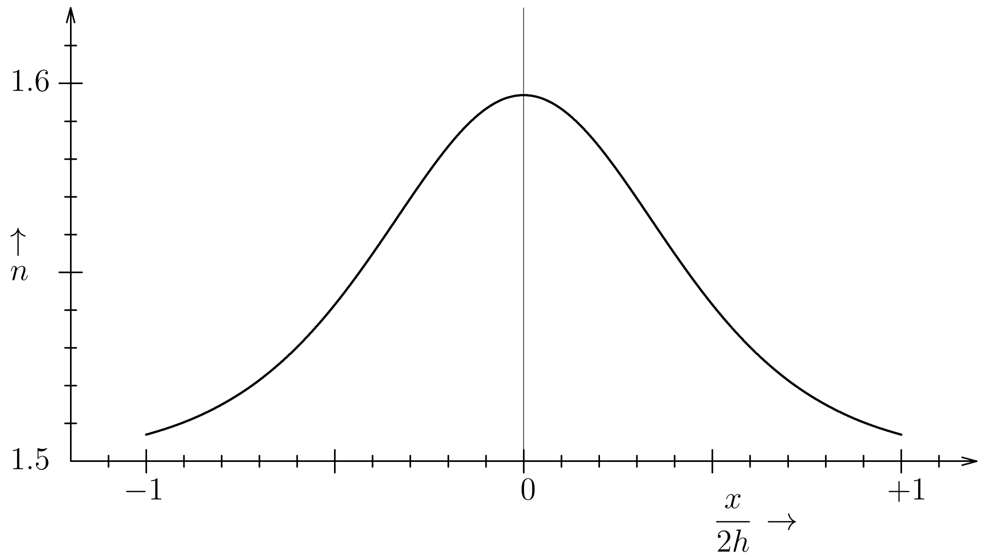

Figure 2.15: Profile of index of refraction, n , in a waveguide with suppressed modal dispersion, $n = \left\{ n_s^2 + 2 n_s \Delta n \left[\cosh\left(\frac{x}{2h}\right)\right]^{-2} \right\}^{1/2}$. Here $n_s = 1.5$ and $\Delta n = 0.1$.

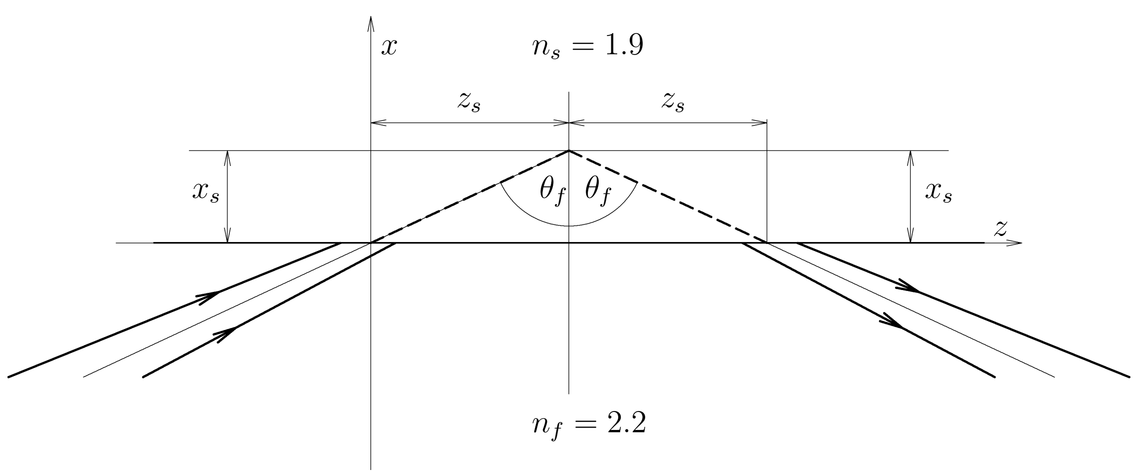

Figure 2.16: Goose – Hänchen shift for TE waves at the film - substrate interface at the vacuum wavelength 1 550 nm and at the angle of incidence, $\theta_f = 65°$. After Herwig Kogelnik, *Theory of Dielectric Waveguides* in Integrated Optics, Editor: Theodor Tamir, Topics in Applied Physics, Vol. 7, Springer Verlag, Berlin, Heidelberg, New York, 1975, p. 26.

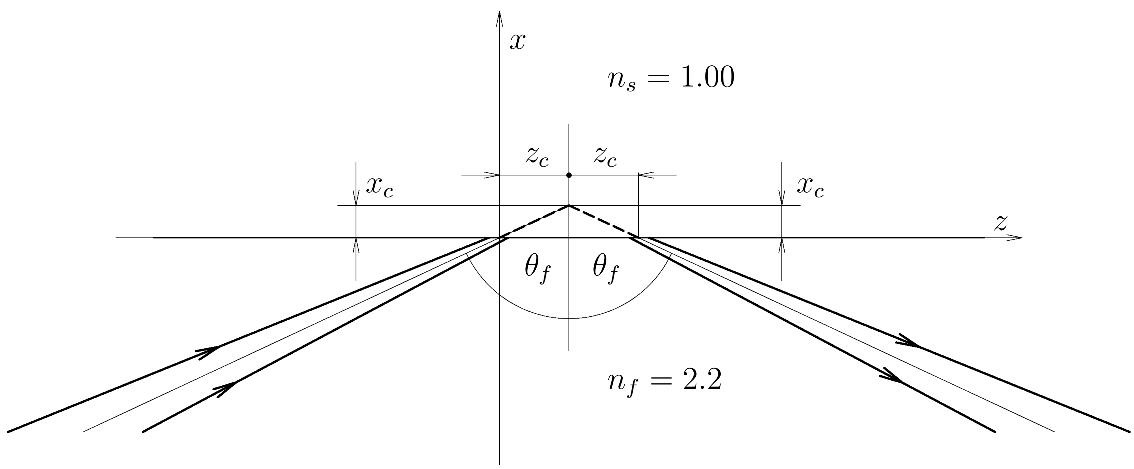

Figure 2.17: Goose – Hänchen shift for TE waves at the interface between the film and the cover (air) at the vacuum wavelength $\lambda_{\text{vac}} = 1\,550\,\text{nm}$ and at an angle of incidence $\theta_f = 65°$. After Herwig Kogelnik, *Theory of Dielectric Waveguides* in Integrated Optics, Editor: Theodor Tamir, Topics in Applied Physics, Vol. 7, Springer Verlag, Berlin, Heidelberg, New York, 1975, p. 27.

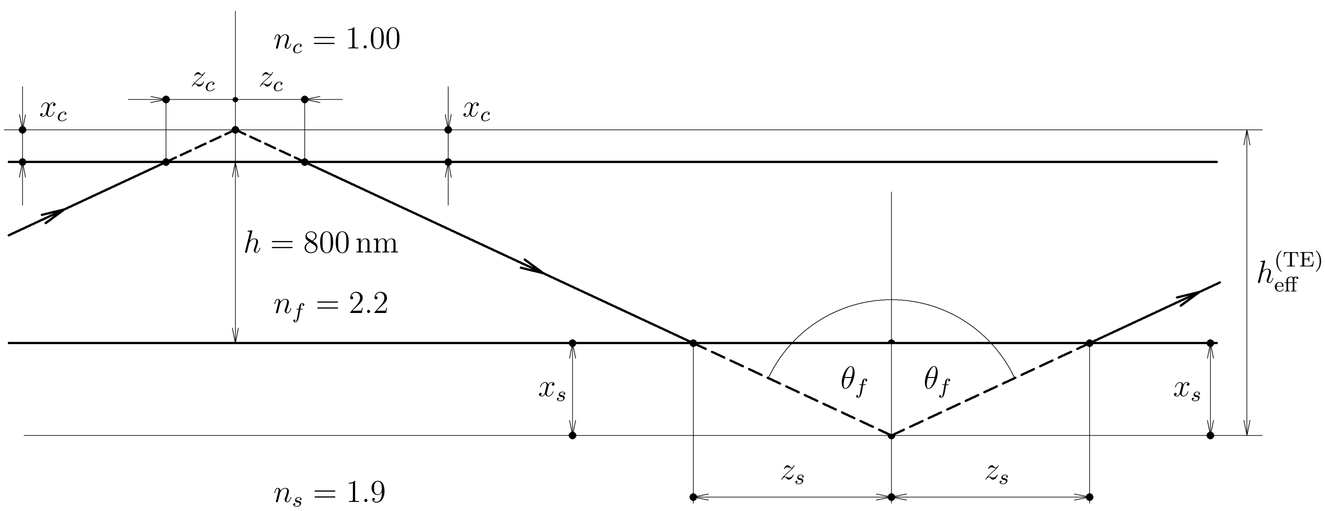

Figure 2.18: Effective guide thickness for the order $\nu = 1$ at the vacuum wavelength $\lambda_{\mathrm{vac}} = 1\,550\,\mathrm{nm}$ for TE waves at an internal angle of incidence, $\theta_f = 65°$. The waveguide consists of a planar film (BiYIG - bismuth substituted yttrium iron garnet) of the index of refraction, $n_f = 2.2$ and of the thickness $h = 800\,\mathrm{nm}$ sandwiched between the cover (air) of the index of refraction, $n_c = 1.0$ and the substrate (GGG - gadolinium gallium garnet) of the index of refraction $n_s = 1.9$. The penetration depths into the cover and into the substrate become $x_c = 143\,\mathrm{nm}$ and $x_s = 408\,\mathrm{nm}$, respectively.

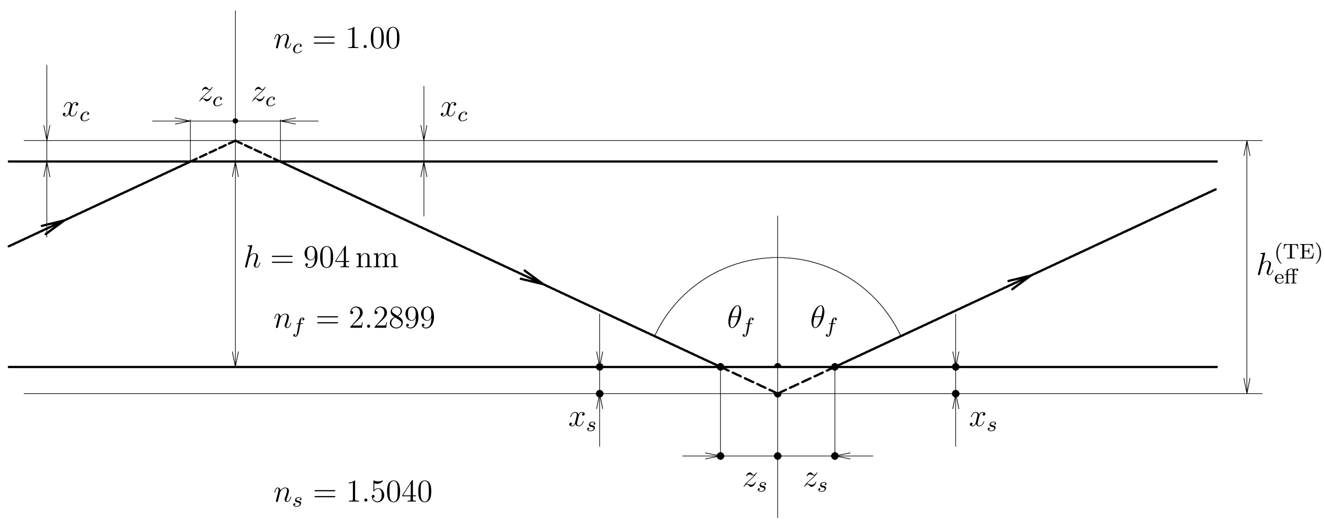

Figure 2.19: Effective guide thickness for the order $\nu = 1$ at the vacuum wavelength $\lambda_{\mathrm{vac}} = 1\,060\,\mathrm{nm}$ for TE waves at an internal angle of incidence, $\theta_f = 65^\circ$. The waveguide consists of a planar film (ZnS) of the index of refraction, $n_f = 2.2899$ and of the thickness $h = 906\,\mathrm{nm}$ sandwiched between the cover (air) of the index of refraction, $n_c = 1.0$ and the substrate (glass) of the index of refraction $n_s = 1.5040$. The penetration depths into the cover and into the substrate become $x_c = 93\,\mathrm{nm}$ and $x_s = 118\,\mathrm{nm}$, respectively. The graphical solution to the eigenvalue equation in Figure 2.11 was employed. After Herwig Kogelnik, *Theory of Dielectric Waveguides* in Integrated Optics, Editor: Theodor Tamir, Topics in Applied Physics, Vol. 7, Springer Verlag, Berlin, Heidelberg, New York, 1975.

Chapter 3

Maxwell equations

In a vacuum with a zero charge density, $\rho = 0$, and a zero current density, $\boldsymbol{J} = 0$, the electric and magnetic flux density vectors, $\boldsymbol{E}$ and $\boldsymbol{B}$, are related by Maxwell equations,[1]

$$\nabla \times \boldsymbol{E} + \frac{\partial \boldsymbol{B}}{\partial t} = 0\,, \tag{3.1a}$$

$$\nabla \times \boldsymbol{B} - \frac{1}{c^2}\frac{\partial \boldsymbol{E}}{\partial t} = 0\,. \tag{3.1b}$$

In a medium with a non zero charge density, $\rho \neq 0$, and a non zero current density, $\boldsymbol{J} \neq 0$, the Maxwell equations become

$$\nabla \times \boldsymbol{E} + \frac{\partial \boldsymbol{B}}{\partial t} = 0 \tag{3.2a}$$

$$\nabla \times \boldsymbol{B} - \mu_{\mathrm{vac}}\varepsilon_{\mathrm{vac}}\frac{\partial \boldsymbol{E}}{\partial t} = \mu_{\mathrm{vac}}\boldsymbol{J} \tag{3.2b}$$

where the vacuum phase velocity is given by $c = (\mu_{\mathrm{vac}}\varepsilon_{\mathrm{vac}})^{-1/2}$. The charge conservation (continuity equation) requiring

$$\nabla \cdot \boldsymbol{J} + \frac{\partial \varrho}{\partial t} = 0 \tag{3.3}$$

leads to the expressions for $\nabla \cdot \boldsymbol{E}$ and $\nabla \cdot \boldsymbol{B}$. Consider the identities

$$\begin{aligned} \nabla \cdot (\nabla \times \boldsymbol{E}) &\equiv 0 \\ \nabla \cdot (\nabla \times \boldsymbol{B}) &\equiv 0 \end{aligned}$$

Their use in Eqs. (3.2a) leads to

$$\nabla \cdot (\nabla \times \boldsymbol{E}) + \frac{\partial}{\partial t}(\nabla \cdot \boldsymbol{B}) = 0 \tag{3.4}$$

[1] R. Wangsness, *Electromagnetic Fields*, 2nd Edition, John Wiley & Sons, 1986, Chapter 21.

The time independent could not be generated in the infinite past. It is therefore reasonable to assume

$$\nabla \cdot \boldsymbol{B} \;=\; 0 \tag{3.5}$$

From the second Maxwell equation, Eq. (3.2b)

$$\nabla \cdot (\nabla \times \boldsymbol{B}) - \mu_{\text{vac}}\varepsilon_{\text{vac}}\frac{\partial}{\partial t}(\nabla \cdot \boldsymbol{E}) \;=\; \mu_{\text{vac}}(\nabla \cdot \boldsymbol{J}) \tag{3.6}$$

From this

$$\frac{\partial}{\partial t}\left(\nabla \cdot \boldsymbol{E} - \frac{\varrho}{\varepsilon_{\text{vac}}}\right) \;=\; 0 \tag{3.7}$$

The result is the scalar Maxwell equation representing the Coulomb law of electrostatics,

$$\nabla \cdot \boldsymbol{E} \;=\; \frac{\varrho}{\varepsilon_{\text{vac}}} \tag{3.8}$$

We decompose the total charge density, ϱ, to a free charge density component, ϱ_f, and to a bound charge density component, $\varrho_b = -\nabla \cdot \boldsymbol{P}$,

$$\varrho \;=\; \varrho_f + \varrho_b \tag{3.9}$$

The total current density can be expressed as a multipole development. With the restriction to first terms,

$$\boldsymbol{J} \;=\; \varrho_f\,\boldsymbol{v} + \frac{\partial \boldsymbol{P}}{\partial t} + \nabla \times \boldsymbol{M} + \ldots \tag{3.10}$$

After the substitution into the Maxwell equation,

$$\nabla \times \boldsymbol{B} - \frac{1}{c^2}\frac{\partial \boldsymbol{E}}{\partial t} \;=\; \mu_{\text{vac}}\varrho_f\,\boldsymbol{v} + \mu_{\text{vac}}\frac{\partial \boldsymbol{P}}{\partial t} + \mu_{\text{vac}}(\nabla \times \boldsymbol{M}) + \ldots \tag{3.11}$$

With the restriction to first few terms,

$$\mu_{\text{vac}}^{-1}\left[\nabla \times (\boldsymbol{B} - \mu_{\text{vac}}\boldsymbol{M})\right] \;=\; \varrho_f\,\boldsymbol{v} + \frac{\partial}{\partial t}(\varepsilon_{\text{vac}}\boldsymbol{E} + \boldsymbol{P}) \tag{3.12}$$

We define the magnetic field vector, $\boldsymbol{H}$,

$$\boldsymbol{H} \;=\; \mu_{\text{vac}}^{-1}(\boldsymbol{B} - \mu_{\text{vac}}\boldsymbol{M})\;, \tag{3.13}$$

the electric induction vector, $\boldsymbol{D}$,

$$\boldsymbol{D} \;=\; \varepsilon_{\text{vac}}\boldsymbol{E} + \boldsymbol{P} \tag{3.14}$$

and the free charge density vector, $\boldsymbol{J}_f$,

$$\boldsymbol{J}_f \;=\; \varrho_f\,\boldsymbol{v} \tag{3.15}$$

Consequently,

$$\begin{aligned}
\nabla \times \boldsymbol{H} &= \boldsymbol{J}_f + \frac{\partial \boldsymbol{D}}{\partial t} \\
&= \varrho_f \boldsymbol{v} + \frac{\partial \boldsymbol{P}}{\partial t} + \varepsilon_{\text{vac}} \frac{\partial \boldsymbol{E}}{\partial t} \\
&= \boldsymbol{J}_f + \boldsymbol{J}_b + \varepsilon_{\text{vac}} \frac{\partial \boldsymbol{E}}{\partial t} \\
&= \boldsymbol{J} + \varepsilon_{\text{vac}} \frac{\partial \boldsymbol{E}}{\partial t} \qquad (3.16)
\end{aligned}$$

where $\boldsymbol{J}_b = \dfrac{\partial \boldsymbol{P}}{\partial t}$ represents bound charge current density.

From the continuity equation, Eq. (3.3)

$$\nabla \cdot \boldsymbol{J} + \frac{\partial \varrho}{\partial t} = 0 \qquad (3.17)$$

$$\nabla \cdot \left(\varrho_f \boldsymbol{v} + \frac{\partial \boldsymbol{P}}{\partial t} \right) + \frac{\partial \varrho_f}{\partial t} + \frac{\partial \varrho_b}{\partial t} = 0 \qquad (3.18)$$

$$\nabla \cdot \left(\varrho_f \boldsymbol{v} + \frac{\partial \boldsymbol{P}}{\partial t} \right) + \varepsilon_{\text{vac}} \frac{\partial}{\partial t} (\nabla \cdot \boldsymbol{E}) = 0 \qquad (3.19)$$

$$\nabla \cdot (\varrho_f \boldsymbol{v}) + \frac{\partial}{\partial t} \left[\nabla \cdot (\varepsilon_{\text{vac}} \boldsymbol{E} + \boldsymbol{P}) \right] = 0 \qquad (3.20)$$

$$(3.21)$$

where ϱ_b denotes the bound charge density. We assume that free charges are conserved and bound charges are conserved independent of each other, i.e.,

$$\nabla \cdot \boldsymbol{J}_f + \frac{\partial \varrho_f}{\partial t} = 0 \qquad (3.22)$$

$$\nabla \cdot \boldsymbol{J}_b + \frac{\partial \varrho_b}{\partial t} = 0 \qquad (3.23)$$

The substitution into Eq. (3.17) according to $\nabla \cdot \boldsymbol{J}_f = \nabla \cdot (\varrho_f \boldsymbol{v}) = -\dfrac{\partial \varrho_f}{\partial t}$ provides,

$$\frac{\partial}{\partial t} \left[\nabla \cdot (\varepsilon_{\text{vac}} \boldsymbol{E} + \boldsymbol{P}) \right] = \frac{\partial \varrho_f}{\partial t} \qquad (3.24)$$

From this it follows,

$$\nabla \cdot \boldsymbol{D} = \varrho_f \qquad (3.25)$$

The use of the charge conservation law, Eq. (3.3) in the Maxwell equations, Eqs. (3.2) in the media characterized by the volume density of free charges, $\varrho_f(\boldsymbol{r})$, the volume density of free charge currents, $\boldsymbol{J}_f(\boldsymbol{r})$ and by the volume densities of electric and magnetic dipoles, $\boldsymbol{P}(\boldsymbol{r})$, and $\boldsymbol{M}(\boldsymbol{r})$, respectively, results in the Maxwell equations,

$$\begin{aligned} \nabla \times \boldsymbol{E} &= -\frac{\partial \boldsymbol{B}}{\partial t} && (3.26\text{a}) \\ \nabla \times \boldsymbol{H} &= \boldsymbol{J}_f + \frac{\partial \boldsymbol{D}}{\partial t} && (3.26\text{b}) \\ \nabla \cdot \boldsymbol{D} &= \varrho_f && (3.26\text{c}) \\ \nabla \cdot \boldsymbol{B} &= 0 && (3.26\text{d}) \end{aligned}$$

For our purpose, it will be sufficient to characterize the presence of material medium by distributions of electric and magnetic dipoles, $\boldsymbol{P}(\boldsymbol{r},\, t)$ and $\boldsymbol{M}(\boldsymbol{r},\, t)$, respectively. Without the restriction generality, we can assume harmonic time, t, dependence of the fields characterized by the angular frequency, ω. A more complicated time dependence can always be characterized as a Fourier sum of monochromatic components. By convention, the harmonic time dependence will be from now characterized by a complex factor, $\exp(\mathrm{j}\omega t)$. Maxwell equations, Eqs. (3.26) can be transformed into the following form

$$\begin{aligned} \nabla \times \boldsymbol{E}(\omega) &= -\mathrm{j}\omega \boldsymbol{B}(\omega) && (3.27\text{a}) \\ \nabla \times \boldsymbol{H}(\omega) &= \boldsymbol{J}_f(\omega) + \mathrm{j}\omega \boldsymbol{D}(\omega) && (3.27\text{b}) \\ \nabla \cdot \boldsymbol{D}(\omega) &= \varrho_f(\omega) && (3.27\text{c}) \\ \nabla \cdot \boldsymbol{B}(\omega) &= 0 && (3.27\text{d}) \end{aligned}$$

where the medium linearity is included in the material equations,

$$\boldsymbol{D}(\omega) \;=\; \varepsilon(\omega)\boldsymbol{E}(\omega)\,, \quad \boldsymbol{B}(\omega) \;=\; \mu(\omega)\boldsymbol{H}(\omega)\,, \quad \boldsymbol{J}_f(\omega) = \sigma(\omega)\boldsymbol{E}(\omega) \tag{3.28}$$

Here $\varepsilon(\omega) = \varepsilon_{\mathrm{vac}}\kappa_e(\omega)$ denotes the medium electric permittivity ($\kappa_e(\omega)$ denotes the relative electric permittivity), $\mu(\omega) = \mu_{\mathrm{vac}}\kappa_m(\omega)$ denotes the medium magnetic permeability ($\kappa_m(\omega)$ denotes the relative magnetic permeability) and $\sigma(\omega)$ denotes the medium free charge conductivity. Our focus is on linear isotropic in general non homogeneous media where $\varepsilon(\boldsymbol{r}\,,\omega)$, $\mu(\boldsymbol{r}\,,\omega)$ and $\sigma(\boldsymbol{r}\,,\omega)$ are scalar functions of the position $\boldsymbol{r}$ at the frequency, ω.

In the following, we shall restrict ourselves to electrically neutral non conducting media, $\varrho_f = 0$ and $\sigma = 0$. The Maxwell equations simplify to

$$\begin{aligned} \nabla \times \boldsymbol{E} &= -\mathrm{j}\omega\mu \boldsymbol{H} && (3.29\text{a}) \\ \nabla \times \boldsymbol{H} &= \mathrm{j}\omega\varepsilon \boldsymbol{E} && (3.29\text{b}) \\ \nabla \cdot (\varepsilon \boldsymbol{E}) &= 0 && (3.29\text{c}) \\ \nabla \cdot (\mu \boldsymbol{H}) &= 0 && (3.29\text{d}) \end{aligned}$$

The last two equations, Eqs. (3.29c) and (3.29d) are the consequence of the first two equations, Eqs. (3.29a) and (3.29b). It is sufficient to take the divergence of Eqs. (3.29a) and (3.29b) and employ the identities, $\nabla \cdot (\nabla \times \boldsymbol{E}) \equiv 0$ and $\nabla \cdot (\nabla \times \boldsymbol{H}) \equiv 0$. The time derivatives of the field divergences of $\boldsymbol{D}$ and $\boldsymbol{B}$ permanently vanish provided the divergence vanish, i.e. $\nabla \cdot \boldsymbol{D} = 0$ and $\nabla \cdot \boldsymbol{B} = 0$.

The symmetry of the Maxwell equations, Eqs. (3.29), enable the construction of new solutions thanks to the duality principle. The duality transformation leaves the Maxwell equations, Eqs. (3.29), invariant. It is expressed by the relations,

$$\boldsymbol{E} \rightarrow \pm \boldsymbol{H}\,, \tag{3.30a}$$

$$\boldsymbol{H} \rightarrow \mp \boldsymbol{E}\,, \tag{3.30b}$$

$$\varepsilon \rightarrow \mu\,, \tag{3.30c}$$

$$\mu \rightarrow \varepsilon\,. \tag{3.30d}$$

3.1 Boundary conditions

Maxwell equations do not provide unique solution of the electromagnetic field. From an infinite number of their solutions, we must select those which are consistent with the boundary conditions pertinent to a problem in question. In nonuniform structures without surfaces of discontinuity, the only boundary condition usually requires finite fields and their vanishing in infinitely remote regions. The fields vanishing in the infinity includes the case of guided modes. The fields of guided modes are localized mostly in optical structures. In near adjacent regions, the fields are manifested themselves as evanescent waves. No energy is lost by radiation.

We now focus on the boundary conditions at surfaces of the discontinuity in electromagnetic material parameters, ε and μ. The problem geometry is shown in Figure 3.1.

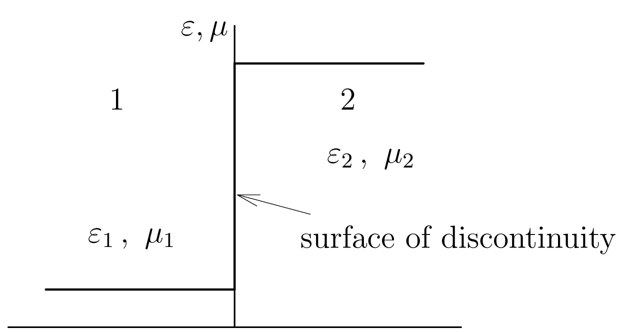

Figure 3.1: An abrupt change in ε and μ along the normal to the interface plane between media 1 and 2.

The time dependent fields, $\boldsymbol{E}$ and $\boldsymbol{B}$, are interdependent as opposite to the time independent fields where $\boldsymbol{E}$ and $\boldsymbol{B}$ are mutually independent. We start from the Maxwell equation in integral form,[2]

$$\oint_C \boldsymbol{E} \cdot \mathrm{d}\boldsymbol{s} = -\mathrm{j}\omega \int_S \mu \boldsymbol{H} \cdot \mathrm{d}\boldsymbol{a} \tag{3.31a}$$

$$\oint_C \boldsymbol{H} \cdot \mathrm{d}\boldsymbol{s} = \mathrm{j}\omega \int_S \varepsilon \boldsymbol{E} \cdot \mathrm{d}\boldsymbol{a} \tag{3.31b}$$

Here C represents a closed curve bounding a two-sided surface S. A vector of an oriented elementary displacement along C is denote as $\mathrm{d}\boldsymbol{s}$. As expected, both the vector integral Maxwell equations are mutually related by the duality transformation. It is therefore sufficient to consider one of them.

Let us consider a small region at the interface stretched into both media. The elementary interface surface can be taken as planar specified by a unit normal, $\hat{\boldsymbol{n}}$, conventionally oriented from the medium characterized by ε_1 and μ_1 to the medium characterized by ε_2 and μ_2 as in Figure 3.2.

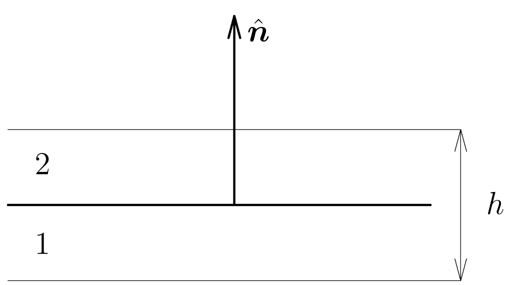

Figure 3.2: The interface unit normal at a surface of discontinuity is oriented from the medium 1 into the medium 2. A transition layer of the thickness h is stretched into both media.

In the elementary interface region, both the media can be taken as homogeneous ones. We draw a rectangular loop bounding the elementary interface region.

Its longer opposite sides of the length, Δs, parallel to the interface plane, are situated either in the medium 1 or in the medium 2. The shorter sides of the length, h, traverse the interface plane. The loop is situated in a plane perpendicular to the interface plane and specified by a unit normal, $\hat{\boldsymbol{n}}'$. Consequently, $\hat{\boldsymbol{n}}'$ is parallel to the interface plane. The orientation of $\hat{\boldsymbol{n}}'$ defines the circulation sense of $\mathrm{d}\boldsymbol{s}$ around C. The orientation of integration path on the longer rectangle side in the medium 2 is given by a unit vector, $\hat{\boldsymbol{t}}_2 = \hat{\boldsymbol{t}}$ and the orientation of integration path on the longer rectangle side in the medium

[2]R. Wangsness, *Electromagnetic Fields*, 2nd Edition, John Wiley & Sons, 1986, Chapter 9.

1 is given by a unit vector, $\hat{\boldsymbol{t}}_1 = -\hat{\boldsymbol{t}}$, consistent with the orientation of $\hat{\boldsymbol{n}}'$. The geometry is explained in Figure 3.3.

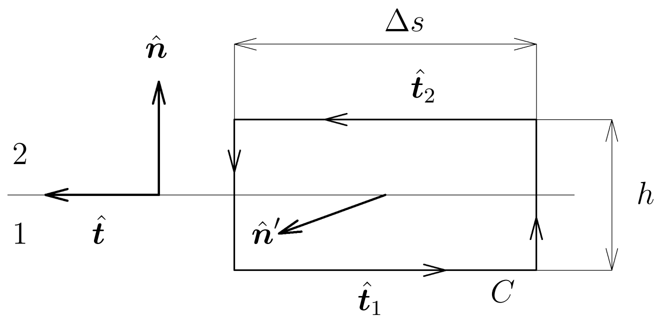

Figure 3.3: The interface unit vector normal, $\hat{\boldsymbol{n}}$, the tangent unit vectors, $\hat{\boldsymbol{t}} = \hat{\boldsymbol{t}}_2 = -\hat{\boldsymbol{t}}_1$, and the unit vector normal, $\hat{\boldsymbol{n}}' = \hat{\boldsymbol{n}} \times \hat{\boldsymbol{t}}$, to the integration loop, C, employed in the derivation of the boundary conditions for tangent components of $\boldsymbol{E}$ or $\boldsymbol{H}$.

From Eq. (3.31b) we get

$$\begin{aligned} \oint_C \boldsymbol{H} \cdot \mathrm{d}\boldsymbol{s} &= \boldsymbol{H}_2 \cdot \boldsymbol{t}_2 \, \Delta s + \boldsymbol{H}_1 \cdot \boldsymbol{t}_1 \, \Delta s + \mathcal{W} \\ &= \boldsymbol{H}_2 \cdot \boldsymbol{t} \, \Delta s - \boldsymbol{H}_1 \cdot \boldsymbol{t} \, \Delta s + \mathcal{W} \end{aligned}$$

$$\mathrm{j}\omega \int_S \varepsilon \boldsymbol{E} \cdot \mathrm{d}\boldsymbol{a} = \mathrm{j}\omega h \, \Delta s \, \varepsilon \boldsymbol{E}$$

The field and its time derivative are everywhere finite. Consequently, in the limit $h \to 0$, the surface integral on the right hand side of Eq. (3.31b) vanishes. The contribution, $\mathcal{W}$, of the shorter rectangle sides to the integral around C, proportional to h, is zero. Then,

$$\boldsymbol{H}_2 \cdot \boldsymbol{t}_2 \, \Delta s + \boldsymbol{H}_1 \cdot \boldsymbol{t}_1 \, \Delta s = 0$$

$$(\boldsymbol{H}_2 - \boldsymbol{H}_1) \cdot \boldsymbol{t} = 0$$

From this, we get for the field components tangent to the interface,

$$\boldsymbol{H}_{2t} = \boldsymbol{H}_{1t} \tag{3.32a}$$

The use of the duality provides,

$$\boldsymbol{E}_{2t} = \boldsymbol{E}_{1t} \tag{3.32b}$$

shown above, Eqs. (3.29c) and (3.29d) follow from Eqs. (3.29b) and (3.29a) and for the time varying fields need not be considered.

3.2 Wave equations in nonuniform media

The wave localization requires structures with non homogeneous electromagnetic material parameters μ and ε. The parameters, μ and ε, may vary either continuously or abruptly, e.g., at interfaces between homogeneous media. We will investigate wave equation in linear, isotropic, non homogeneous media, where magnetic permeability, $\mu = \mu(\boldsymbol{r})$, and electric permittivity, $\varepsilon = \varepsilon(\boldsymbol{r})$ are functions of the position vector, $\boldsymbol{r}$. We are interested in solutions harmonic in time expressed in the phasor (complex vector) representation accounted for by the factor $\exp(\mathrm{j}\omega t)$. We shall start from the Maxwell equations in Eqs. (3.29). We apply the curl operation to Eq. (3.29a) divided by $\mu(\boldsymbol{r})$ and multiply Eq. (3.29b) by $\mathrm{j}\omega$,

$$\nabla \times \left[\mu^{-1}\left(\nabla \times \boldsymbol{E}\right)\right] = -\mathrm{j}\omega\left(\nabla \times \boldsymbol{H}\right) \tag{3.33a}$$

$$\mathrm{j}\omega\left(\nabla \times \boldsymbol{H}\right) = -\varepsilon\omega^2 \boldsymbol{E} \tag{3.33b}$$

We eliminate $\mathrm{j}\omega(\nabla \times \boldsymbol{H})$ and multiply by μ to arrive at the wave equation for $\boldsymbol{E}$,

$$\mu\nabla \times \left[\mu^{-1}\left(\nabla \times \boldsymbol{E}\right)\right] = \mu\varepsilon\omega^2 \boldsymbol{E}\,. \tag{3.34a}$$

The duality provides the corresponding wave equation for pro $\boldsymbol{H}$,

$$\varepsilon\nabla \times \left[\varepsilon^{-1}\left(\nabla \times \boldsymbol{H}\right)\right] = \mu\varepsilon\omega^2 \boldsymbol{H} \tag{3.34b}$$

We employ the identity,

$$\begin{aligned}\mu\nabla \times \left[\mu^{-1}\left(\nabla \times \boldsymbol{E}\right)\right] &= \mu\nabla\left(\mu^{-1}\right) \times \left(\nabla \times \boldsymbol{E}\right) + \left[\nabla \times \left(\nabla \times \boldsymbol{E}\right)\right] \\ &= \mu\nabla\left(\mu^{-1}\right) \times \left(\nabla \times \boldsymbol{E}\right) + \left[\nabla\left(\nabla \cdot \boldsymbol{E}\right) - \left(\nabla^2 \boldsymbol{E}\right)\right]\end{aligned} \tag{3.35}$$

and transform the wave equation into the form

$$\nabla\left(\nabla \cdot \boldsymbol{E}\right) - \left(\nabla^2 \boldsymbol{E}\right) + \mu\nabla\left(\mu^{-1}\right) \times \left(\nabla \times \boldsymbol{E}\right) = \mu\varepsilon\omega^2 \boldsymbol{E} \tag{3.36}$$

Equation (3.27c) in the absence of free charges gives, $\nabla \cdot \boldsymbol{D} = \varrho_f = 0$. However in general, in non homogeneous electrically neutral media, the condition $\nabla \cdot \boldsymbol{E} = 0$ is not valid. Indeed,

$$\nabla \cdot \boldsymbol{D} = \nabla \cdot \left[\varepsilon(\boldsymbol{r})\, \boldsymbol{E}\right] = \left[\nabla\varepsilon(\boldsymbol{r})\right] \cdot \boldsymbol{E} + \varepsilon(\boldsymbol{r})\left(\nabla \cdot \boldsymbol{E}\right) = 0 \tag{3.37}$$

We find that $\nabla \cdot \boldsymbol{E} \neq 0$, i.e.,

$$\nabla \cdot \boldsymbol{E} = -\frac{\nabla\varepsilon}{\varepsilon} \cdot \boldsymbol{E}\,.$$

The ratio can be expressed as $\dfrac{\nabla\varepsilon}{\varepsilon} = \nabla(\ln\varepsilon)$,

$$\nabla\cdot\boldsymbol{E} \;=\; -\left[\nabla(\ln\varepsilon)\right]\cdot\boldsymbol{E} \tag{3.38}$$

The expression, $\mu\nabla(\mu^{-1})$, in Eq. (3.36) may be alternatively written as,

$$\mu\nabla\left(\mu^{-1}\right) \;=\; -\mu\frac{1}{\mu^2}\nabla\mu \;=\; -\frac{\nabla\mu}{\mu} \;=\; -\nabla(\ln\mu) \tag{3.39}$$

By making use of Eqs. (3.37) trough (3.39) and after substituting into Eq. (3.36) we get the wave equation for $\boldsymbol{E}$ in the final form,

$$\nabla^2\boldsymbol{E} + \mu\varepsilon\omega^2\boldsymbol{E} + \nabla\left[(\nabla\ln\varepsilon)\cdot\boldsymbol{E}\right] + (\nabla\ln\mu)\times(\nabla\times\boldsymbol{E}) \;=\; 0 \tag{3.40a}$$

The duality expressed in Eq. (3.30), i.e., $\boldsymbol{E}\to\boldsymbol{H}$, $\mu\leftrightarrow\varepsilon$ applied to Eq. (3.40a) provides the corresponding wave equation for $\boldsymbol{H}$,

$$\nabla^2\boldsymbol{H} + \mu\varepsilon\omega^2\boldsymbol{H} + \nabla\left[(\nabla\ln\mu)\cdot\boldsymbol{H}\right] + (\nabla\ln\varepsilon)\times(\nabla\times\boldsymbol{H}) \;=\; 0 \tag{3.40b}$$

In homogeneous media, where μ and ε are independent of the position vector, $\boldsymbol{r}$, with $\nabla\mu = 0$ and $\nabla\varepsilon = 0$, the wave equations, Eqs. (3.40) simplify to,

$$\nabla^2\boldsymbol{E} + \mu\varepsilon\omega^2\boldsymbol{E} \;=\; 0 \tag{3.41a}$$

$$\nabla^2\boldsymbol{H} + \mu\varepsilon\omega^2\boldsymbol{H} \;=\; 0 \tag{3.41b}$$

If only the condition $\nabla\mu = 0$ is met, e.g., in non homogeneous non magnetic media, the situation is characterized by,

$$\nabla^2\boldsymbol{E} + \mu\varepsilon\omega^2\boldsymbol{E} + \nabla\left[(\nabla\ln\varepsilon)\cdot\boldsymbol{E}\right] \;=\; 0 \tag{3.42}$$

We next look for the circumstances where the term $\nabla\left[(\nabla\ln\varepsilon)\cdot\boldsymbol{E}\right]$ in Eq. (3.42) is negligible with respect the dominating terms,[3]

$$\nabla\left[(\nabla\ln\varepsilon)\cdot\boldsymbol{E}\right] \;\approx\; 0\,. \tag{3.43}$$

The term is identically zero in the special case where the wave polarization of electric field, $\boldsymbol{E}$, is perpendicular to the gradient of permittivity, $\nabla\varepsilon$. In the limiting case of homogeneous media, $\nabla\varepsilon = 0$ and the wave equation reduces to Eq. (3.41a)

$$\nabla^2\boldsymbol{E} + \mu\varepsilon\omega^2\boldsymbol{E} \;=\; 0 \tag{3.44}$$

[3] D. Marcuse, Light Transmission Optics, Van Nostrand Reinhold Company, New York 1972.

where the solution for plane time harmonic, i.e., monochromatic, waves assumes the form

$$\boldsymbol{E} \;=\; \boldsymbol{E}_0 \exp\left[\mathrm{j}\left(\omega\, t - \boldsymbol{k}\cdot\boldsymbol{r}\right)\right] \tag{3.45}$$

with the angular frequency, ω, and the propagation vector, $\boldsymbol{k}$. In the medium characterized by ε and μ, it follows,

$$\boldsymbol{k}^2\boldsymbol{E} - \mu(\omega)\varepsilon(\omega)\omega^2\boldsymbol{E} \;=\; 0 \tag{3.46}$$

The propagation constant $k = |\boldsymbol{k}|$ can be expressed in terms of the vacuum wavelength, λ_{vac}, using the relation $c^2\mu\varepsilon = n^2$,

$$\boldsymbol{k}^2 \;=\; \mu\varepsilon\omega^2 \;=\; \left(n\frac{2\pi}{\lambda_{\mathrm{vac}}}\right)^2 \tag{3.47}$$

The first two dominating terms in Eq. (3.42) are of the order $|k^2E|$. Let us evaluate the third term in Eq. (3.42), i.e., $\nabla\left[(\nabla\ln\varepsilon)\cdot\boldsymbol{E}\right]$, taken as a perturbation. Let us suppose that $(\nabla\ln\varepsilon)\cdot\boldsymbol{E}$ varies the most strongly in the direction of a unit vector, $\hat{\boldsymbol{s}}$, on the s coordinate axis,

$$\begin{aligned}\left|\nabla\left[(\nabla\ln\varepsilon)\cdot\boldsymbol{E}\right]\right| \;&\sim\; \left|\frac{\partial}{\partial s}\left[\left(\frac{\partial}{\partial s}\ln\varepsilon\right)\hat{\boldsymbol{s}}\cdot\boldsymbol{E}\right]\right| \\ &\lesssim\; \left|\frac{\partial}{\partial s}\boldsymbol{E}\right|\left|\frac{\partial}{\partial s}\ln\varepsilon\right| + |\boldsymbol{E}|\left|\frac{\partial}{\partial s}\left(\frac{\partial}{\partial s}\ln\varepsilon\right)\right|\end{aligned} \tag{3.48}$$

The first term in Eq. (3.48) is of the order $|k^1E| = \left|\frac{\partial}{\partial s}\boldsymbol{E}\right|$, the second term is of the order $|k^0E| = |\boldsymbol{E}|$. We restrict ourselves to the case where the second term is negligible with respect to the first one,

$$\left|\frac{\partial}{\partial s}\boldsymbol{E}\right|\left|\frac{\partial}{\partial s}\ln\varepsilon\right| \gg |\boldsymbol{E}|\left|\frac{\partial}{\partial s}\left(\frac{\partial}{\partial s}\ln\varepsilon\right)\right|\,, \tag{3.49}$$

and compare the first term with the dominating terms of the order $|k^2\boldsymbol{E}|$ in Eq. (3.42)

$$\frac{\left|\frac{\partial}{\partial s}\boldsymbol{E}\right|\left|\frac{\partial}{\partial s}\ln\varepsilon\right|}{|k^2\boldsymbol{E}|} \;\sim\; \frac{|k\boldsymbol{E}|\left|\frac{1}{\varepsilon}\frac{\partial\varepsilon}{\partial s}\right|}{|k^2\boldsymbol{E}|} \;\sim\; \frac{\left|\frac{1}{\varepsilon}\frac{\partial\varepsilon}{\partial s}\right|}{|k|}\,.$$

We evaluate $\left|\frac{1}{\varepsilon}\frac{\partial\varepsilon}{\partial s}\right|$ as a relative change of ε on a one wavelength path, $\lambda = 2\pi/k$, inside the material medium, $\partial s \sim \lambda$

$$\left|\frac{1}{\varepsilon}\frac{\partial\varepsilon}{\partial s}\right| \;\approx\; \left|\frac{1}{\lambda}\frac{\varepsilon\left(s+\frac{1}{2}\lambda\right) - \varepsilon\left(s-\frac{1}{2}\lambda\right)}{\varepsilon\,(s)}\right|\,.$$

This is a relative change of ε on the one wavelength path multiplied by λ^{-1}. Here $k = 2\pi/\lambda$. The perturbation term

$$\frac{\left|\dfrac{1}{\varepsilon}\dfrac{\partial \varepsilon}{\partial s}\right|}{|k|} \approx \frac{\lambda}{2\pi}\left|\frac{1}{\lambda}\frac{\varepsilon\left(s+\frac{1}{2}\lambda\right)-\varepsilon\left(s-\frac{1}{2}\lambda\right)}{\varepsilon(s)}\right| ,$$

is negligible at the condition,

$$\frac{1}{2\pi}\left|\frac{\varepsilon\left(s+\frac{1}{2}\lambda\right)-\varepsilon\left(s-\frac{1}{2}\lambda\right)}{\varepsilon(s)}\right| \ll 1 \tag{3.50}$$

Then it is allowed to remove the perturbation term but in the wave equation ε must be taken as dependent on $\boldsymbol{r}$, i.e.,

$$\nabla^2 \boldsymbol{E} + \mu\varepsilon(\boldsymbol{r},\omega)\,\boldsymbol{E} = 0 \tag{3.51}$$

The case of sharp ε changes on the one λ path, e.g., at the interfaces of two homogeneous media is adequately treated by using the boundary conditions for $\boldsymbol{E}$ and $\boldsymbol{H}$ according to Eqs. (3.32) which express the continuity of the $\boldsymbol{E}$ and $\boldsymbol{H}$ components parallel to the interface or, in other words, the continuity of $\boldsymbol{E}$ and $\boldsymbol{H}$ components perpendicular to $\nabla\varepsilon$.

3.3 Waves in media uniform along an axis

We look for monochromatic plane wave solutions to Maxwell equations in media where ε and μ do not change along an axis. We fix the axis to the z axis and denote β the component of the propagation vector parallel to the z axis. The material parameters, ε and μ are therefore independent of z, i.e.,

$$\varepsilon = \varepsilon(x,y)\ , \qquad \mu = \mu(x,y) \tag{3.52}$$

We substitute the solution in the form

$$\boldsymbol{E} = \boldsymbol{E}_0(x,y)\exp\left[\mathrm{j}\left(\omega t - \beta z\right)\right] \tag{3.53a}$$

$$\boldsymbol{H} = \boldsymbol{H}_0(x,y)\exp\left[\mathrm{j}\left(\omega t - \beta z\right)\right] \tag{3.53b}$$

into the Maxwell equations split into the Cartesian components. From the equation

$$\nabla\times\boldsymbol{E} = -\mathrm{j}\omega\mu\boldsymbol{H}$$

we get after expressing the derivative of time, t, and of the z coordinate,

$$\frac{\partial E_z}{\partial y} - \frac{\partial E_y}{\partial z} = -\mathrm{j}\omega\mu H_x\,, \quad \frac{\partial E_z}{\partial y} + \mathrm{j}\beta E_y = -\mathrm{j}\omega\mu H_x \tag{3.54a}$$

$$\frac{\partial E_x}{\partial z} - \frac{\partial E_z}{\partial x} = -\mathrm{j}\omega\mu H_y\,, \quad -\mathrm{j}\beta E_x - \frac{\partial E_z}{\partial x} = -\mathrm{j}\omega\mu H_y \tag{3.54b}$$

$$\frac{\partial E_y}{\partial x} - \frac{\partial E_x}{\partial y} = -\mathrm{j}\omega\mu H_z\,, \quad \frac{\partial E_y}{\partial x} - \frac{\partial E_x}{\partial y} = -\mathrm{j}\omega\mu H_z \tag{3.54c}$$

From the equation

$$\nabla \times \boldsymbol{H} = \mathrm{j}\omega\varepsilon \boldsymbol{E}$$

we have

$$\frac{\partial H_z}{\partial y} - \frac{\partial H_y}{\partial z} = \mathrm{j}\omega\varepsilon E_x\,, \quad \frac{\partial H_z}{\partial y} + \mathrm{j}\beta H_y = \mathrm{j}\omega\varepsilon E_x \tag{3.54d}$$

$$\frac{\partial H_x}{\partial z} - \frac{\partial H_z}{\partial x} = \mathrm{j}\omega\varepsilon E_y\,, \quad -\mathrm{j}\beta H_x - \frac{\partial H_z}{\partial x} = \mathrm{j}\omega\varepsilon E_y \tag{3.54e}$$

$$\frac{\partial H_y}{\partial x} - \frac{\partial H_x}{\partial y} = \mathrm{j}\omega\varepsilon E_z\,, \quad \frac{\partial H_y}{\partial x} - \frac{\partial H_x}{\partial y} = \mathrm{j}\omega\varepsilon E_z \tag{3.54f}$$

Among them, we select those four which express transverse field components, i.e., E_x, E_y, H_x and H_y in terms of derivative of E_z a H_z with respect to x a y,

$$\frac{\partial E_z}{\partial y} + \mathrm{j}\beta E_y = -\mathrm{j}\omega\mu H_x \tag{3.55a}$$

$$\mathrm{j}\beta E_x + \frac{\partial E_z}{\partial x} = \mathrm{j}\omega\mu H_y \tag{3.55b}$$

$$\frac{\partial H_z}{\partial y} + \mathrm{j}\beta H_y = \mathrm{j}\omega\varepsilon E_x \tag{3.55c}$$

$$\mathrm{j}\beta H_x + \frac{\partial H_z}{\partial x} = -\mathrm{j}\omega\varepsilon E_y \tag{3.55d}$$

We select a group containing E_x and H_y

$$\mathrm{j}\beta E_x - \mathrm{j}\omega\mu H_y = -\frac{\partial E_z}{\partial x} \tag{3.56a}$$

$$-\mathrm{j}\omega\varepsilon E_x + \mathrm{j}\beta H_y = -\frac{\partial H_z}{\partial y} \tag{3.56b}$$

and another group containing E_y and H_x

$$\mathrm{j}\beta E_y + \mathrm{j}\omega\mu H_x = -\frac{\partial E_z}{\partial y} \tag{3.56c}$$

$$\mathrm{j}\beta H_x + \mathrm{j}\omega\varepsilon E_y = -\frac{\partial H_z}{\partial x} \tag{3.56d}$$

The set of four equation is summarized in Table 3.1. The 4×4 determinant of the

Table 3.1: Summary of transverse field components

E_x	H_y	E_y	H_x	
$\mathrm{j}\beta$	$-\mathrm{j}\omega\mu$	0	0	$-\dfrac{\partial E_z}{\partial x}$
$-\mathrm{j}\omega\varepsilon$	$\mathrm{j}\beta$	0	0	$-\dfrac{\partial H_z}{\partial y}$
0	0	$\mathrm{j}\beta$	$\mathrm{j}\omega\mu$	$-\dfrac{\partial E_z}{\partial y}$
0	0	$\mathrm{j}\omega\varepsilon$	$\mathrm{j}\beta$	$-\dfrac{\partial H_z}{\partial x}$

equation set can be split into two non zero identical 2×2 determinants,

$$\begin{vmatrix} \mathrm{j}\beta & -\mathrm{j}\omega\mu \\ -\mathrm{j}\omega\varepsilon & \mathrm{j}\beta \end{vmatrix} = \begin{vmatrix} \mathrm{j}\beta & \mathrm{j}\omega\mu \\ \mathrm{j}\omega\varepsilon & \mathrm{j}\beta \end{vmatrix} = \omega^2\varepsilon\mu - \beta^2 \tag{3.57}$$

where β denotes the longitudinal propagation constant. In homogeneous media, $k^2 = \omega^2\varepsilon\mu = (2\pi/\lambda)^2$, represents the square of the propagation vector. There are two cases to be considered,

$$\omega^2\varepsilon\mu - \beta^2 \geq 0 \tag{3.58a}$$

$$\omega^2\varepsilon\mu - \beta^2 \leq 0 \tag{3.58b}$$

The square root of the expression in Eq. (3.58a) represents the propagation vector component perpendicular to the z axis. We shall call it *transverse propagation constant*

$$\kappa \equiv \left(\omega^2\varepsilon\mu - \beta^2\right)^{1/2} \tag{3.59a}$$

The square root in Eq. (3.58b) is imaginary pure. The transverse attenuation constant will be defined by,

$$\gamma \equiv \left(\beta^2 - \omega^2\varepsilon\mu\right)^{1/2} \tag{3.59b}$$

3.3.1 Transverse fields

From the set of four equations, Eqs. (3.56) we compute as unknown the field components E_x , E_y , H_x , and H_y

$$E_x = \frac{1}{\omega^2\varepsilon\mu - \beta^2} \begin{vmatrix} -\dfrac{\partial E_z}{\partial x} & -\mathrm{j}\omega\mu \\ -\dfrac{\partial H_z}{\partial y} & \mathrm{j}\beta \end{vmatrix} \tag{3.60}$$

$$E_x = -\frac{\mathrm{j}}{\omega^2\varepsilon\mu - \beta^2}\left(\beta\frac{\partial E_z}{\partial x} + \omega\mu\frac{\partial H_z}{\partial y}\right) \tag{3.61}$$

The duality of Eq. (3.30) provides H_x ,

$$H_x = -\frac{\mathrm{j}}{\omega^2\varepsilon\mu - \beta^2}\left(\beta\frac{\partial H_z}{\partial x} - \omega\varepsilon\frac{\partial E_z}{\partial y}\right) \tag{3.62}$$

Further,

$$H_y = \frac{1}{\omega^2\varepsilon\mu - \beta^2} \begin{vmatrix} \mathrm{j}\beta & -\dfrac{\partial E_z}{\partial x} \\ -\mathrm{j}\omega\varepsilon & -\dfrac{\partial H_z}{\partial y} \end{vmatrix} \tag{3.63}$$

$$H_y = -\frac{\mathrm{j}}{\omega^2\varepsilon\mu - \beta^2}\left(\beta\frac{\partial H_z}{\partial y} + \omega\varepsilon\frac{\partial E_z}{\partial x}\right) \tag{3.64}$$

and the duality of Eq. (3.30) provides E_y ,

$$E_y = -\frac{\mathrm{j}}{\omega^2\varepsilon\mu - \beta^2}\left(\beta\frac{\partial E_z}{\partial y} - \omega\mu\frac{\partial H_z}{\partial x}\right) \tag{3.65}$$

In summary, we get for E_x , E_y , H_x , and H_y ,

$$E_x = -\frac{\mathrm{j}}{\omega^2\varepsilon\mu - \beta^2}\left(\beta\frac{\partial E_z}{\partial x} + \omega\mu\frac{\partial H_z}{\partial y}\right) \tag{3.66a}$$

$$H_y = -\frac{\mathrm{j}}{\omega^2\varepsilon\mu - \beta^2}\left(\beta\frac{\partial H_z}{\partial y} + \omega\varepsilon\frac{\partial E_z}{\partial x}\right) \tag{3.66b}$$

$$E_y = -\frac{\mathrm{j}}{\omega^2\varepsilon\mu - \beta^2}\left(\beta\frac{\partial E_z}{\partial y} - \omega\mu\frac{\partial H_z}{\partial x}\right) \tag{3.66c}$$

$$H_x = -\frac{\mathrm{j}}{\omega^2\varepsilon\mu - \beta^2}\left(\beta\frac{\partial H_z}{\partial x} - \omega\varepsilon\frac{\partial E_z}{\partial y}\right) \tag{3.66d}$$

For the condition expressed in Eq. (3.59a), we obtain harmonic solutions,

$$E_x = -\frac{\mathrm{j}}{\kappa^2}\left(\beta\frac{\partial E_z}{\partial x} + \omega\mu\frac{\partial H_z}{\partial y}\right) \tag{3.67a}$$

$$H_y = -\frac{\mathrm{j}}{\kappa^2}\left(\beta\frac{\partial H_z}{\partial y} + \omega\varepsilon\frac{\partial E_z}{\partial x}\right) \tag{3.67b}$$

$$E_y = -\frac{\mathrm{j}}{\kappa^2}\left(\beta\frac{\partial E_z}{\partial y} - \omega\mu\frac{\partial H_z}{\partial x}\right) \tag{3.67c}$$

$$H_x = -\frac{\mathrm{j}}{\kappa^2}\left(\beta\frac{\partial H_z}{\partial x} - \omega\varepsilon\frac{\partial E_z}{\partial y}\right) \tag{3.67d}$$

Evanescent solutions result from the condition expressed by Eq. (3.59b),

$$E_x = \frac{\mathrm{j}}{\gamma^2}\left(\beta\frac{\partial E_z}{\partial x} + \omega\mu\frac{\partial H_z}{\partial y}\right) \tag{3.68a}$$

$$H_y = \frac{\mathrm{j}}{\gamma^2}\left(\beta\frac{\partial H_z}{\partial y} + \omega\varepsilon\frac{\partial E_z}{\partial x}\right) \tag{3.68b}$$

$$E_y = \frac{\mathrm{j}}{\gamma^2}\left(\beta\frac{\partial E_z}{\partial y} - \omega\mu\frac{\partial H_z}{\partial x}\right) \tag{3.68c}$$

$$H_x = \frac{\mathrm{j}}{\gamma^2}\left(\beta\frac{\partial H_z}{\partial x} - \omega\varepsilon\frac{\partial E_z}{\partial y}\right) \tag{3.68d}$$

3.3.2 Alternative derivation of transverse fields

The operator ∇ employed in the Maxwell equations

$$\begin{aligned} \nabla \times \boldsymbol{E} &= -\mathrm{j}\omega\mu\boldsymbol{H}\,, \\ \nabla \times \boldsymbol{H} &= \mathrm{j}\omega\varepsilon\boldsymbol{E}\,, \end{aligned}$$

can be split into a transverse and a longitudinal parts.[4]

$$\nabla = \nabla_t + \hat{\boldsymbol{z}}\frac{\partial}{\partial z} \tag{3.70}$$

Also the field vectors, $\boldsymbol{E}$ and $\boldsymbol{H}$ can be split into a transverse and a longitudinal parts,

$$\begin{aligned} \boldsymbol{E} &= \boldsymbol{E}_t + \hat{\boldsymbol{z}}E_z \\ \boldsymbol{H} &= \boldsymbol{H}_t + \hat{\boldsymbol{z}}H_z \end{aligned} \tag{3.71}$$

i.e.,

$$\begin{aligned} \left(\nabla_t + \hat{\boldsymbol{z}}\frac{\partial}{\partial z}\right) \times (\boldsymbol{E}_t + \hat{\boldsymbol{z}}E_z) &= -\mathrm{j}\omega\mu\,(\boldsymbol{H}_t + \hat{\boldsymbol{z}}H_z) \\ \left(\nabla_t + \hat{\boldsymbol{z}}\frac{\partial}{\partial z}\right) \times (\boldsymbol{H}_t + \hat{\boldsymbol{z}}H_z) &= \mathrm{j}\omega\varepsilon\,(\boldsymbol{E}_t + \hat{\boldsymbol{z}}E_z)\ . \end{aligned}$$

[4] Jin Au Kong, Electromagnetic Wave Theory, EMW Publishing, Cambridge, Massachusetts, USA 2000, p. 439.

This can be rearranged,

$$\begin{aligned}
\nabla_t \times \hat{\boldsymbol{z}} E_z + \hat{\boldsymbol{z}} \times \frac{\partial}{\partial z} \boldsymbol{E}_t &= -\mathrm{j}\omega\mu \boldsymbol{H}_t && (3.72a)\\
\nabla_t \times \hat{\boldsymbol{z}} H_z + \hat{\boldsymbol{z}} \times \frac{\partial}{\partial z} \boldsymbol{H}_t &= \mathrm{j}\omega\varepsilon \boldsymbol{E}_t && (3.72b)\\
\nabla_t \times \boldsymbol{E}_t &= -\mathrm{j}\omega\mu \hat{\boldsymbol{z}} H_z && (3.72c)\\
\nabla_t \times \boldsymbol{H}_t &= \mathrm{j}\omega\varepsilon \hat{\boldsymbol{z}} E_z && (3.72d)
\end{aligned}$$

The use has been made of the identities,

$$\hat{\boldsymbol{z}} \times (\hat{\boldsymbol{z}} \times \boldsymbol{E}_t) = -\boldsymbol{E}_t \qquad (3.73)$$

and

$$\hat{\boldsymbol{z}} \times (\nabla_t \times \hat{\boldsymbol{z}} E_z) = -\hat{\boldsymbol{z}} \times (\hat{\boldsymbol{z}} \times \nabla_t E_z) = \nabla_t E_z \qquad (3.74)$$

In the Cartesian coordinates, we have $\nabla_t = \hat{\boldsymbol{x}} \frac{\partial}{\partial x} + \hat{\boldsymbol{y}} \frac{\partial}{\partial y}$,

$$\begin{aligned}
\hat{\boldsymbol{z}} \times (\nabla_t \times \hat{\boldsymbol{z}} E_z) &= \hat{\boldsymbol{z}} \times \left(\hat{\boldsymbol{x}} \times \hat{\boldsymbol{z}} \frac{\partial}{\partial x} E_z\right) + \hat{\boldsymbol{z}} \times \left(\hat{\boldsymbol{y}} \times \hat{\boldsymbol{z}} \frac{\partial}{\partial y} E_z\right)\\
&= \hat{\boldsymbol{z}} \times \left(-\hat{\boldsymbol{y}} \frac{\partial}{\partial x} E_z\right) + \hat{\boldsymbol{z}} \times \left(\hat{\boldsymbol{x}} \frac{\partial}{\partial y} E_z\right)\\
&= \hat{\boldsymbol{x}} \frac{\partial}{\partial x} E_z + \hat{\boldsymbol{y}} \frac{\partial}{\partial y} E_z\\
&= \nabla_t E_z
\end{aligned}$$

We multiply Eq. (3.72a) by $\mathrm{j}\omega\varepsilon$. Then we take the derivative, $\frac{\partial}{\partial z}$, of Eq. (3.72b) and multiply the result by $\hat{\boldsymbol{z}} \times$,

$$\begin{aligned}
\mathrm{j}\omega\varepsilon (\nabla_t \times \hat{\boldsymbol{z}} E_z) + \underline{\mathrm{j}\omega\varepsilon \left(\hat{\boldsymbol{z}} \times \frac{\partial}{\partial z} \boldsymbol{E}_t\right)} &= \omega^2 \mu\varepsilon \boldsymbol{H}_t && (3.75a)\\
\hat{\boldsymbol{z}} \times \left(\nabla_t \times \hat{\boldsymbol{z}} \frac{\partial}{\partial z} H_z\right) + \hat{\boldsymbol{z}} \times \left(\hat{\boldsymbol{z}} \times \frac{\partial^2}{\partial z^2} \boldsymbol{H}_t\right) &= \underline{\mathrm{j}\omega\varepsilon \left(\hat{\boldsymbol{z}} \times \frac{\partial}{\partial z} \boldsymbol{E}_t\right)} && (3.75b)
\end{aligned}$$

We eliminate the underlined expression, $\mathrm{j}\omega\varepsilon \left(\hat{\boldsymbol{z}} \times \frac{\partial}{\partial z} \boldsymbol{E}_t\right)$,

$$\mathrm{j}\omega\varepsilon (\nabla_t \times \hat{\boldsymbol{z}} E_z) + \hat{\boldsymbol{z}} \times \left(\nabla_t \times \hat{\boldsymbol{z}} \frac{\partial}{\partial z} H_z\right) + \hat{\boldsymbol{z}} \times \left(\hat{\boldsymbol{z}} \times \frac{\partial^2}{\partial z^2} \boldsymbol{H}_t\right) = \omega^2 \mu\varepsilon \boldsymbol{H}_t \qquad (3.76)$$

Next, we make use of Eqs. (3.73) and (3.74),

$$\mathrm{j}\omega\varepsilon (\nabla_t \times \hat{\boldsymbol{z}} E_z) + \nabla_t \frac{\partial}{\partial z} H_z - \frac{\partial^2}{\partial z^2} \boldsymbol{H}_t = \omega^2 \mu\varepsilon \boldsymbol{H}_t \qquad (3.77)$$

and of the relation, $\dfrac{\partial^2}{\partial z^2} = -\beta^2$

$$\boldsymbol{H}_t = \frac{1}{(\omega^2\mu\varepsilon - \beta^2)}\left[\nabla_t \frac{\partial}{\partial z} H_z + \mathrm{j}\omega\varepsilon\left(\nabla_t \times \hat{\boldsymbol{z}} E_z\right)\right] \tag{3.78}$$

The duality transformation provides the result summarized as,

$$\boldsymbol{E}_t = \frac{1}{(\omega^2\mu\varepsilon - \beta^2)}\left[\nabla_t\left(\frac{\partial E_z}{\partial z}\right) - \mathrm{j}\omega\varepsilon\left(\nabla_t \times \hat{\boldsymbol{z}} H_z\right)\right] \tag{3.79a}$$

$$\boldsymbol{H}_t = \frac{1}{(\omega^2\mu\varepsilon - \beta^2)}\left[\nabla_t\left(\frac{\partial H_z}{\partial z}\right) + \mathrm{j}\omega\varepsilon\left(\nabla_t \times \hat{\boldsymbol{z}} E_z\right)\right] \tag{3.79b}$$

Using $\dfrac{\partial}{\partial z} \to -\mathrm{j}\beta$,

$$\boldsymbol{E}_t = \frac{1}{(\omega^2\mu\varepsilon - \beta^2)}\left[-\mathrm{j}\beta\left(\nabla_t E_z\right) - \mathrm{j}\omega\varepsilon\left(\nabla_t \times \hat{\boldsymbol{z}} H_z\right)\right] \tag{3.80a}$$

$$\boldsymbol{H}_t = \frac{1}{(\omega^2\mu\varepsilon - \beta^2)}\left[-\mathrm{j}\beta\left(\nabla_t H_z\right) + \mathrm{j}\omega\varepsilon\left(\nabla_t \times \hat{\boldsymbol{z}} E_z\right)\right] \tag{3.80b}$$

3.4 Waves in planarly layered media

Planar structures may be defined as structures homogeneous along two Cartesian axes. So far, we have considered the structures varying along two Cartesian axes, x and y, characterized by the parameters, $\varepsilon = \varepsilon(x, y)$ and $\mu = \mu(x, y)$ and independent on the z coordinate. In planar structures, these parameters vary along a single axis, identified here with the x axis. We therefore set $\varepsilon = \varepsilon(x)$ and $\mu = \mu(x)$. We will show that under these circumstances that the vector wave equations, Eqs. (3.34), split into two independent pairs.[5] Any solution to the vector wave equations in planar isotropic media can be expressed as a linear combination of the solutions to scalar wave equations for transverse electric (TE) and transverse magnetic (TM) waves.

3.4.1 Scalar wave equation

To derive the scalar wave equation, we start Eqs. (3.34)

$$\mu\nabla \times \left[\mu^{-1}\left(\nabla \times \boldsymbol{E}\right)\right] - \mu\varepsilon\omega^2\boldsymbol{E} = 0, \tag{3.81a}$$

$$\varepsilon\nabla \times \left[\varepsilon^{-1}\left(\nabla \times \boldsymbol{H}\right)\right] - \mu\varepsilon\omega^2\boldsymbol{H} = 0, \tag{3.81b}$$

[5] Weng Cho Chew, *Waves and Fields in Inhomogeneous Media*, IEEE Press Series on Electromagnetic Waves, 1995, p. 45

and assume $\boldsymbol{E}$ and $\boldsymbol{H}$ linearly polarized. We set the axis of non homogeneity into the x axis of a Cartesian coordinate system, i.e., $\varepsilon = \varepsilon(x)$ and $\mu = \mu(x)$. With an appropriate rotation transformation, we set the electric field corresponding to the solution of Eq. (3.81a) for TE waves parallel to y axis, $\boldsymbol{E} = \hat{\boldsymbol{y}} E_y$. With a similar procedure, we set the magnetic field corresponding to the solution of Eq. (3.81b) for TM waves oriented parallel to y axis.

From Eqs. (3.29c) and (3.29d)

$$\nabla \cdot (\varepsilon \boldsymbol{E}) = \nabla \cdot [\varepsilon(x) \hat{\boldsymbol{y}} E_y] = 0\,, \tag{3.82a}$$

$$\nabla \cdot (\mu \boldsymbol{H}) = \nabla \cdot [\mu(x) \hat{\boldsymbol{y}} H_y] = 0\,, \tag{3.82b}$$

it is obvious that the derivatives $\partial \boldsymbol{E}/\partial y = \hat{\boldsymbol{y}} \partial E_y/\partial y$ in Eq. (3.81a) and the derivatives $\partial \boldsymbol{H}/\partial y = \hat{\boldsymbol{y}} \partial H_y/\partial y$ in Eq. (3.81b) are zero,

$$\frac{\partial E_y}{\partial y} = 0 \tag{3.83a}$$

$$\frac{\partial H_y}{\partial y} = 0 \tag{3.83b}$$

We take into account,

$$\nabla \times \boldsymbol{E} = \nabla \times (\hat{\boldsymbol{y}} E_y) = \begin{vmatrix} \hat{\boldsymbol{x}} & \hat{\boldsymbol{y}} & \hat{\boldsymbol{z}} \\ \dfrac{\partial}{\partial x} & \dfrac{\partial}{\partial y} & \dfrac{\partial}{\partial z} \\ 0 & E_y & 0 \end{vmatrix} \tag{3.84a}$$

and,

$$\nabla \times \boldsymbol{H} = \nabla \times (\hat{\boldsymbol{y}} H_y) = \begin{vmatrix} \hat{\boldsymbol{x}} & \hat{\boldsymbol{y}} & \hat{\boldsymbol{z}} \\ \dfrac{\partial}{\partial x} & \dfrac{\partial}{\partial y} & \dfrac{\partial}{\partial z} \\ 0 & H_y & 0 \end{vmatrix} \tag{3.84b}$$

The developments of the first terms in Eqs. (3.81) provide,

$$\mu(x) \left[\nabla \mu^{-1}(x)\right] \times (\nabla \times \boldsymbol{E}) + \nabla \times (\nabla \times \boldsymbol{E}) - \mu(x)\varepsilon(x)\omega^2 \boldsymbol{E} = 0 \tag{3.85a}$$

$$\varepsilon(x) \left[\nabla \varepsilon^{-1}(x)\right] \times (\nabla \times \boldsymbol{H}) + \nabla \times (\nabla \times \boldsymbol{H}) - \mu(x)\varepsilon(x)\omega^2 \boldsymbol{H} = 0 \tag{3.85b}$$

We employ the identity $\nabla\times(\nabla\times\boldsymbol{E}) = \nabla(\nabla\cdot\boldsymbol{E}) - \nabla^2\boldsymbol{E}$ and obtain,

$$\mu(x)\left[\nabla\mu^{-1}(x)\right]\times(\nabla\times\boldsymbol{E}) + \nabla(\nabla\cdot\boldsymbol{E}) - \nabla^2\boldsymbol{E} - \mu(x)\varepsilon(x)\omega^2\boldsymbol{E} = 0 \tag{3.86a}$$

Similarly, by making use of the same identity for $\boldsymbol{H}$ $\nabla\times(\nabla\times\boldsymbol{H}) = \nabla(\nabla\cdot\boldsymbol{H}) - \nabla^2\boldsymbol{H}$ we get

$$\varepsilon(x)\left[\nabla\varepsilon^{-1}(x)\right]\times(\nabla\times\boldsymbol{H}) + \nabla(\nabla\cdot\boldsymbol{H}) - \nabla^2\boldsymbol{H} - \mu(x)\varepsilon(x)\omega^2\boldsymbol{H} = 0 \tag{3.86b}$$

By exploiting the independence of $\boldsymbol{E} = \hat{\boldsymbol{y}}E_y$ and $\boldsymbol{H} = \hat{\boldsymbol{y}}H_y$ on y expressed in Eqs. (3.83), and by making use of Eq. (3.84), we have

$$\hat{\boldsymbol{x}}\mu(x)\frac{\partial\mu^{-1}(x)}{\partial x}\times\left(\hat{\boldsymbol{z}}\frac{\partial E_y}{\partial x} - \hat{\boldsymbol{x}}\frac{\partial E_y}{\partial z}\right) - \hat{\boldsymbol{y}}\frac{\partial^2 E_y}{\partial z^2} - \hat{\boldsymbol{y}}\frac{\partial^2 E_y}{\partial x^2} - \hat{\boldsymbol{y}}\mu(x)\varepsilon(x)\omega^2 E_y = 0 \tag{3.87a}$$

$$\hat{\boldsymbol{x}}\varepsilon(x)\frac{\partial\varepsilon^{-1}(x)}{\partial x}\times\left(\hat{\boldsymbol{z}}\frac{\partial H_y}{\partial x} - \hat{\boldsymbol{x}}\frac{\partial H_y}{\partial z}\right) - \hat{\boldsymbol{y}}\frac{\partial^2 H_y}{\partial z^2} - \hat{\boldsymbol{y}}\frac{\partial^2 H_y}{\partial x^2} - \hat{\boldsymbol{y}}\mu(x)\varepsilon(x)\omega^2 H_y = 0 \tag{3.87b}$$

or,

$$-\hat{\boldsymbol{y}}\mu(x)\frac{\partial\mu^{-1}(x)}{\partial x}\frac{\partial E_y}{\partial x} - \hat{\boldsymbol{y}}\frac{\partial^2 E_y}{\partial z^2} - \hat{\boldsymbol{y}}\frac{\partial^2 E_y}{\partial x^2} - \hat{\boldsymbol{y}}\mu(x)\varepsilon(x)\omega^2 E_y = 0$$

$$-\hat{\boldsymbol{y}}\varepsilon(x)\frac{\partial\varepsilon^{-1}(x)}{\partial x}\frac{\partial H_y}{\partial x} - \hat{\boldsymbol{y}}\frac{\partial^2 H_y}{\partial z^2} - \hat{\boldsymbol{y}}\frac{\partial^2 H_y}{\partial x^2} - \hat{\boldsymbol{y}}\mu(x)\varepsilon(x)\omega^2 H_y = 0$$

We have arrived at scalar equations

$$\mu(x)\frac{\partial\mu^{-1}(x)}{\partial x}\frac{\partial E_y}{\partial x} + \frac{\partial^2 E_y}{\partial z^2} + \frac{\partial^2 E_y}{\partial x^2} + \mu(x)\varepsilon(x)\omega^2 E_y = 0 \tag{3.89a}$$

$$\varepsilon(x)\frac{\partial\varepsilon^{-1}(x)}{\partial x}\frac{\partial H_y}{\partial x} + \frac{\partial^2 H_y}{\partial z^2} + \frac{\partial^2 H_y}{\partial x^2} + \mu(x)\varepsilon(x)\omega^2 H_y = 0 \tag{3.89b}$$

Alternatively, they can be expressed,

$$\mu(x)\frac{\partial}{\partial x}\left[\mu^{-1}(x)\frac{\partial E_y}{\partial x}\right] + \frac{\partial^2 E_y}{\partial z^2} + \mu(x)\varepsilon(x)\omega^2 E_y = 0 \tag{3.90a}$$

$$\varepsilon(x)\frac{\partial}{\partial x}\left[\varepsilon^{-1}(x)\frac{\partial H_y}{\partial x}\right] + \frac{\partial^2 H_y}{\partial z^2} + \mu(x)\varepsilon(x)\omega^2 H_y = 0 \tag{3.90b}$$

or,

$$\left\{\frac{\partial^2}{\partial z^2} + \mu(x)\frac{\partial}{\partial x}\left[\mu^{-1}(x)\frac{\partial}{\partial x}\right] + \mu(x)\varepsilon(x)\omega^2\right\} E_y = 0 \tag{3.91a}$$

$$\left\{\frac{\partial^2}{\partial z^2} + \varepsilon(x)\frac{\partial}{\partial x}\left[\varepsilon^{-1}(x)\frac{\partial}{\partial x}\right] + \mu(x)\varepsilon(x)\omega^2\right\} H_y = 0 \tag{3.91b}$$

From the Maxwell equations, Eqs. (3.29), it follows in planar structures where $\boldsymbol{E} = \hat{\boldsymbol{y}} E_y$,

$$\begin{aligned} \hat{\boldsymbol{z}}\frac{\partial E_y}{\partial x} - \hat{\boldsymbol{x}}\frac{\partial E_y}{\partial z} &= -\mathrm{j}\omega\mu(x)\boldsymbol{H} \\ \hat{\boldsymbol{y}}\frac{\partial H_x}{\partial z} - \hat{\boldsymbol{y}}\frac{\partial H_z}{\partial x} &= \mathrm{j}\omega\varepsilon(x)\hat{\boldsymbol{y}}E_y \end{aligned}$$

that the only remaining non zero field components are H_z and H_x. From the independence of E_y on y, given by Eq. (3.83a) as a conclusion of Eq. (3.82a), it is obvious that both H_z and H_x are independent of y

$$\frac{\partial H_z}{\partial y} = 0\,, \qquad \frac{\partial H_x}{\partial y} = 0$$

In a similar way, we get from the Maxwell equations in planar structures, Eqs. (3.29), where $\boldsymbol{H} = \hat{\boldsymbol{y}} H_y$,

$$\begin{aligned} \hat{\boldsymbol{z}}\frac{\partial H_y}{\partial x} - \hat{\boldsymbol{x}}\frac{\partial H_y}{\partial z} &= \mathrm{j}\omega\varepsilon(x)\boldsymbol{E} \\ \hat{\boldsymbol{y}}\frac{\partial E_x}{\partial z} - \hat{\boldsymbol{y}}\frac{\partial E_z}{\partial x} &= -\mathrm{j}\omega\mu(x)\hat{\boldsymbol{y}}H_y \end{aligned}$$

that the only non zero field components associated with $\boldsymbol{H} = \hat{\boldsymbol{y}} H_y$ are E_z and E_x. From the independence of y of H_y given by Eq. (3.83b) as a consequence of Eq. (3.82b) it is obvious that also the field components E_z and E_x are independent of y,

$$\frac{\partial E_z}{\partial y} = 0\,, \qquad \frac{\partial E_x}{\partial y} = 0\,.$$

In our planar structure with $\varepsilon = \varepsilon(x)$ and $\mu = \mu(x)$, all components of $\boldsymbol{E}$ and $\boldsymbol{H}$ are independent of y. Consequently,

$$\frac{\partial}{\partial y} = 0 \tag{3.92}$$

with the corresponding form of $\nabla = \hat{\boldsymbol{x}}\frac{\partial}{\partial x} + \hat{\boldsymbol{z}}\frac{\partial}{\partial z}$.

Table 3.2: Field in planar structures.

E_x	H_y	E_y	H_x	
$\mathrm{j}\beta$	$-\mathrm{j}\omega\mu$	0	0	$-\dfrac{\mathrm{d}E_z}{\mathrm{d}x}$
$-\mathrm{j}\omega\varepsilon$	$\mathrm{j}\beta$	0	0	0
0	0	$\mathrm{j}\beta$	$\mathrm{j}\omega\mu$	0
0	0	$\mathrm{j}\omega\varepsilon$	$\mathrm{j}\beta$	$-\dfrac{\mathrm{d}H_z}{\mathrm{d}x}$

Table 3.3: TE and TM modes in planar structures.

TE	H_x	E_y	H_z
TM	E_x	H_y	E_z

3.4.2 TE and TM modes

We conclude that in planar structures the set of four Maxwell equations, Eqs. (3.56), for transverse fields splits into two sets of mutually independent sets of two equations as shown in Table 3.2. The six field components are classified into two groups, The TE group with $E_z = 0$ and TM group with $H_z = 0$, according to Table 3.3.

Chapter 4

Optical fibers

4.1 Introduction

Optical fibers represent dielectric cylindrical waveguides most often of circular cross section employed to the propagation of electromagnetic waves in the infrared and visible spectral regions.[1] We wish to determine the conditions for the wave propagation in the optical fibers. As we focus on circular cylindrical waveguides fibers, we employ the Maxwell equation and Helmholtz wave equations in circular cylinder representation. The transverse profile, i.e., the dependence on radial coordinate, ϱ, of the electromagnetic parameters, electric permittivity, $\varepsilon(\varrho)$ and magnetic permeability, $\mu(\varrho)$, may be rather complicated. It is determined by the requirement on the wave mode properties in a particular fiber. The waveguiding in circular cylindrical waveguides similarly to that in planar symmetric waveguides is characterized by zero cut-off frequency/thickness for the fundamental mode.

The analysis can be performed analytically to the highest degree for a waveguide consisting of a homogeneous core and a homogeneous cladding bound by circular cylindrical surfaces with a common axis.[2] Their radii are denoted as a_1 and a_2, $a_1 < a_2$. The homogeneous core region, $0 \le \varrho \le a_1$ is characterized by ε_1 and μ_1 and by a corresponding real index of refraction, n_1. The homogeneous cladding occupies the region $a_1 \le \varrho \le a_2$ characterized by ε_2 and μ_2 and by a corresponding real index of refraction, $n_2 < n_1$ (Figure 4.1). This is a fiber waveguide with a step profile of $\varepsilon(\varrho)$ and $\mu(\varrho)$ i.e., with a step index profile, $n(\varrho)$. The notation may be simplified by taking $a_1 \equiv a$ and by assuming $a_2 \to \infty$. Indeed, in a reasonably designed optical waveguide, the radius, a_2 must be chosen sufficiently high in order to make the evanescent wave penetration into

[1]Optical fibers of elliptical cross sections present interest in the applications where the wave polarization must be stabilized.

[2]D. Marcuse, Light Transmission Optics, Van Nostrand Reinhold Company, New York 1972, pp. 286–305

outer medium negligible. This justifies the approximation $a_2 \to \infty$. The present chapter is devoted to the analysis of this step index profile optical fiber.

4.2 Field equations in circular cylinder coordinates

4.2.1 Unit vectors

The unit vectors in circular cylinder coordinates are related to the Cartesian unit vectors by the relations,

$$\begin{aligned} \hat{\boldsymbol{\varrho}} &= \hat{\boldsymbol{x}}\cos\varphi + \hat{\boldsymbol{y}}\sin\varphi / \cdot \cos\varphi / \cdot \sin\varphi \\ \hat{\boldsymbol{\varphi}} &= -\hat{\boldsymbol{x}}\sin\varphi + \hat{\boldsymbol{y}}\cos\varphi / \cdot (-\sin\varphi) / \cdot \cos\varphi \\ \hat{\boldsymbol{z}} &= \hat{\boldsymbol{z}} \end{aligned} \tag{4.1a}$$

The inverse transformation requires

$$\begin{aligned} \hat{\boldsymbol{\varrho}}\cos\varphi - \hat{\boldsymbol{\varphi}}\sin\varphi &= \hat{\boldsymbol{x}} \\ \hat{\boldsymbol{\varrho}}\sin\varphi + \hat{\boldsymbol{\varphi}}\cos\varphi &= \hat{\boldsymbol{y}} \\ \hat{\boldsymbol{z}} &= \hat{\boldsymbol{z}} \end{aligned} \tag{4.1b}$$

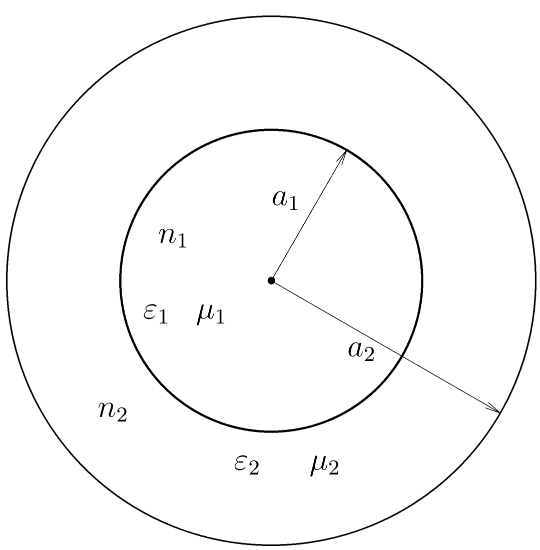

Figure 4.1: Cross section of a circular cylindrical dielectric waveguide.

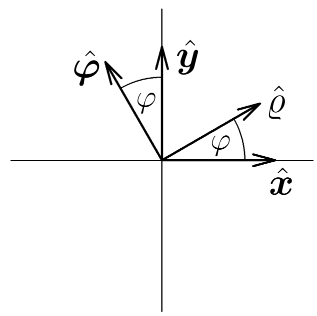

Figure 4.2: Cartesian and circular cylinder unit vectors are related by a transformation of rotation about the z axis. The z axis is perpendicular to the page and the unit vector $\hat{\boldsymbol{z}}$ is oriented out of the page.

The unit vectors, $\hat{\boldsymbol{\varrho}}$ and $\hat{\boldsymbol{\varphi}}$ depend on the azimuthal angle, φ

$$\frac{\partial}{\partial\varphi}\hat{\boldsymbol{\varrho}} = \hat{\boldsymbol{\varphi}}\,, \tag{4.2a}$$

$$\frac{\partial}{\partial\varphi}\hat{\boldsymbol{\varphi}} = -\hat{\boldsymbol{\varrho}} \tag{4.2b}$$

The vector products of unit vectors are given by $\hat{\boldsymbol{\varrho}} \times \hat{\boldsymbol{\varphi}} = \hat{\boldsymbol{z}}$, $\hat{\boldsymbol{\varphi}} \times \hat{\boldsymbol{z}} = \hat{\boldsymbol{\varrho}}$ a $\hat{\boldsymbol{z}} \times \hat{\boldsymbol{\varrho}} = \hat{\boldsymbol{\varphi}}$.

4.2.2 Operator ∇ in circular cylindrical coordinates

Let us remember the operator ∇ in the Cartesian coordinates. For a scalar function of position, $u = u\,(x,\, y,\, z)$, the total differential becomes,

$$\mathrm{d}u = \frac{\partial u}{\partial x}\,\mathrm{d}x + \frac{\partial u}{\partial y}\,\mathrm{d}y + \frac{\partial u}{\partial z}\,\mathrm{d}z$$

product of two vectors,

$$\mathrm{d}u = \mathrm{d}\boldsymbol{r}\cdot\nabla u = (\hat{\boldsymbol{x}}\,\mathrm{d}x + \hat{\boldsymbol{y}}\,\mathrm{d}y + \hat{\boldsymbol{z}}\,\mathrm{d}z)\cdot\left(\hat{\boldsymbol{x}}\,\frac{\partial u}{\partial x} + \hat{\boldsymbol{y}}\,\frac{\partial u}{\partial y} + \hat{\boldsymbol{z}}\frac{\partial u}{\partial z}\right)$$

From this, we can deduced the gradient of the scalar function $u(\boldsymbol{r})$ of a position vector, $\boldsymbol{r} = x\hat{\boldsymbol{x}} + y\hat{\boldsymbol{y}} + z\hat{\boldsymbol{z}}$,

$$\nabla u = \hat{\boldsymbol{x}}\frac{\partial u}{\partial x} + \hat{\boldsymbol{y}}\frac{\partial u}{\partial y} + \hat{\boldsymbol{z}}\frac{\partial u}{\partial z} \tag{4.3}$$

$$\nabla = \hat{\boldsymbol{x}}\frac{\partial}{\partial x} + \hat{\boldsymbol{y}}\frac{\partial}{\partial y} + \hat{\boldsymbol{z}}\frac{\partial}{\partial z} \tag{4.4}$$

the differential operators in circular cylinder coordinates. If $u = u\,(\varrho, \varphi, z)$ represents a scalar function of position, then its total differential becomes,

$$\mathrm{d}u = \frac{\partial u}{\partial \varrho}\,\mathrm{d}\varrho + \frac{\partial u}{\partial \varphi}\,\mathrm{d}\varphi + \frac{\partial u}{\partial z}\,\mathrm{d}z$$

be expressed as a scalar product of two vectors

$$\mathrm{d}u = \mathrm{d}\boldsymbol{r}\cdot\nabla u = (\hat{\boldsymbol{\varrho}}\mathrm{d}\varrho + \hat{\boldsymbol{\varphi}}\varrho\,\mathrm{d}\varphi + \hat{\boldsymbol{z}}\,\mathrm{d}z)\cdot\left(\hat{\boldsymbol{\varrho}}\frac{\partial u}{\partial\varrho} + \hat{\boldsymbol{\varphi}}\frac{1}{\varrho}\frac{\partial u}{\partial\varphi} + \hat{\boldsymbol{z}}\frac{\partial u}{\partial z}\right)$$

From this, it follows for the gradient of a scalar function $u(\boldsymbol{r})$ of a position vector $\boldsymbol{r} = \varrho\hat{\boldsymbol{\varrho}} + z\hat{\boldsymbol{z}}$,

$$\nabla u = \hat{\boldsymbol{\varrho}}\frac{\partial u}{\partial\varrho} + \hat{\boldsymbol{\varphi}}\frac{1}{\varrho}\frac{\partial u}{\partial\varphi} + \hat{\boldsymbol{z}}\frac{\partial u}{\partial z} \tag{4.5}$$

$$\boxed{\nabla = \hat{\boldsymbol{\varrho}}\frac{\partial}{\partial\varrho} + \hat{\boldsymbol{\varphi}}\frac{1}{\varrho}\frac{\partial}{\partial\varphi} + \hat{\boldsymbol{z}}\frac{\partial}{\partial z}} \tag{4.6}$$

To find the relations between the Cartesian and circular cylinder differential operation, we compare the expressions for ∇

$$\nabla_{xyz} = \hat{\boldsymbol{x}}\frac{\partial}{\partial x} + \hat{\boldsymbol{y}}\frac{\partial}{\partial y} + \hat{\boldsymbol{z}}\frac{\partial}{\partial z}. \tag{4.7}$$

and,

$$\nabla_{\varrho\varphi z} = \hat{\boldsymbol{\varrho}}\frac{\partial}{\partial\varrho} + \hat{\boldsymbol{\varphi}}\frac{1}{\varrho}\frac{\partial}{\partial\varphi} + \hat{\boldsymbol{z}}\frac{\partial}{\partial z} \tag{4.8}$$

where $x = \varrho\cos\varphi$, $y = \varrho\sin\varphi$ and $z = z$. The scalar products (Figure 4.2) are given by,

$$\hat{\boldsymbol{\varrho}}\cdot\hat{\boldsymbol{x}} = \cos\varphi,\quad \hat{\boldsymbol{\varphi}}\cdot\hat{\boldsymbol{x}} = -\sin\varphi \tag{4.9a}$$

$$\hat{\boldsymbol{\varrho}}\cdot\hat{\boldsymbol{y}} = \sin\varphi,\quad \hat{\boldsymbol{\varphi}}\cdot\hat{\boldsymbol{y}} = \cos\varphi \tag{4.9b}$$

The derivatives with respect to ϱ and φ can be expressed in terms of the derivatives with respect to x and y,

$$\begin{aligned}\frac{\partial}{\partial\varrho} &= \hat{\boldsymbol{\varrho}}\cdot\nabla_{\varrho\varphi z} = \hat{\boldsymbol{\varrho}}\cdot\nabla_{xyz}\\ &= (\hat{\boldsymbol{\varrho}}\cdot\hat{\boldsymbol{x}})\frac{\partial}{\partial x} + (\hat{\boldsymbol{\varrho}}\cdot\hat{\boldsymbol{y}})\frac{\partial}{\partial y}\\ &= \cos\varphi\frac{\partial}{\partial x} + \sin\varphi\frac{\partial}{\partial y} \qquad (4.10\text{a})\\ \frac{1}{\varrho}\frac{\partial}{\partial\varphi} &= \hat{\boldsymbol{\varphi}}\cdot\nabla_{\varrho\varphi z} = \hat{\boldsymbol{\varphi}}\cdot\nabla_{xyz}\\ &= (\hat{\boldsymbol{\varphi}}\cdot\hat{\boldsymbol{x}})\frac{\partial}{\partial x} + (\hat{\boldsymbol{\varphi}}\cdot\hat{\boldsymbol{y}})\frac{\partial}{\partial y}\\ &= -\sin\varphi\frac{\partial}{\partial x} + \cos\varphi\frac{\partial}{\partial y} \qquad (4.10\text{b})\end{aligned}$$

This can be concisely written in a matrix form,

$$\begin{pmatrix} \dfrac{\partial}{\partial \varrho} \\ \\ \dfrac{1}{\varrho}\dfrac{\partial}{\partial \varphi} \end{pmatrix} = \begin{pmatrix} \cos\varphi & \sin\varphi \\ -\sin\varphi & \cos\varphi \end{pmatrix} \begin{pmatrix} \dfrac{\partial}{\partial x} \\ \\ \dfrac{\partial}{\partial y} \end{pmatrix} \tag{4.11}$$

The inverse transformation, i.e. the derivatives with respect to x and y expressed in terms of the derivatives with respect to ϱ and φ,

$$\begin{aligned} \frac{\partial}{\partial x} &= \hat{\boldsymbol{x}} \cdot \nabla_{xyz} = \hat{\boldsymbol{x}} \cdot \nabla_{\varrho\varphi z} \\ &= (\hat{\boldsymbol{x}} \cdot \hat{\boldsymbol{\varrho}})\frac{\partial}{\partial \varrho} + (\hat{\boldsymbol{x}} \cdot \hat{\boldsymbol{\varphi}})\frac{1}{\varrho}\frac{\partial}{\partial \varphi} \\ &= \cos\varphi\frac{\partial}{\partial \varrho} - \frac{\sin\varphi}{\varrho}\frac{\partial}{\partial \varphi} && (4.12a) \\ \frac{\partial}{\partial y} &= \hat{\boldsymbol{y}} \cdot \nabla_{xyz} = \hat{\boldsymbol{y}} \cdot \nabla_{\varrho\varphi z} \\ &= \sin\varphi\frac{\partial}{\partial \varrho} + \frac{\cos\varphi}{\varrho}\frac{\partial}{\partial \varphi} && (4.12b) \end{aligned}$$

or in a matrix form,

$$\begin{pmatrix} \dfrac{\partial}{\partial x} \\ \\ \dfrac{\partial}{\partial y} \end{pmatrix} = \begin{pmatrix} \cos\varphi & -\sin\varphi \\ \sin\varphi & \cos\varphi \end{pmatrix} \begin{pmatrix} \dfrac{\partial}{\partial \varrho} \\ \\ \dfrac{1}{\varrho}\dfrac{\partial}{\partial \varphi} \end{pmatrix} . \tag{4.13}$$

4.2.3 Vector field in circular cylindrical coordinates

The vector field in circular cylinder coordinates follows from the transformation of the Cartesian field,

$$\begin{aligned} \boldsymbol{A}(\boldsymbol{r}) &= A_x\hat{\boldsymbol{x}} + A_y\hat{\boldsymbol{y}} + A_z\hat{\boldsymbol{z}} \\ &= A_\varrho\hat{\boldsymbol{\varrho}} + A_\varphi\hat{\boldsymbol{\varphi}} + A_z\hat{\boldsymbol{z}} \end{aligned}$$

using the relations (Figures 4.3 and 4.4)

$$\begin{aligned} A_\varrho &= A_x\cos\varphi + A_y\sin\varphi && (4.14a) \\ A_\varphi &= -A_x\sin\varphi + A_y\cos\varphi && (4.14b) \end{aligned}$$

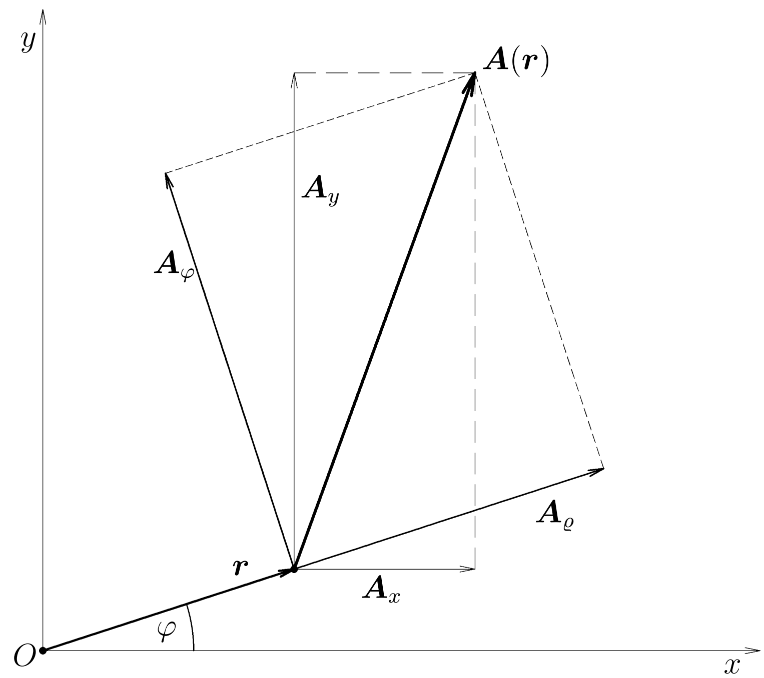

Figure 4.3: The vector field $\boldsymbol{A}(\boldsymbol{r})$ in the point determined by the position vector $\boldsymbol{r} = \varrho\hat{\boldsymbol{\varrho}}$ decomposed into the Cartesian and circular cylinder component.

4.2.4 Maxwell equations

We start from the Maxwell equations in a linear, isotropic, lossless, nondispersive, and homogeneous medium with a zero free charge and free current densities, i.e., in a source free region[3]

$$\begin{aligned}
\nabla \times \boldsymbol{E} &= -\mu \frac{\partial}{\partial t}\boldsymbol{H}\,, \\
\nabla \times \boldsymbol{H} &= \varepsilon \frac{\partial}{\partial t}\boldsymbol{E}\,, \\
\nabla \cdot \boldsymbol{E} &= 0\,, \\
\nabla \cdot \boldsymbol{H} &= 0\,.
\end{aligned}$$

For a time, t, harmonic dependence accounted for by a factor $\exp(\mathrm{j}\omega t)$ the Maxwell equations assume the form,

$$\nabla \times \boldsymbol{E} = -\mathrm{j}\omega\mu\boldsymbol{H}\,, \tag{4.16a}$$

$$\nabla \times \boldsymbol{H} = \mathrm{j}\omega\varepsilon\boldsymbol{E}\,, \tag{4.16b}$$

$$\nabla \cdot \boldsymbol{E} = 0\,, \tag{4.16c}$$

$$\nabla \cdot \boldsymbol{H} = 0\,. \tag{4.16d}$$

[3]The sources responsible for the generation of the field are located outside the considered region.

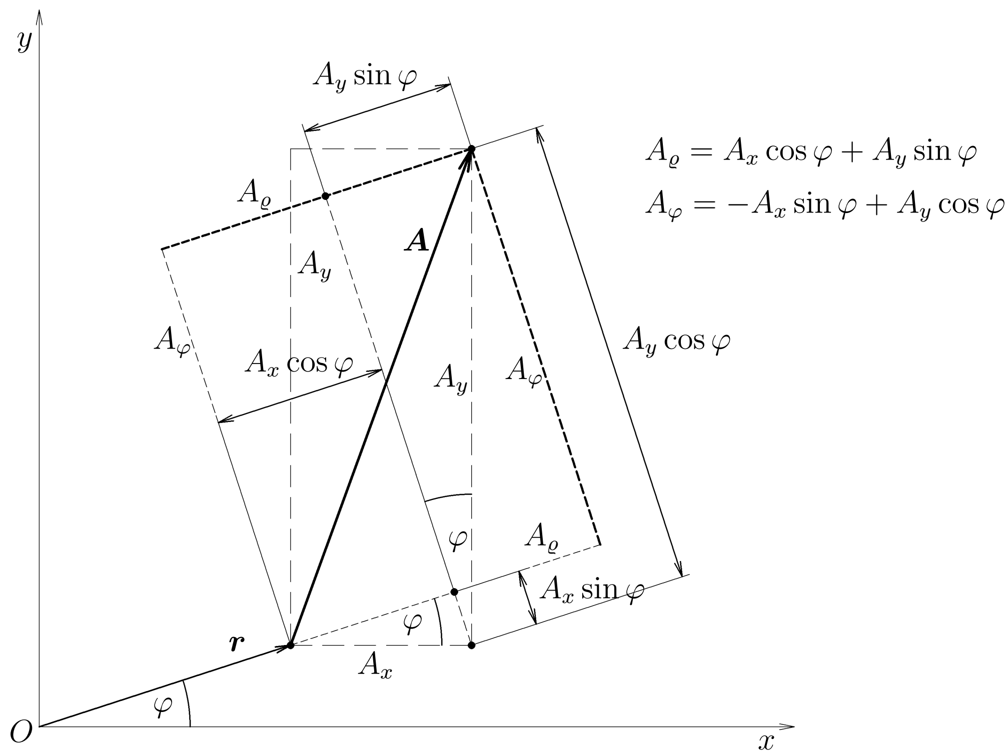

Figure 4.4: A two dimensional Cartesian vector field $\boldsymbol{A}(\boldsymbol{r}) = \boldsymbol{A}\left(x\hat{\boldsymbol{x}} + y\hat{\boldsymbol{y}}\right)$ transformed into the circular cylinder coordinates $\boldsymbol{A}(\boldsymbol{r}) = \boldsymbol{A}(\hat{\boldsymbol{\varrho}}\varrho)$ in the plane perpendicular to the z axis.

The fields can be decomposed into the components parallel to the unit vector of circular cylinder coordinates,

$$\boldsymbol{E} = E_\varrho \hat{\boldsymbol{\varrho}} + E_\varphi \hat{\boldsymbol{\varphi}} + E_z \hat{\boldsymbol{z}} \tag{4.17a}$$

$$\boldsymbol{H} = H_\varrho \hat{\boldsymbol{\varrho}} + H_\varphi \hat{\boldsymbol{\varphi}} + H_z \hat{\boldsymbol{z}} \tag{4.17b}$$

The Maxwell equations (4.16) can be expressed decomposed into the components using Eq. (4.4) for the operator ∇ in circular cylinder coordinates,

$$\frac{1}{\varrho}\frac{\partial}{\partial\varphi}E_z - \frac{\partial}{\partial z}E_\varphi = -\mu\frac{\partial}{\partial t}H_\varrho \tag{4.18a}$$

$$\frac{\partial}{\partial z}E_\varrho - \frac{\partial}{\partial\varrho}E_z = -\mu\frac{\partial}{\partial t}H_\varphi \tag{4.18b}$$

$$\frac{1}{\varrho}\left[\frac{\partial}{\partial\varrho}\left(\varrho E_\varphi\right) - \frac{\partial}{\partial\varphi}E_\varrho\right] = -\mu\frac{\partial}{\partial t}H_z \tag{4.18c}$$

$$\frac{1}{\varrho}\frac{\partial}{\partial\varphi}H_z - \frac{\partial}{\partial z}H_\varphi = \varepsilon\frac{\partial}{\partial t}E_\varrho\,, \tag{4.18d}$$

$$\frac{\partial}{\partial z}H_\varrho - \frac{\partial}{\partial\varrho}H_z = \varepsilon\frac{\partial}{\partial t}E_\varphi\,, \tag{4.18e}$$

$$\frac{1}{\varrho}\left[\frac{\partial}{\partial\varrho}\left(\varrho H_\varphi\right) - \frac{\partial}{\partial\varphi}H_\varrho\right] = \varepsilon\frac{\partial}{\partial t}E_z\,, \tag{4.18f}$$

The dependence of the unit vectors on the azimuthal angle, φ, given in Eqs. (4.2),

$$\frac{\partial}{\partial\varphi}\hat{\boldsymbol{\varrho}} = \hat{\boldsymbol{\varphi}}\,, \tag{4.19a}$$

$$\frac{\partial}{\partial\varphi}\hat{\boldsymbol{\varphi}} = -\hat{\boldsymbol{\varrho}} \tag{4.19b}$$

and the vector products of the unit vectors, i.e., $\hat{\boldsymbol{\varrho}}\times\hat{\boldsymbol{\varphi}} = \hat{\boldsymbol{z}}$, $\hat{\boldsymbol{\varphi}}\times\hat{\boldsymbol{z}} = \hat{\boldsymbol{\varrho}}$ and $\hat{\boldsymbol{z}}\times\hat{\boldsymbol{\varrho}} = \hat{\boldsymbol{\varphi}}$ have been taken into account. In homogeneous media in the absence of free charges, the scalar Maxwell equation, not relevant for the present purpose, take the form

$$\nabla\cdot\boldsymbol{E} = \frac{\partial}{\partial\varrho}E_\varrho + \frac{1}{\varrho}E_\varrho + \frac{1}{\varrho}\frac{\partial}{\partial\varphi}E_\varphi + \frac{\partial}{\partial z}E_z = 0\,, \tag{4.20a}$$

$$\nabla\cdot\boldsymbol{H} = \frac{\partial}{\partial\varrho}H_\varrho + \frac{1}{\varrho}H_\varrho + \frac{1}{\varrho}\frac{\partial}{\partial\varphi}H_\varphi + \frac{\partial}{\partial z}H_z = 0\,. \tag{4.20b}$$

With the restriction to the harmonic time dependence, Eqs. (4.18) are transformed into the form,

$$\frac{1}{\varrho}\frac{\partial}{\partial\varphi}E_z - \frac{\partial}{\partial z}E_\varphi = -\mathrm{j}\omega\mu H_\varrho \tag{4.21a}$$

$$\frac{\partial}{\partial z}E_\varrho - \frac{\partial}{\partial\varrho}E_z = --\mathrm{j}\omega\mu H_\varphi \tag{4.21b}$$

$$\frac{1}{\varrho}\left[\frac{\partial}{\partial\varrho}(\varrho E_\varphi) - \frac{\partial}{\partial\varphi}E_\varrho\right] = -\mathrm{j}\omega\mu H_z \tag{4.21c}$$

$$\frac{1}{\varrho}\frac{\partial}{\partial\varphi}H_z - \frac{\partial}{\partial z}H_\varphi = \mathrm{j}\omega\varepsilon E_\varrho\,, \tag{4.21d}$$

$$\frac{\partial}{\partial z}H_\varrho - \frac{\partial}{\partial\varrho}H_z = \mathrm{j}\omega\varepsilon E_\varphi\,, \tag{4.21e}$$

$$\frac{1}{\varrho}\left[\frac{\partial}{\partial\varrho}(\varrho H_\varphi) - \frac{\partial}{\partial\varphi}H_\varrho\right] = \mathrm{j}\omega\varepsilon E_z\,, \tag{4.21f}$$

The account of the harmonic dependence on both time and the z coordinate expressed by the factor $\exp\mathrm{j}\,(\omega t - \beta z)$ in Eqs. (4.21) provides,

$$\frac{1}{\varrho}\frac{\partial}{\partial\varphi}E_z + \mathrm{j}\beta E_\varphi = -\mathrm{j}\omega\mu H_\varrho \tag{4.22a}$$

$$-\mathrm{j}\beta E_\varrho - \frac{\partial}{\partial\varrho}E_z = -\mathrm{j}\omega\mu H_\varphi \tag{4.22b}$$

$$\frac{1}{\varrho}\left[\frac{\partial}{\partial\varrho}(\varrho E_\varphi) - \frac{\partial}{\partial\varphi}E_\varrho\right] = -\mathrm{j}\omega\mu H_z \tag{4.22c}$$

$$\frac{1}{\varrho}\frac{\partial}{\partial\varphi}H_z + \mathrm{j}\beta H_\varphi = \mathrm{j}\omega\varepsilon E_\varrho\,, \tag{4.22d}$$

$$-\mathrm{j}\beta H_\varrho - \frac{\partial}{\partial\varrho}H_z = \mathrm{j}\omega\varepsilon E_\varphi\,, \tag{4.22e}$$

$$\frac{1}{\varrho}\left[\frac{\partial}{\partial\varrho}(\varrho H_\varphi) - \frac{\partial}{\partial\varphi}H_\varrho\right] = \mathrm{j}\omega\varepsilon E_z\,, \tag{4.22f}$$

The transverse field components, E_ϱ, E_φ, H_ϱ, and H_φ are related to the corresponding Cartesian components,

$$\begin{aligned} E_\varrho &= E_x \cos\varphi + E_y \sin\varphi && \text{(4.23a)} \\ E_\varphi &= -E_x \sin\varphi + E_y \cos\varphi && \text{(4.23b)} \end{aligned}$$

$$\begin{aligned} H_\varrho &= H_x \cos\varphi + H_y \sin\varphi && \text{(4.23c)} \\ H_\varphi &= -H_x \sin\varphi + H_y \cos\varphi && \text{(4.23d)} \end{aligned}$$

We also list the inverse relations, the Cartesian field components, E_x, E_y, H_x, and H_y in terms of the corresponding components E_ϱ, E_φ, H_ϱ, and H_φ

$$\begin{aligned} E_x &= E_\varrho \cos\varphi - E_\varphi \sin\varphi && \text{(4.24a)} \\ E_y &= E_\varrho \sin\varphi + E_\varphi \cos\varphi && \text{(4.24b)} \end{aligned}$$

$$\begin{aligned} H_x &= H_\varrho \cos\varphi - H_\varphi \sin\varphi && \text{(4.24c)} \\ H_y &= H_\varrho \sin\varphi + H_\varphi \cos\varphi && \text{(4.24d)} \end{aligned}$$

The transformation from the Cartesian coordinates into the circular cylinder coordinates, it is advantageous to employ the matrix presented in Eq. (4.11)

$$\mathfrak{R}(\varphi) = \begin{pmatrix} \cos\varphi & \sin\varphi \\ -\sin\varphi & \cos\varphi \end{pmatrix} \tag{4.25}$$

The matrix transforms the unit vectors in Eq. (4.1)

$$\begin{pmatrix} \hat{\boldsymbol{\varrho}} \\ \hat{\boldsymbol{\varphi}} \end{pmatrix} = \begin{pmatrix} \cos\varphi & \sin\varphi \\ -\sin\varphi & \cos\varphi \end{pmatrix} \begin{pmatrix} \hat{\boldsymbol{x}} \\ \hat{\boldsymbol{y}} \end{pmatrix} \tag{4.26}$$

In the matrix form, Eqs. (4.23) can be written as follows,

$$\begin{pmatrix} E_\varrho \\ E_\varphi \end{pmatrix} = \begin{pmatrix} \cos\varphi & \sin\varphi \\ -\sin\varphi & \cos\varphi \end{pmatrix} \begin{pmatrix} E_x \\ E_y \end{pmatrix} \tag{4.27a}$$

$$\begin{pmatrix} H_\varrho \\ H_\varphi \end{pmatrix} = \begin{pmatrix} \cos\varphi & \sin\varphi \\ -\sin\varphi & \cos\varphi \end{pmatrix} \begin{pmatrix} H_x \\ H_y \end{pmatrix} \tag{4.27b}$$

The same 2×2 matrix relates the derivatives of z components in agreement with Eq. (4.11)

$$\begin{pmatrix} \dfrac{\partial E_z}{\partial \varrho} \\[2ex] \dfrac{1}{\varrho}\dfrac{\partial E_z}{\partial \varphi} \end{pmatrix} = \begin{pmatrix} \cos\varphi & \sin\varphi \\ -\sin\varphi & \cos\varphi \end{pmatrix} \begin{pmatrix} \dfrac{\partial E_z}{\partial x} \\[2ex] \dfrac{\partial E_z}{\partial y} \end{pmatrix} \tag{4.28a}$$

$$\begin{pmatrix} \dfrac{\partial H_z}{\partial \varrho} \\ \\ \dfrac{1}{\varrho}\dfrac{\partial H_z}{\partial \varphi} \end{pmatrix} = \begin{pmatrix} \cos\varphi & \sin\varphi \\ -\sin\varphi & \cos\varphi \end{pmatrix} \begin{pmatrix} \dfrac{\partial H_z}{\partial x} \\ \\ \dfrac{\partial H_z}{\partial y} \end{pmatrix} \tag{4.28b}$$

The inverse transform employs the matrix,

$$\mathfrak{R}^{-1}(\varphi) = \begin{pmatrix} \cos\varphi & -\sin\varphi \\ \sin\varphi & \cos\varphi \end{pmatrix} \tag{4.29}$$

The unit vectors transform according to Eq. (4.1)

$$\begin{pmatrix} \hat{\boldsymbol{x}} \\ \hat{\boldsymbol{y}} \end{pmatrix} = \begin{pmatrix} \cos\varphi & -\sin\varphi \\ \sin\varphi & \cos\varphi \end{pmatrix} \begin{pmatrix} \hat{\boldsymbol{\varrho}} \\ \hat{\boldsymbol{\varphi}} \end{pmatrix} \tag{4.30}$$

The transform inverse to the transform in Eqs. (4.27),

$$\begin{pmatrix} E_x \\ E_y \end{pmatrix} = \begin{pmatrix} \cos\varphi & -\sin\varphi \\ \sin\varphi & \cos\varphi \end{pmatrix} \begin{pmatrix} E_\varrho \\ E_\varphi \end{pmatrix} \tag{4.31a}$$

$$\begin{pmatrix} H_x \\ H_y \end{pmatrix} = \begin{pmatrix} \cos\varphi & -\sin\varphi \\ \sin\varphi & \cos\varphi \end{pmatrix} \begin{pmatrix} H_\varrho \\ H_\varphi \end{pmatrix} \tag{4.31b}$$

The transform inverse to the transform of derivatives in Eqs. (4.28) becomes,

$$\begin{pmatrix} \dfrac{\partial E_z}{\partial x} \\ \\ \dfrac{\partial E_z}{\partial y} \end{pmatrix} = \begin{pmatrix} \cos\varphi & -\sin\varphi \\ \sin\varphi & \cos\varphi \end{pmatrix} \begin{pmatrix} \dfrac{\partial E_z}{\partial \varrho} \\ \\ \dfrac{1}{\varrho}\dfrac{\partial E_z}{\partial \varphi} \end{pmatrix} \tag{4.32a}$$

$$\begin{pmatrix} \dfrac{\partial H_z}{\partial x} \\ \\ \dfrac{\partial H_z}{\partial y} \end{pmatrix} = \begin{pmatrix} \cos\varphi & -\sin\varphi \\ \sin\varphi & \cos\varphi \end{pmatrix} \begin{pmatrix} \dfrac{\partial H_z}{\partial \varrho} \\ \\ \dfrac{1}{\varrho}\dfrac{\partial H_z}{\partial \varphi} \end{pmatrix} \tag{4.32b}$$

In the Cartesian coordinates, the transverse field x and y components may be expressed in terms of the derivatives of the longitudinal field components as in Eqs. (3.66) valid for the solutions proportional to the factor $\exp[\mathrm{j}(\omega t - \beta z)]$,

$$E_x = -\mathrm{j}\frac{1}{\omega^2\varepsilon\mu - \beta^2}\left(\beta\frac{\partial E_z}{\partial x} + \omega\mu\frac{\partial H_z}{\partial y}\right) \tag{4.33a}$$

$$E_y = -\mathrm{j}\frac{1}{\omega^2\varepsilon\mu - \beta^2}\left(\beta\frac{\partial E_z}{\partial y} - \omega\mu\frac{\partial H_z}{\partial x}\right) \tag{4.33b}$$

$$H_x = -\mathrm{j}\frac{1}{\omega^2\varepsilon\mu - \beta^2}\left(\beta\frac{\partial H_z}{\partial x} - \omega\varepsilon\frac{\partial E_z}{\partial y}\right) \tag{4.33c}$$

$$H_y = -\mathrm{j}\frac{1}{\omega^2\varepsilon\mu - \beta^2}\left(\beta\frac{\partial H_z}{\partial y} + \omega\varepsilon\frac{\partial E_z}{\partial x}\right) \tag{4.33d}$$

The transform to the circular cylinder coordinates provides,

$$\begin{aligned}
E_\varrho &= E_x\cos\varphi + E_y\sin\varphi \\
&= -\mathrm{j}\frac{1}{\omega^2\varepsilon\mu - \beta^2}\left[\cos\varphi\left(\beta\frac{\partial E_z}{\partial x} + \omega\mu\frac{\partial H_z}{\partial y}\right) + \sin\varphi\left(\beta\frac{\partial E_z}{\partial y} - \omega\mu\frac{\partial H_z}{\partial x}\right)\right] \\
&= -\mathrm{j}\frac{1}{\omega^2\varepsilon\mu - \beta^2}\left[\beta\left(\cos\varphi\frac{\partial E_z}{\partial x} + \sin\varphi\frac{\partial E_z}{\partial y}\right) + \omega\mu\left(\cos\varphi\frac{\partial H_z}{\partial y} - \sin\varphi\frac{\partial H_z}{\partial x}\right)\right] \\
&= -\mathrm{j}\frac{1}{\omega^2\varepsilon\mu - \beta^2}\left[\beta\underbrace{\left(\cos\varphi\frac{\partial}{\partial x} + \sin\varphi\frac{\partial}{\partial y}\right)}_{\frac{\partial}{\partial\varrho}}E_z + \omega\mu\underbrace{\left(\cos\varphi\frac{\partial}{\partial y} - \sin\varphi\frac{\partial}{\partial x}\right)}_{\frac{1}{\varrho}\frac{\partial}{\partial\varphi}}H_z\right] \\
&= -\mathrm{j}\frac{1}{\omega^2\varepsilon\mu - \beta^2}\left(\beta\frac{\partial E_z}{\partial\varrho} + \omega\mu\frac{1}{\varrho}\frac{\partial H_z}{\partial\varphi}\right),
\end{aligned}$$

$$\begin{aligned}
E_\varphi &= -E_x\sin\varphi + E_y\cos\varphi \\
&= -\mathrm{j}\frac{1}{\omega^2\varepsilon\mu - \beta^2}\left[-\sin\varphi\left(\beta\frac{\partial E_z}{\partial x} + \omega\mu\frac{\partial H_z}{\partial y}\right) + \cos\varphi\left(\beta\frac{\partial E_z}{\partial y} - \omega\mu\frac{\partial H_z}{\partial x}\right)\right] \\
&= -\mathrm{j}\frac{1}{\omega^2\varepsilon\mu - \beta^2}\left[\beta\left(-\sin\varphi\frac{\partial E_z}{\partial x} + \cos\varphi\frac{\partial E_z}{\partial y}\right) + \omega\mu\left(\sin\varphi\frac{\partial H_z}{\partial y} + \cos\varphi\frac{\partial H_z}{\partial x}\right)\right] \\
&= -\mathrm{j}\frac{1}{\omega^2\varepsilon\mu - \beta^2}\left[\beta\underbrace{\left(-\sin\varphi\frac{\partial}{\partial x} + \cos\varphi\frac{\partial}{\partial y}\right)}_{\frac{1}{\varrho}\frac{\partial}{\partial\varphi}}E_z + \omega\mu\underbrace{\left(\sin\varphi\frac{\partial}{\partial y} + \cos\varphi\frac{\partial}{\partial x}\right)}_{\frac{\partial}{\partial\varrho}}H_z\right] \\
&= -\mathrm{j}\frac{1}{\omega^2\varepsilon\mu - \beta^2}\left(\beta\frac{1}{\varrho}\frac{\partial E_z}{\partial\varphi} - \omega\mu\frac{\partial H_z}{\partial\varrho}\right)
\end{aligned}$$

The use has been made of Eqs. (4.10).[4] The results for H_ϱ and H_φ follows from the duality transform according to Eq. (3.30).

In summary, the relations for transverse field components are listed bellow,

$$E_\varrho = -\mathrm{j}\frac{1}{\omega^2\varepsilon\mu-\beta^2}\left(\beta\frac{\partial E_z}{\partial\varrho}+\omega\mu\frac{1}{\varrho}\frac{\partial H_z}{\partial\varphi}\right), \tag{4.34a}$$

$$E_\varphi = -\mathrm{j}\frac{1}{\omega^2\varepsilon\mu-\beta^2}\left(\beta\frac{1}{\varrho}\frac{\partial E_z}{\partial\varphi}-\omega\mu\frac{\partial H_z}{\partial\varrho}\right), \tag{4.34b}$$

$$H_\varrho = -\mathrm{j}\frac{1}{\omega^2\varepsilon\mu-\beta^2}\left(\beta\frac{\partial H_z}{\partial\varrho}-\omega\varepsilon\frac{1}{\varrho}\frac{\partial E_z}{\partial\varphi}\right), \tag{4.34c}$$

$$H_\varphi = -\mathrm{j}\frac{1}{\omega^2\varepsilon\mu-\beta^2}\left(\beta\frac{1}{\varrho}\frac{\partial H_z}{\partial\varphi}+\omega\varepsilon\frac{\partial E_z}{\partial\varrho}\right). \tag{4.34d}$$

Alternatively, Eqs. (4.34) can be deduced from Eqs. (3.80) using the transverse gradient operator, $\nabla_t = \hat{\boldsymbol{\varrho}}\frac{\partial}{\partial\varrho}+\hat{\boldsymbol{\varphi}}\frac{1}{\varrho}\frac{\partial}{\partial\varphi}$, extracted from Eq. (4.8).

4.2.5 Helmholtz equations

In linear isotropic homogeneous non dispersive media, the wave equations for the vector wave fields, $\boldsymbol{E}$ and $\boldsymbol{H}$ are given by,

$$\nabla\times(\nabla\times\boldsymbol{E}) = -\mu\varepsilon\frac{\partial^2}{\partial t^2}\boldsymbol{E} \tag{4.35a}$$

$$\nabla\times(\nabla\times\boldsymbol{H}) = -\mu\varepsilon\frac{\partial^2}{\partial t^2}\boldsymbol{H} \tag{4.35b}$$

where $\nabla\times(\nabla\times\boldsymbol{E}) = \nabla(\nabla\cdot\boldsymbol{E})-\nabla^2\boldsymbol{E}$ a $\nabla\times(\nabla\times\boldsymbol{H}) = \nabla(\nabla\cdot\boldsymbol{H})-\nabla^2\boldsymbol{H}$. For $\nabla\cdot\boldsymbol{E}=0$ and $\nabla\cdot\boldsymbol{H}=0$ in the absence of free charges and free currents in homogeneous media according to Eq. (3.41), and the harmonic time dependence of monochromatic wave fields accounted for by the conventional factor $\exp(\mathrm{j}\omega t)$, we get

$$\nabla^2\boldsymbol{E}+\omega^2\mu\varepsilon\boldsymbol{E} = 0 \tag{4.36a}$$

$$\nabla^2\boldsymbol{H}+\omega^2\mu\varepsilon\boldsymbol{H} = 0 \tag{4.36b}$$

Here ∇^2 denotes the Laplacian which in circular cylindrical coordinates assumes the form

$$\nabla^2 = \frac{1}{\varrho}\frac{\partial}{\partial\varrho}\left(\varrho\frac{\partial}{\partial\varrho}\right)+\frac{1}{\varrho^2}\frac{\partial^2}{\partial\varphi^2}+\frac{\partial^2}{\partial z^2}$$

or more conveniently,

$$\boxed{\nabla^2 = \frac{\partial^2}{\partial\varrho^2}+\frac{1}{\varrho}\frac{\partial}{\partial\varrho}+\frac{1}{\varrho^2}\frac{\partial^2}{\partial\varphi^2}+\frac{\partial^2}{\partial z^2}} \tag{4.37}$$

[4] E_φ can be deduced from E_ϱ by the exchange $\frac{\partial}{\partial\varrho}\to\frac{1}{\varrho}\frac{\partial}{\partial\varphi}$ and $\frac{1}{\varrho}\frac{\partial}{\partial\varphi}\to-\frac{\partial}{\partial\varrho}$.

We should not forget to account the dependence of the unit vectors, $\hat{\boldsymbol{\varrho}}$ and $\hat{\boldsymbol{\varphi}}$ on the azimuthal angle, φ, in Eqs. (4.19). The Laplacian, ∇^2 applied to a vector function of position $\boldsymbol{E}(\boldsymbol{r})$ provides,

$$\nabla^2 \boldsymbol{E} = \hat{\boldsymbol{\varrho}}\left(\nabla^2 E_\varrho - \frac{2}{\varrho^2}\frac{\partial E_\varphi}{\partial \varphi} - \frac{E_\varrho}{\varrho^2}\right) + \hat{\boldsymbol{\varphi}}\left(\nabla^2 E_\varphi + \frac{2}{\varrho^2}\frac{\partial E_\varrho}{\partial \varphi} - \frac{E_\varphi}{\varrho^2}\right) + \hat{\boldsymbol{z}}\nabla^2 E_z$$

Equation (4.36a) for the electric field vector developed in circular cylinder components displayed in detail becomes,

$$\begin{aligned}
0 &= \left(\frac{1}{\varrho}\frac{\partial}{\partial \varrho}\varrho\frac{\partial}{\partial \varrho} + \frac{1}{\varrho^2}\frac{\partial^2}{\partial \varphi^2} + \frac{\partial^2}{\partial z^2} + \omega^2\mu\varepsilon\right)\left(\hat{\boldsymbol{\varrho}}E_\varrho + \hat{\boldsymbol{\varphi}}E_\varphi + \hat{\boldsymbol{z}}E_z\right)\\
&= \hat{\boldsymbol{\varrho}}\left[\left(\frac{1}{\varrho}\frac{\partial}{\partial \varrho}\varrho\frac{\partial}{\partial \varrho}\right)E_\varrho + \frac{1}{\varrho^2}\frac{\partial^2}{\partial \varphi^2}E_\varrho + \frac{\partial^2}{\partial z^2}E_\varrho - \frac{1}{\varrho^2}\left(E_\varrho + 2\frac{\partial E_\varphi}{\partial \varphi}\right) + \omega^2\mu\varepsilon E_\varrho\right]\\
&+ \hat{\boldsymbol{\varphi}}\left[\left(\frac{1}{\varrho}\frac{\partial}{\partial \varrho}\varrho\frac{\partial}{\partial \varrho}\right)E_\varphi + \frac{1}{\varrho^2}\frac{\partial^2}{\partial \varphi^2}E_\varphi + \frac{\partial^2}{\partial z^2}E_\varphi - \frac{1}{\varrho^2}\left(E_\varphi - 2\frac{\partial E_\varrho}{\partial \varphi}\right) + \omega^2\mu\varepsilon E_\varphi\right]\\
&+ \hat{\boldsymbol{z}}\left[\left(\frac{1}{\varrho}\frac{\partial}{\partial \varrho}\varrho\frac{\partial}{\partial \varrho}\right)E_z + \frac{1}{\varrho^2}\frac{\partial^2}{\partial \varphi^2}E_z + \frac{\partial^2}{\partial z^2}E_z + \omega^2\mu\varepsilon E_z\right]\\
&= \hat{\boldsymbol{\varrho}}\left[\nabla^2 E_\varrho - \frac{1}{\varrho^2}\left(E_\varrho + 2\frac{\partial E_\varphi}{\partial \varphi}\right) + \omega^2\mu\varepsilon E_\varrho\right]\\
&+ \hat{\boldsymbol{\varphi}}\left[\nabla^2 E_\varphi - \frac{1}{\varrho^2}\left(E_\varphi - 2\frac{\partial E_\varrho}{\partial \varphi}\right) + \omega^2\mu\varepsilon E_\varphi\right]
\end{aligned} \tag{4.38a}$$

The same procedures provides for the vector magnetic field,

$$\nabla^2 \boldsymbol{H} = \hat{\boldsymbol{\varrho}}\left(\nabla^2 H_\varrho - \frac{2}{\varrho^2}\frac{\partial H_\varphi}{\partial \varphi} - \frac{H_\varrho}{\varrho^2}\right) + \hat{\boldsymbol{\varphi}}\left(\nabla^2 H_\varphi + \frac{2}{\varrho^2}\frac{\partial H_\varrho}{\partial \varphi} - \frac{H_\varphi}{\varrho^2}\right) + \hat{\boldsymbol{z}}\nabla^2 H_z$$

After the substitution into Eq. (4.36b), we have,

$$\begin{aligned}
0 &= \left(\frac{1}{\varrho}\frac{\partial}{\partial \varrho}\varrho\frac{\partial}{\partial \varrho} + \frac{1}{\varrho^2}\frac{\partial^2}{\partial \varphi^2} + \frac{\partial^2}{\partial z^2} + \omega^2\mu\varepsilon\right)\left(\hat{\boldsymbol{\varrho}}H_\varrho + \hat{\boldsymbol{\varphi}}H_\varphi + \hat{\boldsymbol{z}}H_z\right)\\
&= \hat{\boldsymbol{\varrho}}\left[\left(\frac{1}{\varrho}\frac{\partial}{\partial \varrho}\varrho\frac{\partial}{\partial \varrho}\right)H_\varrho + \frac{1}{\varrho^2}\frac{\partial^2}{\partial \varphi^2}H_\varrho + \frac{\partial^2}{\partial z^2}H_\varrho - \frac{1}{\varrho^2}\left(H_\varrho + 2\frac{\partial H_\varphi}{\partial \varphi}\right) + \omega^2\mu\varepsilon H_\varrho\right]\\
&+ \hat{\boldsymbol{\varphi}}\left[\left(\frac{1}{\varrho}\frac{\partial}{\partial \varrho}\varrho\frac{\partial}{\partial \varrho}\right)H_\varphi + \frac{1}{\varrho^2}\frac{\partial^2}{\partial \varphi^2}H_\varphi + \frac{\partial^2}{\partial z^2}H_\varphi - \frac{1}{\varrho^2}\left(H_\varphi - 2\frac{\partial H_\varrho}{\partial \varphi}\right) + \omega^2\mu\varepsilon H_\varphi\right]\\
&+ \hat{\boldsymbol{z}}\left[\left(\frac{1}{\varrho}\frac{\partial}{\partial \varrho}\varrho\frac{\partial}{\partial \varrho}\right)H_z + \frac{1}{\varrho^2}\frac{\partial^2}{\partial \varphi^2}H_z + \frac{\partial^2}{\partial z^2}H_z + \omega^2\mu\varepsilon H_z\right]\\
&= \hat{\boldsymbol{\varrho}}\left[\nabla^2 H_\varrho - \frac{1}{\varrho^2}\left(H_\varrho + 2\frac{\partial H_\varphi}{\partial \varphi}\right) + \omega^2\mu\varepsilon H_\varrho\right]\\
&+ \hat{\boldsymbol{\varphi}}\left[\nabla^2 H_\varphi - \frac{1}{\varrho^2}\left(H_\varphi - 2\frac{\partial H_\varrho}{\partial \varphi}\right) + \omega^2\mu\varepsilon H_\varphi\right]\\
&+ \hat{\boldsymbol{z}}\left[\nabla^2 H_z + \omega^2\mu\varepsilon H_z\right]
\end{aligned} \tag{4.38b}$$

In Eq. (4.38a), the component parallel to $\hat{\boldsymbol{\varrho}}$ involves not only the field component E_ϱ, i.e., $E_\varrho(\varrho, \varphi, z, t)$, but also the field component $E_\varphi(\varrho, \varphi, z, t)$. Likewise, the component parallel to $\hat{\boldsymbol{\varphi}}$ contains in addition to the field component $E_\varphi(\varrho, \varphi, z, t)$, the field component $E_\varrho(\varrho, \varphi, z, t)$. The same situation takes place in Eq. (4.38b). The solutions for the harmonic waves traveling parallel to the z axis with the increasing z coordinate applied in the waveguiding studies already employed in Eqs. (3.53) become,

$$\boldsymbol{E} = \boldsymbol{E}_0 \exp\left[\mathrm{j}\left(\omega t - \beta z\right)\right] \tag{4.39a}$$

$$\boldsymbol{H} = \boldsymbol{H}_0 \exp\left[\mathrm{j}\left(\omega t - \beta z\right)\right] \tag{4.39b}$$

We have therefore to confine ourselves to find the solutions for the E_z and H_z components

$$E_z = E_{z0} \exp\left[\mathrm{j}\left(\omega t - \beta z\right)\right] \tag{4.40a}$$

$$H_z = H_{z0} \exp\left[\mathrm{j}\left(\omega t - \beta z\right)\right] \tag{4.40b}$$

and to deduce the transverse components from Eqs. (4.34).

We start from the Helmholtz wave equations,

$$\nabla^2 E_z = \nabla_t^2 E_z + \frac{\partial^2}{\partial z^2} E_z = -\mu\varepsilon\omega^2 E_z \tag{4.41a}$$

$$\nabla^2 H_z = \nabla_t^2 H_z + \frac{\partial^2}{\partial z^2} H_z = -\mu\varepsilon\omega^2 H_z \tag{4.41b}$$

and account for the z dependence according to Eqs. (4.39),

$$\nabla^2 E_z = \nabla_t^2 E_z - \beta^2 E_z = -\mu\varepsilon\omega^2 E_z \tag{4.42a}$$

$$\nabla^2 H_z = \nabla_t^2 H_z - \beta^2 H_z = -\mu\varepsilon\omega^2 H_z \tag{4.42b}$$

We have employed the transverse gradient defined as,

$$\nabla_t = \hat{\boldsymbol{\varrho}} \frac{\partial}{\partial \varrho} + \hat{\boldsymbol{\varphi}} \frac{1}{\varrho} \frac{\partial}{\partial \varphi} \tag{4.43}$$

The transverse component of the Laplacian becomes

$$\nabla_t^2 = \frac{1}{\varrho} \frac{\partial}{\partial \varrho}\left(\varrho \frac{\partial}{\partial \varrho}\right) + \frac{1}{\varrho^2} \frac{\partial^2}{\partial \varphi^2} = \frac{\partial^2}{\partial \varrho^2} + \frac{1}{\varrho} \frac{\partial}{\partial \varrho} + \frac{1}{\varrho^2} \frac{\partial^2}{\partial \varphi^2} \tag{4.44}$$

4.2.6 Wave equations in the core, Bessel functions

The region of the cylinder, $0 \leq \varrho \leq a$, is characterized by the material parameters, μ_1 and ε_1. We make use of the solutions proposed in Eqs. (4.39) and obtain,

$$\begin{aligned} \nabla_t^2 E_z - \beta^2 E_z &= -\mu_1 \varepsilon_1 \omega^2 E_z \\ \nabla_t^2 E_z + \kappa^2 E_z &= 0 \end{aligned} \tag{4.45a}$$

$$\begin{aligned} \nabla_t^2 H_z - \beta^2 H_z &= -\mu_1 \varepsilon_1 \omega^2 H_z \\ \nabla_t^2 H_z + \kappa^2 H_z &= 0 \end{aligned} \tag{4.45b}$$

For $\mu_1 \varepsilon_1 \omega^2 \geq \beta^2$, we define,

$$\mu_1 \varepsilon_1 \omega^2 - \beta^2 = \kappa^2 \tag{4.46}$$

To solve the Helmholtz equations (4.38) with the proposed solution according to Eqs. (4.39), we have to start from the component parallel to $\hat{\boldsymbol{z}}$ containing exclusively a single field component, $E_z(\varrho, \varphi)$, or $H_z(\varrho, \varphi)$

$$\begin{aligned} \nabla^2 E_z + \mu_1 \varepsilon_1 \omega^2 E_z &= 0 \\ \frac{\partial^2 E_z}{\partial \varrho^2} + \frac{1}{\varrho}\frac{\partial E_z}{\partial \varrho} + \frac{1}{\varrho^2}\frac{\partial^2 E_z}{\partial \varphi^2} + \frac{\partial^2 E_z}{\partial z^2} + \mu_1 \varepsilon_1 \omega^2 E_z &= 0 \\ \frac{\partial^2 E_z}{\partial \varrho^2} + \frac{1}{\varrho}\frac{\partial E_z}{\partial \varrho} + \frac{1}{\varrho^2}\frac{\partial^2 E_z}{\partial \varphi^2} - \beta^2 E_z + \mu_1 \varepsilon_1 \omega^2 E_z &= 0 \\ \frac{\partial^2 E_z}{\partial \varrho^2} + \frac{1}{\varrho}\frac{\partial E_z}{\partial \varrho} + \frac{1}{\varrho^2}\frac{\partial^2 E_z}{\partial \varphi^2} + \kappa^2 E_z &= 0 \end{aligned} \tag{4.47a}$$

$$\begin{aligned} \nabla^2 H_z + \mu_1 \varepsilon_1 \omega^2 H_z &= 0 \\ \frac{\partial^2 H_z}{\partial \varrho^2} + \frac{1}{\varrho}\frac{\partial H_z}{\partial \varrho} + \frac{1}{\varrho^2}\frac{\partial^2 H_z}{\partial \varphi^2} + \frac{\partial^2 H_z}{\partial z^2} + \mu_1 \varepsilon_1 \omega^2 H_z &= 0 \\ \frac{\partial^2 H_z}{\partial \varrho^2} + \frac{1}{\varrho}\frac{\partial H_z}{\partial \varrho} + \frac{1}{\varrho^2}\frac{\partial^2 H_z}{\partial \varphi^2} - \beta^2 H_z + \mu_1 \varepsilon_1 \omega^2 H_z &= 0 \\ \frac{\partial^2 H_z}{\partial \varrho^2} + \frac{1}{\varrho}\frac{\partial H_z}{\partial \varrho} + \frac{1}{\varrho^2}\frac{\partial^2 H_z}{\partial \varphi^2} + \kappa^2 H_z &= 0 \end{aligned} \tag{4.47b}$$

In summary, we have the following results. The fields $E_\varrho(\varrho, \varphi)$, $E_\varphi(\varrho, \varphi)$, $H_\varrho(\varrho, \varphi)$, and $H_\varphi(\varrho,\varphi)$ are given by Eqs. (4.34) with the substitutions according to Eqs. (4.46)

$$\begin{aligned}
E_\varrho &= -\mathrm{j}\frac{1}{\kappa^2}\left(\beta\frac{\partial E_z}{\partial\varrho}+\omega\mu_1\frac{1}{\varrho}\frac{\partial H_z}{\partial\varphi}\right), && (4.48a)\\
E_\varphi &= -\mathrm{j}\frac{1}{\kappa^2}\left(\beta\frac{1}{\varrho}\frac{\partial E_z}{\partial\varphi}-\omega\mu_1\frac{\partial H_z}{\partial\varrho}\right), && (4.48b)\\
H_\varrho &= -\mathrm{j}\frac{1}{\kappa^2}\left(\beta\frac{\partial H_z}{\partial\varrho}-\omega\varepsilon_1\frac{1}{\varrho}\frac{\partial E_z}{\partial\varphi}\right), && (4.48c)\\
H_\varphi &= -\mathrm{j}\frac{1}{\kappa^2}\left(\beta\frac{1}{\varrho}\frac{\partial H_z}{\partial\varphi}+\omega\varepsilon_1\frac{\partial E_z}{\partial\varrho}\right). && (4.48d)
\end{aligned}$$

The fields $E_z(\varrho,\varphi)$ and $H_z(\varrho,\varphi)$ are the solutions of the partial differential equations (4.47)

$$\begin{aligned}
\frac{\partial^2 E_z}{\partial\varrho^2}+\frac{1}{\varrho}\frac{\partial E_z}{\partial\varrho}+\frac{1}{\varrho^2}\frac{\partial^2 E_z}{\partial\varphi^2}+\kappa^2 E_z &= 0 && (4.49a)\\
\frac{\partial^2 H_z}{\partial\varrho^2}+\frac{1}{\varrho}\frac{\partial H_z}{\partial\varrho}+\frac{1}{\varrho^2}\frac{\partial^2 H_z}{\partial\varphi^2}+\kappa^2 H_z &= 0 && (4.49b)
\end{aligned}$$

or in a concise form, still in circular cylinder coordinates, using Eq. (4.44)

$$\begin{aligned}
\nabla_t^2 E_z+\kappa^2 E_z &= 0 && (4.50a)\\
\nabla_t^2 H_z+\kappa^2 H_z &= 0 && (4.50b)
\end{aligned}$$

We have already removed the second derivatives with respect to t and z of the fields in the wave equations (4.36) using the proposed solutions given in Eqs. (4.39)

$$\begin{aligned}
\frac{\partial^2 E_z(\varrho,\varphi,z,t)}{\partial t^2} &= -\omega^2 E_z(\varrho,\varphi,z,t) && (4.51a)\\
\frac{\partial^2 H_z(\varrho,\varphi,z,t)}{\partial t^2} &= -\omega^2 H_z(\varrho,\varphi,z,t) && (4.51b)\\
\frac{\partial^2 E_z(\varrho,\varphi,z,t)}{\partial z^2} &= -\beta^2 E_z(\varrho,\varphi,z,t) && (4.51c)\\
\frac{\partial^2 H_z(\varrho,\varphi,z,t)}{\partial z^2} &= -\beta^2 H_z(\varrho,\varphi,z,t) && (4.51d)
\end{aligned}$$

Next we choose the dependence on φ according to the requirement where the transform $\varphi\to\varphi+2\pi$ should not change the φ dependence of the fields. For a Laplace product as a choice for the solution of the partial differential equations, here the wave equations (4.36), we take

$$\begin{aligned}
E_z(\varrho,\varphi,z,t) &= E_z(\varrho)\,\mathrm{e}^{\mathrm{j}\nu\varphi}\exp\left[\mathrm{j}(\omega t-\beta z)\right] && (4.52a)\\
H_z(\varrho,\varphi,z,t) &= H_z(\varrho)\,\mathrm{e}^{\mathrm{j}\nu\varphi}\exp\left[\mathrm{j}(\omega t-\beta z)\right] && (4.52b)
\end{aligned}$$

where ν must be an integer. The solutions to the transverse components take the same form which follow from Eqs. (4.34),

$$\begin{aligned}
E_\varrho(\varrho,\varphi,z,t) &= E_\varrho(\varrho)\,\mathrm{e}^{\mathrm{j}\nu\varphi}\exp\left[\mathrm{j}\left(\omega t-\beta z\right)\right] && \text{(4.53a)}\\
E_\varphi(\varrho,\varphi,z,t) &= E_\varphi(\varrho)\,\mathrm{e}^{\mathrm{j}\nu\varphi}\exp\left[\mathrm{j}\left(\omega t-\beta z\right)\right] && \text{(4.53b)}\\
H_\varrho(\varrho,\varphi,z,t) &= H_\varrho(\varrho)\,\mathrm{e}^{\mathrm{j}\nu\varphi}\exp\left[\mathrm{j}\left(\omega t-\beta z\right)\right] && \text{(4.53c)}\\
H_\varphi(\varrho,\varphi,z,t) &= H_\varphi(\varrho)\,\mathrm{e}^{\mathrm{j}\nu\varphi}\exp\left[\mathrm{j}\left(\omega t-\beta z\right)\right] && \text{(4.53d)}
\end{aligned}$$

We can now eliminate the derivatives with respect to φ using the proposed dependence in the form of a factor $\exp(\mathrm{j}\nu\varphi)$ .The substitution into Eq. (4.38a) according to Eq. (4.52a), and the account of $\dfrac{\partial}{\partial\varphi}\rightarrow \mathrm{j}\nu$ and $\dfrac{\partial^2}{\partial z^2}\rightarrow -\beta^2$ provides,

$$\begin{aligned}
&\left(\frac{1}{\varrho}\frac{\partial}{\partial\varrho}\varrho\frac{\partial}{\partial\varrho}+\frac{1}{\varrho^2}\frac{\partial^2}{\partial\varphi^2}+\frac{\partial^2}{\partial z^2}+\omega^2\mu\varepsilon\right)\left(\hat{\boldsymbol{\varrho}}E_\varrho+\hat{\boldsymbol{\varphi}}E_\varphi+\hat{\boldsymbol{z}}E_z\right)\\
&= \hat{\boldsymbol{\varrho}}\left[\left(\frac{1}{\varrho}\frac{\mathrm{d}}{\mathrm{d}\varrho}\varrho\frac{\mathrm{d}}{\mathrm{d}\varrho}\right)E_\varrho-\frac{1}{\varrho^2}\left(E_\varrho+2\mathrm{j}\nu E_\varphi\right)+\left(\omega^2\mu\varepsilon-\beta^2-\frac{\nu^2}{\varrho^2}\right)E_\varrho\right]\\
&+ \hat{\boldsymbol{\varphi}}\left[\left(\frac{1}{\varrho}\frac{\mathrm{d}}{\mathrm{d}\varrho}\varrho\frac{\mathrm{d}}{\mathrm{d}\varrho}\right)E_\varphi-\frac{1}{\varrho^2}\left(E_\varphi-2\mathrm{j}\nu E_\varrho\right)+\left(\omega^2\mu\varepsilon-\beta^2-\frac{\nu^2}{\varrho^2}\right)E_\varphi\right]\\
&+ \hat{\boldsymbol{z}}\left[\left(\frac{1}{\varrho}\frac{\mathrm{d}}{\mathrm{d}\varrho}\varrho\frac{\mathrm{d}}{\mathrm{d}\varrho}\right)E_z+\left(\omega^2\mu\varepsilon-\beta^2-\frac{\nu^2}{\varrho^2}\right)E_z\right]\\
&= \hat{\boldsymbol{\varrho}}\left[\left(\frac{1}{\varrho}\frac{\mathrm{d}}{\mathrm{d}\varrho}\varrho\frac{\mathrm{d}}{\mathrm{d}\varrho}\right)E_\varrho-\frac{2\mathrm{j}\nu}{\varrho^2}E_\varphi+\left(\omega^2\mu\varepsilon-\beta^2-\frac{\nu^2+1}{\varrho^2}\right)E_\varrho\right]\\
&+ \hat{\boldsymbol{\varphi}}\left[\left(\frac{1}{\varrho}\frac{\mathrm{d}}{\mathrm{d}\varrho}\varrho\frac{\mathrm{d}}{\mathrm{d}\varrho}\right)E_\varphi+\frac{2\mathrm{j}\nu}{\varrho^2}E_\varrho+\left(\omega^2\mu\varepsilon-\beta^2-\frac{\nu^2+1}{\varrho^2}\right)E_\varphi\right]\\
&+ \hat{\boldsymbol{z}}\left[\left(\frac{1}{\varrho}\frac{\mathrm{d}}{\mathrm{d}\varrho}\varrho\frac{\mathrm{d}}{\mathrm{d}\varrho}\right)E_z+\left(\omega^2\mu\varepsilon-\beta^2-\frac{\nu^2}{\varrho^2}\right)E_z\right] \qquad \text{(4.54)}
\end{aligned}$$

In a similar way, we can transform Eq. (4.38b) with the help of Eq. (4.52b).

Equations (4.49a) and (4.49b) are reduced to ordinary differential equations, so called *Bessel–Euler equations* for $E_z(\varrho)$ and $H_z(\varrho)$ with a variable ϱ ,

$$\frac{\mathrm{d}^2E_z}{\mathrm{d}\varrho^2}+\frac{1}{\varrho}\frac{\mathrm{d}E_z}{\mathrm{d}\varrho}+\left(\kappa^2-\frac{\nu^2}{\varrho^2}\right)E_z = 0 \qquad \text{(4.55a)}$$

$$\frac{\mathrm{d}^2H_z}{\mathrm{d}\varrho^2}+\frac{1}{\varrho}\frac{\mathrm{d}H_z}{\mathrm{d}\varrho}+\left(\kappa^2-\frac{\nu^2}{\varrho^2}\right)H_z = 0 \qquad \text{(4.55b)}$$

Alternatively, these equations are expressed with a dimensionless variable $\kappa\varrho$ as $E_z(\kappa\varrho)$ and $H_z(\kappa\varrho)$

$$(\kappa\varrho)^2\frac{\mathrm{d}^2}{\mathrm{d}(\kappa\varrho)^2}E_z+(\kappa\varrho)\frac{\mathrm{d}}{\mathrm{d}(\kappa\varrho)}E_z+\left[(\kappa\varrho)^2-\nu^2\right]E_z = 0 \qquad \text{(4.56a)}$$

$$(\kappa\varrho)^2\frac{\mathrm{d}^2}{\mathrm{d}(\kappa\varrho)^2}H_z+(\kappa\varrho)\frac{\mathrm{d}}{\mathrm{d}(\kappa\varrho)}H_z+\left[(\kappa\varrho)^2-\nu^2\right]H_z = 0 \qquad \text{(4.56b)}$$

The Laplace product as a solutions of the wave equations (4.36) in a more specific notation becomes,

$$E_z^{(\nu)}(\kappa\varrho, \varphi, z, t) = E_z^{(\nu)}(\kappa\varrho)\,\mathrm{e}^{\mathrm{j}\nu\varphi}\exp\left[\mathrm{j}\left(\omega t - \beta^{(\nu)} z\right)\right] \tag{4.57a}$$

$$H_z^{(\nu)}(\kappa\varrho, \varphi, z, t) = H_z^{(\nu)}(\kappa\varrho)\,\mathrm{e}^{\mathrm{j}\nu\varphi}\exp\left[\mathrm{j}\left(\omega t - \beta^{(\nu)} z\right)\right] \tag{4.57b}$$

In the mathematical analysis, the Bessel–Euler equation is written as

$$\boxed{x^2\frac{\mathrm{d}^2 y}{\mathrm{d}x^2} + x\frac{\mathrm{d}y}{\mathrm{d}x} + \left(x^2 - \nu^2\right)y = 0\,.} \tag{4.58}$$

or

$$\frac{\mathrm{d}^2 y}{\mathrm{d}x^2} + \frac{1}{x}\frac{\mathrm{d}y}{\mathrm{d}x} + \left(1 - \frac{\nu^2}{x^2}\right)y = 0\,. \tag{4.59}$$

It can be transformed in the form

$$x\frac{\mathrm{d}}{\mathrm{d}x}\left(x\frac{\mathrm{d}y}{\mathrm{d}x}\right) + \left(x^2 - \nu^2\right)y = 0\,. \tag{4.60}$$

It is a second order homogeneous ordinary differential linear equation which has two linearly independent solutions. One of them is represented by the Bessel function (of the order ν), i.e., $\mathcal{J}_\nu(\kappa\varrho)$ (also the Bessel function of the first kind),

$$\boxed{\mathcal{J}_\nu(\kappa\varrho) = \sum_{q=0}^{\infty}\frac{(-1)^q}{q!(q+\nu)!}\left(\frac{\kappa\varrho}{2}\right)^{\nu+2q}} \tag{4.61}$$

The second solution is represented by the Neumann function (of the order ν), i.e., $\mathcal{N}_\nu(\kappa\varrho)$ (also the Bessel function of the second kind)

$$\begin{aligned}
\mathcal{N}_\nu(\kappa\varrho) &= \frac{2}{\pi}\ln\left(\frac{\Upsilon\kappa\varrho}{2}\right)\mathcal{J}_\nu(\kappa\varrho) \\
&- \frac{1}{\pi}\left(\frac{\kappa\varrho}{2}\right)^{-\nu}\sum_{q=0}^{\nu-1}\frac{(\nu-q-1)!}{q!}\left(\frac{\kappa\varrho}{2}\right)^{2q} \\
&- \frac{1}{\pi}\left(\frac{\kappa\varrho}{2}\right)^{\nu}\sum_{q=0}^{\infty}\frac{(-1)^q}{q!\,(q+\nu)!}\left(\sum_{s=1}^{q}\frac{1}{s} + \sum_{s=1}^{q+\nu}\frac{1}{s}\right)\left(\frac{\kappa\varrho}{2}\right)^{2q}
\end{aligned} \tag{4.62}$$

At $q = 0$, the sum $\sum_{s=1}^{q}\frac{1}{s}$ is zero. Here $\Upsilon = \exp\upsilon \approx 1,78107$ with,

$$\upsilon = \lim_{m\to\infty}\left[\sum_{s=1}^{m}\left(\frac{1}{s} - \ln s\right)\right] \approx \frac{228}{395} \approx 0,5772157$$

υ is the Euler–Mascheroni constant.[5]

The solutions to the Bessel equation can be alternatively expressed in terms of Hankel functions (also the Bessel functions of the third kind). The Hankel functions in a modified form are important in our analysis as they will be employed as solutions in the region $a \leq \varrho < \infty$. The Hankel functions of the first and second kind (of the order ν) are denoted as $\mathcal{H}_{\nu}^{(1)}(\kappa\varrho)$ and $\mathcal{H}_{\nu}^{(2)}(\kappa\varrho)$, respectively. They are related to the previous solutions by the relations,

$$\mathcal{H}_{\nu}^{(1)}(\kappa\varrho) = \mathcal{J}_{\nu}(\kappa\varrho) + \mathrm{j}\mathcal{N}_{\nu}(\kappa\varrho) \tag{4.63a}$$

$$\mathcal{H}_{\nu}^{(2)}(\kappa\varrho) = \mathcal{J}_{\nu}(\kappa\varrho) - \mathrm{j}\mathcal{N}_{\nu}(\kappa\varrho) \tag{4.63b}$$

The Bessel functions, Neumann functions, and Hankel functions belong to the family of cylindrical functions (of the order ν). In general, the order of cylindrical functions need not be an integer. However, for our purpose we are restricted to the case where ν is an integer, as required by the condition expressed in Eq. (4.52). The restriction to integer ν complicates the search for the second solution represented by the Neumann function.

The general cylindrical functions are denoted as $\mathcal{Z}_{\nu}(\kappa\varrho)$. The Bessel functions of the zero and first order are shown in Figure 4.5. Figures 4.6–4.8 compare the Bessel and Neumann functions of the zero and first order. The higher order Bessel functions are shown in Figure 4.9.

4.2.7 Wave equations in the cladding. Hankel functions

The outer region, $a \leq \varrho < \infty$, is characterized by the material parameters μ_2 and ε_2 . We are interested in the solutions pertinent to the waveguide modes in the fibers and require the solutions for the region $a \leq \varrho < \infty$ in the form of evanescent waves of amplitudes sufficiently quickly decaying with the distance $\varrho \to \infty$ from the fiber axis z . The transverse fields, $E_{\varrho}(\varrho, \varphi)$, $E_{\varphi}(\varrho, \varphi)$, $H_{\varrho}(\varrho, \varphi)$, and $H_{\varphi}(\varrho, \varphi)$ follow from Eqs. (4.34) after the substitution for $\omega^2\varepsilon\mu - \beta^2 = \omega^2\varepsilon_2\mu_2 - \beta^2 = -\gamma^2$ or from the Eqs. (4.49) by the exchange $\kappa \to \mathrm{j}\gamma$.

[5] In the convention notation, the Eulero–Mascheroni constant is denoted as γ . In the present electromagnetic theory of dielectric waveguides, the symbol γ is employed for the transverse damping constant. We therefore represent the Euler–Mascheroni constant by υ and define $\Upsilon = \mathrm{e}^{\upsilon}$.

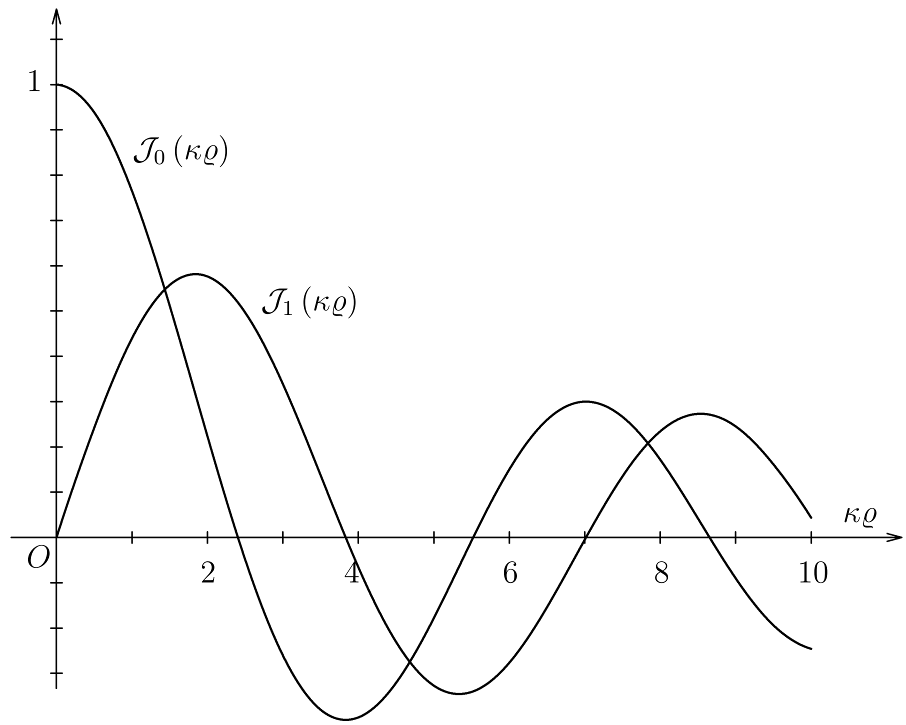

Figure 4.5: Plot of the Bessel functions of the zero and first order, $\mathcal{J}_0(\kappa\varrho)$ and $\mathcal{J}_1(\kappa\varrho)$.

We get

$$E_\varrho = \mathrm{j}\frac{1}{\gamma^2}\left(\beta\frac{\partial E_z}{\partial\varrho} + \omega\mu_2\frac{1}{\varrho}\frac{\partial H_z}{\partial\varphi}\right), \tag{4.64a}$$

$$E_\varphi = \mathrm{j}\frac{1}{\gamma^2}\left(\beta\frac{1}{\varrho}\frac{\partial E_z}{\partial\varphi} - \omega\mu_2\frac{\partial H_z}{\partial\varrho}\right), \tag{4.64b}$$

$$H_\varrho = \mathrm{j}\frac{1}{\gamma^2}\left(\beta\frac{\partial H_z}{\partial\varrho} - \omega\varepsilon_2\frac{1}{\varrho}\frac{\partial E_z}{\partial\varphi}\right), \tag{4.64c}$$

$$H_\varphi = \mathrm{j}\frac{1}{\gamma^2}\left(\beta\frac{1}{\varrho}\frac{\partial H_z}{\partial\varphi} + \omega\varepsilon_2\frac{\partial E_z}{\partial\varrho}\right). \tag{4.64d}$$

The fields $E_z(\varrho,\varphi)$ and $H_z(\varrho,\varphi)$ are the solutions to the partial differential equations,

$$\frac{\partial^2 E_z}{\partial\varrho^2} + \frac{1}{\varrho}\frac{\partial E_z}{\partial\varrho} + \frac{1}{\varrho^2}\frac{\partial^2 E_z}{\partial\varphi^2} - \gamma^2 E_z = 0 \tag{4.65a}$$

$$\frac{\partial^2 H_z}{\partial\varrho^2} + \frac{1}{\varrho}\frac{\partial H_z}{\partial\varrho} + \frac{1}{\varrho^2}\frac{\partial^2 H_z}{\partial\varphi^2} - \gamma^2 H_z = 0 \tag{4.65b}$$

or in a more concise notation,

$$\nabla_t^2 E_z - \gamma^2 E_z = 0 \tag{4.66a}$$

$$\nabla_t^2 H_z - \gamma^2 H_z = 0 \tag{4.66b}$$

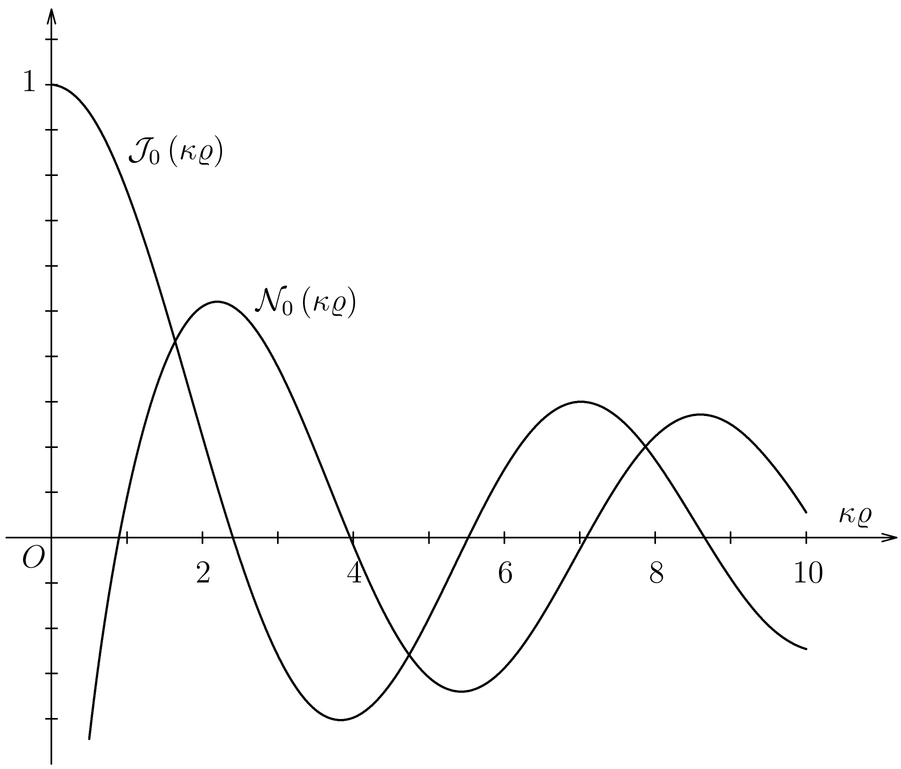

Figure 4.6: Plot of the Bessel and Neumann functions of the zero order, $\mathcal{J}_0(\kappa\varrho)$ and $\mathcal{N}_0(\kappa\varrho)$.

The diffusion equations (4.65) and (4.66) follow from the wave equations (4.49) and (4.50) by the same exchange $\kappa \to \mathrm{j}\gamma$.[6] The required solution for the fields $E_z(\varrho,\varphi)$ and $H_z(\varrho,\varphi)$ sufficiently quickly decaying with $\varrho \to \infty$, corresponding to the evanescent waves represent the solution to the modified Bessel equation,

$$\boxed{x^2 \frac{\mathrm{d}^2 \mathrm{y}}{\mathrm{d}x^2} + x\frac{\mathrm{d}y}{\mathrm{d}x} - \left(x^2+\nu^2\right) y = 0}. \tag{4.67}$$

which can be deduced from Eq. (4.58) by the exchange $x \to \mathrm{j}x$. For our purpose, we write them in a way similar to that already employed in Eqs. (4.55)

$$\frac{\mathrm{d}^2 E_z}{\mathrm{d}\varrho^2} + \frac{1}{\varrho}\frac{\mathrm{d}E_z}{\mathrm{d}\varrho} - \left(\gamma^2 + \frac{\nu^2}{\varrho^2}\right) E_z = 0 \tag{4.68a}$$

$$\frac{\mathrm{d}^2 H_z}{\mathrm{d}\varrho^2} + \frac{1}{\varrho}\frac{\mathrm{d}H_z}{\mathrm{d}\varrho} - \left(\gamma^2 + \frac{\nu^2}{\varrho^2}\right) H_z = 0 \tag{4.68b}$$

or to the Bessel equation with a dimensionless variable, in a close analogy with the rep-

[6] The replacement of the real parameter κ by an imaginary pure one, $\mathrm{j}\gamma$ transforms the Helmholtz wave equation into a diffuse equation. The solutions to the Helmholtz equations are the Bessel functions, the solutions to the diffuse equations are the modified (or hyperbolic) Bessel functions.

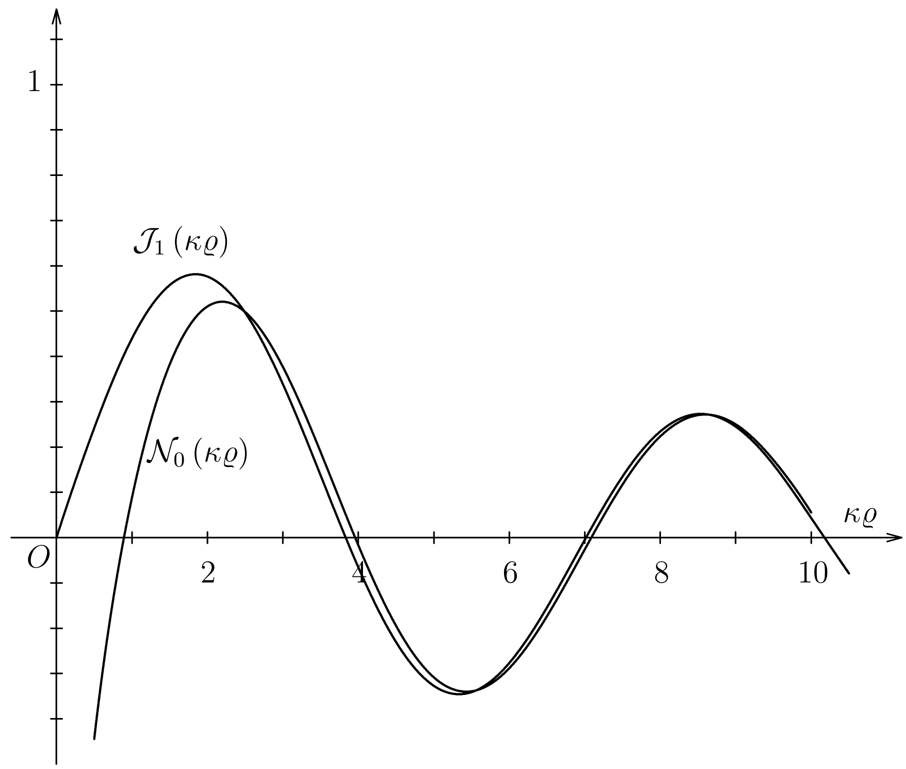

Figure 4.7: The Bessel function of the first order, $\mathcal{J}_1(\kappa\varrho)$ and the Neumann function of the zero order, $\mathcal{N}_0(\kappa\varrho)$.

resentation in Eqs. (4.56)

$$(\mathrm{j}\gamma\varrho)^2 \frac{\mathrm{d}^2 E_z}{\mathrm{d}(\mathrm{j}\gamma\varrho)^2} + (\mathrm{j}\gamma\varrho)\frac{\mathrm{d}E_z}{\mathrm{d}(\mathrm{j}\gamma\varrho)} + \left[(\mathrm{j}\gamma\varrho)^2 - \nu^2\right] E_z = 0 \tag{4.69a}$$

$$(\mathrm{j}\gamma\varrho)^2 \frac{\mathrm{d}^2 H_z}{\mathrm{d}(\mathrm{j}\gamma\varrho)^2} + (\mathrm{j}\gamma\varrho)\frac{\mathrm{d}H_z}{\mathrm{d}(\mathrm{j}\gamma\varrho)} + \left[(\mathrm{j}\gamma\varrho)^2 - \nu^2\right] H_z = 0 \tag{4.69b}$$

After the removal of the imaginary unit j,

$$(\gamma\varrho)^2 \frac{\mathrm{d}^2 E_z}{\mathrm{d}(\gamma\varrho)^2} + (\gamma\varrho)\frac{\mathrm{d}E_z}{\mathrm{d}(\gamma\varrho)} - \left[(\gamma\varrho)^2 + \nu^2\right] E_z = 0\,, \tag{4.70a}$$

$$(\gamma\varrho)^2 \frac{\mathrm{d}^2 H_z}{\mathrm{d}(\gamma\varrho)^2} + (\gamma\varrho)\frac{\mathrm{d}H_z}{\mathrm{d}(\gamma\varrho)} - \left[(\gamma\varrho)^2 + \nu^2\right] H_z = 0\,. \tag{4.70b}$$

We have started from the equations corresponding to Eqs. (4.45)

$$\begin{aligned} \nabla_t^2 E_z - \beta^2 E_z &= -\mu\varepsilon\omega^2 E_z \\ \nabla_t^2 E_z - \gamma^2 E_z &= 0 \end{aligned} \tag{4.71a}$$

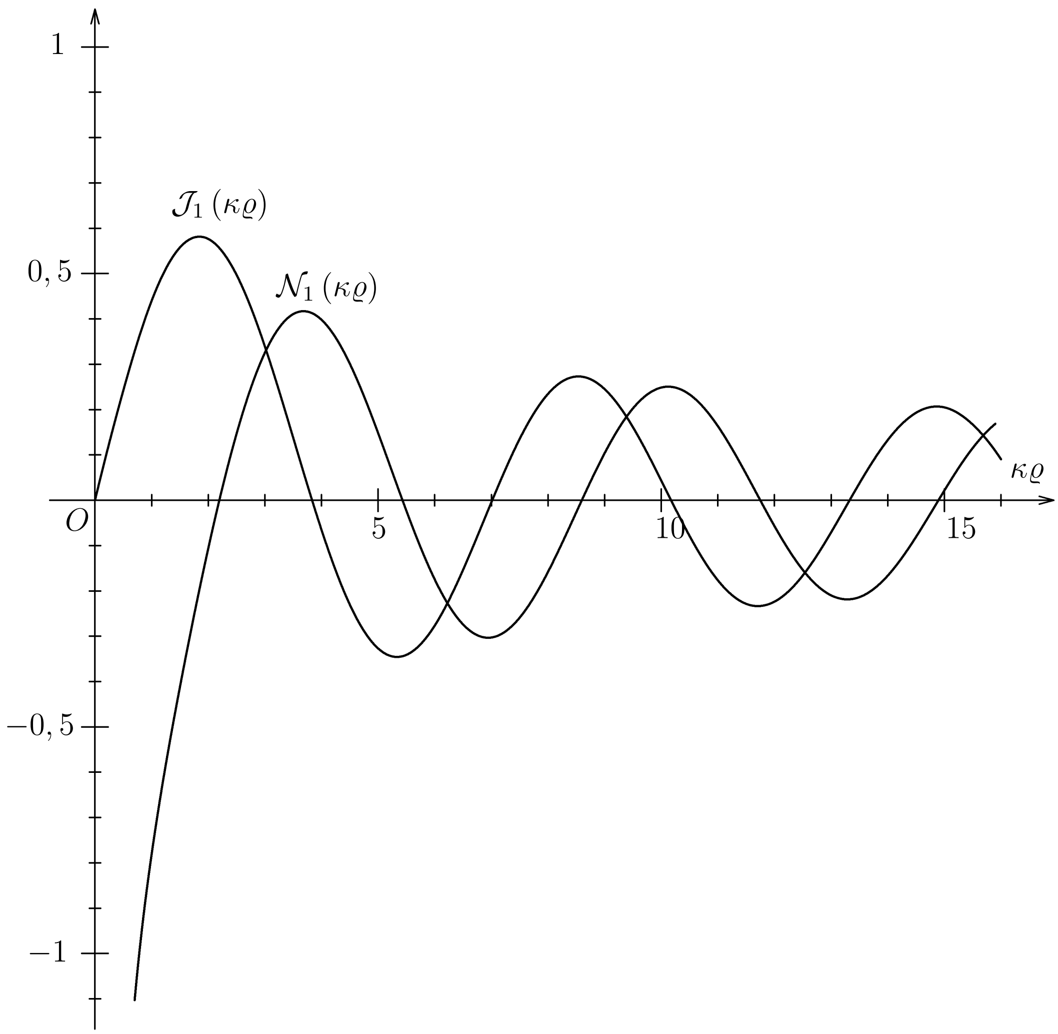

Figure 4.8: Plot of the Bessel function and Neumann function of the first order, $\mathcal{J}_1(\kappa\varrho)$ and $\mathcal{N}_1(\kappa\varrho)$.

$$\begin{aligned} \nabla_t^2 H_z - \beta^2 H_z &= -\mu\varepsilon\omega^2 H_z \\ \nabla_t^2 H_z - \gamma^2 H_z &= 0 \end{aligned} \tag{4.71b}$$

For the evanescent solution, $\mu_2\varepsilon_2\omega^2 \leq \beta^2$,

$$\beta^2 - \mu_2\varepsilon_2\omega^2 = \gamma^2 \tag{4.72}$$

The solutions to the modified Bessel equations (4.68) and (4.69) are represented by cylindrical functions of an imaginary variable, $\mathcal{Z}_\nu(\mathrm{j}\gamma\varrho)$. Between the two solutions represented by modified Hankel functions, $\mathcal{H}_\nu^{(1)}(\mathrm{j}\gamma\varrho)$ and $\mathcal{H}_\nu^{(2)}(\mathrm{j}\gamma\varrho)$ we choose the solution consistent with the boundary condition for the guided waves. i.e., that sufficiently quickly decaying with the distance, ϱ from the fiber axis.

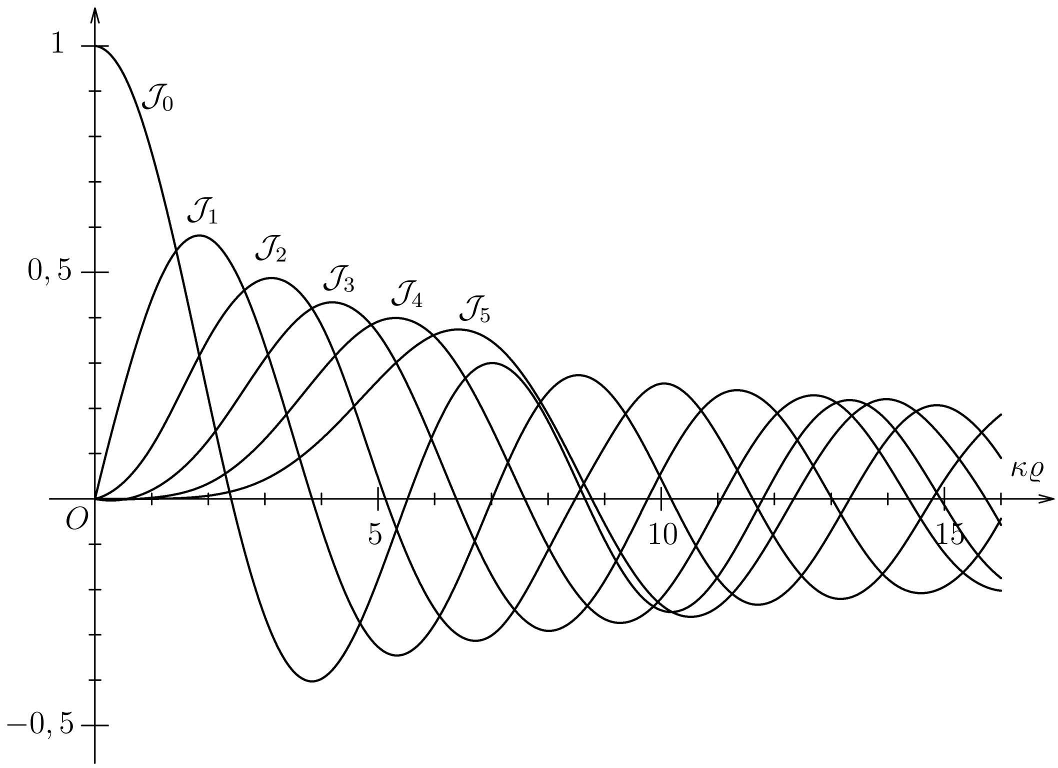

Figure 4.9: Bessel functions $\mathcal{J}_0(\kappa\varrho)$, $\mathcal{J}_1(\kappa\varrho)$, $\mathcal{J}_2(\kappa\varrho)$, $\mathcal{J}_3(\kappa\varrho)$, $\mathcal{J}_4(\kappa\varrho)$, and $\mathcal{J}_5(\kappa\varrho)$.

4.2.8 Acceptable solutions

We first solve the Helmholtz wave equation in a homogeneous unbound medium characterized by the material parameters ε_1 and μ_1 using Eqs. (4.47) pertinent to the fiber core region, $0 \le \varrho \le a$. In the next step we solve the diffuse equation in a homogeneous unbound medium characterized by the material parameters ε_2 and μ_2 using Eqs. (4.72) pertinent to the fiber cladding region, $\varrho \ge a$. We assume that the solutions are also valid in the corresponding regions, $0 \le \varrho \le a$ and $\varrho \ge a$ with the common boundary surface, $\varrho = a$. At the boundary surface, $\varrho = a$, we require the continuity of the field $\boldsymbol{E}$ and $\boldsymbol{H}$ components parallel to the boundary surface, $\varrho = a$. In addition, we require the fields $\boldsymbol{E}$ and $\boldsymbol{H}$ of the guided modes to be non zero and finite in the region $0 \le \varrho \le a$, and to be finite and decaying sufficiently quickly in the region $\varrho \ge a$ at $\varrho \to \infty$.

In the region $0 \le \varrho \le a$ we choose Bessel functions, $\mathcal{J}_\nu(\kappa\varrho)$, as solutions to Eqs. (4.49) Besselovy funkce $\mathcal{J}_\nu(\kappa\varrho)$. Neumann functions, $\mathcal{N}_\nu(\kappa\varrho)$ as well as Hankel functions $\mathcal{H}_\nu^{(1)}(\kappa\varrho)$ and $\mathcal{H}_\nu^{(2)}(\kappa\varrho)$ display singularities on the fiber axis, $\varrho = 0$ and must be therefore rejected. At $\varrho = 0$ all Bessel functions are finite. The Bessel function of zero order, $\nu = 0$, assumes the value, $\mathcal{J}_0(0) = 1$ while those of non zero order, $\nu > 0$ display a nodal point at $\varrho = 0$, i.e., $\mathcal{J}_\nu(0) = 0$.

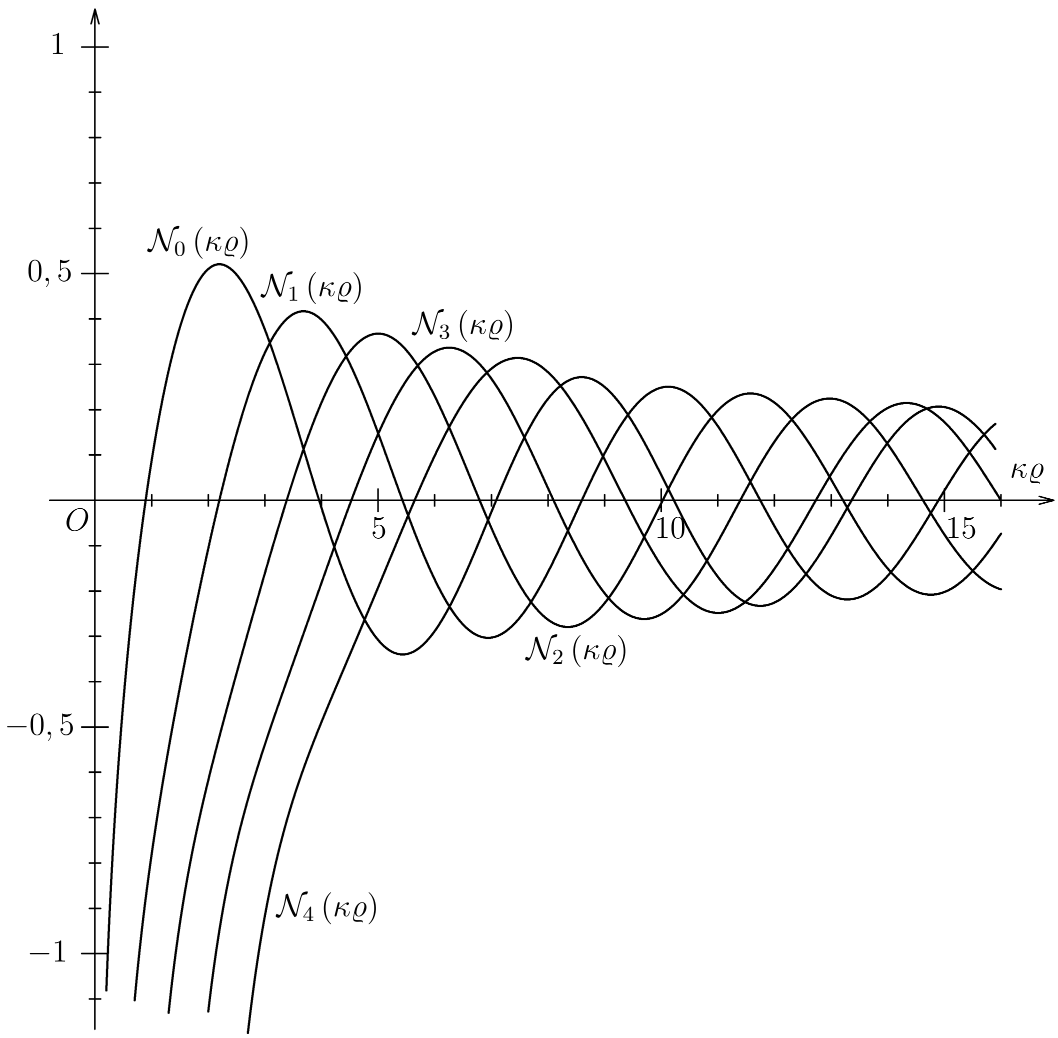

Figure 4.10: Plot of Neumann functions, $\mathcal{N}_0\left(\kappa\varrho\right)$, $\mathcal{N}_1\left(\kappa\varrho\right)$, $\mathcal{N}_2\left(\kappa\varrho\right)$, $\mathcal{N}_3\left(\kappa\varrho\right)$, and $\mathcal{N}_4\left(\kappa\varrho\right)$.

In the region, $\varrho \geq a$, we choose modified Hankel functions of the first kind, $\mathcal{H}_\nu^{(1)}\left(\mathrm{j}\gamma\varrho\right) \propto \exp\left(-\gamma\varrho\right)$, decaying with $\varrho \to \infty$ and reject modified Hankel functions of the second kind, $\mathcal{H}_\nu^{(2)}\left(\mathrm{j}\gamma\varrho\right) \propto \exp\left(\gamma\varrho\right)$ increasing to infinity for $\varrho \to \infty$.

Alternatively, the solutions for the region, $\varrho \geq a$, consistent with the boundary conditions at infinity can be expressed in terms real functions of real variable $(\gamma\varrho)$, represented by modified Bessel functions, $\mathcal{K}_\nu(\gamma\varrho)$ [7]

$$\mathcal{K}_\nu(\gamma\varrho) = \frac{\pi}{2}\mathrm{j}^{\nu+1}\mathcal{H}_\nu^{(1)}(\mathrm{j}\gamma\varrho) = \frac{\pi}{2}\mathrm{j}^{\nu+1}\left[\mathcal{J}_\nu(\mathrm{j}\gamma\varrho) + \mathrm{j}\mathcal{N}_\nu(\mathrm{j}\gamma\varrho)\right] \tag{4.73}$$

[7] Mary L. Boas, Mathematical Methods in Physical Sciences, 3rd Edition, J. Wiley & Sons 2006, p. 595.

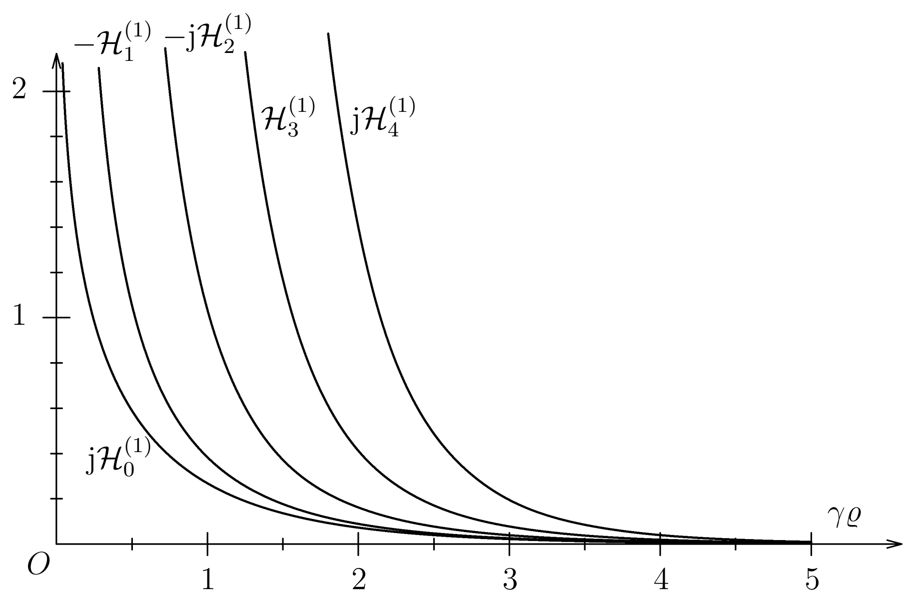

Figure 4.11: Modified Hankel functions of the first kind, $\mathcal{H}_\nu^{(1)}(\mathrm{j}\,\gamma\varrho)$ of the order $\nu = 0, 1, 2, 3, 4$. The displayed curves represent the functions $\mathcal{H}_\nu^{(1)}(\mathrm{j}\,\gamma\varrho)$ multiplied by a phase factor $\exp[\mathrm{j}\,(\nu+1)\,\pi/2]$, The factor transforms the functions $\mathcal{H}_0^{(1)}(\mathrm{j}\,\gamma\varrho)$, $\mathcal{H}_1^{(1)}(\mathrm{j}\,\gamma\varrho)$, $\mathcal{H}_2^{(1)}(\mathrm{j}\,\gamma\varrho)$, $\mathcal{H}_3^{(1)}(\mathrm{j}\,\gamma\varrho)$ and $\mathcal{H}_4^{(1)}(\mathrm{j}\,\gamma\varrho)$ to the functions of real positive values.

4.2.9 Fields in the core

In the core region, $0 \le \varrho \le a$, we have,

$$\kappa^2 = n_1^2\frac{\omega^2}{c^2} - \beta^2\,, \tag{4.74}$$

where $n_1^2 = \varepsilon_1\mu_1 c^2$, The symbol $c = \left(\varepsilon^{(\mathrm{vac})}\mu^{(\mathrm{vac})}\right)^{-1/2}$ conventionally denotes the speed of electromagnetic waves in a vacuum; $\varepsilon^{(\mathrm{vac})}$ and $\mu^{(\mathrm{vac})}$ stand for the electric permittivity in a vacuum and magnetic permeability in a vacuum, respectively.

We write for the electric and magnetic fields,

$$E_z^{(\nu)}(\varrho,\varphi) = A_\nu\mathcal{J}_\nu(\kappa\varrho)\,\mathrm{e}^{\mathrm{j}\nu\varphi} \tag{4.75a}$$

$$H_z^{(\nu)}(\varrho,\varphi) = B_\nu\mathcal{J}_\nu(\kappa\varrho)\,\mathrm{e}^{\mathrm{j}\nu\varphi} \tag{4.75b}$$

The factor $\exp[\mathrm{j}\,(\omega t - \beta z)]$ was dropped out. We find for the first and second derivatives of fields $E_z^{(\nu)}$ and $H_z^{(\nu)}$,

$$\frac{\partial E_z^{(\nu)}(\varrho,\varphi)}{\partial \varrho} = \kappa A_\nu \frac{\mathrm{d}\mathcal{J}_\nu(\kappa\varrho)}{\mathrm{d}(\kappa\varrho)} \mathrm{e}^{\mathrm{j}\nu\varphi} \tag{4.76a}$$

$$\frac{\partial^2 E_z^{(\nu)}(\varrho,\varphi)}{\partial \varrho^2} = \kappa^2 A_\nu \frac{\mathrm{d}^2\mathcal{J}_\nu(\kappa\varrho)}{\mathrm{d}(\kappa\varrho)^2} \mathrm{e}^{\mathrm{j}\nu\varphi} \tag{4.76b}$$

$$\frac{\partial E_z^{(\nu)}(\varrho,\varphi)}{\partial \varphi} = \mathrm{j}\nu A_\nu \mathcal{J}_\nu(\kappa\varrho) \mathrm{e}^{\mathrm{j}\nu\varphi} \tag{4.76c}$$

$$\frac{\partial^2 E_z^{(\nu)}(\varrho,\varphi)}{\partial \varphi^2} = -\nu^2 A_\nu \mathcal{J}_\nu(\kappa\varrho) \mathrm{e}^{\mathrm{j}\nu\varphi} \tag{4.76d}$$

$$\frac{\partial H_z^{(\nu)}(\varrho,\varphi)}{\partial \varrho} = \kappa B_\nu \frac{\mathrm{d}\mathcal{J}_\nu(\kappa\varrho)}{\mathrm{d}(\kappa\varrho)} \mathrm{e}^{\mathrm{j}\nu\varphi} \tag{4.76e}$$

$$\frac{\partial^2 H_z^{(\nu)}(\varrho,\varphi)}{\partial \varrho^2} = \kappa^2 B_\nu \frac{\mathrm{d}^2\mathcal{J}_\nu(\kappa\varrho)}{\mathrm{d}(\kappa\varrho)^2} \mathrm{e}^{\mathrm{j}\nu\varphi} \tag{4.76f}$$

$$\frac{\partial H_z^{(\nu)}(\varrho,\varphi)}{\partial \varphi} = \mathrm{j}\nu B_\nu \mathcal{J}_\nu(\kappa\varrho) \mathrm{e}^{\mathrm{j}\nu\varphi} \tag{4.76g}$$

$$\frac{\partial^2 H_z^{(\nu)}(\varrho,\varphi)}{\partial \varphi^2} = -\nu^2 B_\nu \mathcal{J}_\nu(\kappa\varrho) \mathrm{e}^{\mathrm{j}\nu\varphi} \tag{4.76h}$$

The field components, $E_z^{(\nu)}$ and $H_z^{(\nu)}$, are parallel to the fiber cylinder axis and tangential with respect to the cylindrical surface boundary $\varrho = a$. The electric field components perpendicular (transverse) with respect to the cylinder axis are given by,

$$\begin{aligned} E_\varrho^{(\nu)} &= -\frac{\mathrm{j}}{\kappa^2}\left(\beta\frac{\partial E_z^{(\nu)}}{\partial\varrho} + \omega\mu_1\frac{1}{\varrho}\frac{\partial H_z^{(\nu)}}{\partial\varphi}\right) \\ &= -\frac{\mathrm{j}}{\kappa^2}\left[\beta\kappa A_\nu\frac{\mathrm{d}\mathcal{J}_\nu(\kappa\varrho)}{\mathrm{d}(\kappa\varrho)} + \frac{\mathrm{j}\nu\omega\mu_1}{\varrho}B_\nu\mathcal{J}_\nu(\kappa\varrho)\right]\mathrm{e}^{\mathrm{j}\nu\varphi} \end{aligned} \tag{4.77a}$$

$$\begin{aligned} E_\varphi^{(\nu)} &= -\frac{\mathrm{j}}{\kappa^2}\left(\beta\frac{1}{\varrho}\frac{\partial E_z^{(\nu)}}{\partial\varphi} - \omega\mu_1\frac{\partial H_z^{(\nu)}}{\partial\varrho}\right) \\ &= -\frac{\mathrm{j}}{\kappa^2}\left[\frac{\mathrm{j}\nu\beta}{\varrho}A_\nu\mathcal{J}_\nu(\kappa\varrho) - \omega\mu_1\kappa B_\nu\frac{\mathrm{d}\mathcal{J}_\nu(\kappa\varrho)}{\mathrm{d}(\kappa\varrho)}\right]\mathrm{e}^{\mathrm{j}\nu\varphi} \end{aligned} \tag{4.77b}$$

The electric field component, $E_\varphi^{(\nu)}$ is tangential with respect to the boundary surface $\varrho = a$.

We consider the duality tansform

$$\boldsymbol{E} \to \pm\boldsymbol{H}\,,\ \text{i.e., } A_\nu \to \pm B_\nu$$
$$\boldsymbol{H} \to \mp\boldsymbol{E}\,,\ \text{i.e., } B_\nu \to \mp A_\nu$$
$$\mu_1 \leftrightarrow \varepsilon_1$$

and find,

$$H_{\varrho}^{(\nu)} = -\frac{\mathrm{j}}{\kappa^2}\left(\beta\frac{\partial H_z^{(\nu)}}{\partial\varrho} - \omega\varepsilon_1\frac{1}{\varrho}\frac{\partial E_z^{(\nu)}}{\partial\varphi}\right)$$
$$= -\frac{\mathrm{j}}{\kappa^2}\left[\beta\kappa B_\nu\frac{\mathrm{d}\mathcal{J}_\nu(\kappa\varrho)}{\mathrm{d}(\kappa\varrho)} - \mathrm{j}\nu\omega\varepsilon_1\frac{1}{\varrho}A_\nu\mathcal{J}_\nu(\kappa\varrho)\right]\mathrm{e}^{\mathrm{j}\nu\varphi} \tag{4.78a}$$

$$H_{\varphi}^{(\nu)} = -\frac{\mathrm{j}}{\kappa^2}\left(\beta\frac{1}{\varrho}\frac{\partial H_z^{(\nu)}}{\partial\varphi} + \omega\varepsilon_1\frac{\partial E_z^{(\nu)}}{\partial\varrho}\right)$$
$$= -\frac{\mathrm{j}}{\kappa^2}\left[\frac{\mathrm{j}\nu\beta}{\varrho}B_\nu\mathcal{J}_\nu(\kappa\varrho) + \omega\varepsilon_1\kappa A_\nu\frac{\mathrm{d}\mathcal{J}_\nu(\kappa\varrho)}{\mathrm{d}(\kappa\varrho)}\right]\mathrm{e}^{\mathrm{j}\nu\varphi} \tag{4.78b}$$

The magnetic field component, $H_{\varphi}^{(\nu)}$ is tangential with respect to the boundary surface, $\varrho = a$.

4.2.10 Fields in the cladding

In the cladding region, $a \le \varrho < \infty$, we have

$$\gamma^2 = \beta^2 - n_2^2\frac{\omega^2}{c^2}, \tag{4.79}$$

where $n_2^2 = \varepsilon_2\mu_2 c^2$. The electromagnetic wave velocity in a vacuum is denoted by $c = \left(\varepsilon^{(\mathrm{vac})}\mu^{(\mathrm{vac})}\right)^{-1/2}$. We express the fields without the factor $\exp\left[\mathrm{j}\left(\omega t - \beta z\right)\right]$

$$E_z^{(\nu)}(\varrho,\varphi) = C_\nu\mathcal{H}_\nu^{(1)}(\mathrm{j}\gamma\varrho)\,\mathrm{e}^{\mathrm{j}\nu\varphi} \tag{4.80a}$$
$$H_z^{(\nu)}(\varrho,\varphi) = D_\nu\mathcal{H}_\nu^{(1)}(\mathrm{j}\gamma\varrho)\,\mathrm{e}^{\mathrm{j}\nu\varphi} \tag{4.80b}$$

The first and second derivatives of the fields $E_z^{(\nu)}$ and $H_z^{(\nu)}$ are given by,

$$\frac{\partial E_z^{(\nu)}(\varrho,\varphi)}{\partial\varrho} = \mathrm{j}\gamma C_\nu\frac{\mathrm{d}\mathcal{H}_\nu^{(1)}(\mathrm{j}\gamma\varrho)}{\mathrm{d}(\mathrm{j}\gamma\varrho)}\mathrm{e}^{\mathrm{j}\nu\varphi} \tag{4.81a}$$
$$\frac{\partial^2 E_z^{(\nu)}(\varrho,\varphi)}{\partial\varrho^2} = -\gamma^2 C_\nu\frac{\mathrm{d}^2\mathcal{H}_\nu^{(1)}(\mathrm{j}\gamma\varrho)}{\mathrm{d}(\mathrm{j}\gamma\varrho)^2}\mathrm{e}^{\mathrm{j}\nu\varphi} \tag{4.81b}$$
$$\frac{\partial E_z^{(\nu)}(\varrho,\varphi)}{\partial\varphi} = \mathrm{j}\nu C_\nu\mathcal{H}_\nu^{(1)}(\mathrm{j}\gamma\varrho)\,\mathrm{e}^{\mathrm{j}\nu\varphi} \tag{4.81c}$$
$$\frac{\partial^2 E_z^{(\nu)}(\varrho,\varphi)}{\partial\varphi^2} = -\nu^2 C_\nu\mathcal{H}_\nu^{(1)}(\mathrm{j}\gamma\varrho)\,\mathrm{e}^{\mathrm{j}\nu\varphi} \tag{4.81d}$$

$$\frac{\partial H_z^{(\nu)}(\varrho,\varphi)}{\partial\varrho} = \mathrm{j}\gamma D_\nu \frac{\mathrm{d}\mathcal{H}_\nu^{(1)}(\mathrm{j}\gamma\varrho)}{\mathrm{d}(\mathrm{j}\gamma\varrho)}\mathrm{e}^{\mathrm{j}\nu\varphi} \tag{4.81e}$$

$$\frac{\partial^2 H_z^{(\nu)}(\varrho,\varphi)}{\partial\varrho^2} = -\gamma^2 D_\nu \frac{\mathrm{d}^2\mathcal{H}_\nu^{(1)}(\mathrm{j}\gamma\varrho)}{\mathrm{d}(\mathrm{j}\gamma\varrho)^2}\mathrm{e}^{\mathrm{j}\nu\varphi} \tag{4.81f}$$

$$\frac{\partial H_z^{(\nu)}(\varrho,\varphi)}{\partial\varphi} = \mathrm{j}\nu D_\nu \mathcal{H}_\nu^{(1)}(\mathrm{j}\gamma\varrho)\,\mathrm{e}^{\mathrm{j}\nu\varphi} \tag{4.81g}$$

$$\frac{\partial^2 H_z^{(\nu)}(\varrho,\varphi)}{\partial\varphi^2} = -\nu^2 D_\nu \mathcal{H}_\nu^{(1)}(\mathrm{j}\gamma\varrho)\,\mathrm{e}^{\mathrm{j}\nu\varphi} \tag{4.81h}$$

The field components, $E_z^{(\nu)}$ and $H_z^{(\nu)}$, are parallel to the fiber cylinder axis and tangential with respect to the cylindrical surface boundary $\varrho = a$. The electric field components perpendicular (transverse) with respect to the cylinder axis are given by,

$$\begin{aligned} E_\varrho^{(\nu)} &= \frac{\mathrm{j}}{\gamma^2}\left(\beta\frac{\partial E_z^{(\nu)}}{\partial\varrho} + \omega\mu_2\frac{1}{\varrho}\frac{\partial H_z^{(\nu)}}{\partial\varphi}\right) \\ &= \frac{\mathrm{j}}{\gamma^2}\left[\mathrm{j}\gamma\beta C_\nu\frac{\mathrm{d}\mathcal{H}_\nu^{(1)}(\mathrm{j}\gamma\varrho)}{\mathrm{d}(\mathrm{j}\gamma\varrho)} + \mathrm{j}\nu\omega\mu_2\frac{1}{\varrho}D_\nu\mathcal{J}_\nu(\mathrm{j}\gamma\varrho)\right]\mathrm{e}^{\mathrm{j}\nu\varphi} \end{aligned} \tag{4.82a}$$

$$\begin{aligned} E_\varphi^{(\nu)} &= \frac{\mathrm{j}}{\gamma^2}\left(\beta\frac{1}{\varrho}\frac{\partial E_z^{(\nu)}}{\partial\varphi} - \omega\mu_2\frac{\partial H_z^{(\nu)}}{\partial\varrho}\right) \\ &= \frac{\mathrm{j}}{\gamma^2}\left[\mathrm{j}\nu\beta\frac{1}{\varrho}C_\nu\mathcal{H}_\nu^{(1)}(\mathrm{j}\gamma\varrho) - \mathrm{j}\gamma\omega\mu_2 D_\nu\frac{\mathrm{d}\mathcal{H}_\nu^{(1)}(\mathrm{j}\gamma\varrho)}{\mathrm{d}(\mathrm{j}\gamma\varrho)}\right]\mathrm{e}^{\mathrm{j}\nu\varphi} \end{aligned} \tag{4.82b}$$

The electric field component, $E_\varphi^{(\nu)}$ is tangential with respect to the boundary surface $\varrho = a$.

The duality transform provides,

$$\begin{gathered} \boldsymbol{E} \to \pm\boldsymbol{H}\,,\ \text{i.e.,}\ C_\nu \to \pm D_\nu \\ \boldsymbol{H} \to \mp\boldsymbol{E}\,,\ \text{i.e.,}\ D_\nu \to \mp C_\nu \\ \mu_1 \leftrightarrow \varepsilon_1 \end{gathered}$$

$$\begin{aligned} H_\varrho^{(\nu)} &= \frac{\mathrm{j}}{\gamma^2}\left(\beta\frac{\partial H_z^{(\nu)}}{\partial\varrho} - \omega\varepsilon_2\frac{1}{\varrho}\frac{\partial E_z^{(\nu)}}{\partial\varphi}\right) \\ &= \frac{\mathrm{j}}{\gamma^2}\left[\mathrm{j}\gamma\beta D_\nu\frac{\mathrm{d}\mathcal{H}_\nu^{(1)}(\mathrm{j}\gamma\varrho)}{\mathrm{d}(\mathrm{j}\gamma\varrho)} - \mathrm{j}\nu\omega\varepsilon_2\frac{1}{\varrho}C_\nu\mathcal{H}_\nu^{(1)}(\mathrm{j}\gamma\varrho)\right]\mathrm{e}^{\mathrm{j}\nu\varphi} \end{aligned} \tag{4.83a}$$

$$\begin{aligned} H_\varphi^{(\nu)} &= \frac{\mathrm{j}}{\gamma^2}\left(\beta\frac{1}{\varrho}\frac{\partial H_z^{(\nu)}}{\partial\varphi} + \omega\varepsilon_2\frac{\partial E_z^{(\nu)}}{\partial\varrho}\right) \\ &= \frac{\mathrm{j}}{\gamma^2}\left[\mathrm{j}\nu\beta\frac{1}{\varrho}D_\nu\mathcal{H}_\nu^{(1)}(\mathrm{j}\gamma\varrho) + \mathrm{j}\gamma\omega\varepsilon_2 C_\nu\frac{\mathrm{d}\mathcal{H}_\nu^{(1)}(\mathrm{j}\gamma\varrho)}{\mathrm{d}(\mathrm{j}\gamma\varrho)}\right]\mathrm{e}^{\mathrm{j}\nu\varphi} \end{aligned} \tag{4.83b}$$

The magnetic field component, $H_\varphi^{(\nu)}$ is tangential with respect to the boundary surface $\varrho = a$.

4.3 Characteristic equation

The relations among the amplitudes, A_ν, B_ν, C_ν and D_ν follow from the continuity condition for tangential field components, $E_\varphi^{(\nu)}$, $H_z^{(\nu)}$, $H_\varphi^{(\nu)}$, and $E_z^{(\nu)}$ at the boundary surface, $\varrho = a$, expressed in Eqs. (3.32),

$$\lim_{\varrho\to a_-} E_z^{(\nu)}(\varrho) = \lim_{\varrho\to a_+} E_z^{(\nu)}(\varrho) \tag{4.84a}$$

$$\lim_{\varrho\to a_-} H_z^{(\nu)}(\varrho) = \lim_{\varrho\to a_+} H_z^{(\nu)}(\varrho) \tag{4.84b}$$

$$\lim_{\varrho\to a_-} E_\varphi^{(\nu)}(\varrho) = \lim_{\varrho\to a_+} E_\varphi^{(\nu)}(\varrho) \tag{4.84c}$$

$$\lim_{\varrho\to a_-} H_\varphi^{(\nu)}(\varrho) = \lim_{\varrho\to a_+} H_\varphi^{(\nu)}(\varrho) \tag{4.84d}$$

where the limits $\lim\limits_{\varrho\to a_-}$ denote limits for ϱ approaching the boundary, $\varrho = a$ from the core region $\varrho < a$, and the limits $\lim\limits_{\varrho\to a_+}$ denote limits for ϱ approaching the boundary, $\varrho = a$, from the cladding region, $\varrho > a$.

We introduce a concise notation for the derivatives at the surface $\varrho = a$

$$\left[\frac{\mathrm{d}\mathcal{J}_\nu(\kappa\varrho)}{\mathrm{d}(\kappa\varrho)}\right]_{\varrho=a} = \frac{\mathrm{d}\mathcal{J}_\nu(\kappa a)}{\mathrm{d}(\kappa a)} \tag{4.85a}$$

$$\left[\frac{\mathrm{d}\mathcal{H}_\nu^{(1)}(\mathrm{j}\gamma\varrho)}{\mathrm{d}(\mathrm{j}\gamma\varrho)}\right]_{\varrho=a} = \frac{\mathrm{d}\mathcal{H}_\nu^{(1)}(\mathrm{j}\gamma a)}{\mathrm{d}(\mathrm{j}\gamma a)} \tag{4.85b}$$

We arrive at four relations,
$E_\varphi^{(\nu)}$ continuous

$$\begin{aligned} & -\frac{\mathrm{j}}{\kappa^2}\left[\frac{\mathrm{j}\nu\beta}{a}A_\nu\mathcal{J}_\nu(\kappa a) - \omega\mu_1\kappa B_\nu\frac{\mathrm{d}\mathcal{J}_\nu(\kappa a)}{\mathrm{d}(\kappa a)}\right] \\ &= \frac{\mathrm{j}}{\gamma^2}\left[\mathrm{j}\nu\beta\frac{1}{a}C_\nu\mathcal{H}_\nu^{(1)}(\mathrm{j}\gamma a) - \mathrm{j}\gamma\omega\mu_2 D_\nu\frac{\mathrm{d}\mathcal{H}_\nu^{(1)}(\mathrm{j}\gamma a)}{\mathrm{d}(\mathrm{j}\gamma a)}\right] \end{aligned} \tag{4.86a}$$

$H_z^{(\nu)}$ continuous

$$B_\nu\mathcal{J}_\nu(\kappa a) = D_\nu\mathcal{H}_\nu^{(1)}(\mathrm{j}\gamma a) \tag{4.86b}$$

$H_\varphi^{(\nu)}$ continuous

$$\begin{aligned} & -\frac{\mathrm{j}}{\kappa^2}\left[\mathrm{j}\nu\beta\frac{1}{a}B_\nu\mathcal{J}_\nu(\kappa a) + \omega\varepsilon_1\kappa A_\nu\frac{\mathrm{d}\mathcal{J}_\nu(\kappa a)}{\mathrm{d}(\kappa a)}\right] \\ &= \frac{\mathrm{j}}{\gamma^2}\left[\mathrm{j}\nu\beta\frac{1}{a}D_\nu\mathcal{H}_\nu^{(1)}(\mathrm{j}\gamma a) + \mathrm{j}\gamma\omega\varepsilon_2 C_\nu\frac{\mathrm{d}\mathcal{H}_\nu^{(1)}(\mathrm{j}\gamma a)}{\mathrm{d}(\mathrm{j}\gamma a)}\right] \end{aligned} \tag{4.86c}$$

$E_z^{(\nu)}$ continuous

$$A_\nu \mathcal{J}_\nu(\kappa a) = C_\nu \mathcal{H}_\nu^{(1)}(\mathrm{j}\gamma a) \tag{4.86d}$$

The relations are coupled by the duality transform, $A_\nu \to \pm B_\nu$, $B_\nu \to \mp A_\nu$ and $\mu_1 \leftrightarrow \varepsilon_1$ in the core region, $\varrho \le a$, and by the duality transform, $C_\nu \to \pm D_\nu$, $D_\nu \to \mp C_\nu$ and $\mu_2 \leftrightarrow \varepsilon_2$ in the cladding region, $\varrho \ge a$.

The boundary conditions provide a homogeneous set of four equations for unknown amplitudes, A_ν, B_ν, C_ν and D_ν. We further simplify the notation for the cylindrical functions $\mathcal{Z}_\nu$ and their derivatives on the boundary surface $\varrho = a$ in Eqs. (4.85),

$$\mathcal{J}_\nu = \mathcal{J}_\nu(\kappa a) \tag{4.87a}$$

$$\mathcal{H}_\nu^{(1)} = \mathcal{H}_\nu^{(1)}(\mathrm{j}\gamma a) \tag{4.87b}$$

$$\mathcal{J}_\nu' = \frac{\mathrm{d}\mathcal{J}_\nu(\kappa a)}{\mathrm{d}(\kappa a)} \tag{4.87c}$$

$$\mathcal{H}_\nu^{(1)\prime} = \frac{\mathrm{d}\mathcal{H}_\nu^{(1)}(\mathrm{j}\gamma a)}{\mathrm{d}(\mathrm{j}\gamma a)} \tag{4.87d}$$

A nontrivial solution to Eqs. (4.87) follows from the condition for the zero determinant of this set. The arrangement of the determinant is shown in Table 4.1. In our concise notation, a condition for the zero determinant takes the form,

$$\begin{vmatrix} \dfrac{\nu\beta}{\kappa^2 a}\mathcal{J}_\nu & \dfrac{\mathrm{j}\omega\mu_1}{\kappa}\mathcal{J}_\nu' & \dfrac{\nu\beta}{\gamma^2 a}\mathcal{H}_\nu^{(1)} & -\dfrac{\omega\mu_2}{\gamma}\mathcal{H}_\nu^{(1)\prime} \\ 0 & \mathcal{J}_\nu & 0 & -\mathcal{H}_\nu^{(1)} \\ -\dfrac{\mathrm{j}\omega\varepsilon_1}{\kappa}\mathcal{J}_\nu' & \dfrac{\nu\beta}{\kappa^2 a}\mathcal{J}_\nu & \dfrac{\omega\varepsilon_2}{\gamma}\mathcal{H}_\nu^{(1)\prime} & \dfrac{\nu\beta}{\gamma^2 a}\mathcal{H}_\nu^{(1)} \\ \mathcal{J}_\nu & 0 & -\mathcal{H}_\nu^{(1)} & 0 \end{vmatrix} = 0 \tag{4.88}$$

It represents the eigenvalue equation for guided modes. The determinant on the left hand side of Eq. (4.88) is of the type,

$$
\begin{vmatrix} a_{11} & a_{12} & a_{13} & a_{14} \\ 0 & a_{22} & 0 & a_{24} \\ a_{31} & a_{11} & a_{33} & a_{13} \\ a_{22} & 0 & a_{24} & 0 \end{vmatrix}
$$

$$
\begin{aligned}
&= a_{11}\begin{vmatrix} a_{22} & 0 & a_{24} \\ a_{11} & a_{33} & a_{13} \\ 0 & a_{24} & 0 \end{vmatrix} - a_{12}\begin{vmatrix} 0 & 0 & a_{24} \\ a_{31} & a_{33} & a_{13} \\ a_{22} & a_{24} & 0 \end{vmatrix} + a_{13}\begin{vmatrix} 0 & a_{22} & a_{24} \\ a_{31} & a_{11} & a_{13} \\ a_{22} & 0 & 0 \end{vmatrix} - a_{14}\begin{vmatrix} 0 & a_{22} & 0 \\ a_{31} & a_{11} & a_{33} \\ a_{22} & 0 & a_{24} \end{vmatrix} \\
&= a_{11}\left(a_{11}a_{24}^2 - a_{13}a_{22}a_{24}\right) - a_{12}\left(a_{24}^2 a_{31} - a_{22}a_{24}a_{33}\right) \\
&+ a_{13}\left(a_{13}a_{22}^2 - a_{11}a_{22}a_{24}\right) - a_{14}\left(a_{22}^2 a_{33} - a_{22}a_{24}a_{31}\right) \\
&= a_{11}a_{24}\left(a_{11}a_{24} - a_{13}a_{22}\right) - a_{12}a_{24}\left(a_{24}a_{31} - a_{22}a_{33}\right) \\
&+ a_{13}a_{22}\left(a_{13}a_{22} - a_{11}a_{24}\right) - a_{14}a_{22}\left(a_{22}a_{33} - a_{24}a_{31}\right) \\
&= \left(a_{11}a_{24} - a_{13}a_{22}\right)\left(a_{11}a_{24} - a_{13}a_{22}\right) - \left(a_{12}a_{24} - a_{14}a_{22}\right)\left(a_{24}a_{31} - a_{22}a_{33}\right) \\
&= \left(a_{11}a_{24} - a_{13}a_{22}\right)^2 - \left(a_{12}a_{24} - a_{14}a_{22}\right)\left(a_{24}a_{31} - a_{22}a_{33}\right)
\end{aligned}
$$

The structure of the eigenvalue equation simplifies to the form,

$$
\left(a_{11}a_{24} - a_{13}a_{22}\right)^2 - \left(a_{12}a_{24} - a_{14}a_{22}\right)\left(a_{24}a_{31} - a_{22}a_{33}\right) = 0 \tag{4.89}
$$

The substitution for the determinant elements according to Eq. (4.88) provides

$$
\begin{aligned}
&\left[\frac{\nu\beta}{\kappa^2 a}\mathcal{J}_\nu\left(-\mathcal{H}_\nu^{(1)}\right) - \frac{\nu\beta}{\gamma^2 a}\mathcal{H}_\nu^{(1)}\mathcal{J}_\nu\right]^2 \\
&- \left[\frac{\mathrm{j}\omega\mu_1}{\kappa}\mathcal{J}_\nu'\left(-\mathcal{H}_\nu^{(1)}\right) - \left(-\frac{\omega\mu_2}{\gamma}\mathcal{H}_\nu^{(1)\prime}\right)\mathcal{J}_\nu\right]\left[\left(-\mathcal{H}_\nu^{(1)}\right)\left(-\frac{\mathrm{j}\omega\varepsilon_1}{\kappa}\mathcal{J}_\nu'\right) - \mathcal{J}_\nu\frac{\omega\varepsilon_2}{\gamma}\mathcal{H}_\nu^{(1)\prime}\right] = 0
\end{aligned} \tag{4.90}
$$

The eigenvalues equation rearranged becomes,

$$
\begin{aligned}
&\left[\frac{\nu\beta}{\omega}\left(\frac{1}{\kappa^2 a^2} + \frac{1}{\gamma^2 a^2}\right)\mathcal{J}_\nu\mathcal{H}_\nu^{(1)}\right]^2 \\
&- \left[\frac{\mu_1}{\kappa a}\mathcal{J}_\nu'\mathcal{H}_\nu^{(1)} - \frac{\mu_2}{\mathrm{j}\gamma a}\mathcal{J}_\nu\mathcal{H}_\nu^{(1)\prime}\right]\left[\frac{\mathrm{j}\varepsilon_1}{\kappa a}\mathcal{J}_\nu'\mathcal{H}_\nu^{(1)} - \frac{\varepsilon_2}{\mathrm{j}\gamma a}\mathcal{J}_\nu\mathcal{H}_\nu^{(1)\prime}\right] = 0
\end{aligned} \tag{4.91}
$$

A further rearrangement using $\kappa^2 + \gamma^2 = (\varepsilon_1\mu_1 - \varepsilon_2\mu_2)\,\omega^2$

$$
\begin{aligned}
&\left[\frac{\nu\beta}{a}\frac{\omega}{\kappa^2\gamma^2}\left(\varepsilon_1\mu_1 - \varepsilon_2\mu_2\right)\right]^2 \\
&= \left[\frac{\mu_1}{\kappa}\frac{\mathcal{J}_\nu'(\kappa a)}{\mathcal{J}_\nu(\kappa a)} + \mathrm{j}\frac{\mu_2}{\gamma}\frac{\mathcal{H}_\nu^{(1)\prime}(\mathrm{j}\gamma a)}{\mathcal{H}_\nu^{(1)}(\mathrm{j}\gamma a)}\right]\left[\frac{\varepsilon_1}{\kappa}\frac{\mathcal{J}_\nu'(\kappa a)}{\mathcal{J}_\nu(\kappa a)} + \mathrm{j}\frac{\varepsilon_2}{\gamma}\frac{\mathcal{H}_\nu^{(1)\prime}(\mathrm{j}\gamma a)}{\mathcal{H}_\nu^{(1)}(\mathrm{j}\gamma a)}\right]
\end{aligned}
$$

Table 4.1: Arrangement of the determinant employed in the computation of the eigenvalue equation

	A_ν	B_ν	C_ν	D_ν
E_φ	$\dfrac{\nu\beta}{\kappa^2 a}\mathcal{J}$	$\dfrac{\mathrm{j}\omega\mu_1}{\kappa}\mathcal{J}'$	$\dfrac{\nu\beta}{\gamma^2 a}\mathcal{H}$	$-\dfrac{\omega\mu_2}{\gamma}\mathcal{H}'$
H_z	0	$\mathcal{J}$	0	$-\mathcal{H}$
H_φ	$-\dfrac{\mathrm{j}\omega\varepsilon_1}{\kappa}\mathcal{J}'$	$\dfrac{\nu\beta}{\kappa^2 a}\mathcal{J}$	$\dfrac{\omega\varepsilon_2}{\gamma}\mathcal{H}'$	$\dfrac{\nu\beta}{\gamma^2 a}\mathcal{H}$
E_z	$\mathcal{J}$	0	$-\mathcal{H}$	0

Equation (4.91) can be transformed to the form with dimensionless arguments, βa, κa and $\mathrm{j}\gamma a$

$$\boxed{\left[\frac{\nu\omega a\,\beta a}{\kappa^2 a^2\,\gamma^2 a^2}\left(\varepsilon_1\mu_1-\varepsilon_2\mu_2\right)\right]^2=\left[\frac{\mu_1}{\kappa a}\frac{\mathcal{J}_\nu'\left(\kappa a\right)}{\mathcal{J}_\nu\left(\kappa a\right)}-\frac{\mu_2}{\mathrm{j}\gamma a}\frac{\mathcal{H}_\nu^{(1)'}\left(\mathrm{j}\gamma a\right)}{\mathcal{H}_\nu^{(1)}\left(\mathrm{j}\gamma a\right)}\right]\left[\frac{\varepsilon_1}{\kappa a}\frac{\mathcal{J}_\nu'\left(\kappa a\right)}{\mathcal{J}_\nu\left(\kappa a\right)}-\frac{\varepsilon_2}{\mathrm{j}\gamma a}\frac{\mathcal{H}_\nu^{(1)'}\left(\mathrm{j}\gamma a\right)}{\mathcal{H}_\nu^{(1)}\left(\mathrm{j}\gamma a\right)}\right]} \tag{4.92}$$

We can also employ $\dfrac{1}{\mathrm{j}\gamma a}\dfrac{\mathcal{H}_\nu^{(1)'}\left(\mathrm{j}\gamma a\right)}{\mathcal{H}_\nu\left(\mathrm{j}\gamma a\right)}=-\dfrac{1}{\gamma a}\dfrac{\mathcal{K}_\nu'\left(\gamma a\right)}{\mathcal{K}_\nu\left(\gamma a\right)}$, and write,

$$\left[\frac{\nu\omega a\,\beta a}{\kappa^2 a^2\,\gamma^2 a^2}\left(\varepsilon_1\mu_1-\varepsilon_2\mu_2\right)\right]^2=\left[\frac{\mu_1}{\kappa a}\frac{\mathcal{J}_\nu'\left(\kappa a\right)}{\mathcal{J}_\nu\left(\kappa a\right)}+\mu_2\frac{1}{\gamma a}\frac{\mathcal{K}_\nu'\left(\gamma a\right)}{\mathcal{K}_\nu\left(\gamma a\right)}\right]\left[\frac{\varepsilon_1}{\kappa a}\frac{\mathcal{J}_\nu'\left(\kappa a\right)}{\mathcal{J}_\nu\left(\kappa a\right)}+\varepsilon_2\frac{1}{\gamma a}\frac{\mathcal{K}_\nu'\left(\gamma a\right)}{\mathcal{K}_\nu\left(\gamma a\right)}\right]. \tag{4.93}$$

The expressions in square brackets on the right hand side are related by the duality transform $\mu_i \leftrightarrow \varepsilon_i$, $i=1,2$ while the eigenvalue equation itself is invariant with respect to the duality transform.

To find another alternative form, we multiply both sides of Eq. (4.92) by $\gamma^4 a^2$

$$\left[\frac{\nu\beta\omega}{\kappa^2}(\varepsilon_1\mu_1-\varepsilon_2\mu_2)\right]^2=\left[\frac{\mu_1\gamma^2 a}{\kappa}\frac{\mathcal{J}_\nu'(\kappa a)}{\mathcal{J}_\nu(\kappa a)}+\mathrm{j}\mu_2\gamma a\frac{\mathcal{H}_\nu^{(1)'}(\mathrm{j}\gamma a)}{\mathcal{H}_\nu^{(1)}(\mathrm{j}\gamma a)}\right]\left[\frac{\varepsilon_1\gamma^2 a}{\kappa}\frac{\mathcal{J}_\nu'(\kappa a)}{\mathcal{J}_\nu(\kappa a)}+\mathrm{j}\varepsilon_2\gamma a\frac{\mathcal{H}_\nu^{(1)'}(\mathrm{j}\gamma a)}{\mathcal{H}_\nu^{(1)}(\mathrm{j}\gamma a)}\right]$$

In the first step, we rearrange the result to get,

$$\left[\frac{\nu\beta\omega}{\kappa^2}\varepsilon_2\mu_2\left(\frac{\varepsilon_1\mu_1}{\varepsilon_2\mu_2}-1\right)\right]^2=\left[\frac{\mu_1\gamma^2 a}{\kappa}\frac{\mathcal{J}_\nu'(\kappa a)}{\mathcal{J}_\nu(\kappa a)}+\mathrm{j}\mu_2\gamma a\frac{\mathcal{H}_\nu^{(1)'}(\mathrm{j}\gamma a)}{\mathcal{H}_\nu^{(1)}(\mathrm{j}\gamma a)}\right]\left[\frac{\varepsilon_1\gamma^2 a}{\kappa}\frac{\mathcal{J}_\nu'(\kappa a)}{\mathcal{J}_\nu(\kappa a)}+\mathrm{j}\varepsilon_2\gamma a\frac{\mathcal{H}_\nu^{(1)'}(\mathrm{j}\gamma a)}{\mathcal{H}_\nu^{(1)}(\mathrm{j}\gamma a)}\right]$$

Then in the second step, we have

$$\begin{aligned}&\varepsilon_2\mu_2\left[\frac{\nu\beta\omega\left(\varepsilon_2\mu_2\right)^{1/2}}{\kappa^2}\left(\frac{\varepsilon_1\mu_1}{\varepsilon_2\mu_2}-1\right)\right]^2\\&=\left[\frac{\mu_1\gamma^2 a}{\kappa}\frac{\mathcal{J}_\nu'(\kappa a)}{\mathcal{J}_\nu(\kappa a)}+\mathrm{j}\mu_2\gamma a\frac{\mathcal{H}_\nu^{(1)'}(\mathrm{j}\gamma a)}{\mathcal{H}_\nu^{(1)}(\mathrm{j}\gamma a)}\right]\left[\frac{\varepsilon_1\gamma^2 a}{\kappa}\frac{\mathcal{J}_\nu'(\kappa a)}{\mathcal{J}_\nu(\kappa a)}+\mathrm{j}\varepsilon_2\gamma a\frac{\mathcal{H}_\nu^{(1)'}(\mathrm{j}\gamma a)}{\mathcal{H}_\nu^{(1)}(\mathrm{j}\gamma a)}\right]\end{aligned}$$

We introduce the propagation constant in the cladding medium (2), $k_2 = \omega\left(\varepsilon_2\mu_2\right)^{1/2}$. Then

$$\begin{aligned}&\left[\nu\frac{\beta k_2}{\kappa^2}\left(\frac{\varepsilon_1\mu_1}{\varepsilon_2\mu_2}-1\right)\right]^2\\&=\left[\frac{\mu_1\gamma^2 a}{\mu_2\kappa}\frac{\mathcal{J}_\nu'(\kappa a)}{\mathcal{J}_\nu(\kappa a)}+\mathrm{j}\gamma a\frac{\mathcal{H}_\nu^{(1)'}(\mathrm{j}\gamma a)}{\mathcal{H}_\nu^{(1)}(\mathrm{j}\gamma a)}\right]\left[\frac{\varepsilon_1\gamma^2 a}{\varepsilon_2\kappa}\frac{\mathcal{J}_\nu'(\kappa a)}{\mathcal{J}_\nu(\kappa a)}+\mathrm{j}\gamma a\frac{\mathcal{H}_\nu^{(1)'}(\mathrm{j}\gamma a)}{\mathcal{H}_\nu^{(1)}(\mathrm{j}\gamma a)}\right]\end{aligned}$$

Often, it is useful employ the indices of refraction on the left hand side of Eq. (4.92). We make use of $\varepsilon_i\mu_i = n_i^2 c^{-2}$, $i = 1, 2$

$$\begin{aligned}&\left[\frac{\nu\beta a\,\omega a}{\kappa^2 a^2\gamma^2 a^2 c^2}\left(n_1^2-n_2^2\right)\right]^2\\&=\left[\mu_1\frac{1}{\kappa a}\frac{\mathcal{J}_\nu'\left(\kappa a\right)}{\mathcal{J}_\nu\left(\kappa a\right)}-\mu_2\frac{1}{\mathrm{j}\gamma a}\frac{\mathcal{H}_\nu^{(1)'}\left(\mathrm{j}\gamma a\right)}{\mathcal{H}_\nu^{(1)}\left(\mathrm{j}\gamma a\right)}\right]\left[\varepsilon_1\frac{1}{\kappa a}\frac{\mathcal{J}_\nu'\left(\kappa a\right)}{\mathcal{J}_\nu\left(\kappa a\right)}-\varepsilon_2\frac{1}{\mathrm{j}\gamma a}\frac{\mathcal{H}_\nu^{(1)'}\left(\mathrm{j}\gamma a\right)}{\mathcal{H}_\nu^{(1)}\left(\mathrm{j}\gamma a\right)}\right]\end{aligned} \tag{4.94}$$

In the original treatment, the eigenvalue equation has been displayed with a simplified assumption, $\mu_1 = \mu_2$.[8] Here we reproduce the original treatment keeping $\mu_1 \neq \mu_2$ to emphasize the duality relation between the expressions on the right hand side,

$$\left[\frac{\nu\beta\omega}{\kappa^2 c^2}\left(n_1^2-n_2^2\right)\right]^2=\left[\frac{\mu_1\gamma^2 a^2}{\kappa a}\frac{\mathcal{J}_\nu'(\kappa a)}{\mathcal{J}_\nu(\kappa a)}+\mathrm{j}\mu_2\gamma a\frac{\mathcal{H}_\nu^{(1)'}(\mathrm{j}\gamma a)}{\mathcal{H}_\nu^{(1)}(\mathrm{j}\gamma a)}\right]\left[\frac{\varepsilon_1\gamma^2 a^2}{\kappa a}\frac{\mathcal{J}_\nu'(\kappa a)}{\mathcal{J}_\nu(\kappa a)}+\mathrm{j}\varepsilon_2\gamma a\frac{\mathcal{H}_\nu^{(1)'}(\mathrm{j}\gamma a)}{\mathcal{H}_\nu^{(1)}(\mathrm{j}\gamma a)}\right] \tag{4.95}$$

The required solution to the eigenvalue equation presents a set of eigenvalues expressed in terms of κ, γ, or β associated to the given real indices of refraction in the core, n_1 and in the cladding, n_2 along with the core radius, a and frequency, ω, for the orders $\nu = 0, 1, 2, \ldots$. The number of eigenvalues, κ, or γ, or β gives the number of modes which are allowed to propagate in the fiber. The eigenvalues, κ, γ, and β are interrelated

[8] Dietrich Marcuse, *Light Transmission Optics*, Bell Laboratories Series, Van Nostrand Reinhold Company, New York 1972, pp. 286 - 305.

according to Eqs. (4.74) and (4.79)

$$\kappa^2 = n_1^2 \frac{\omega^2}{c^2} - \beta^2$$
$$\gamma^2 = \beta^2 - n_2^2 \frac{\omega^2}{c^2}$$

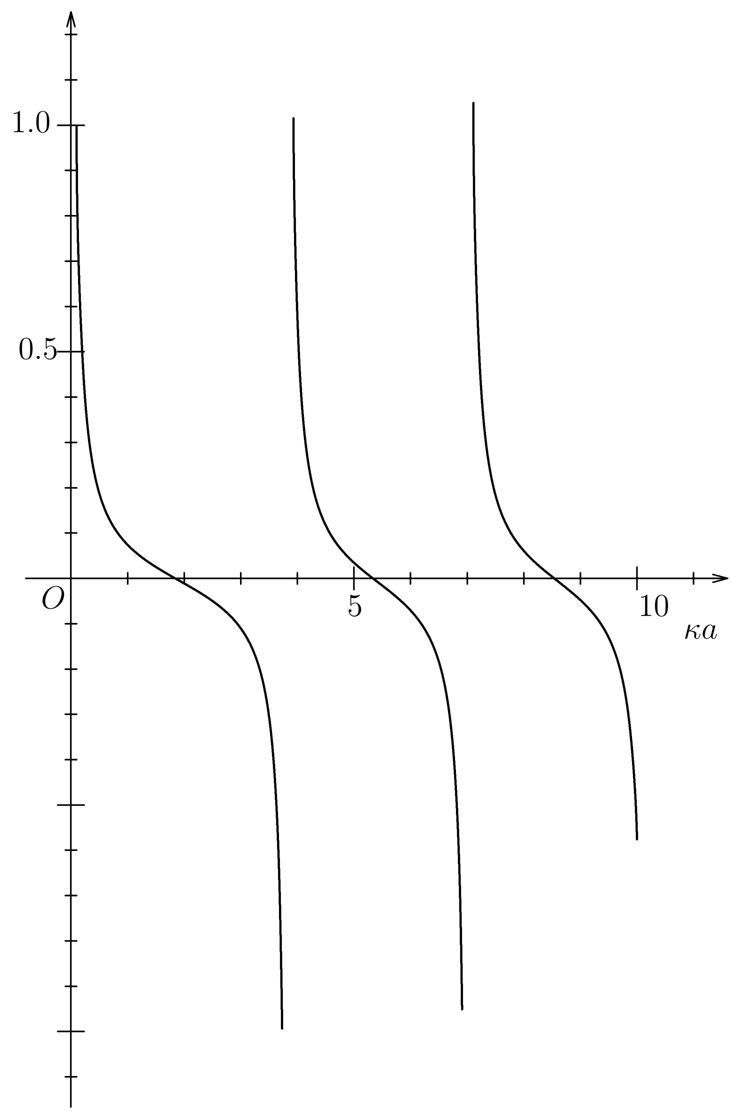

Figure 4.12: Plot of the function $\dfrac{\mathcal{J}_1'(\kappa a)}{\mathcal{J}_1(\kappa a)}$.

Figures 4.12, 4.14 and 4.16 display the plots of functions $\dfrac{\mathcal{J}_i'(\kappa a)}{\mathcal{J}_i(\kappa a)}$, $i = 1, 2, 3$ employed in the eigenvalue equation Eq. (4.95). Figures 4.13, 4.15 and 4.17 illustrates the behavior of the functions $\dfrac{1}{\kappa a} \dfrac{\mathcal{J}_i'(\kappa a)}{\mathcal{J}_i(\kappa a)}$, $i = 1, 2, 3$. The nodal points of Bessel functions and their derivatives are listed in Table 4.2.

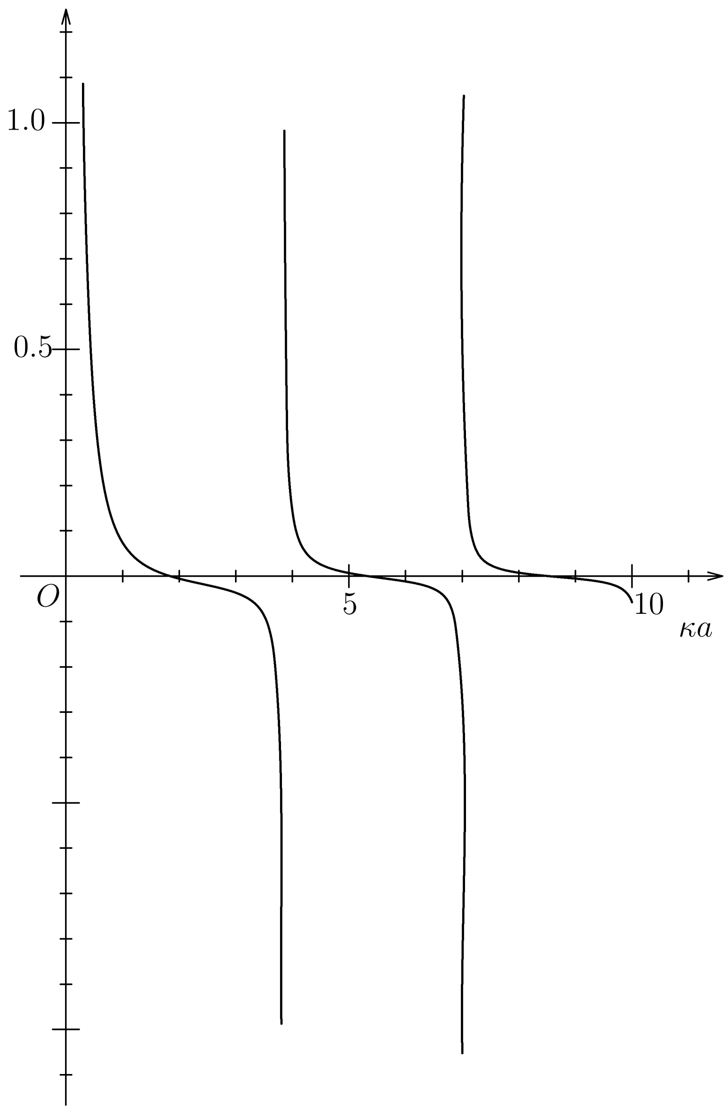

Figure 4.13: Plot of the function $\dfrac{1}{\kappa a}\dfrac{\mathcal{J}_1'(\kappa a)}{\mathcal{J}_1(\kappa a)}$.

4.4 Guided TE and TM modes

In general, the eigenmodes consist of all six components. The eigen modes where $E_z \neq 0$ and $H_z \neq 0$ simultaneously are called hybrid modes. They are characterized by $\nu \neq 0$. On the other hand, at $\nu = 0$ the dependence on the φ coordinate disappears and the left hand side of the eigenvalue equation $E_z \neq 0$ a $H_z \neq 0$ vanish. Then, the eigenvalue equation splits into two independent parts,

$$\left[\frac{\mu_1}{\kappa a}\frac{\mathcal{J}_0'(\kappa a)}{\mathcal{J}_0(\kappa a)} + \mathrm{j}\frac{\mu_2}{\gamma a}\frac{\mathcal{H}_0^{(1)'}(\mathrm{j}\gamma a)}{\mathcal{H}_0^{(1)}(\mathrm{j}\gamma a)}\right] = 0 \tag{4.96a}$$

$$\left[\frac{\varepsilon_1}{\kappa a}\frac{\mathcal{J}_0'(\kappa a)}{\mathcal{J}_0(\kappa a)} + \mathrm{j}\frac{\varepsilon_2}{\gamma a}\frac{\mathcal{H}_0^{(1)'}(\mathrm{j}\gamma a)}{\mathcal{H}_0^{(1)}(\mathrm{j}\gamma a)}\right] = 0 \tag{4.96b}$$

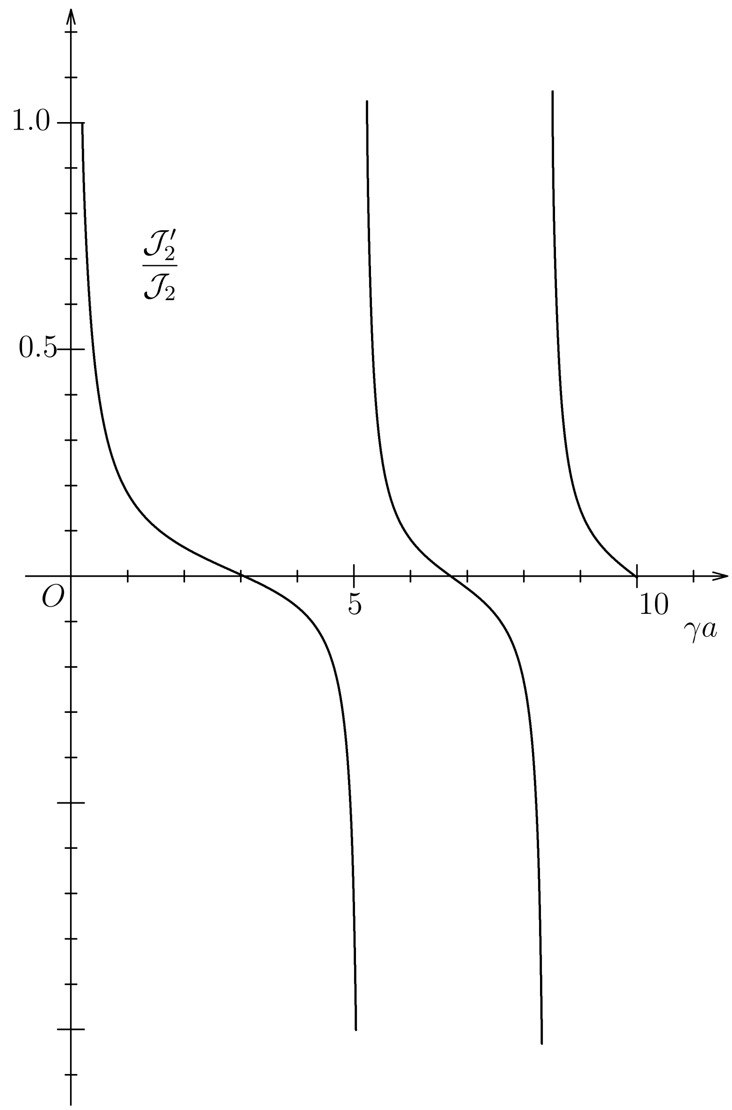

Figure 4.14: Plot of the function $\dfrac{\mathcal{J}_2'(\kappa a)}{\mathcal{J}_2(\kappa a)}$.

Because of the φ independence, all the derivatives with respect to φ in Eqs. (4.34) vanish, i.e., $\dfrac{\partial}{\partial\varphi} \to 0$. Equations (4.34) simplify to

$$E_\varrho = -\mathrm{j}\frac{1}{\kappa^2}\beta\frac{\partial E_z}{\partial\varrho} \tag{4.97a}$$

$$E_\varphi = \mathrm{j}\frac{1}{\kappa^2}\omega\mu\frac{\partial H_z}{\partial\varrho} \tag{4.97b}$$

$$H_\varrho = -\mathrm{j}\frac{1}{\kappa^2}\beta\frac{\partial H_z}{\partial\varrho} \tag{4.97c}$$

$$H_\varphi = -\mathrm{j}\frac{1}{\kappa^2}\omega\varepsilon\frac{\partial E_z}{\partial\varrho} \tag{4.97d}$$

We arrive at two independent field sets. In the first one, the E_z component is missing.

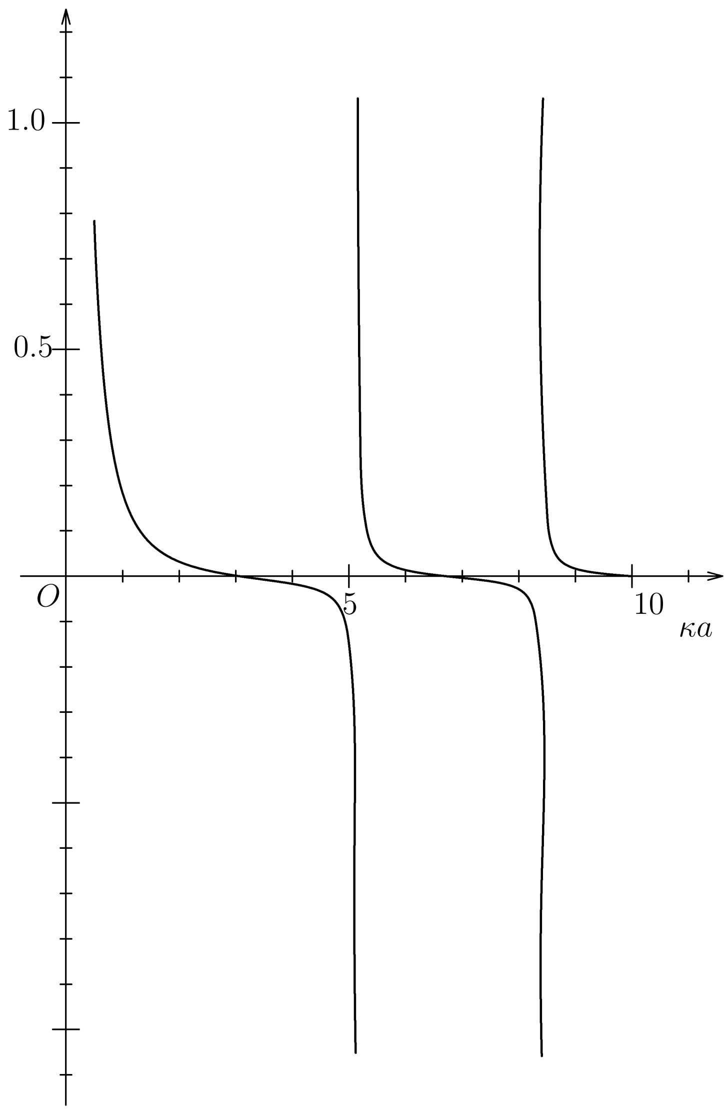

Figure 4.15: Plot of the function $\dfrac{1}{\kappa a}\dfrac{\mathcal{J}_2'(\kappa a)}{\mathcal{J}_2(\kappa a)}$.

The set represents TE modes consisting of the E_φ, H_ϱ and H_z components. It is the H_z field component which is missing in the second set. This represent TM modes consisting of the H_φ, E_ϱ and E_z components. Equations (4.97) confirm the splitting into the two sets, each consisting of three field components independent of the φ coordinate. Equation (4.96a) represents the eigenvalue equation for TE modes, while Eq. (4.96b) represents that one for TM modes.

4.4.1 Characteristic equations for TE and TM modes

The eigenvalue equations for TE and TM modes can be derived using a easier procedure. We employ a simplified notation for cylindrical functions of zero order, $\mathcal{Z}_0 = \mathcal{J}_0\,, \mathcal{H}_0^{(1)}$, for the values of their derivatives on the surface $\varrho = a$ similar to that employed in Eqs. (4.87),

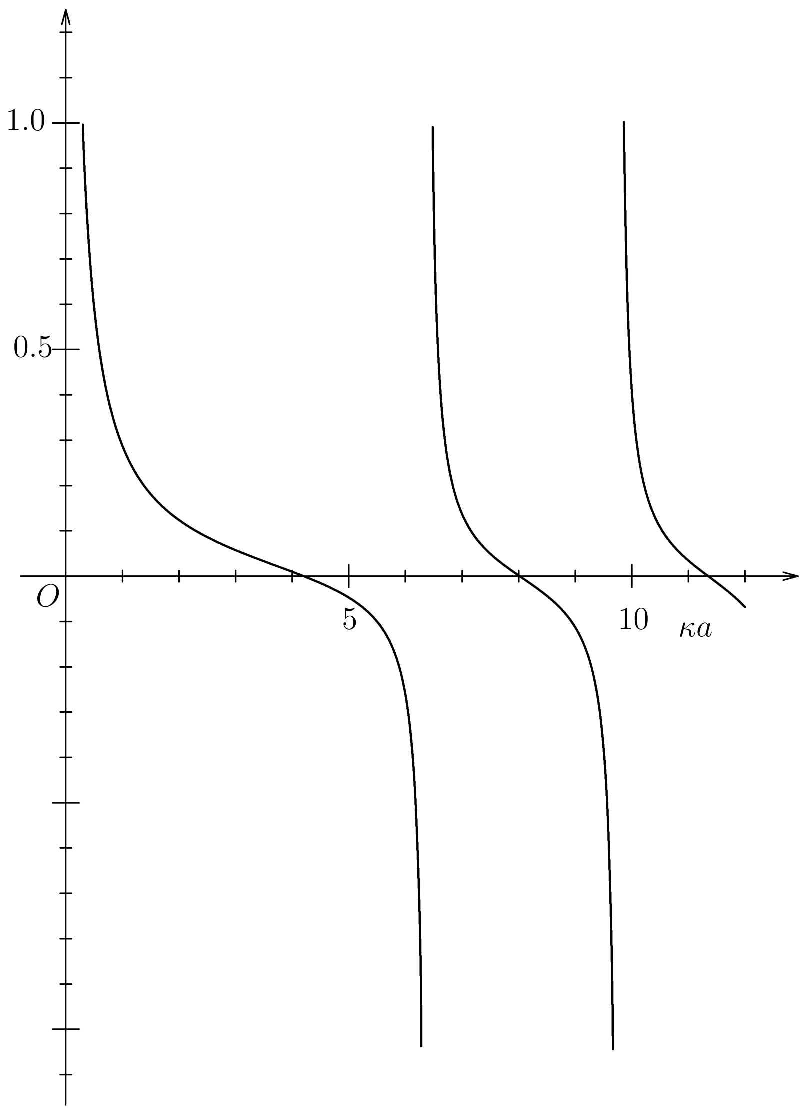

Figure 4.16: Plot of the function $\dfrac{\mathcal{J}_3'(\kappa a)}{\mathcal{J}_3(\kappa a)}$.

$$\mathcal{J}_0 = \mathcal{J}_0(\kappa a) \tag{4.98a}$$

$$\mathcal{H}_0^{(1)} = \mathcal{H}_0^{(1)}(\mathrm{j}\gamma a) \tag{4.98b}$$

$$\mathcal{J}_0' = \frac{\mathrm{d}\mathcal{J}_0(\kappa a)}{\mathrm{d}(\kappa a)} \tag{4.98c}$$

$$\mathcal{H}_0^{(1)'} = \frac{\mathrm{d}\mathcal{H}_0^{(1)}(\mathrm{j}\gamma a)}{\mathrm{d}(\mathrm{j}\gamma a)} \tag{4.98d}$$

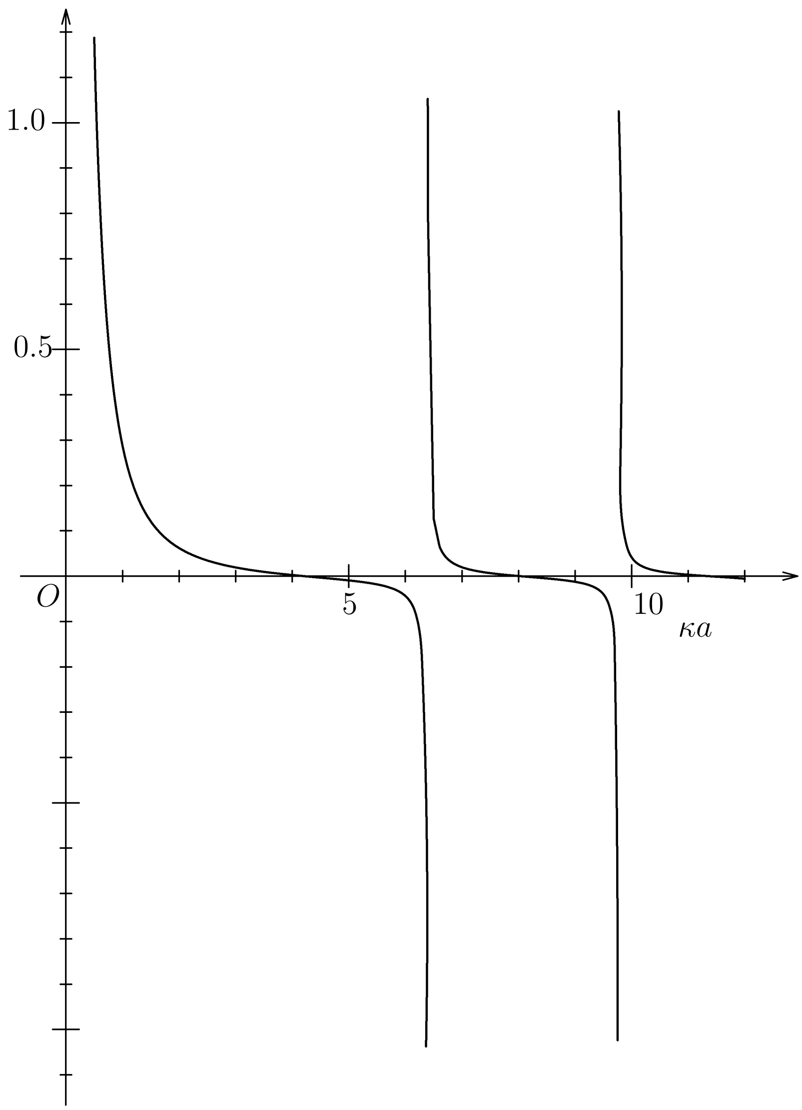

Figure 4.17: Plot of the function $\dfrac{1}{\kappa a}\dfrac{\mathcal{J}_3'(\kappa a)}{\mathcal{J}_3(\kappa a)}$.

Core region

In the core region, $0 \le \varrho \le a$ we express the field components as,

$$E_z^{(0)} = A_0 \mathcal{J}_0(\kappa\varrho)\, \mathrm{e}^{\mathrm{j}(\omega t - \beta z)} \tag{4.99a}$$

$$H_z^{(0)} = B_0 \mathcal{J}_0(\kappa\varrho)\, \mathrm{e}^{\mathrm{j}(\omega t - \beta z)} \tag{4.99b}$$

$$E_\varrho^{(0)} = -\frac{\mathrm{j}}{\kappa^2}\beta\frac{\partial E_z^{(0)}}{\partial\varrho} A_0 \frac{\mathrm{j}}{\kappa}\beta\frac{\mathrm{d}\mathcal{J}_0(\kappa\varrho)}{\mathrm{d}(\kappa\varrho)}\ \mathrm{e}^{\mathrm{j}(\omega t - \beta z)} \tag{4.99c}$$

$$E_\varphi^{(0)} = \frac{\mathrm{j}}{\kappa^2}\omega\mu_1\frac{\partial H_z^{(0)}}{\partial\varrho} = B_0 \frac{\mathrm{j}}{\kappa}\omega\mu_1\frac{\mathrm{d}\mathcal{J}_0(\kappa\varrho)}{\mathrm{d}(\kappa\varrho)}\ \mathrm{e}^{\mathrm{j}(\omega t - \beta z)} \tag{4.99d}$$

$$H_\varrho^{(0)} = -\frac{\mathrm{j}}{\kappa^2}\beta\frac{\partial H_z^{(0)}}{\partial\varrho} = -B_0 \frac{\mathrm{j}}{\kappa}\beta\frac{\mathrm{d}\mathcal{J}_0(\kappa\varrho)}{\mathrm{d}(\kappa\varrho)}\ \mathrm{e}^{\mathrm{j}(\omega t - \beta z)} \tag{4.99e}$$

Table 4.2: Nodal points of Bessel functions, $\mathcal{J}_\nu(x)$ and their derivatives, $\mathcal{J}'_\nu(x)$. (André Angot, *Compléments de mathématiques*, Paris 1957.)

	$\mathcal{J}_0(x)$	$\mathcal{J}_1(x)$	$\mathcal{J}_2(x)$	$\mathcal{J}_3(x)$	$\mathcal{J}_4(x)$	$\mathcal{J}_5(x)$
1	2.4048	3.8317	5.1356	6.3802	7.5883	8.7715
2	5.5201	7.0156	8.4172	9.7610	11.0647	12.3386
3	8.6537	10.1735	11.6198	13.0152	14.3725	15.7002
4	11.7915	13.3237	14.7960	16.2235	17.6160	18.9801
5	14.9309	16.4706	17.9598	19.4094	20.8269	22.2178
	$\mathcal{J}'_0(x)$	$\mathcal{J}'_1(x)$	$\mathcal{J}'_2(x)$	$\mathcal{J}'_3(x)$	$\mathcal{J}'_4(x)$	$\mathcal{J}'_5(x)$
1	0.0000	1.8412	3.0542	4.2012	5.3175	6.4156
2	3.8317	5.3314	6.7061	8.0152	9.2824	10.5199
3	7.0156	8.5363	9.9695	11.3459	12.6819	13.9872
4	10.1735	11.7060	13.1704	14.5859	15.9641	17.3128
5	13.3237	14.8636	16.3475	17.7888	19.1960	20.5755

$$H_\varphi^{(0)} = -\frac{\mathrm{j}}{\kappa^2}\omega\varepsilon_1\frac{\partial E_z^{(0)}}{\partial\varrho} = -\frac{\mathrm{j}}{\kappa}\omega\varepsilon_1 A_0\frac{\mathrm{d}\mathcal{J}_0\left(\kappa\varrho\right)}{\mathrm{d}\left(\kappa\varrho\right)}\ \mathrm{e}^{\mathrm{j}(\omega t-\beta z)} \tag{4.99f}$$

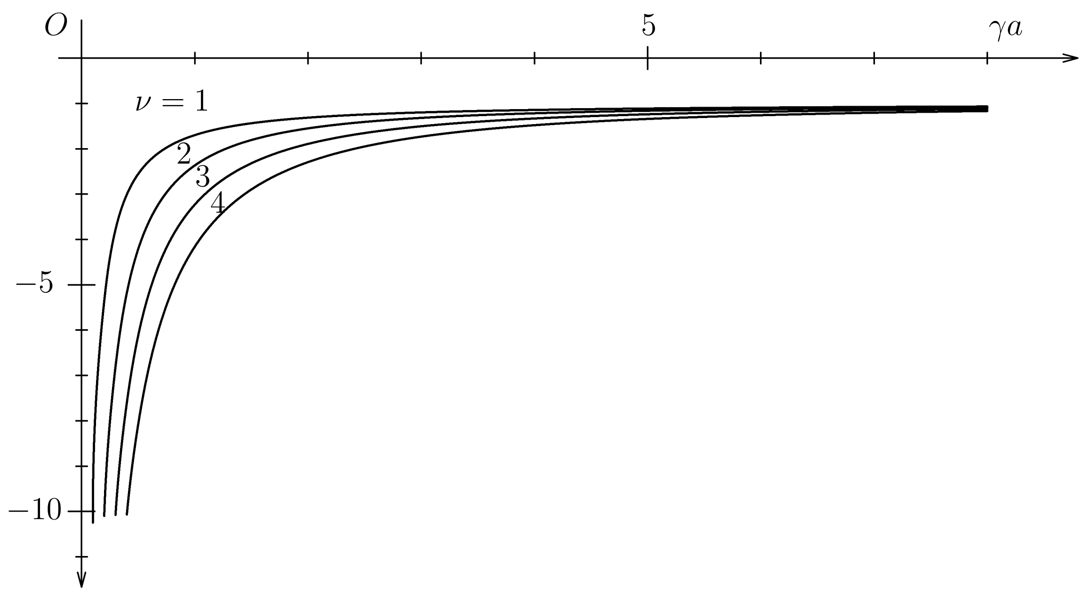

Figure 4.18: Plot of the functions $\dfrac{\mathcal{K}_\nu'(\gamma a)}{\mathcal{K}_\nu(\gamma a)} = \mathrm{j}\dfrac{\mathcal{H}_\nu^{(1)'}(\gamma a)}{\mathcal{H}_\nu^{(1)}(\gamma a)}$, $\nu = 1,\ 2,\ 3, 4$.

Cladding region

In the cladding region, $a \le \varrho$, we express the field components as

$$E_z^{(0)} = C_0\mathcal{H}_0^{(1)}(\mathrm{j}\gamma\varrho)\,\mathrm{e}^{\mathrm{j}(\omega t-\beta z)} \tag{4.100a}$$

$$H_z^{(0)} = D_0\mathcal{H}_0^{(1)}(\mathrm{j}\gamma\varrho)\,\mathrm{e}^{\mathrm{j}(\omega t-\beta z)} \tag{4.100b}$$

$$E_\varrho^{(0)} = \frac{\mathrm{j}}{\gamma^2}\left(\beta\frac{\partial E_z^{(0)}}{\partial\varrho}\right) = -C_0\frac{\beta}{\gamma}\frac{\mathrm{d}\mathcal{H}_0^{(1)}(\mathrm{j}\gamma\varrho)}{\mathrm{d}(\mathrm{j}\gamma\varrho)}\;\mathrm{e}^{\mathrm{j}(\omega t-\beta z)} \tag{4.100c}$$

$$E_\varphi^{(0)} = -\frac{\mathrm{j}}{\gamma^2}\omega\mu_2\frac{\partial H_z^{(0)}}{\partial\varrho} = D_0\frac{\omega\mu_2}{\gamma}\frac{\mathrm{d}\mathcal{H}_0^{(1)}(\mathrm{j}\gamma\varrho)}{\mathrm{d}(\mathrm{j}\gamma\varrho)}\;\mathrm{e}^{\mathrm{j}(\omega t-\beta z)} \tag{4.100d}$$

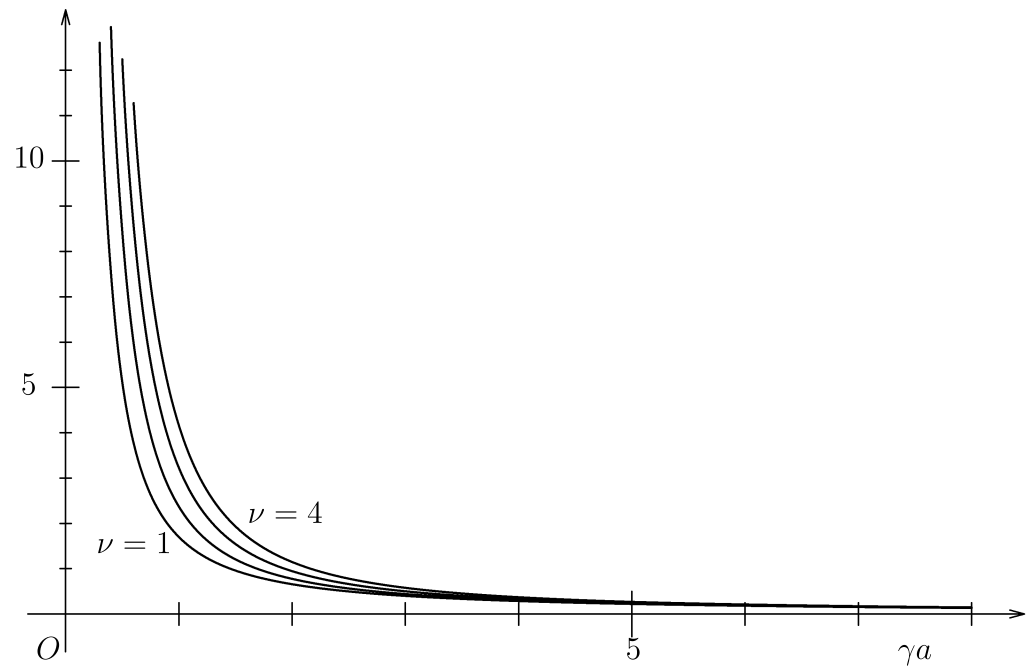

Figure 4.19: Plot of the functions $\dfrac{1}{\mathrm{j}\gamma a}\dfrac{\mathcal{H}_\nu^{(1)'}(\mathrm{j}\gamma a)}{\mathcal{H}_\nu(\mathrm{j}\gamma a)} = -\dfrac{1}{\gamma a}\dfrac{\mathcal{K}_\nu'(\gamma a)}{\mathcal{K}_\nu(\gamma a)}$, $\nu = 1,\, 2,\, 3,\, 4$.

$$H_\varrho^{(0)} = \frac{\mathrm{j}}{\gamma^2}\beta\frac{\partial H_z^{(0)}}{\partial\varrho}\frac{\mathrm{d}\mathcal{H}_0^{(1)}(\mathrm{j}\gamma\varrho)}{\mathrm{d}(\mathrm{j}\gamma\varrho)}\;\mathrm{e}^{\mathrm{j}(\omega t-\beta z)} \tag{4.100e}$$

$$H_\varphi^{(0)} = \frac{\mathrm{j}}{\gamma^2}\omega\varepsilon_2\frac{\partial E_z^{(0)}}{\partial\varrho} = -C_0\frac{\omega\varepsilon_2}{\gamma}\frac{\mathrm{d}\mathcal{H}_0^{(1)}(\mathrm{j}\gamma\varrho)}{\mathrm{d}(\mathrm{j}\gamma\varrho)}\;\mathrm{e}^{\mathrm{j}(\omega t-\beta z)} \tag{4.100f}$$

As already found, the components form the two sets,

$$\begin{array}{c}\text{TE } (E_z^{(0)} = 0)\text{: } E_\varphi^{(0)},\, H_z^{(0)},\, H_\varrho^{(0)}\\ \text{TM } (H_z^{(0)} = 0)\text{: } H_\varphi^{(0)},\, E_z^{(0)},\, E_\varrho^{(0)}\end{array}$$

$\varrho = a$ according to Eqs. (4.84) for $\nu = 0$,

$$\lim_{\varrho\to a_-} E_z^{(0)}(\varrho) = \lim_{\varrho\to a_+} E_z^{(0)}(\varrho) \tag{4.101a}$$

$$\lim_{\varrho\to a_-} H_z^{(0)}(\varrho) = \lim_{\varrho\to a_+} H_z^{(0)}(\varrho) \tag{4.101b}$$

$$\lim_{\varrho\to a_-} E_\varphi^{(0)}(\varrho) = \lim_{\varrho\to a_+} E_\varphi^{(0)}(\varrho) \tag{4.101c}$$

$$\lim_{\varrho\to a_-} H_\varphi^{(0)}(\varrho) = \lim_{\varrho\to a_+} H_\varphi^{(0)}(\varrho) \tag{4.101d}$$

The continuity conditions can be established with the help of Eqs. (4.99) and (4.100) for the fields,

E_φ continuous

$$B_0 \frac{\mathrm{j}}{\kappa} \mu_1 \frac{\mathrm{d}\mathcal{J}_0(\kappa\varrho)}{\mathrm{d}(\kappa\varrho)}\bigg|_{\varrho\to a^-} = D_0 \frac{\mu_2}{\gamma} \frac{\mathrm{d}\mathcal{H}_0^{(1)}(\mathrm{j}\gamma\varrho)}{\mathrm{d}(\mathrm{j}\gamma\varrho)}\Bigg|_{\varrho\to a^+} \tag{4.102a}$$

H_z continuous

$$B_0 \mathcal{J}_0(\kappa\varrho)\big|_{\varrho\to a^-} = D_0 \mathcal{H}_0^{(1)}(\mathrm{j}\gamma\varrho)\Big|_{\varrho\to a^+} \tag{4.102b}$$

H_φ continuous

$$-\frac{\mathrm{j}}{\kappa} \omega\varepsilon_1 A_0 \frac{\mathrm{d}\mathcal{J}_0(\kappa\varrho)}{\mathrm{d}(\kappa\varrho)}\bigg|_{\varrho\to a^-} = -C_0 \frac{\omega\varepsilon_2}{\gamma} \frac{\mathrm{d}\mathcal{H}_0^{(1)}(\mathrm{j}\gamma\varrho)}{\mathrm{d}(\mathrm{j}\gamma\varrho)} \mathrm{e}^{\mathrm{j}(\omega t-\beta z)}\Bigg|_{\varrho\to a^+} \tag{4.102c}$$

E_z continuous

$$A_0 \mathcal{J}_0(\kappa\varrho)\big|_{\varrho\to a^-} = C_0 \mathcal{H}_0^{(1)}(\mathrm{j}\gamma\varrho)\Big|_{\varrho\to a^+} \tag{4.102d}$$

We rewrite this homogeneous equation set with the help of a more concise notation.

E_φ continuous

$$B_0 \frac{\mathrm{j}}{\kappa} \mu_1 \mathcal{J}_0'(\kappa a) - D_0 \frac{\mu_2}{\gamma} \mathcal{H}_0^{(1)'}(\mathrm{j}\gamma a) = 0 \tag{4.103a}$$

H_z continuous

$$B_0 \mathcal{J}_0(\kappa a) - D_0 \mathcal{H}_0^{(1)}(\mathrm{j}\gamma a) = 0 \tag{4.103b}$$

H_φ continuous

$$-\frac{\mathrm{j}}{\kappa} \omega\varepsilon_1 A_0 \mathcal{J}_0'(\kappa a) + C_0 \frac{\omega\varepsilon_2}{\gamma} \mathcal{H}_0^{(1)'}(\mathrm{j}\gamma a) = 0 \tag{4.103c}$$

E_z continuous

$$A_0 \mathcal{J}_0(\kappa a) - C_0 \mathcal{H}_0^{(1)}(\mathrm{j}\gamma a) = 0 \tag{4.103d}$$

This homogeneous equation set of four linear equations for the amplitudes A_0, B_0, C_0 and D_0, has a nontrivial solution at the vanishing determinant constructed from the elements of a block diagonal matrix representing the left hand side of the equation set. The determinant has the structure displayed in Table 4.3,

Table 4.3: Tangential field components of TE and TM modes at the boundary surface $\varrho = a$.

	A_0	C_0	B_0	D_0
E_φ	0	0	$\frac{\mathrm{j}\omega\mu_1}{\kappa}\mathcal{J}_0'$	$-\frac{\omega\mu_2}{\gamma}\mathcal{H}_0^{(1)'}$
H_z	0	0	$\mathcal{J}_0$	$-\mathcal{H}_0^{(1)}$
H_φ	$-\frac{\mathrm{j}\omega\varepsilon_1}{\kappa}\mathcal{J}_0'$	$-\frac{\omega\varepsilon_2}{\gamma}\mathcal{H}_0^{(1)'}$	0	0
E_z	$\mathcal{J}_0$	$-\mathcal{H}_0^{(1)}$	0	0

$$\begin{vmatrix} 0 & 0 & \frac{\mathrm{j}\omega\mu_1}{\kappa}\mathcal{J}_0' & -\frac{\omega\mu_2}{\gamma}\mathcal{H}_0^{(1)'} \\ 0 & 0 & \mathcal{J}_0 & -\mathcal{H}_0^{(1)} \\ -\frac{\mathrm{j}\omega\varepsilon_1}{\kappa}\mathcal{J}_0' & -\frac{\omega\varepsilon_2}{\gamma}\mathcal{H}_0^{(1)'} & 0 & 0 \\ \mathcal{J}_0 & -\mathcal{H}_0^{(1)} & 0 & 0 \end{vmatrix} = 0$$

The eigenvalue equation for TE modes

$$\frac{\mu_1}{\kappa}\frac{\mathcal{J}_0'(\kappa a)}{\mathcal{J}_0(\kappa a)} + \frac{\mathrm{j}\mu_2}{\gamma}\frac{\mathcal{H}_0^{(1)'}(\mathrm{j}\gamma a)}{\mathcal{H}_0^{(1)}(\mathrm{j}\gamma a)} = 0 \tag{4.104a}$$

corresponds to Eq. (4.96a). The eigenvalue equation for TM modes,

$$\frac{\varepsilon_1}{\kappa}\frac{\mathcal{J}_0'(\kappa a)}{\mathcal{J}_0(\kappa a)} + \frac{\mathrm{j}\varepsilon_2}{\gamma}\frac{\mathcal{H}_0^{(1)'}(\mathrm{j}\gamma a)}{\mathcal{H}_0^{(1)}(\mathrm{j}\gamma a)} = 0 \tag{4.104b}$$

corresponds to Eq. (4.96b). The eigenvalue equation for TE modes can be rearranged to the form,

$$\frac{\mu_1}{\mu_2}\frac{\gamma^2 a^2}{\kappa a}\frac{\mathcal{J}_0'(\kappa a)}{\mathcal{J}_0(\kappa a)} + \mathrm{j}\gamma a\frac{\mathcal{H}_0^{(1)'}(\mathrm{j}\gamma a)}{\mathcal{H}_0^{(1)}(\mathrm{j}\gamma a)} = 0 \tag{4.105a}$$

and the eigenvalue equation for TM modes can be rearranged to the form,

$$\frac{\varepsilon_1}{\varepsilon_2}\frac{\gamma^2 a^2}{\kappa a}\frac{\mathcal{J}_0'(\kappa a)}{\mathcal{J}_0(\kappa a)} + \mathrm{j}\gamma a\frac{\mathcal{H}_0^{(1)'}(\mathrm{j}\gamma a)}{\mathcal{H}_0^{(1)}(\mathrm{j}\gamma a)} = 0 \tag{4.105b}$$

Next, we employ the recursion relations for cylindrical function including the cases $\nu = 0$ and $\nu = \pm 1$,

$$\mathcal{Z}_{-1}(z) = -\mathcal{Z}_1(z) \tag{4.106a}$$

$$\begin{aligned}\mathcal{Z}_0'(z) = \frac{\mathrm{d}\mathcal{Z}_0(z)}{\mathrm{d}z} &= \frac{1}{2}\left[\mathcal{Z}_{-1}(z) - \mathcal{Z}_1(z)\right] \\ &= \frac{1}{2}\left[-\mathcal{Z}_1(z) - \mathcal{Z}_1(z)\right] \\ &= -\mathcal{Z}_1 \qquad (4.106b)\end{aligned}$$

This allows us to eliminate from the eigenvalue equations (4.105) the derivatives of cylindrical functions with respect to the argument,

$$\frac{\mu_1}{\mu_2}\frac{\gamma a}{\kappa a}\frac{\mathcal{J}_1(\kappa a)}{\mathcal{J}_0(\kappa a)} + \mathrm{j}\frac{\mathcal{H}_1^{(1)}(\mathrm{j}\gamma a)}{\mathcal{H}_0^{(1)}(\mathrm{j}\gamma a)} = 0\,, \qquad \text{(TE)} \qquad (4.107a)$$

$$\frac{\varepsilon_1}{\varepsilon_2}\frac{\gamma a}{\kappa a}\frac{\mathcal{J}_1(\kappa a)}{\mathcal{J}_0(\kappa a)} + \mathrm{j}\frac{\mathcal{H}_1^{(1)}(\mathrm{j}\gamma a)}{\mathcal{H}_0^{(1)}(\mathrm{j}\gamma a)} = 0\,, \qquad \text{(TM)} \qquad (4.107b)$$

4.4.2 Fields of TE modes

The profile of TE modes can be appreciated from Figure 4.20.

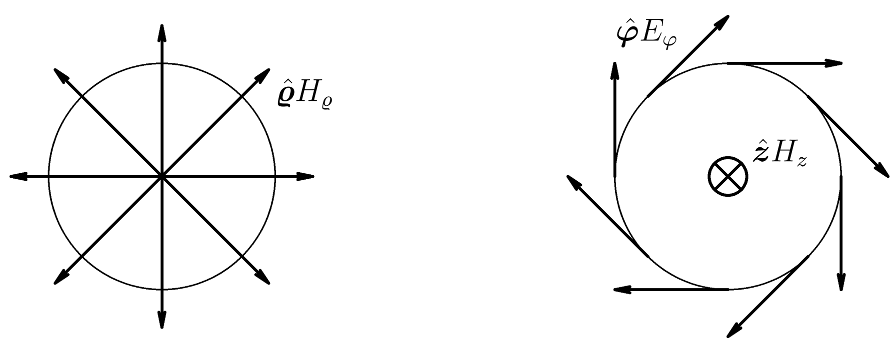

Figure 4.20: The field components of TE modes in circular cylindrical dielectric waveguides. The unit vector, $\hat{\boldsymbol{z}}$ is oriented into the page.

$$\begin{aligned}H_z^{(0)} &= B_0\mathcal{J}_0(\kappa\varrho) \qquad (4.108a)\\ H_\varrho^{(0)} &= \frac{\mathrm{j}\beta}{\kappa}B_0\mathcal{J}_1(\kappa\varrho) \qquad (4.108b)\\ E_\varphi^{(0)} &= -\frac{\mathrm{j}\omega\mu_1}{\kappa}B_0\mathcal{J}_1(\kappa\varrho) \qquad (4.108c)\end{aligned}$$

4.4.3 Fields of TM modes

The profile of TM modes can be appreciated from Figure 4.21.

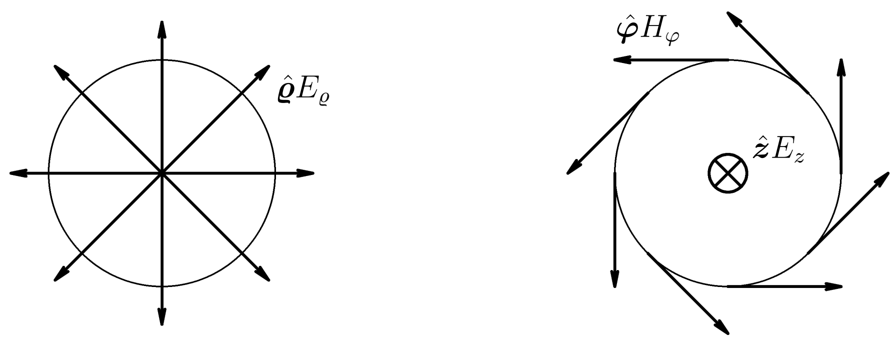

Figure 4.21: The field components of TM modes módů in circular cylindrical dielectric waveguides. The unit vector, $\hat{\boldsymbol{z}}$ is oriented into the page.

$$E_z^{(0)} = A_0 \mathcal{J}_0(\kappa\varrho) \tag{4.109a}$$

$$E_\varrho^{(0)} = \frac{\mathrm{j}\beta}{\kappa} B_0 \mathcal{J}_1(\kappa\varrho) \tag{4.109b}$$

$$H_\varphi^{(0)} = \frac{\mathrm{j}\omega\varepsilon_1}{\kappa} A_0 \mathcal{J}_1(\kappa\varrho) \tag{4.109c}$$

4.4.4 Cut-off frequencies for TE and TM modes

The cut–off conditions follow from the condition $\gamma \to 0$. We make the use of Eqs. (4.61) and (4.62). For small γa, the cylindrical functions can be approximated,

$$\begin{aligned}\mathcal{H}_0^{(1)}(\mathrm{j}\gamma a) = \mathcal{J}_0(\mathrm{j}\gamma a) + \mathrm{j}\mathcal{N}_0(\mathrm{j}\gamma a) &\approx 1 + \mathrm{j}\frac{2}{\pi}\ln\left(\frac{\Upsilon\gamma a}{2}\right) \\ &\approx \mathrm{j}\frac{2}{\pi}\ln\left(\frac{\Upsilon\gamma a}{2}\right),\end{aligned} \tag{4.110a}$$

thanks to $\left|\ln\left(\frac{\Upsilon\gamma a}{2}\right)\right| \gg 1$. Here $\Upsilon \approx 1,78107 = \mathrm{e}^{\upsilon} = \mathrm{e}^{0,5772156619}$. The symbol υ denotes so called Euler–Mascheroni constant (p. 93). defined by the series,

$$\upsilon = \lim_{m\to\infty}\left(1 + \frac{1}{2} + \frac{1}{3} + \frac{1}{4} + \cdots + \frac{1}{m} - \ln m\right)$$

For small γa we further have

$$\mathcal{H}_1^{(1)}(\mathrm{j}\gamma a) \approx \mathrm{j}\frac{1}{2}\gamma a - \frac{2}{\pi\gamma a} \approx -\frac{2}{\pi\gamma a}, \quad \gamma a \ll 1 \tag{4.110b}$$

The substitution to the eigenvalue equation (4.107b) for TM eigenmodes provides step by step,

$$
\begin{aligned}
\frac{\varepsilon_1}{\varepsilon_2}\frac{1}{\kappa a}\frac{\mathcal{J}_1(\kappa a)}{\mathcal{J}_0(\kappa a)} + \mathrm{j}\frac{1}{\gamma a}\frac{\mathcal{H}_1^{(1)}(\mathrm{j}\gamma a)}{\mathcal{H}_0^{(1)}(\mathrm{j}\gamma a)} &= 0 \\
\frac{\varepsilon_2}{\varepsilon_1}\kappa a\frac{\mathcal{J}_0(\kappa a)}{\mathcal{J}_1(\kappa a)} - \mathrm{j}\gamma a\frac{\mathcal{H}_0^{(1)}(\mathrm{j}\gamma a)}{\mathcal{H}_1^{(1)}(\mathrm{j}\gamma a)} &= 0 \\
\frac{\varepsilon_2}{\varepsilon_1}\kappa a\frac{\mathcal{J}_0(\kappa a)}{\mathcal{J}_1(\kappa a)} - \mathrm{j}\gamma a\frac{\mathrm{j}\frac{2}{\pi}\ln\left(\frac{\Upsilon\gamma a}{2}\right)}{-\frac{2}{\pi\gamma a}} &= 0 \\
\frac{\varepsilon_2}{\varepsilon_1}\kappa a\,\frac{\mathcal{J}_0(\kappa a)}{\mathcal{J}_1(\kappa a)} - \gamma^2 a^2\ln\left(\frac{\Upsilon\gamma a}{2}\right) &= 0
\end{aligned}
\tag{4.111}
$$

The condition may be rearranged,

$$
\frac{\varepsilon_2}{\varepsilon_1}\kappa a\frac{\mathcal{J}_0(\kappa a)}{\mathcal{J}_1(\kappa a)} = (\gamma a)^2\ln\left(\frac{\Upsilon\gamma a}{2}\right) \tag{4.112}
$$

The limits $\gamma a \to 0$ can be found by making use of the l'Hospital rule applied to a indefinite expression of the type $0 \times (-\infty)$ on the right hand side

$$
\begin{aligned}
&\lim_{\gamma a\to 0}\mathrm{j}\gamma a\left[\frac{\mathcal{H}_0^{(1)}(\mathrm{j}\gamma a)}{\mathcal{H}_1^{(1)}(\mathrm{j}\gamma a)}\right] \\
&= \lim_{\gamma a\to 0}\frac{\ln\left(\frac{\Upsilon\gamma a}{2}\right)}{\frac{1}{(\gamma a)^2}} = \frac{\frac{1}{(\gamma a)}}{\frac{-2}{(\gamma a)^3}} = -\frac{(\gamma a)^2}{2} = 0
\end{aligned}
\tag{4.113}
$$

At $\gamma a \to 0$, the right hand side of Eq. (4.112) goes to zero and the solution is given by[9]

$$
\frac{\varepsilon_2}{\varepsilon_1}\kappa a\frac{\mathcal{J}_0(\kappa a)}{\mathcal{J}_1(\kappa a)} = 0 \tag{4.114}
$$

The cut–off frequencies/thicknesses are specified by the nodal points of the Bessel function of zero order, $\mathcal{J}_0(\kappa a)$

$$
\mathcal{J}_0(\kappa a) = 0 \tag{4.115}
$$

The same condition, $\mathcal{J}_0(\kappa a) = 0$ determines the cut–off condition for TE modes. The first zero point of $\mathcal{J}_0(\kappa)$ determines the lowest frequency/thickness for both TE and TM modes, is located at $(\kappa a)_c \approx 2,405$. The TE and TM modes have common cut–off frequencies/thicknesses but above them their parameters, β, κ, and γ are different.

[9]The zero of the κa argument, $\kappa a = 0$, of the Bessel function does not represent the solution as at $\kappa a \to 0$, $\mathcal{J}_0(\kappa a) \to 1$ and $\mathcal{J}_1(\kappa a) \to \kappa a/2$. Consequently, $\kappa a = 0$ is not a solution to Eq. (4.114).

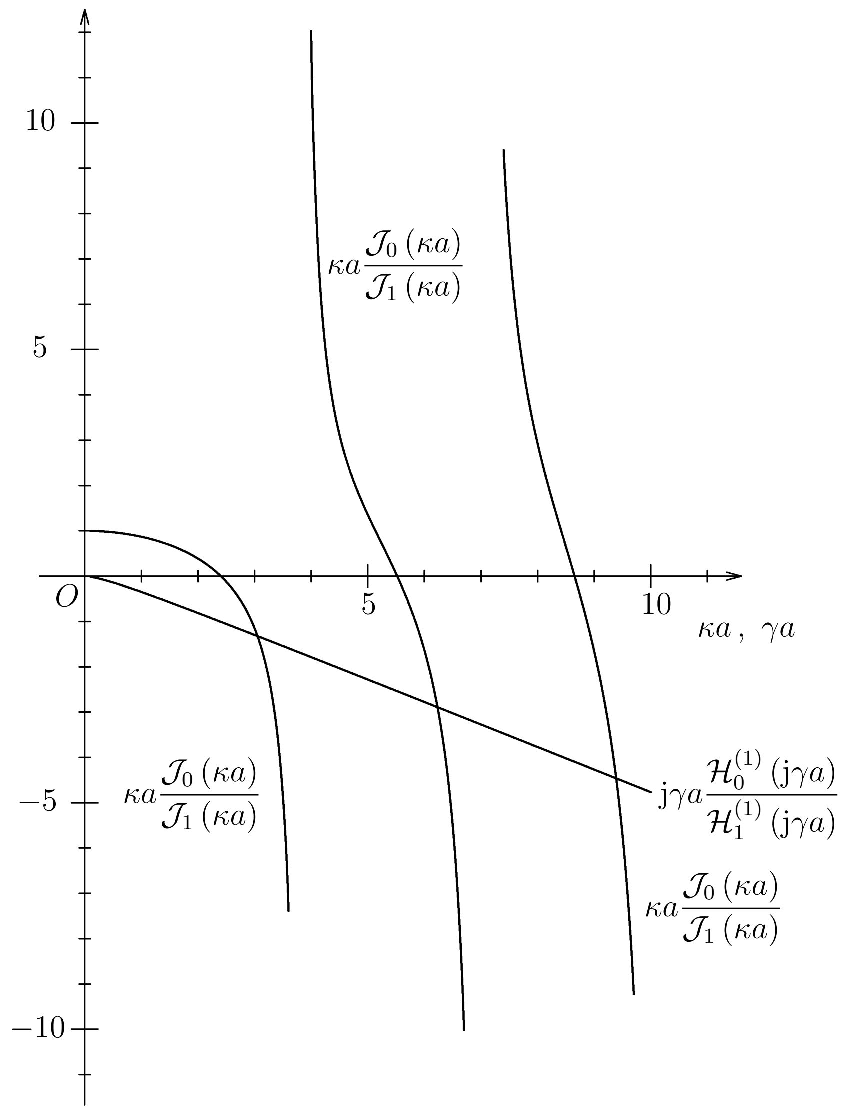

Figure 4.22: Plot of the functions $\kappa a \dfrac{\mathcal{J}_0(\kappa a)}{\mathcal{J}_1(\kappa a)}$ and $\mathrm{j}\gamma a \dfrac{\mathcal{H}_0^{(1)}(\mathrm{j}\gamma a)}{\mathcal{H}_1^{(1)}(\mathrm{j}\gamma a)}$ entering the eigenvalue equations for TE and TM modes.

4.5 Hybrid modes

In Section 4.4 we were concerned with the cut–off conditions for TE and TM modes. In this section, we investigate cut–off frequencies/thicknesses of EH and HE modes, characterized by $\nu \neq 0$. The fields of these so called hybrid modes have non zero both z field components, $E_z \neq 0$ a $H_z \neq 0$ (see the introduction to Section 4.4). Because of Eqs. (4.34), they are formed by all six field components.

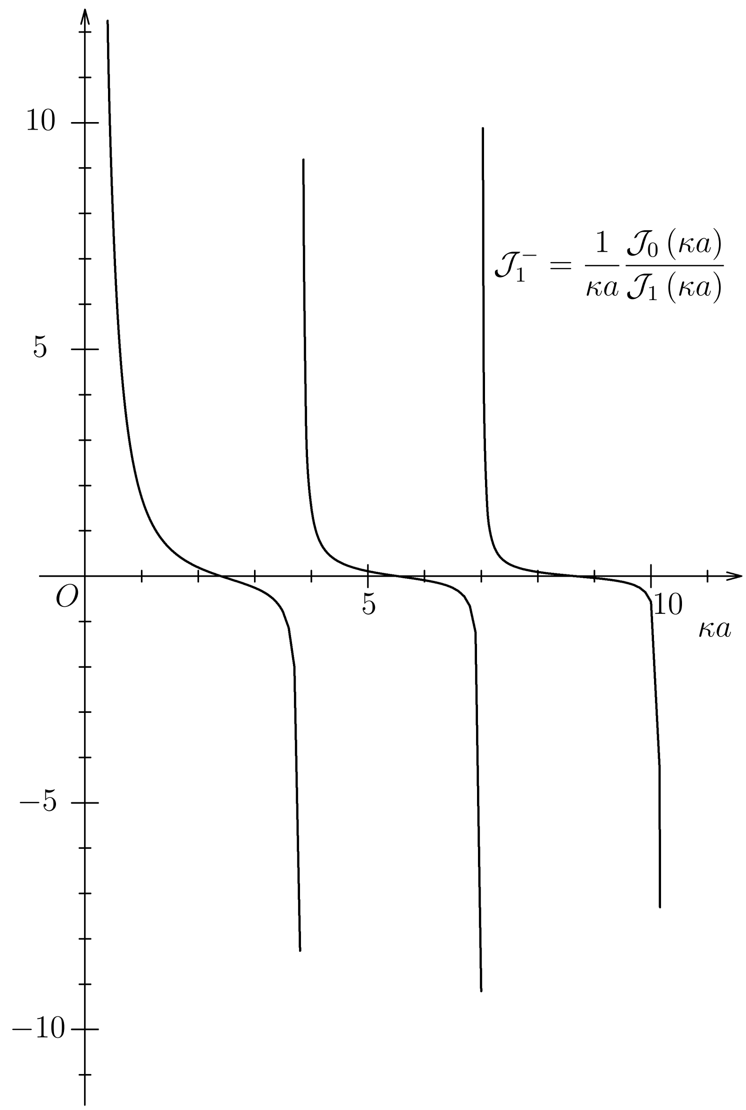

Figure 4.23: Plot of the function, $\mathcal{J}_1^-(\kappa a)$.

4.5.1 Transformation of the characteristic equation

To find the cut–off frequecies/thicknesses (core radii), we transform the eigenvalue equation (4.92). We take into account the properties of cylindrical functions. These are of defined parity,

$$\mathcal{Z}_{-\nu}(z) = (-1)^{\nu}\,\mathcal{Z}_{\nu}(z) \tag{4.116a}$$

We further employ the recursion relations for cylindrical functions,

$$\mathcal{Z}'_{\nu}(z) = \frac{\mathrm{d}\mathcal{Z}_{\nu}(z)}{\mathrm{d}z} = \frac{1}{2}\left[\mathcal{Z}_{\nu-1}(z) - \mathcal{Z}_{\nu+1}(z)\right] \tag{4.116b}$$

$$\mathcal{Z}_{\nu}(z) = \frac{z}{2\nu}\left[\mathcal{Z}_{\nu-1}(z) + \mathcal{Z}_{\nu+1}(z)\right] \tag{4.116c}$$

Please note that the recursion relations must be modified for the Bessel functions of third kind, employed as the solutions to the diffuse equation, $\mathcal{I}_{\nu}(z)$ and $\mathcal{K}_{\nu}(z)$. In particular,

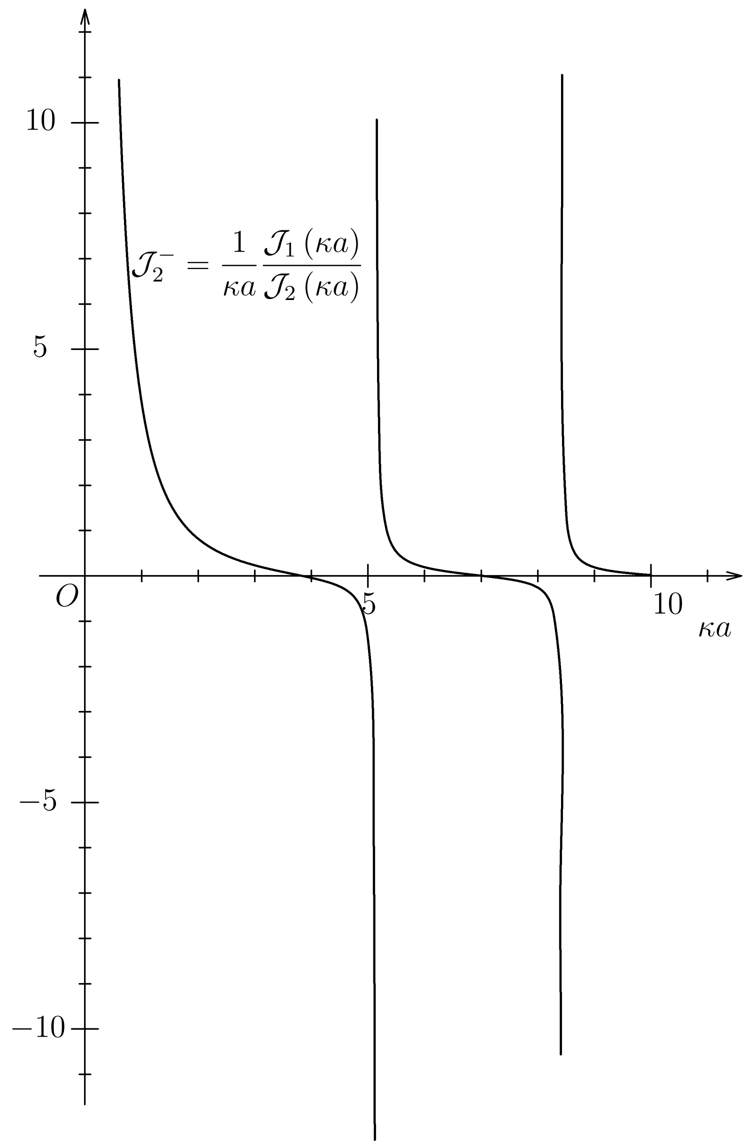

Figure 4.24: Plot of the function, $\mathcal{J}_2^-(\kappa a)$.

for the solutions to the modified Bessel equation in terms of $\mathcal{K}_\nu(\gamma\varrho)$ defined by Eq. (4.73),

$$\begin{aligned}
\mathcal{K}_\nu(\gamma\varrho) &= \frac{\pi}{2}\mathrm{j}^{\nu+1}\mathcal{H}_\nu^{(1)}(\mathrm{j}\gamma\varrho) \\
\frac{\mathrm{d}\mathcal{K}_\nu(\gamma\varrho)}{\mathrm{d}(\gamma\varrho)} &= \frac{\pi}{2}\mathrm{j}^{\nu+2}\frac{\mathrm{d}\mathcal{H}_\nu^{(1)}(\mathrm{j}\gamma\varrho)}{\mathrm{d}(\mathrm{j}\gamma\varrho)} = -\frac{\pi}{2}\mathrm{j}^{\nu}\frac{\mathrm{d}\mathcal{H}_\nu^{(1)}(\mathrm{j}\gamma\varrho)}{\mathrm{d}(\mathrm{j}\gamma\varrho)}
\end{aligned}$$

we have,

$$\mathcal{K}'_\nu(\gamma\varrho) = \frac{\mathrm{d}\mathcal{K}_\nu(\gamma\varrho)}{\mathrm{d}(\gamma\varrho)} = -\frac{1}{2}\left[\mathcal{K}_{\nu-1}(\gamma\varrho) + \mathcal{K}_{\nu+1}(\gamma\varrho)\right] \tag{4.117a}$$

$$-\frac{2\nu}{\gamma\varrho}\mathcal{K}_\nu(\gamma\varrho) = \mathcal{K}_{\nu-1}(\gamma\varrho) - \mathcal{K}_{\nu+1}(\gamma\varrho) \tag{4.117b}$$

which differs from the results given in Eqs. (4.116b) and (4.116c) valid for Bessel and Hankel functions.

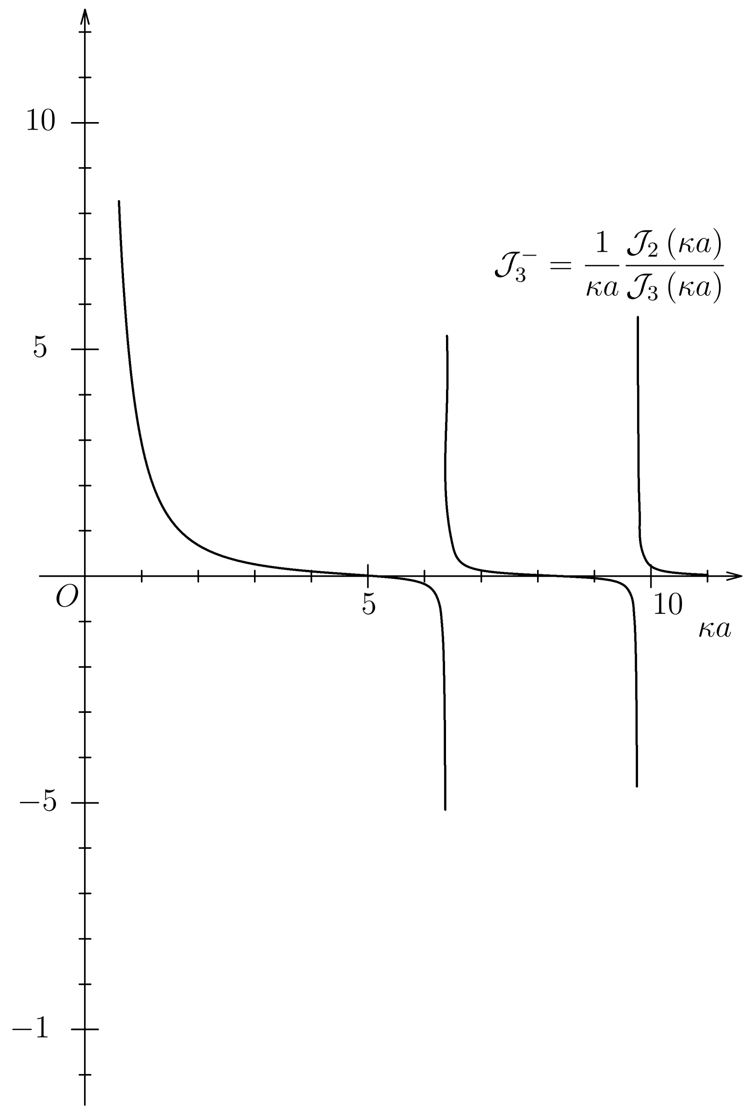

Figure 4.25: Plot of the function, $\mathcal{J}_3^-(\kappa a)$.

The sum of Eqs. (4.116b) and (4.116c)

$$\begin{aligned}\mathcal{Z}_{\nu-1}(z) - \mathcal{Z}_{\nu+1}(z) &= 2\mathcal{Z}'_\nu(z)\\ \mathcal{Z}_{\nu-1}(z) + \mathcal{Z}_{\nu+1}(z) &= \frac{2\nu}{z}\mathcal{Z}_\nu(z)\end{aligned}$$

divided by two,

$$\mathcal{Z}_{\nu-1}(z) = \mathcal{Z}'_\nu(z) + \frac{\nu}{z}\mathcal{Z}_\nu(z)$$

The difference of Eqs. (4.116b) and (4.116c) divided by two gives,

$$\mathcal{Z}_{\nu+1}(z) = -\mathcal{Z}'_\nu(z) + \frac{\nu}{z}\mathcal{Z}_\nu(z)$$

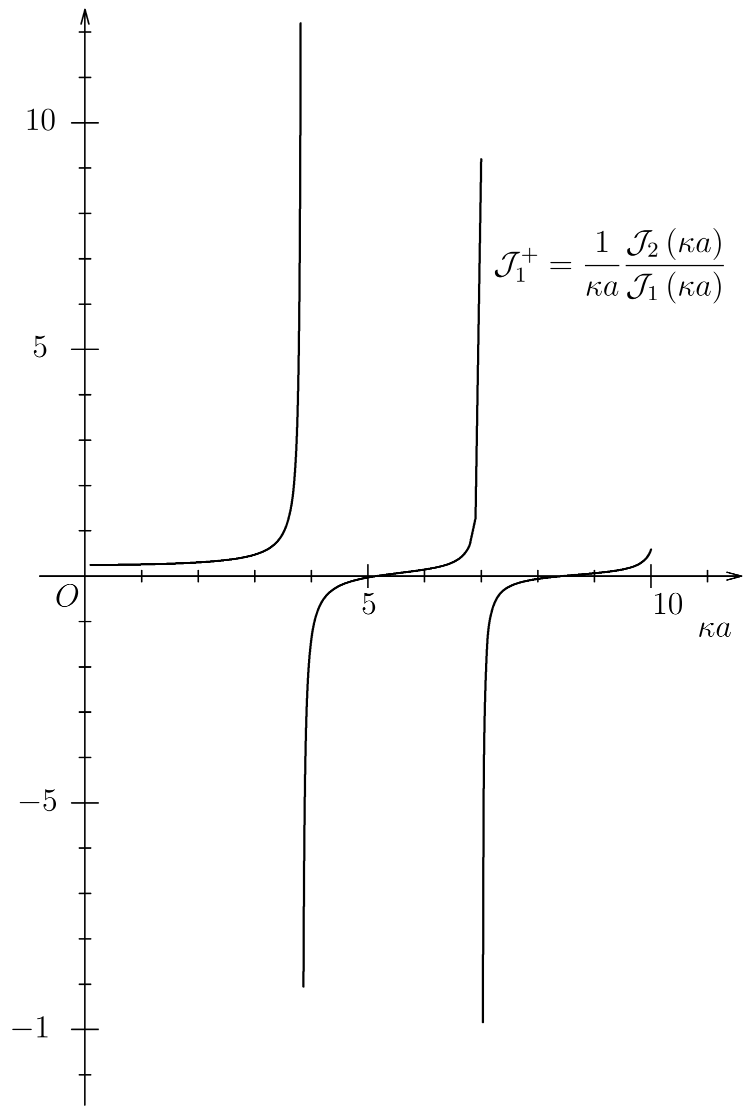

Figure 4.26: Plot of the function, $\mathcal{J}_1^+(\kappa a)$.

The division of both equations by $\mathcal{Z}_\nu(z)$ results in,

$$\frac{\mathcal{Z}_{\nu-1}(z)}{\mathcal{Z}_\nu(z)} = \frac{\mathcal{Z}_\nu'(z)}{\mathcal{Z}_\nu(z)} + \frac{\nu}{z} \tag{4.118a}$$

$$\frac{\mathcal{Z}_{\nu+1}(z)}{\mathcal{Z}_\nu(z)} = -\frac{\mathcal{Z}_\nu'(z)}{\mathcal{Z}_\nu(z)} + \frac{\nu}{z} \tag{4.118b}$$

We further divide the difference by the variable z and obtain,

$$\frac{1}{z}\frac{\mathcal{Z}_\nu'(z)}{\mathcal{Z}_\nu(z)} = \frac{1}{2}\left[\frac{1}{z}\frac{\mathcal{Z}_{\nu-1}(z)}{\mathcal{Z}_\nu(z)} - \frac{1}{z}\frac{\mathcal{Z}_{\nu+1}(z)}{\mathcal{Z}_\nu(z)}\right]$$

We introduce the notation,

$$\frac{1}{z}\frac{\mathcal{Z}_\nu'(z)}{\mathcal{Z}_\nu(z)} = \frac{1}{2}\left[\mathcal{Z}_\nu^-(z) - \mathcal{Z}_\nu^+(z)\right] \tag{4.119}$$

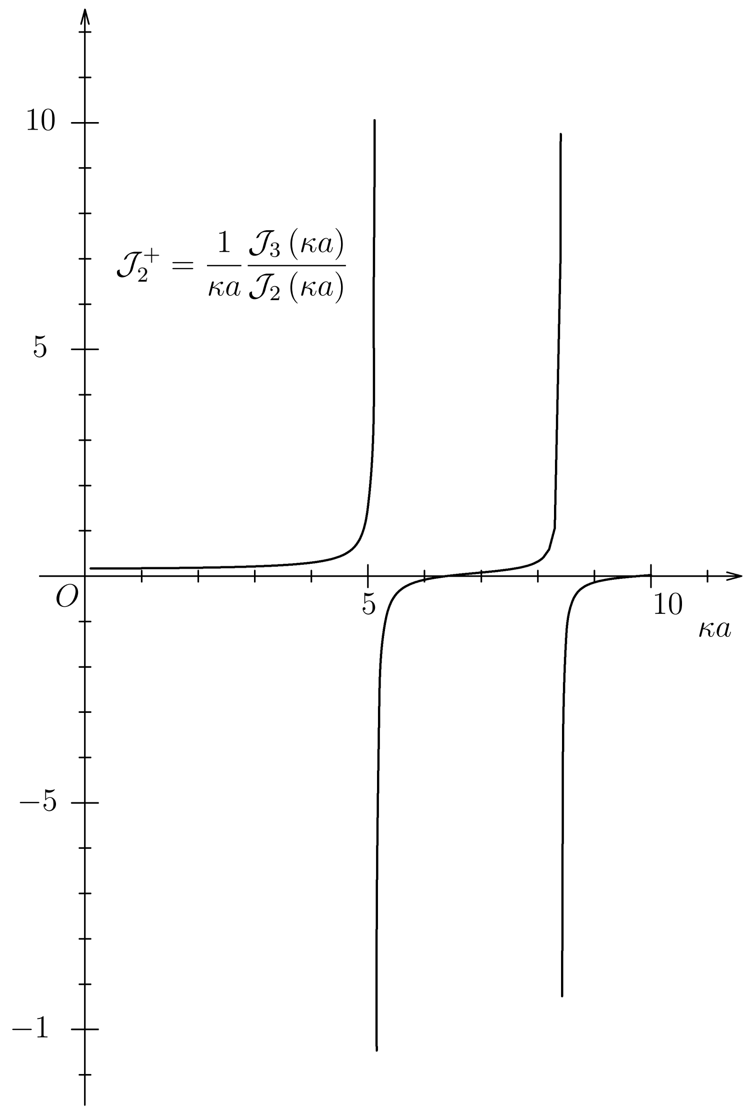

Figure 4.27: Plot of the function, $\mathcal{J}_2^+(\kappa a)$.

with

$$\mathcal{Z}_\nu^\pm(z) = \frac{1}{z}\frac{\mathcal{Z}_{\nu\pm1}(z)}{\mathcal{Z}_\nu(z)} \tag{4.120}$$

In the special cases,

$$\mathcal{J}_\nu^\pm(\kappa a) = \frac{1}{\kappa a}\frac{\mathcal{J}_{\nu\pm1}(\kappa a)}{\mathcal{J}_\nu(\kappa a)} \tag{4.121a}$$

$$\mathcal{H}_\nu^\pm(\mathrm{j}\gamma a) = \frac{1}{\mathrm{j}\gamma a}\frac{\mathcal{H}_{\nu\pm1}^{(1)}(\mathrm{j}\gamma a)}{\mathcal{H}_\nu^{(1)}(\mathrm{j}\gamma a)} \tag{4.121b}$$

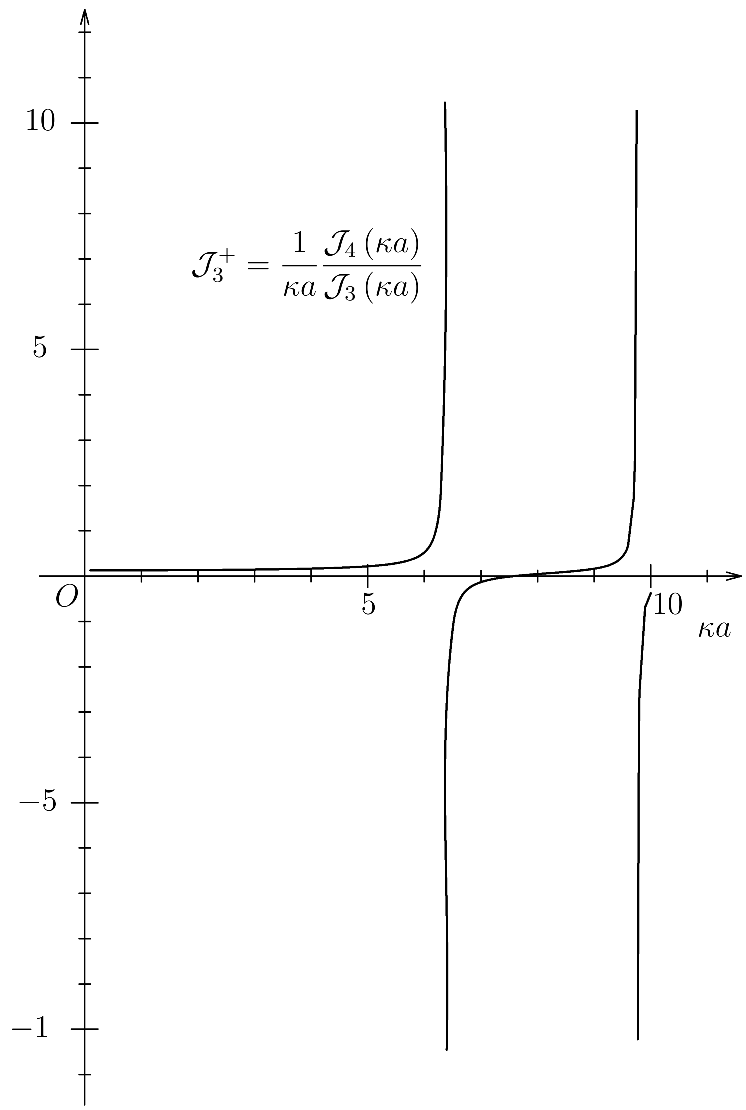

Figure 4.28: Plot of the function, $\mathcal{J}_3^+(\kappa a)$.

The substitution according to Eq. (4.119)

$$\frac{1}{\kappa a}\frac{\mathcal{J}_\nu'(\kappa a)}{\mathcal{J}_\nu(\kappa a)} = \frac{1}{2}\left[\mathcal{J}_\nu^-(\kappa a) - \mathcal{J}_\nu^+(\kappa a)\right] \tag{4.122}$$

$$\frac{1}{\mathrm{j}\gamma a}\frac{\mathcal{H}_\nu^{(1)'}(\mathrm{j}\gamma a)}{\mathcal{H}_\nu^{(1)}(\mathrm{j}\gamma a)} = \frac{1}{2}\left[\mathcal{H}_\nu^-(\mathrm{j}\gamma a) - \mathcal{H}_\nu^+(\mathrm{j}\gamma a)\right] \tag{4.123}$$

into the eigenvalue equation (4.92),

$$\left[\frac{\nu\omega a\,\beta a}{\kappa^2 a^2\,\gamma^2 a^2}\left(\varepsilon_1\mu_1 - \varepsilon_2\mu_2\right)\right]^2$$
$$= \left[\mu_1\frac{1}{\kappa a}\frac{\mathcal{J}_\nu'(\kappa a)}{\mathcal{J}_\nu(\kappa a)} - \mu_2\frac{1}{\mathrm{j}\gamma a}\frac{\mathcal{H}_\nu^{(1)'}(\mathrm{j}\gamma a)}{\mathcal{H}_\nu^{(1)}(\mathrm{j}\gamma a)}\right]\left[\varepsilon_1\frac{1}{\kappa a}\frac{\mathcal{J}_\nu'(\kappa a)}{\mathcal{J}_\nu(\kappa a)} - \varepsilon_2\frac{1}{\mathrm{j}\gamma a}\frac{\mathcal{H}_\nu^{(1)'}(\mathrm{j}\gamma a)}{\mathcal{H}_\nu^{(1)}(\mathrm{j}\gamma a)}\right]$$

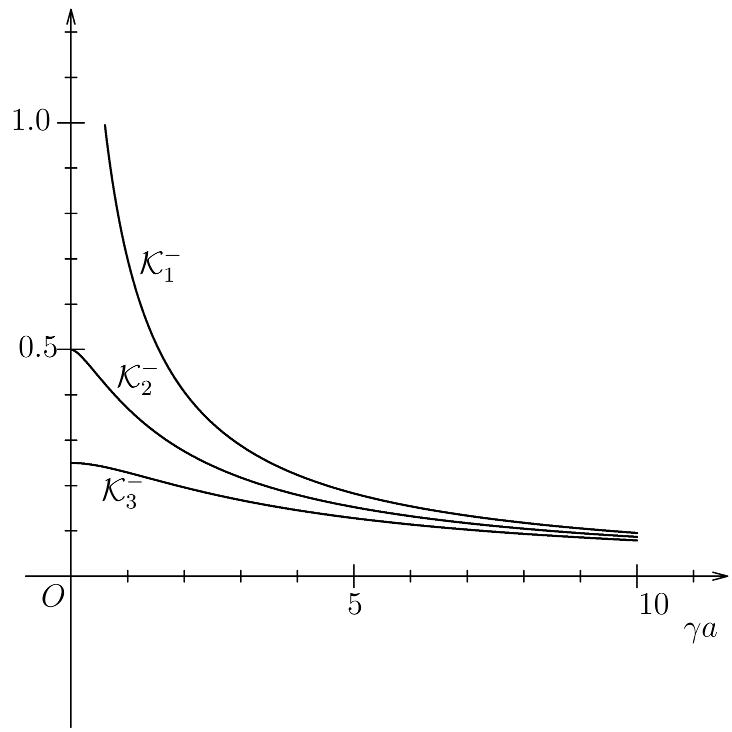

Figure 4.29: Plot of the functions, $\mathcal{K}_\nu^- = \dfrac{1}{\gamma a}\dfrac{\mathcal{K}_{\nu-1}(\gamma a)}{\mathcal{K}_\nu(\gamma a)} = \dfrac{1}{\mathrm{j}\gamma a}\dfrac{\mathcal{H}_{\nu-1}(\mathrm{j}\gamma a)}{\mathcal{H}_\nu(\mathrm{j}\gamma a)} = \mathcal{H}_\nu^-$, $\nu = 1,\, 2,\, 3$.

provides, by making use of Eq. (4.122) and after the division by the product $\varepsilon_2\mu_2$

$$\begin{aligned} &\left[\frac{2\nu\omega a\,\beta a\,(\varepsilon_2\mu_2)^{1/2}}{\kappa^2a^2\gamma^2a^2}\left(\frac{\varepsilon_1\mu_1}{\varepsilon_2\mu_2}-1\right)\right]^2 \\ &= \left[\frac{\mu_1}{\mu_2}\left(\mathcal{J}_\nu^- - \mathcal{J}_\nu^+\right) - \left(\mathcal{H}_\nu^- - \mathcal{H}_\nu^+\right)\right] \\ &\times \left[\frac{\varepsilon_1}{\varepsilon_2}\left(\mathcal{J}_\nu^- - \mathcal{J}_\nu^+\right) - \left(\mathcal{H}_\nu^- - \mathcal{H}_\nu^+\right)\right] \end{aligned} \tag{4.124}$$

We denote,

$$\frac{\varepsilon_1}{\varepsilon_2} \equiv \varepsilon\,, \quad \frac{\mu_1}{\mu_2} \equiv \mu\,, \quad (\varepsilon_1\mu_1)^{1/2}\,\omega \equiv k_1\,, \quad (\varepsilon_2\mu_2)^{1/2}\,\omega \equiv k_2 \tag{4.125}$$

and transform Eq. (4.124),

$$\begin{aligned} &\left[2\nu\,(\varepsilon\mu-1)\,\frac{k_2a\,\beta a}{\kappa^2a^2\,\gamma^2a^2}\right]^2 \\ &= \left[\mu\left(\mathcal{J}_\nu^- - \mathcal{J}_\nu^+\right) - \left(\mathcal{H}_\nu^- - \mathcal{H}_\nu^+\right)\right]\left[\varepsilon\left(\mathcal{J}_\nu^- - \mathcal{J}_\nu^+\right) - \left(\mathcal{H}_\nu^- - \mathcal{H}_\nu^+\right)\right] \end{aligned} \tag{4.126}$$

We now have to perform a rather cumbersome rearranging on the right hand side of this equation. This will allow us, by making use of the recursion relation, to eliminate

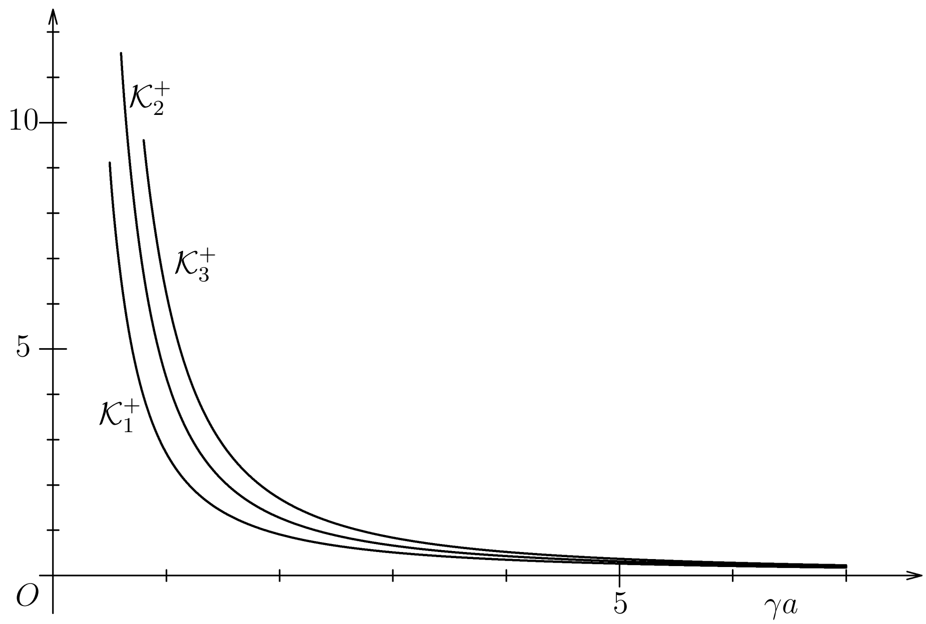

Figure 4.30: Plot of the functions, $\mathcal{K}_\nu^+ = \dfrac{1}{\gamma a}\dfrac{\mathcal{K}_{\nu+1}(\gamma a)}{\mathcal{K}_\nu(\gamma a)} = -\dfrac{1}{\mathrm{j}\gamma a}\dfrac{\mathcal{H}_{\nu+1}(\mathrm{j}\gamma a)}{\mathcal{H}_\nu(\mathrm{j}\gamma a)} = -\mathcal{H}_\nu^+$, $\nu = 1, 2, 3$.

cylindrical functions from the sums $\mathcal{J}_\nu^- + \mathcal{J}_\nu^+$ and $\mathcal{H}_\nu^- + \mathcal{H}_\nu^+$. This will be the first step in a procedure leading to a considerable simplification of the eigenvalue equation. We have

$$\begin{aligned}
&\left[\mu\left(\mathcal{J}_\nu^- - \mathcal{J}_\nu^+\right) - \left(\mathcal{H}_\nu^- - \mathcal{H}_\nu^+\right)\right]\left[\varepsilon\left(\mathcal{J}_\nu^- - \mathcal{J}_\nu^+\right) - \left(\mathcal{H}_\nu^- - \mathcal{H}_\nu^+\right)\right] \\
&= \left[\left(\mu\mathcal{J}_\nu^- - \mathcal{H}_\nu^-\right) - \left(\mu\mathcal{J}_\nu^+ - \mathcal{H}_\nu^+\right)\right]\left[\left(\varepsilon\mathcal{J}_\nu^- - \mathcal{H}_\nu^-\right) - \left(\varepsilon\mathcal{J}_\nu^+ - \mathcal{H}_\nu^+\right)\right] \\
&= \left(\mu\mathcal{J}_\nu^- - \mathcal{H}_\nu^-\right)\left(\varepsilon\mathcal{J}_\nu^- - \mathcal{H}_\nu^-\right) + \left(\mu\mathcal{J}_\nu^+ - \mathcal{H}_\nu^+\right)\left(\varepsilon\mathcal{J}_\nu^+ - \mathcal{H}_\nu^+\right) \\
&- \left(\mu\mathcal{J}_\nu^- - \mathcal{H}_\nu^-\right)\left(\varepsilon\mathcal{J}_\nu^+ - \mathcal{H}_\nu^+\right) - \left(\mu\mathcal{J}_\nu^+ - \mathcal{H}_\nu^+\right)\left(\varepsilon\mathcal{J}_\nu^- - \mathcal{H}_\nu^-\right)
\end{aligned} \tag{4.127}$$

We subtract and add the expression in the last row in Eq. (4.127), i.e.,

$$\left(\mu\mathcal{J}_\nu^- - \mathcal{H}_\nu^-\right)\left(\varepsilon\mathcal{J}_\nu^+ - \mathcal{H}_\nu^+\right) + \left(\mu\mathcal{J}_\nu^+ - \mathcal{H}_\nu^+\right)\left(\varepsilon\mathcal{J}_\nu^- - \mathcal{H}_\nu^-\right)$$

to get

$$\begin{aligned}
&\left[\mu\left(\mathcal{J}_\nu^- - \mathcal{J}_\nu^+\right) - \left(\mathcal{H}_\nu^- - \mathcal{H}_\nu^+\right)\right]\left[\varepsilon\left(\mathcal{J}_\nu^- - \mathcal{J}_\nu^+\right) - \left(\mathcal{H}_\nu^- - \mathcal{H}_\nu^+\right)\right] \\
&= \left(\mu\mathcal{J}_\nu^- - \mathcal{H}_\nu^-\right)\left(\varepsilon\mathcal{J}_\nu^- - \mathcal{H}_\nu^-\right) + \left(\mu\mathcal{J}_\nu^+ - \mathcal{H}_\nu^+\right)\left(\varepsilon\mathcal{J}_\nu^+ - \mathcal{H}_\nu^+\right) \\
&+ \left(\mu\mathcal{J}_\nu^- - \mathcal{H}_\nu^-\right)\left(\varepsilon\mathcal{J}_\nu^+ - \mathcal{H}_\nu^+\right) + \left(\mu\mathcal{J}_\nu^+ - \mathcal{H}_\nu^+\right)\left(\varepsilon\mathcal{J}_\nu^- - \mathcal{H}_\nu^-\right) \\
&- 2\left(\mu\mathcal{J}_\nu^- - \mathcal{H}_\nu^-\right)\left(\varepsilon\mathcal{J}_\nu^+ - \mathcal{H}_\nu^+\right) - 2\left(\mu\mathcal{J}_\nu^+ - \mathcal{H}_\nu^+\right)\left(\varepsilon\mathcal{J}_\nu^- - \mathcal{H}_\nu^-\right)
\end{aligned}$$

We rearrange the first four terms (underlined) on the right hand side of this equation,

$$\begin{aligned}
&\left[\mu\left(\mathcal{J}_\nu^- - \mathcal{J}_\nu^+\right) - \left(\mathcal{H}_\nu^- - \mathcal{H}_\nu^+\right)\right]\left[\varepsilon\left(\mathcal{J}_\nu^- - \mathcal{J}_\nu^+\right) - \left(\mathcal{H}_\nu^- - \mathcal{H}_\nu^+\right)\right] \\
&= \underline{\left(\mu\mathcal{J}_\nu^- - \mathcal{H}_\nu^-\right)\left(\varepsilon\mathcal{J}_\nu^- - \mathcal{H}_\nu^-\right) + \left(\mu\mathcal{J}_\nu^- - \mathcal{H}_\nu^-\right)\left(\varepsilon\mathcal{J}_\nu^+ - \mathcal{H}_\nu^+\right)} \\
&+ \underline{\left(\mu\mathcal{J}_\nu^+ - \mathcal{H}_\nu^+\right)\left(\varepsilon\mathcal{J}_\nu^+ - \mathcal{H}_\nu^+\right) + \left(\mu\mathcal{J}_\nu^+ - \mathcal{H}_\nu^+\right)\left(\varepsilon\mathcal{J}_\nu^- - \mathcal{H}_\nu^-\right)} \\
&- 2\left(\mu\mathcal{J}_\nu^- - \mathcal{H}_\nu^-\right)\left(\varepsilon\mathcal{J}_\nu^+ - \mathcal{H}_\nu^+\right) - 2\left(\mu\mathcal{J}_\nu^+ - \mathcal{H}_\nu^+\right)\left(\varepsilon\mathcal{J}_\nu^- - \mathcal{H}_\nu^-\right)
\end{aligned}$$

We leave unchanged the left hand side and last two terms on the right hand side of this equation,

$$\begin{aligned}
&\left[\mu\left(\mathcal{J}_\nu^- - \mathcal{J}_\nu^+\right) - \left(\mathcal{H}_\nu^- - \mathcal{H}_\nu^+\right)\right]\left[\varepsilon\left(\mathcal{J}_\nu^- - \mathcal{J}_\nu^+\right) - \left(\mathcal{H}_\nu^- - \mathcal{H}_\nu^+\right)\right] \\
&= \left(\mu\mathcal{J}_\nu^- - \mathcal{H}_\nu^-\right)\left[\left(\varepsilon\mathcal{J}_\nu^- - \mathcal{H}_\nu^-\right) + \left(\varepsilon\mathcal{J}_\nu^+ - \mathcal{H}_\nu^+\right)\right] \\
&+ \left(\mu\mathcal{J}_\nu^+ - \mathcal{H}_\nu^+\right)\left[\left(\varepsilon\mathcal{J}_\nu^- - \mathcal{H}_\nu^-\right) + \left(\varepsilon\mathcal{J}_\nu^+ - \mathcal{H}_\nu^+\right)\right] \\
&- 2\left(\mu\mathcal{J}_\nu^- - \mathcal{H}_\nu^-\right)\left(\varepsilon\mathcal{J}_\nu^+ - \mathcal{H}_\nu^+\right) - 2\left(\mu\mathcal{J}_\nu^+ - \mathcal{H}_\nu^+\right)\left(\varepsilon\mathcal{J}_\nu^- - \mathcal{H}_\nu^-\right) \\
&= \left[\left(\mu\mathcal{J}_\nu^- - \mathcal{H}_\nu^-\right) + \left(\mu\mathcal{J}_\nu^+ - \mathcal{H}_\nu^+\right)\right]\left[\left(\varepsilon\mathcal{J}_\nu^- - \mathcal{H}_\nu^-\right) + \left(\varepsilon\mathcal{J}_\nu^+ - \mathcal{H}_\nu^+\right)\right] \\
&- 2\left(\mu\mathcal{J}_\nu^- - \mathcal{H}_\nu^-\right)\left(\varepsilon\mathcal{J}_\nu^+ - \mathcal{H}_\nu^+\right) - 2\left(\mu\mathcal{J}_\nu^+ - \mathcal{H}_\nu^+\right)\left(\varepsilon\mathcal{J}_\nu^- - \mathcal{H}_\nu^-\right)
\end{aligned}$$

and get on the right hand side,

$$\begin{aligned}
&\left[\mu\left(\mathcal{J}_\nu^- - \mathcal{J}_\nu^+\right) - \left(\mathcal{H}_\nu^- - \mathcal{H}_\nu^+\right)\right]\left[\varepsilon\left(\mathcal{J}_\nu^- - \mathcal{J}_\nu^+\right) - \left(\mathcal{H}_\nu^- - \mathcal{H}_\nu^+\right)\right] \\
&= \underline{\left[\mu\left(\mathcal{J}_\nu^- + \mathcal{J}_\nu^+\right) - \left(\mathcal{H}_\nu^- + \mathcal{H}_\nu^+\right)\right]\left[\varepsilon\left(\mathcal{J}_\nu^- + \mathcal{J}_\nu^+\right) - \left(\mathcal{H}_\nu^- + \mathcal{H}_\nu^+\right)\right]} \\
&- 2\left[\left(\mu\mathcal{J}_\nu^- - \mathcal{H}_\nu^-\right)\left(\varepsilon\mathcal{J}_\nu^+ - \mathcal{H}_\nu^+\right) + \left(\mu\mathcal{J}_\nu^+ - \mathcal{H}_\nu^+\right)\left(\varepsilon\mathcal{J}_\nu^- - \mathcal{H}_\nu^-\right)\right] \qquad (4.128)
\end{aligned}$$

The sums $\mathcal{J}_\nu^- + \mathcal{J}_\nu^+$ and $\mathcal{H}_\nu^- + \mathcal{H}_\nu^+$ were underlined. We take into account the recursion relation, Eq. (4.116c),

$$\frac{\mathcal{Z}_{\nu-1}(z) + \mathcal{Z}_{\nu+1}(z)}{\mathcal{Z}_\nu(z)} = \frac{2\nu}{z} \qquad (4.129)$$

and compute, with the help of Eq. (4.120),

$$\frac{1}{z}\frac{\mathcal{Z}_{\nu-1}(z)}{\mathcal{Z}_\nu(z)} + \frac{1}{z}\frac{\mathcal{Z}_{\nu+1}(z)}{\mathcal{Z}_\nu(z)} = \mathcal{Z}_\nu^-(z) + \mathcal{Z}_\nu^+(z) = \frac{2\nu}{z^2} \qquad (4.130)$$

We apply this general result to the special cases, $\mathcal{J}_\nu^- + \mathcal{J}_\nu^+$ and $\mathcal{H}_\nu^- + \mathcal{H}_\nu^+$

$$\mathcal{J}_\nu^-(\kappa a) + \mathcal{J}_\nu^+(\kappa a) = \frac{2\nu}{\kappa^2 a^2} \qquad (4.131a)$$

$$\mathcal{H}_\nu^-(\mathrm{j}\gamma a) + \mathcal{H}_\nu^+(\mathrm{j}\gamma a) = -\frac{2\nu}{\gamma^2 a^2} \qquad (4.131b)$$

From the first term on the right hand side (underlined) of Eq. (4.128) we eliminate the cylindrical functions,

$$\begin{aligned}
&\left[\mu\left(\mathcal{J}_\nu^- + \mathcal{J}_\nu^+\right) - \left(\mathcal{H}_\nu^- + \mathcal{H}_\nu^+\right)\right]\left[\varepsilon\left(\mathcal{J}_\nu^- + \mathcal{J}_\nu^+\right) - \left(\mathcal{H}_\nu^- + \mathcal{H}_\nu^+\right)\right] \\
&= \left(\mu\frac{2\nu}{\kappa^2a^2} + \frac{2\nu}{\gamma^2a^2}\right)\left(\varepsilon\frac{2\nu}{\kappa^2a^2} + \frac{2\nu}{\gamma^2a^2}\right) \\
&= \left(\frac{2\nu}{a^2}\right)^2\left(\frac{\mu}{\kappa^2} + \frac{1}{\gamma^2}\right)\left(\frac{\varepsilon}{\kappa^2} + \frac{1}{\gamma^2}\right) \\
&= \left(\frac{2\nu}{a^2\kappa^2\gamma^2}\right)^2\left(\mu\gamma^2 + \kappa^2\right)\left(\varepsilon\gamma^2 + \kappa^2\right)
\end{aligned} \tag{4.132}$$

The expression $(\mu\gamma^2 + \kappa^2)(\varepsilon\gamma^2 + \kappa^2)$ rearranged becomes,

$$\left(\mu\gamma^2 + \kappa^2\right)\left(\varepsilon\gamma^2 + \kappa^2\right) = \epsilon\mu\gamma^4 + (\varepsilon + \mu)\gamma^2\kappa^2 + \kappa^4 \tag{4.133}$$

We apply the relations from Eqs. (4.74) and (4.79)

$$\gamma^2 = \beta^2 - \left(\omega^2\varepsilon_2\mu_2\right) = \beta^2 - k_2^2 \tag{4.134a}$$

$$\begin{aligned}
\kappa^2 &= \left(\omega^2\varepsilon_1\mu_1\right) - \beta^2 = k_1^2 - \beta^2 = \varepsilon\mu\left(\omega^2\varepsilon_2\mu_2\right) - \beta^2 \\
&= \varepsilon\mu k_2^2 - \beta^2
\end{aligned} \tag{4.134b}$$

where, because of Eq. (4.125), the propagation constant in the core equals $k_1^2 = \varepsilon\mu k_2^2$. We eliminate γ^2 and κ^2 from Eq. (4.133)

$$\begin{aligned}
&\left(\mu\gamma^2 + \kappa^2\right)\left(\varepsilon\gamma^2 + \kappa^2\right) \\
&= \epsilon\mu\left(\beta^2 - k_2^2\right)^2 + (\varepsilon + \mu)\left(\beta^2 - k_2^2\right)\left(\varepsilon\mu k_2^2 - \beta^2\right) + \left(\varepsilon\mu k_2^2 - \beta^2\right)^2 \\
&= \epsilon\mu\beta^4 - 2\epsilon\mu\beta^2k_2^2 + \epsilon\mu k_2^4 + (\varepsilon + \mu)\left(\varepsilon\mu k_2^2\beta^2 - \varepsilon\mu k_2^4 - \beta^4 + k_2^2\beta^2\right) \\
&\quad + \varepsilon^2\mu^2k_2^4 - 2\varepsilon\mu k_2^2\beta^2 + \beta^4
\end{aligned} \tag{4.135}$$

We rewrite this expression as a sum of terms proportional to β^4, k_2^4 and $k_2^2\beta^2$,

$$\begin{aligned}
&\left(\mu\gamma^2 + \kappa^2\right)\left(\varepsilon\gamma^2 + \kappa^2\right) \\
&= \left[(\epsilon\mu + 1) - (\varepsilon + \mu)\right]\beta^4 + \varepsilon\mu\left[\varepsilon\mu - (\varepsilon + \mu) + 1\right]k_2^4 \\
&\quad + \left[-4\varepsilon\mu + (\varepsilon + \mu)(\varepsilon\mu + 1)\right]k_2^2\beta^2 \\
&= (\epsilon - 1)(\mu - 1)\beta^4 + (\varepsilon - 1)(\mu - 1)\varepsilon\mu k_2^4 + k_2^2\beta^2\left[-4\varepsilon\mu + (\varepsilon + \mu)(\varepsilon\mu + 1)\right] \\
&= (\epsilon - 1)(\mu - 1)\left(\beta^4 + \varepsilon\mu k_2^4\right) + k_2^2\beta^2\left[-4\varepsilon\mu + (\varepsilon + \mu)(\varepsilon\mu + 1)\right]
\end{aligned} \tag{4.136}$$

The term proportional to $k_2^2\beta^2$ can be rearranged to,

$$\begin{aligned}
&-4\varepsilon\mu + (\varepsilon+\mu)(\varepsilon\mu+1) \\
&= -4\varepsilon\mu + (\varepsilon+\mu)(\varepsilon\mu+1) + (\varepsilon\mu+1)(\varepsilon-1)(\mu-1) - (\varepsilon\mu+1)(\varepsilon-1)(\mu-1) \\
&= -4\varepsilon\mu + (\varepsilon\mu+1)\left[(\varepsilon+\mu) + (\varepsilon-1)(\mu-1)\right] - (\varepsilon\mu+1)(\varepsilon-1)(\mu-1) \\
&= -4\varepsilon\mu + (\varepsilon\mu+1)^2 - (\varepsilon\mu+1)(\varepsilon-1)(\mu-1) \\
&= (\varepsilon\mu-1)^2 - (\varepsilon\mu+1)(\varepsilon-1)(\mu-1) \qquad (4.137)
\end{aligned}$$

Then we have

$$\begin{aligned}
&\left(\mu\gamma^2+\kappa^2\right)\left(\varepsilon\gamma^2+\kappa^2\right) \\
&= (\epsilon-1)(\mu-1)\left(\beta^4+\varepsilon\mu k_2^4\right) + k_2^2\beta^2\left[(\varepsilon\mu-1)^2 - (\varepsilon\mu+1)(\varepsilon-1)(\mu-1)\right] \\
&= (\epsilon-1)(\mu-1)\left[\beta^4 - (\varepsilon\mu+1)k_2^2\beta^2 + \varepsilon\mu k_2^4\right] + k_2^2\beta^2(\varepsilon\mu-1)^2 \\
&= (\epsilon-1)(\mu-1)\left(\beta^2-k_2^2\right)\left(\beta^2-\varepsilon\mu k_2^2\right) + k_2^2\beta^2(\varepsilon\mu-1)^2 \\
&= -(\epsilon-1)(\mu-1)\gamma^2\kappa^2 + k_2^2\beta^2(\varepsilon\mu-1)^2 \qquad (4.138)
\end{aligned}$$

In the last step, we have employed Eqs. (4.134) for $\gamma^2 = \beta^2 - k_2^2$ and $-\kappa^2 = \beta^2 - \varepsilon\mu k_2^2$. In this way, we have acquired all partial results required for the final transformation of the eigenvalue equation (4.126),

$$\begin{aligned}
&\left[2\nu(\varepsilon\mu-1)\frac{k_2\beta}{\kappa^2\gamma^2a^2}\right]^2 \\
&= \left[\mu\left(\mathcal{J}_\nu^- - \mathcal{J}_\nu^+\right) - \left(\mathcal{H}_\nu^- - \mathcal{H}_\nu^+\right)\right]\left[\varepsilon\left(\mathcal{J}_\nu^- - \mathcal{J}_\nu^+\right) - \left(\mathcal{H}_\nu^- - \mathcal{H}_\nu^+\right)\right]
\end{aligned}$$

In the first step, we transform the right hand side of this equation according our results and leave the left hand side unchanged. The use of Eq. (4.138) leads to the form,

$$\begin{aligned}
&\left(\frac{2\nu}{\kappa^2\gamma^2a^2}\right)^2\left[(\varepsilon\mu-1)k_2\beta\right]^2 \\
&= \left[\mu\left(\mathcal{J}_\nu^- + \mathcal{J}_\nu^+\right) - \left(\mathcal{H}_\nu^- + \mathcal{H}_\nu^+\right)\right]\left[\varepsilon\left(\mathcal{J}_\nu^- + \mathcal{J}_\nu^+\right) - \left(\mathcal{H}_\nu^- + \mathcal{H}_\nu^+\right)\right] \\
&- 2\left[\left(\mu\mathcal{J}_\nu^- - \mathcal{H}_\nu^-\right)\left(\varepsilon\mathcal{J}_\nu^+ - \mathcal{H}_\nu^+\right) + \left(\mu\mathcal{J}_\nu^+ - \mathcal{H}_\nu^+\right)\left(\varepsilon\mathcal{J}_\nu^- - \mathcal{H}_\nu^-\right)\right]
\end{aligned}$$

In the second step, we eliminate the cylindrical functions by making use of Eq. (4.132)

$$\begin{aligned}
&\left(\frac{2\nu}{a^2\kappa^2\gamma^2}\right)^2\left[(\varepsilon\mu-1)k_2\beta\right]^2 \\
&= \left(\frac{2\nu}{a^2\kappa^2\gamma^2}\right)^2\left(\mu\gamma^2+\kappa^2\right)\left(\varepsilon\gamma^2+\kappa^2\right) \\
&- 2\left[\left(\mu\mathcal{J}_\nu^- - \mathcal{H}_\nu^-\right)\left(\varepsilon\mathcal{J}_\nu^+ - \mathcal{H}_\nu^+\right) + \left(\mu\mathcal{J}_\nu^+ - \mathcal{H}_\nu^+\right)\left(\varepsilon\mathcal{J}_\nu^- - \mathcal{H}_\nu^-\right)\right]
\end{aligned}$$

The use of Eq. (4.138) gives,

$$
\begin{aligned}
&\left(\frac{2\nu}{a^2\kappa^2\gamma^2}\right)^2 \left[(\varepsilon\mu-1)\,k_2\beta\right]^2 \\
&= \left(\frac{2\nu}{a^2\kappa^2\gamma^2}\right)^2 \left\{-\left(\epsilon-1\right)\left(\mu-1\right)\gamma^2\kappa^2+\left[(\varepsilon\mu-1)\,k_2\beta\right]^2\right\} \\
&- 2\left[\left(\mu\mathcal{J}_\nu^- - \mathcal{H}_\nu^-\right)\left(\varepsilon\mathcal{J}_\nu^+ - \mathcal{H}_\nu^+\right)+\left(\mu\mathcal{J}_\nu^+ - \mathcal{H}_\nu^+\right)\left(\varepsilon\mathcal{J}_\nu^- - \mathcal{H}_\nu^-\right)\right]
\end{aligned}
$$

The distribution of the curly brackets, $\{\}$, in the first term on the right hand side,

$$
\begin{aligned}
&\left(\frac{2\nu}{a^2\kappa^2\gamma^2}\right)^2 \left[(\varepsilon\mu-1)\,k_2\beta\right]^2 \\
&= -\left(\frac{2\nu}{a^2\kappa^2\gamma^2}\right)^2 \left(\epsilon-1\right)\left(\mu-1\right)\gamma^2\kappa^2+\underline{\left(\frac{2\nu}{a^2\kappa^2\gamma^2}\right)^2 \left[(\varepsilon\mu-1)\,k_2\beta\right]^2} \\
&- 2\left[\left(\mu\mathcal{J}_\nu^- - \mathcal{H}_\nu^-\right)\left(\varepsilon\mathcal{J}_\nu^+ - \mathcal{H}_\nu^+\right)+\left(\mu\mathcal{J}_\nu^+ - \mathcal{H}_\nu^+\right)\left(\varepsilon\mathcal{J}_\nu^- - \mathcal{H}_\nu^-\right)\right]
\end{aligned}
\tag{4.139}
$$

The single term on the left hand side is canceled with the underlined term on the right hand side of this equation. We finally arrive at an alternative form of the eigenvalue equation in cylindrical dielectric fiber waveguides with a step index profile,

$$
\boxed{\left(\mu\mathcal{J}_\nu^- - \mathcal{H}_\nu^-\right)\left(\varepsilon\mathcal{J}_\nu^+ - \mathcal{H}_\nu^+\right)+\left(\mu\mathcal{J}_\nu^+ - \mathcal{H}_\nu^+\right)\left(\varepsilon\mathcal{J}_\nu^- - \mathcal{H}_\nu^-\right) = -2\left(\frac{\nu}{a^2\kappa\gamma}\right)^2 \left(\epsilon-1\right)\left(\mu-1\right)}
\tag{4.140}
$$

where the meaning of $\mathcal{J}_\nu^\pm$ and $\mathcal{H}_\nu^\pm$ is given by Eqs. (4.120),

$$
\begin{aligned}
\mathcal{J}_\nu^\pm(\kappa a) &= \frac{1}{\kappa a}\frac{\mathcal{J}_{\nu\pm1}(\kappa a)}{\mathcal{J}_\nu(\kappa a)} \\
\mathcal{H}_\nu^\pm(\mathrm{j}\gamma a) &= \frac{1}{\mathrm{j}\gamma a}\frac{\mathcal{H}_{\nu\pm1}^{(1)}(\mathrm{j}\gamma a)}{\mathcal{H}_\nu^{(1)}(\mathrm{j}\gamma a)}
\end{aligned}
$$

We have left the concise notation, $\varepsilon = \varepsilon_1/\varepsilon_2$ and $\mu = \mu_1/\mu_2$. Equation (4.140) will be employed in the search for cut–off product of frequencies and core radii.

The eigenvalue equation can also be written in the form,

$$
2\left(\mu\varepsilon\mathcal{J}_\nu^-\mathcal{J}_\nu^+ + \mathcal{H}_\nu^-\mathcal{H}_\nu^+\right) - \left(\mu+\varepsilon\right)\left(\mathcal{J}_\nu^-\mathcal{H}_\nu^+ + \mathcal{J}_\nu^+\mathcal{H}_\nu^-\right) = -2\left(\frac{\nu}{a^2\kappa\gamma}\right)^2 \left(\epsilon-1\right)\left(\mu-1\right)
\tag{4.141}
$$

The eigenvalue equation can be simplified for $\epsilon - 1 = 0$ or $\mu - 1 = 0$. In fibers of nonmagnetic core and cladding (or in fiber with both core and cladding of the same magnetic permeability), corresponding to $\mu - 1 = 0$, we get a simplified form of the eigenvalue equation,

$$
\left(\mathcal{J}_\nu^- - \mathcal{H}_\nu^-\right)\left(\varepsilon\mathcal{J}_\nu^+ - \mathcal{H}_\nu^+\right)+\left(\mathcal{J}_\nu^+ - \mathcal{H}_\nu^+\right)\left(\varepsilon\mathcal{J}_\nu^- - \mathcal{H}_\nu^-\right) = 0
\tag{4.142}
$$

4.5.2 Approximation for Hankel functions of small arguments

The cut–off frequencies/thicknesses correspond to the situations where $\gamma a \to 0$. To find the cut–off frequencies/thicknesses we need the approximations for Hankel functions of the first kind at small arguments, γa, i.e., for $\gamma a \ll 1$. Please note that for $\nu = 0$ a $\nu = 1$ the approximations have been already employed in Eqs. (4.110). The approximations can be deduced from Eqs. (4.61), (4.62) and (4.63),

$$\mathcal{H}_0^{(1)}(\mathrm{j}\gamma a) \approx \mathrm{j}\frac{2}{\pi}\ln\left(\frac{\Upsilon\gamma a}{2}\right), \quad \Upsilon \approx 1,78107 = \mathrm{e}^{\upsilon} = \mathrm{e}^{0,5772156619} \tag{4.143a}$$

$$\mathcal{H}_\nu^{(1)}(\mathrm{j}\gamma a) \approx -\mathrm{j}\frac{(\nu-1)!}{\pi}\left(\frac{2}{\mathrm{j}\gamma a}\right)^{\nu}, \quad \nu \geq 1 \tag{4.143b}$$

We remind the relevant properties of cylindrical functions from Eqs. (4.116),

$$\begin{aligned}
\mathcal{Z}_{-\nu}(z) &= (-1)^{\nu}\mathcal{Z}_\nu(z) \\
\mathcal{Z}'_\nu(z) = \frac{\mathrm{d}\mathcal{Z}_\nu(z)}{\mathrm{d}z} &= \frac{1}{2}\left[\mathcal{Z}_{\nu-1}(z) - \mathcal{Z}_{\nu+1}(z)\right] \\
\mathcal{Z}_{\nu-1}(z) + \mathcal{Z}_{\nu+1}(z) &= \frac{2\nu}{z}\mathcal{Z}_\nu(z)
\end{aligned}$$

The approximations to $\mathcal{H}_\nu^-$ (Figure 4.29),

$$\mathcal{H}_\nu^- \equiv \frac{1}{\mathrm{j}\gamma a}\frac{\mathcal{H}_{\nu-1}^{(1)}(\mathrm{j}\gamma a)}{\mathcal{H}_\nu^{(1)}(\mathrm{j}\gamma a)} \tag{4.145}$$

must be deduced from Eqs. (4.143) separately for $\nu = 1$ and for $\nu > 1$.

$$\mathcal{H}_1^- \equiv \frac{1}{\mathrm{j}\gamma a}\frac{\mathcal{H}_0^{(1)}(\mathrm{j}\gamma a)}{\mathcal{H}_1^{(1)}(\mathrm{j}\gamma a)}$$

$$\mathcal{H}_1^- \approx \frac{1}{\mathrm{j}\gamma a}\frac{\mathrm{j}\frac{2}{\pi}\ln\left(\frac{\Upsilon\gamma a}{2}\right)}{-\mathrm{j}\frac{0!}{\pi}\left(\frac{2}{\mathrm{j}\gamma a}\right)}$$

i.e.,

$$\mathcal{H}_1^- \approx -\ln\left(\frac{\Upsilon\gamma a}{2}\right), \quad \gamma a \ll 1 \tag{4.146}$$

For $\nu > 1$, we get,

$$\begin{aligned}
\mathcal{H}_\nu^- &\approx \frac{1}{\mathrm{j}\gamma a}\frac{-\mathrm{j}\frac{(\nu-2)!}{\pi}\left(\frac{2}{\mathrm{j}\gamma a}\right)^{\nu-1}}{-\mathrm{j}\frac{(\nu-1)!}{\pi}\left(\frac{2}{\mathrm{j}\gamma a}\right)^{\nu}} \\
&\approx \frac{1}{\mathrm{j}\gamma a}\frac{1}{(\nu-1)}\frac{\mathrm{j}\gamma a}{2}
\end{aligned} \tag{4.147}$$

i.e.,

$$\mathcal{H}_\nu^- \;\approx\; \frac{1}{2\,(\nu-1)}\,, \quad \nu > 1\,, \quad \gamma a \ll 1 \tag{4.148}$$

$$\begin{aligned}\mathcal{H}_\nu^+ \equiv \frac{1}{\mathrm{j}\gamma a}\frac{\mathcal{H}_{\nu+1}^{(1)}(\mathrm{j}\gamma a)}{\mathcal{H}_\nu^{(1)}(\mathrm{j}\gamma a)} \;&\approx\; \frac{1}{\mathrm{j}\gamma a}\frac{-\mathrm{j}\dfrac{\nu!}{\pi}\left(\dfrac{2}{\mathrm{j}\gamma a}\right)^{\nu+1}}{-\mathrm{j}\dfrac{(\nu-1)!}{\pi}\left(\dfrac{2}{\mathrm{j}\gamma a}\right)^{\nu}} \\ &\approx\; \frac{1}{\mathrm{j}\gamma a}\frac{2\nu}{\mathrm{j}\gamma a}\end{aligned} \tag{4.149}$$

i.e.,

$$\mathcal{H}_\nu^+ \;\approx\; -\frac{2\nu}{(\gamma a)^2}\,, \quad \nu \geq 1\,, \quad \gamma a \ll 1 \tag{4.150}$$

4.5.3 Mode $\nu = 1$ of zero cut-off frequency

We look for the fundamental mode of zero cut –off frequency/thickness, if exists. To the cut–off condition, $\gamma a \to 0$ we associate the condition $\kappa a \to 0$. We employ the approximations to Bessel functions at $\kappa a \to 0$. These can be found from Eq. (4.61)

$$\mathcal{J}_\nu(\kappa a) \;\approx\; \frac{1}{\nu\,!}\left(\frac{\kappa a}{2}\right)^\nu, \quad \kappa a \ll 1\,, \quad \nu \geq 0 \tag{4.151}$$

In particular,

$$\mathcal{J}_0(\kappa a) \;\approx\; 1\,, \quad \kappa a \ll 1 \tag{4.152}$$

We establish

$$\mathcal{J}_\nu^+ \;\equiv\; \frac{1}{\kappa a}\frac{\mathcal{J}_{\nu+1}(\kappa a)}{\mathcal{J}_\nu(\kappa a)} \tag{4.153}$$

and

$$\mathcal{J}_\nu^- \;\equiv\; \frac{1}{\kappa a}\frac{\mathcal{J}_{\nu-1}(\kappa a)}{\mathcal{J}_\nu(\kappa a)} \tag{4.154}$$

at $\kappa a \to 0$. We obtain

$$\begin{aligned}\mathcal{J}_\nu^+ \;&\approx\; \frac{1}{\kappa a}\frac{\dfrac{1}{(\nu+1)!}\left(\dfrac{\kappa a}{2}\right)^{\nu+1}}{\dfrac{1}{\nu\,!}\left(\dfrac{\kappa a}{2}\right)^{\nu}} \\ &\approx\; \frac{1}{\kappa a}\frac{\nu\,!}{(\nu+1)!}\frac{\kappa a}{2}\end{aligned}$$

i.e.,

$$\mathcal{J}_\nu^+ \approx \frac{1}{2(\nu+1)}\,, \quad \kappa a \ll 1 \tag{4.155}$$

$$\mathcal{J}_\nu^- \approx \frac{1}{\kappa a}\frac{\frac{1}{(\nu-1)!}\left(\frac{\kappa a}{2}\right)^{\nu-1}}{\frac{1}{\nu\,!}\left(\frac{\kappa a}{2}\right)^{\nu}}$$

$$\mathcal{J}_\nu^- \approx \frac{2\nu}{(\kappa a)^2}\,, \quad \kappa a \ll 1 \tag{4.156}$$

In the special case, $\nu = 1$

$$\mathcal{J}_1^+ = \frac{1}{\kappa a}\frac{\mathcal{J}_2(\kappa a)}{\mathcal{J}_1(\kappa a)} \approx \frac{1}{4}\,, \quad \kappa a \ll 1 \tag{4.157a}$$

$$\mathcal{J}_1^- = \frac{1}{\kappa a}\frac{\mathcal{J}_0(\kappa a)}{\mathcal{J}_1(\kappa a)} \approx \frac{2}{(\kappa a)^2}\,, \quad \kappa a \ll 1 \tag{4.157b}$$

$$\mathcal{H}_1^+ \approx -\frac{2}{(\gamma a)^2}\,, \quad \gamma a \ll 1 \tag{4.157c}$$

$$\mathcal{H}_1^- \approx -\ln\left(\frac{\Upsilon\gamma a}{2}\right)\,, \quad \Upsilon \approx 1,78107\,, \quad \gamma a \ll 1 \tag{4.157d}$$

Here, we have included the previous results for $\mathcal{H}_1^+$ and $\mathcal{H}_1^-$ at $\gamma a \to 0$ given in Eqs. (4.146) and (4.150).

We can now apply the approximations to the eigenvalue equation (4.140) restricted to the order $\nu = 1$,

$$\left(\mu\mathcal{J}_1^- - \mathcal{H}_1^-\right)\left(\varepsilon\mathcal{J}_1^+ - \mathcal{H}_1^+\right) + \left(\mu\mathcal{J}_1^+ - \mathcal{H}_1^+\right)\left(\varepsilon\mathcal{J}_1^- - \mathcal{H}_1^-\right) = -2\left(\frac{1}{a^2\kappa\gamma}\right)^2(\epsilon-1)(\mu-1) \tag{4.158}$$

We get,

$$\begin{aligned}&\left[\frac{2\mu}{(\kappa a)^2} + \ln\left(\frac{\Upsilon\gamma a}{2}\right)\right]\left[\frac{\varepsilon}{4} + \frac{2}{(\gamma a)^2}\right] + \left[\frac{\mu}{4} + \frac{2}{(\gamma a)^2}\right]\left[\frac{2\varepsilon}{(\kappa a)^2} + \ln\left(\frac{\Upsilon\gamma a}{2}\right)\right] \\ \approx\ & -2\left(\frac{1}{a^2\kappa\gamma}\right)^2(\epsilon-1)(\mu-1)\end{aligned} \tag{4.159}$$

Obviously for $\gamma a \to 0$, we have $\dfrac{2}{(\gamma a)^2} \gg \dfrac{\varepsilon}{4}$ and $\dfrac{2}{(\gamma a)^2} \gg \dfrac{\mu}{4}$. This allows us to write,

$$\begin{aligned}
&\left[\frac{2\mu}{(\kappa a)^2} + \ln\left(\frac{\Upsilon\gamma a}{2}\right)\right]\frac{2}{(\gamma a)^2} + \frac{2}{(\gamma a)^2}\left[\frac{2\varepsilon}{(\kappa a)^2} + \ln\left(\frac{\Upsilon\gamma a}{2}\right)\right] \\
&\quad \approx -2\left(\frac{1}{\kappa a\,\gamma a}\right)^2(\epsilon-1)(\mu-1)
\end{aligned}$$

We remove the common factor, $\dfrac{2}{(\gamma a)^2}$,

$$\left[\frac{2\mu}{(\kappa a)^2} + \ln\left(\frac{\Upsilon\gamma a}{2}\right)\right] + \left[\frac{2\varepsilon}{(\kappa a)^2} + \ln\left(\frac{\Upsilon\gamma a}{2}\right)\right] \approx -\frac{1}{(\kappa a)^2}(\epsilon-1)(\mu-1)$$

and after some manipulations,

$$\begin{aligned}
\frac{2(\mu+\varepsilon)}{(\kappa a)^2} + 2\ln\left(\frac{\Upsilon\gamma a}{2}\right) &\approx -\frac{1}{(\kappa a)^2}(\epsilon-1)(\mu-1) \\
\frac{2(\mu+\varepsilon)+(\epsilon-1)(\mu-1)}{(\kappa a)^2} + 2\ln\left(\frac{\Upsilon\gamma a}{2}\right) &\approx 0 \\
\frac{(\mu+1)(\varepsilon+1)}{(\kappa a)^2} &\approx -2\ln\left(\frac{\Upsilon\gamma a}{2}\right)
\end{aligned}$$

we arrive at

$$\frac{(\mu+1)(\varepsilon+1)}{(\kappa a)^2} \approx \ln\left[\left(\frac{2}{\Upsilon\gamma a}\right)^2\right] \tag{4.160}$$

At $\gamma a \to 0$ and $\kappa a \to 0$, both the left hand side and the right hand side increase to $+\infty$. This equation has the solution for both $\gamma a \to 0$ and $\kappa a \to 0$.

We rewrite Eq. (4.160) in terms of effective guide index, $N = c\beta/\omega$. In the limits $\gamma a \to 0$ and $\kappa a \to 0$ N goes to n_2, i.e., $N \to n_2$

$$\frac{(\mu+1)(\varepsilon+1)}{2\left(\dfrac{\omega a}{c}\right)^2(n_1^2-N^2)} + \ln\left[\frac{\dfrac{\omega a}{c}\Upsilon\left(N^2-n_2^2\right)^{1/2}}{2}\right] \approx 0 \tag{4.161}$$

For the sake of simplicity, we confine ourselves to the situations where the magnetic permeabilities in the core and in the cladding are equal to each other, which is often the case. Then $\mu_1 = \mu_2$, consequently $\mu = 1$. Equation (4.161) simplifies to the form where $\varepsilon = \dfrac{n_1^2}{n_2^2}$,

$$\frac{2\left(1+\dfrac{n_1^2}{n_2^2}\right)}{\left(\dfrac{\omega a}{c}\right)^2(n_1^2-N^2)} \approx \ln\left[\frac{4}{\left(\dfrac{\omega a}{c}\Upsilon\right)^2\left(N^2-n_2^2\right)}\right] \tag{4.162}$$

We compare the expressions on the left hand side and on the right hand side of this equation. For $N \to n_2$ the solutions to this approximate eigenvalue equation are the values, $\dfrac{\omega a}{c} \to 0$. Indeed, the graphical solutions to Eq. (4.162) in Figure 4.31 are given by the intersections of the function of N

$$f_\kappa(N, \omega a) = \frac{2\left(1 + \dfrac{n_1^2}{n_2^2}\right)}{\left(\dfrac{\omega a}{c}\right)^2 (n_1^2 - N^2)} \tag{4.163a}$$

which, at a fixed value of ωa varies slowly when $N \to n_2$, and the function of N

$$f_\gamma(N, \omega a) = \ln\left[\frac{4}{\left(\dfrac{\omega a}{c}\Upsilon\right)^2 \left(N^2 - n_2^2\right)}\right] \tag{4.163b}$$

which asymptotically approaches the vertical axis as $N \to n_2$. Both the functions increase to infinity as $\omega a \to 0$. Figure 4.31 displays the intersection points of these functions associated to a particular value N and $\dfrac{\omega a}{c}$ representing the solutions in the region of small arguments, γa and κa. The solution to the approximate eigenvalue equation, Eq. (4.162) at a given value of $\omega a/c$ can be expressed in terms N, or in terms γ, or κ for a given radius of the core, a. These parameters are coupled by equations

$$\begin{aligned}
\kappa &= \left(\omega^2 \varepsilon_1 \mu_1 - \beta^2\right)^{1/2} = \frac{\omega}{c}\left(n_1^2 - N^2\right)^{1/2} \\
\gamma &= \left(\beta^2 - \omega^2 \varepsilon_2 \mu_2\right)^{1/2} = \frac{\omega}{c}\left(N^2 - n_2^2\right)^{1/2}
\end{aligned}$$

results of numerical evaluation of Eq. (4.161) at $\mu = 1$ are shown in Figure 4.32.

4.5.4 Cut-off frequencies of higher $\nu = 1$ modes

We consider the cases $\gamma a \to 0$ but $\kappa a \neq 0$. We substitute into the eigenvalue equation

$$\left(\mu \mathcal{J}_1^- - \mathcal{H}_1^-\right)\left(\varepsilon \mathcal{J}_1^+ - \mathcal{H}_1^+\right) + \left(\mu \mathcal{J}_1^+ - \mathcal{H}_1^+\right)\left(\varepsilon \mathcal{J}_1^- - \mathcal{H}_1^-\right) = -2\left(\frac{1}{a^2 \kappa \gamma}\right)^2 (\epsilon - 1)(\mu - 1) \tag{4.164}$$

the approximations to the Hankel functions, $\mathcal{H}_1^+$ and $\mathcal{H}_1^-$ according to Eqs. (4.157c) and (4.157d),

$$\begin{aligned}
&\left[\mu \frac{1}{\kappa a}\frac{\mathcal{J}_0(\kappa a)}{\mathcal{J}_1(\kappa a)} + \ln\left(\frac{\Upsilon \gamma a}{2}\right)\right]\left[\varepsilon \frac{1}{\kappa a}\frac{\mathcal{J}_2(\kappa a)}{\mathcal{J}_1(\kappa a)} + \frac{2}{(\gamma a)^2}\right] \\
+ &\left[\varepsilon \frac{1}{\kappa a}\frac{\mathcal{J}_0(\kappa a)}{\mathcal{J}_1(\kappa a)} + \ln\left(\frac{\Upsilon \gamma a}{2}\right)\right]\left[\mu \frac{1}{\kappa a}\frac{\mathcal{J}_2(\kappa a)}{\mathcal{J}_1(\kappa a)} + \frac{2}{(\gamma a)^2}\right] \\
&= \frac{-2}{(\kappa a)^2 (\gamma a)^2}(\epsilon - 1)(\mu - 1)
\end{aligned} \tag{4.165}$$

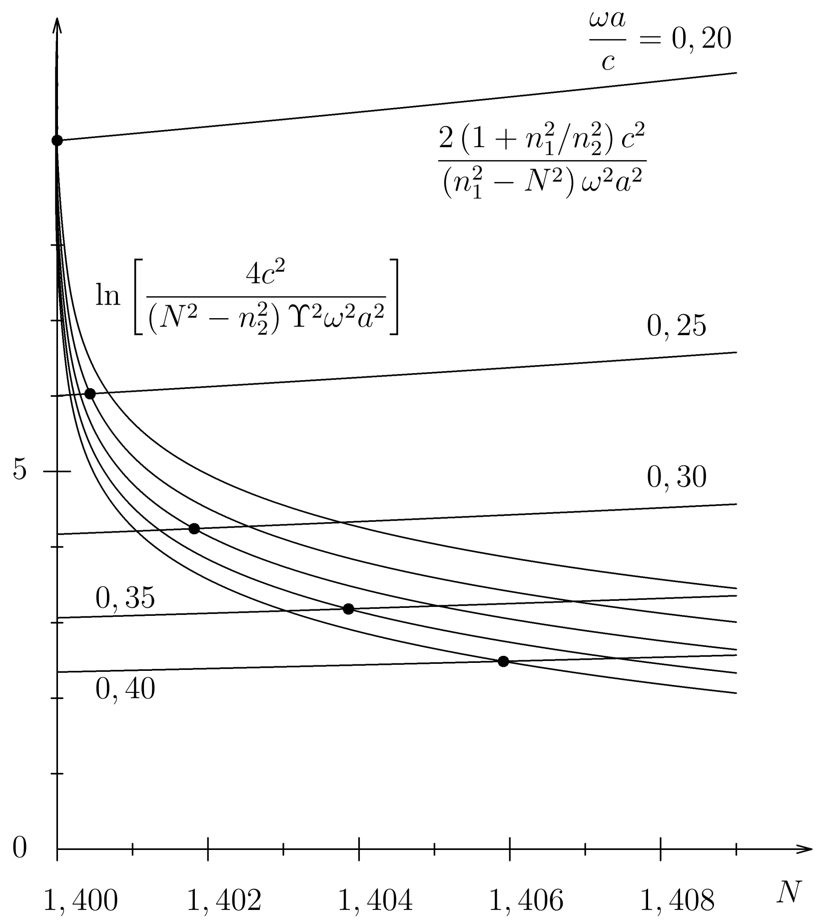

Figure 4.31: Graphical solution to the eigenvalue equation in a cylindrical dielectric fiber waveguide for small values of the vacuum propagation constant, ω/c and/or for small values of the core radius, a, i.e., for the values $\omega a/c = 0,20 \;\; 0,25 \;\; 0,30 \;\; 0,35$ and $0,40$. The magnetic permeabilities in the core and in the cladding are equal. The real index of refraction in the core assumes the value, $n_1 = 1,5$. The real index of refraction in the cladding assumes the value, $n_2 = 1,4$. The effective guide index is confined to the range, $n_2 < N < n_1$. The figure shows the region where $N \to n_2$. The full circles indicate intersections of the functions with the same values of the parameter, $\omega a/c$.

This equation can be rearranged by the multiplication of both sides with $(\kappa a)^2\,\mathcal{J}_0\,(\kappa a)$

$$\begin{aligned} &\left[\mu\mathcal{J}_0 + \kappa a\mathcal{J}_1 \ln\left(\frac{\Upsilon\gamma a}{2}\right)\right]\left[\varepsilon\mathcal{J}_2 + \kappa a\mathcal{J}_1\frac{2}{(\gamma a)^2}\right] \\ + \;\; &\left[\varepsilon\mathcal{J}_0 + \kappa a\mathcal{J}_1 \ln\left(\frac{\Upsilon\gamma a}{2}\right)\right]\left[\mu\mathcal{J}_2 + \kappa a\mathcal{J}_1\frac{2}{(\gamma a)^2}\right] \\ &= \frac{-2\mathcal{J}_1^2}{(\gamma a)^2}\,(\epsilon - 1)\,(\mu - 1) \end{aligned} \tag{4.166}$$

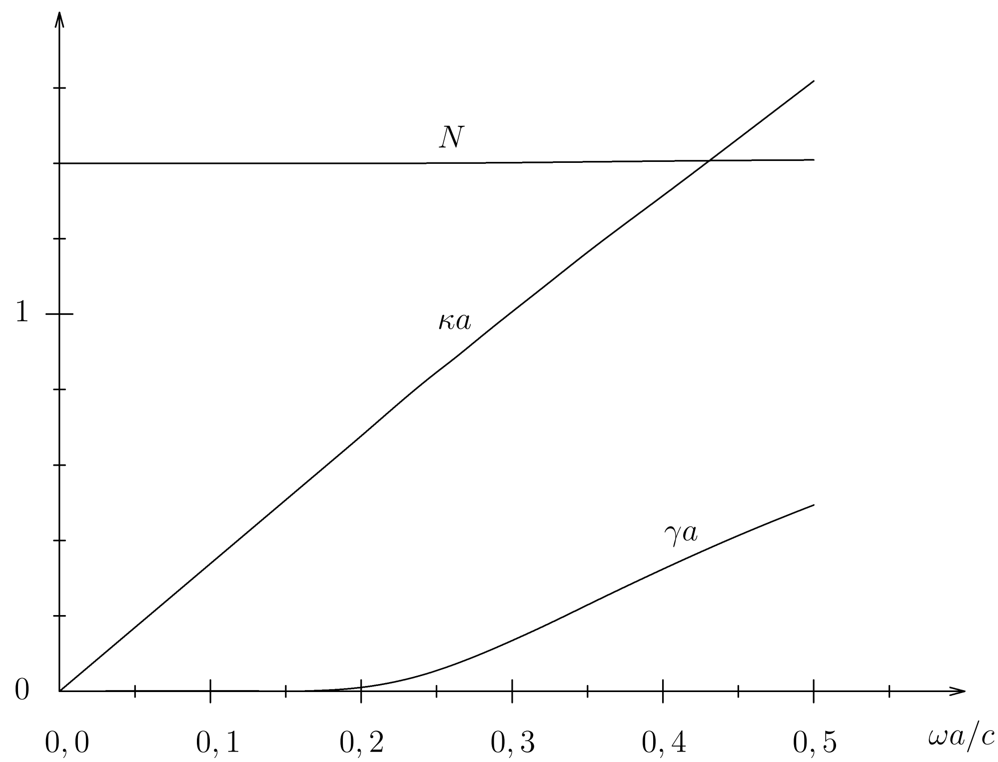

Figure 4.32: Approximate solutions to the eigenvalue equation in a cylindrical dielectric fiber waveguide in terms of the effective guide index, N, in terms of product of the transverse propagation constant, κ, and the core radius, a, i.e., κa, and in terms of product of the damping constant, γ and the core radius, a, i.e., γa, expressed as functions of the product of the vacuum propagation constant, ω/c and the core radius, a, i.e., $\omega a/c$. The magnetic permeabilities in the core and in the cladding are equal. The real index of refraction in the core assumes the value, $n_1 = 1,5$. The real index of refraction in the cladding assumes the value, $n_2 = 1,4$. The effective guide index is confined to the range, $n_2 < N < n_1$. In the region, $\frac{\omega a}{c} \to 0$ the effective guide index N tends to n_2, $N \to n_2$.

At $(\gamma a)^2 \to 0$

$$\varepsilon \mathcal{J}_2 \ll (\kappa a)\, \mathcal{J}_1 \frac{2}{(\gamma a)^2} \tag{4.167a}$$

$$\mu \mathcal{J}_2 \ll \kappa a \mathcal{J}_1 \frac{2}{(\gamma a)^2} \tag{4.167b}$$

(excluding, perhaps, the nodal points of $\mathcal{J}_1$)

$$\begin{aligned} & \left[\mu \mathcal{J}_0 + \kappa a \mathcal{J}_1 \ln\left(\frac{\Upsilon \gamma a}{2}\right)\right] \kappa a \mathcal{J}_1 \frac{2}{(\gamma a)^2} \\ + \quad & \left[\varepsilon \mathcal{J}_0 + \kappa a \mathcal{J}_1 \ln\left(\frac{\Upsilon \gamma a}{2}\right)\right] \kappa a \mathcal{J}_1 \frac{2}{(\gamma a)^2} \\ & = \frac{-2\mathcal{J}_1^2}{(\gamma a)^2} (\epsilon - 1)(\mu - 1) \end{aligned} \tag{4.168}$$

Equation (4.168) can rearranged after the division by $\dfrac{2}{(\gamma a)^2}$. We get,

$$\left[(\mu + \varepsilon) \kappa a \mathcal{J}_0 + 2 (\kappa a)^2 \mathcal{J}_1 \ln\left(\frac{\Upsilon \gamma a}{2}\right) + (\epsilon - 1)(\mu - 1) \mathcal{J}_1\right] \mathcal{J}_1 \quad = \quad 0 \tag{4.169}$$

One set of solutions is given by nodal points of the Bessel function $\mathcal{J}_1(\kappa a)$, excluding $\kappa a = 0$, i.e.,

$$\mathcal{J}_1(\kappa a) \quad = \quad 0 \,, \qquad \kappa a \neq 0 \tag{4.170}$$

and determines the cut–off frequencies/thicknesses of so called EH modes numbered as EH_{11}, EH_{12}, EH_{13}, EH_{14}, $\ldots$ $\mathrm{EH}_{1\mu}$.

The nomenclature of guided modes in cylindrical dielectric waveguides with a step index profile employs the notation $\mathrm{EH}_{\nu\mu}$ and $\mathrm{HE}_{\nu\mu}$. The first subscript gives the azimuthal number, ν , or the order of a corresponding cylindrical function (associated with the z field components) and the second one gives the radial number, μ, or the numerical order of nodal points associated with the Bessel function, $\mathcal{J}_\nu(\kappa a)$.[10]

Another set of solutions follows from

$$(\mu + \varepsilon) \kappa a \mathcal{J}_0 + 2 (\kappa a)^2 \mathcal{J}_1 \ln\left(\frac{\Upsilon \gamma a}{2}\right) + (\epsilon - 1)(\mu - 1) \mathcal{J}_1 \quad = \quad 0 \tag{4.171}$$

which can also be expressed as,

$$\mathcal{J}_1 = \mathcal{J}_1(\kappa a) \quad = \quad \frac{(\mu + \varepsilon) \kappa a}{2 (\kappa a)^2 \ln\left(\dfrac{2}{\Upsilon \gamma a}\right) - (\epsilon - 1)(\mu - 1)} \mathcal{J}_0(\kappa a) \tag{4.172}$$

[10]The conventional notation of the radial number is employed as a subscript and cannot be confused with the permeability ratio, $\mu = \mu_1/\mu_2$.

The limits on the right hand side

$$\lim_{\gamma a\to 0}\frac{(\mu+\varepsilon)\,\kappa a\mathcal{J}_0(\kappa a)}{2(\kappa a)^2\ln\left(\dfrac{2}{\Upsilon\gamma a}\right)-(\epsilon-1)(\mu-1)}=0 \tag{4.173}$$

is zero. Consequently, the cut–off frequencies/thicknesses are determined by the same condition,

$$\mathcal{J}_1(\kappa a) \;=\; 0\,,\quad \kappa a\neq 0 \tag{4.174}$$

as in the case of $\mathrm{EH}_{1\mu}$ modes. These modes are denoted as $\mathrm{HE}_{1\mu}$. Above the cut–off, they are not degenerate with $\mathrm{EH}_{1\mu}$ modes. The numerical order starts at HE_{12}, as HE_{11} is reserved for the fundamental mode of zero cut–off, $\kappa a\to 0$.

4.5.5 Cut-off frequencies of $\nu\geq 2$ modes

In the eigenvalue equation,

$$\left(\mu\mathcal{J}_\nu^- - \mathcal{H}_\nu^-\right)\left(\varepsilon\mathcal{J}_\nu^+ - \mathcal{H}_\nu^+\right)+\left(\mu\mathcal{J}_\nu^+ - \mathcal{H}_\nu^+\right)\left(\varepsilon\mathcal{J}_\nu^- - \mathcal{H}_\nu^-\right)=-2\left(\frac{\nu}{a^2\kappa\gamma}\right)^2(\epsilon-1)(\mu-1) \tag{4.175}$$

we replace $\mathcal{J}_\nu^\pm$ according to

$$\mathcal{J}_\nu^\pm \;\equiv\; \frac{1}{\kappa a}\frac{\mathcal{J}_{\nu\pm1}(\kappa a)}{\mathcal{J}_\nu(\kappa a)} \tag{4.176}$$

and employ the approximations for $\mathcal{H}_\nu^-$ and $\mathcal{H}_\nu^+$ from Eqs. (4.148) and (4.150),

$$\mathcal{H}_\nu^+ \;\approx\; -\frac{2\nu}{(\gamma a)^2}\,,\quad \nu\geq 1 \tag{4.177}$$

$$\mathcal{H}_\nu^- \;\approx\; \frac{1}{2(\nu-1)}\,,\quad \nu>1 \tag{4.178}$$

We get,

$$\begin{aligned}
&\left[\frac{\mu}{\kappa a}\frac{\mathcal{J}_{\nu-1}}{\mathcal{J}_\nu}-\frac{1}{2(\nu-1)}\right]\left[\frac{\varepsilon}{\kappa a}\frac{\mathcal{J}_{\nu+1}}{\mathcal{J}_\nu}+\frac{2\nu}{(\gamma a)^2}\right]\\
+\;&\left[\frac{\varepsilon}{\kappa a}\frac{\mathcal{J}_{\nu-1}}{\mathcal{J}_\nu}-\frac{1}{2(\nu-1)}\right]\left[\frac{\mu}{\kappa a}\frac{\mathcal{J}_{\nu+1}}{\mathcal{J}_\nu}+\frac{2\nu}{(\gamma a)^2}\right]\\
=\;&-2\left(\frac{\nu}{a^2\kappa\gamma}\right)^2(\epsilon-1)(\mu-1)
\end{aligned} \tag{4.179}$$

After the multiplication of both sides by $(\kappa a)^2 \mathcal{J}_\nu^2$, the equation transforms to

$$\begin{aligned}
& \left[\mu \mathcal{J}_{\nu-1} - \frac{\kappa a \mathcal{J}_\nu}{2(\nu-1)}\right]\left[\varepsilon \mathcal{J}_{\nu+1} + \kappa a \mathcal{J}_\nu \frac{2\nu}{(\gamma a)^2}\right] \\
+ & \left[\varepsilon \mathcal{J}_{\nu-1} - \frac{\kappa a \mathcal{J}_\nu}{2(\nu-1)}\right]\left[\mu \mathcal{J}_{\nu+1} + \kappa a \mathcal{J}_\nu \frac{2\nu}{(\gamma a)^2}\right] \\
= & \frac{-2\nu^2}{(\gamma a)^2}(\epsilon - 1)(\mu - 1)\mathcal{J}_\nu^2 \qquad (4.180)
\end{aligned}$$

The terms $\dfrac{2\nu}{(\gamma a)^2}\kappa a \mathcal{J}_\nu$ dominate at $\gamma a \to 0$. Then the terms $\varepsilon \mathcal{J}_{\nu+1}$ and $\mu \mathcal{J}_{\nu+1}$ become negligible with respect to them, and we can write,

$$\begin{aligned}
& \left[\mu \mathcal{J}_{\nu-1} - \frac{\kappa a \mathcal{J}_\nu}{2(\nu-1)}\right]\kappa a \mathcal{J}_\nu \frac{2\nu}{(\gamma a)^2} + \left[\varepsilon \mathcal{J}_{\nu-1} - \frac{\kappa a \mathcal{J}_\nu}{2(\nu-1)}\right]\kappa a \mathcal{J}_\nu \frac{2\nu}{(\gamma a)^2} \\
& + \frac{2\nu^2}{(\gamma a)^2}(\epsilon - 1)(\mu - 1)\mathcal{J}_\nu^2 = 0 \qquad (4.181)
\end{aligned}$$

This can be rearranged to

$$\frac{2\nu}{(\gamma a)^2}\kappa a \mathcal{J}_\nu \left[(\mu + \varepsilon)\mathcal{J}_{\nu-1} - \frac{\kappa a \mathcal{J}_\nu}{(\nu-1)}\right] + \frac{2\nu^2}{(\gamma a)^2}(\epsilon - 1)(\mu - 1)\mathcal{J}_\nu^2 = 0 \qquad (4.182)$$

The division by $\dfrac{2\nu}{(\gamma a)^2}$ provides,

$$\underbrace{\kappa a \mathcal{J}_\nu}_{\text{EH}} \underbrace{\left[(\mu + \varepsilon)\mathcal{J}_{\nu-1} - \frac{\kappa a \mathcal{J}_\nu}{(\nu-1)} + \frac{\nu}{\kappa a}(\epsilon - 1)(\mu - 1)\mathcal{J}_\nu\right]}_{\text{HE}} = 0 \qquad (4.183)$$

There exist the solutions of two types for the cut–off. One is determined by the condition,

$$\mathcal{J}_\nu(\kappa a) \;=\; 0\,, \quad \kappa a \neq 0\,, \quad \nu = 2, 3, 4, \ldots \qquad (4.184)$$

and defines the cut–off for $\text{EH}_{\nu 1}$, $\text{EH}_{\nu 2}$, $\text{EH}_{\nu 3}$, $\text{EH}_{\nu 4}$, ... $\text{EH}_{\nu\mu}$, $\nu \geq 2$. Another one follows from the equation (4.183) after the removal of $\kappa a \mathcal{J}_\nu \neq 0$

$$(\mu + \varepsilon)\mathcal{J}_{\nu-1} - \left[\frac{\kappa a}{(\nu-1)} - \frac{\nu(\epsilon - 1)(\mu - 1)}{\kappa a}\right]\mathcal{J}_\nu = 0\,, \quad \nu \geq 2 \qquad (4.185)$$

and defines the cut–off for $\text{HE}_{\nu\mu}$ modes.

It can be shown that $\kappa a \to 0$ is not a solution for the cut–off for the modes of the order $\nu > 1$. In the opposite case, the monomode regime would not be possible.

The substitution into Eq. (4.175) for the approximate $\mathcal{H}_\nu^+$ and $\mathcal{H}_\nu^-$ from Eqs. (4.177) and (4.177) for $\nu > 1$ in the limits, $\gamma a \to 0$ has given

$$\left[\mu \mathcal{J}_\nu^- - \frac{1}{2(\nu-1)}\right]\left[\varepsilon \mathcal{J}_\nu^+ + \frac{2\nu}{(\gamma a)^2}\right] + \left[\mu \mathcal{J}_\nu^+ + \frac{2\nu}{(\gamma a)^2}\right]\left[\varepsilon \mathcal{J}_\nu^- - \frac{1}{2(\nu-1)}\right]$$
$$= -2\left(\frac{\nu}{a^2\kappa\gamma}\right)^2 (\epsilon - 1)(\mu - 1) \tag{4.186}$$

We introduce

$$\mathcal{J}_\nu^\pm \equiv \frac{1}{\kappa a}\frac{\mathcal{J}_{\nu\pm1}(\kappa a)}{\mathcal{J}_\nu(\kappa a)} \tag{4.187}$$

and suppose $\kappa a \ll 1$. The use of the approximation from Eq. (4.151) and the definition for $\mathcal{J}_\nu^+$ and $\mathcal{J}_\nu^-$ given in Eqs. (4.119) or (4.121a) provides,

$$\mathcal{J}_\nu \approx \frac{1}{\nu\,!}\left(\frac{\kappa a}{2}\right)^\nu, \quad \kappa a \ll 1, \quad \nu \geq 0 \tag{4.188}$$

and,

$$\mathcal{J}_\nu^+ = \frac{1}{\kappa a}\frac{\mathcal{J}_{\nu+1}(\kappa a)}{\mathcal{J}_\nu(\kappa a)} \approx \frac{1}{\kappa a}\frac{\frac{1}{(\nu+1)!}\left(\frac{\kappa a}{2}\right)^{\nu+1}}{\frac{1}{\nu\,!}\left(\frac{\kappa a}{2}\right)^\nu}$$
$$\approx \frac{1}{\kappa a}\frac{\nu\,!}{(\nu+1)!}\frac{\kappa a}{2}$$

i.e.,

$$\mathcal{J}_\nu^+ \approx \frac{1}{2(\nu+1)} \tag{4.189}$$

and,

$$\mathcal{J}_\nu^- = \frac{1}{\kappa a}\frac{\mathcal{J}_{\nu-1}(\kappa a)}{\mathcal{J}_\nu(\kappa a)} \approx \frac{1}{\kappa a}\frac{\frac{1}{(\nu-1)!}\left(\frac{\kappa a}{2}\right)^{\nu-1}}{\frac{1}{\nu\,!}\left(\frac{\kappa a}{2}\right)^\nu}$$
$$\approx \frac{1}{\kappa a}\frac{\nu\,!}{(\nu-1)!}\frac{2}{\kappa a}$$

i.e.,

$$\mathcal{J}_\nu^- \approx \frac{2\nu}{(\kappa a)^2}, \qquad \nu \geq 1 \tag{4.190}$$

The substitutions for $\mathcal{J}_\nu^\pm$ into Eq. (4.186) gives,

$$\left[\mu\frac{2\nu}{(\kappa a)^2} - \frac{1}{2(\nu-1)}\right]\left[\varepsilon\frac{1}{2(\nu+1)} + \frac{2\nu}{(\gamma a)^2}\right]$$
$$+ \left[\mu\frac{1}{2(\nu+1)} + \frac{2\nu}{(\gamma a)^2}\right]\left[\varepsilon\frac{2\nu}{(\kappa a)^2} - \frac{1}{2(\nu-1)}\right]$$
$$= -2\left(\frac{\nu}{a^2\kappa\gamma}\right)^2 (\epsilon - 1)(\mu - 1) \tag{4.191}$$

With the restriction to the terms dominating at $\gamma a \to 0$ and $\kappa a \to 0$, we have

$$\mu\frac{2\nu}{(\kappa a)^2}\frac{2\nu}{(\gamma a)^2}+\varepsilon\frac{2\nu}{(\gamma a)^2}\frac{2\nu}{(\kappa a)^2}+2\left(\frac{\nu}{a^2\kappa\gamma}\right)^2(\epsilon-1)(\mu-1)=0 \tag{4.192}$$

simplified step by step to

$$\begin{aligned}\frac{2\nu^2\left[2(\varepsilon+\mu)+(\epsilon-1)(\mu-1)\right]}{(\gamma a)^2(\kappa a)^2}&=0\\ \frac{2\nu^2(\varepsilon+1)(\mu+1)}{(\gamma a)^2(\kappa a)^2}&=0\,,\qquad \nu>1\end{aligned} \tag{4.193}$$

This equation has no solution for $\gamma a \to 0$ and $\kappa a \to 0$. Consequently, $\kappa a \to 0$ cannot be a solution for cut–off of modes of the order $\nu > 1$.

4.6 Weak guiding approximation

In practical fibers, $\varepsilon \approx 1$ and $\mu \approx 1$. From the cut–off condition for $\mathrm{HE}_{\nu\mu}$ modes given by Eq. (4.185)

$$(\mu+\varepsilon)\mathcal{J}_{\nu-1}-\left[\frac{\kappa a}{(\nu-1)}-\frac{\nu(\epsilon-1)(\mu-1)}{\kappa a}\right]\mathcal{J}_\nu=0\,,\quad \nu\geq 2$$

we get with the small term proportional to $(\epsilon-1)(\mu-1)$ removed,

$$2\mathcal{J}_{\nu-1}-\frac{\kappa a}{(\nu-1)}\mathcal{J}_\nu\approx 0 \tag{4.194}$$

i.e.,

$$\mathcal{J}_\nu \;\approx\; 2\frac{(\nu-1)}{\kappa a}\mathcal{J}_{\nu-1} \tag{4.195}$$

In the recursion relation given in Eq. (4.116c)

$$\mathcal{Z}_{\nu-1}(z)+\mathcal{Z}_{\nu+1}(z) \;=\; \frac{2\nu}{z}\mathcal{Z}_\nu(z) \tag{4.196}$$

we shift the order, $\nu \to \nu - 1$ and get

$$\mathcal{Z}_{\nu-2}(z)+\mathcal{Z}_\nu(z) \;=\; \frac{2(\nu-1)}{z}\mathcal{Z}_{\nu-1}(z) \tag{4.197}$$

In the special case of Bessel functions, $\mathcal{Z}_\nu(z)$ is replaced by $\mathcal{J}_\nu(\kappa a)$

$$\mathcal{J}_{\nu-2}(\kappa a)+\mathcal{J}_\nu(\kappa a) \;=\; \frac{2(\nu-1)}{\kappa a}\mathcal{J}_{\nu-1}(\kappa a) \tag{4.198}$$

Table 4.4: The cut–off condition, $(\kappa a)_c$, for the modes of orders $\nu = 0, 1, \ldots 3$, in the fiber characterized by $\varepsilon_1/\varepsilon_2 = 1,1$ and $\mu_1/\mu_2 = 1,0$. After Dietrich Marcuse, *Light Transmission Optics*, Bell Laboratories Series, Van Nostrand Reinhold Company, New York 1972, pp. 305 - 313.

$\nu \backslash \mu$	1	2	3	4	5	Mode	Cut–off
0	2,405	5,520	8,654	11.792	14.931	TE,TM	$\mathcal{J}_0(\kappa a) = 0$
1	0	3,832	7,016	10.174	13.324	HE	$\mathcal{J}_1(\kappa a) = 0$
1	3,832	7,016	10,174	13.324	16.471	EH	$\mathcal{J}_1(\kappa a) = 0$
2	2,44	5,54	8,67	11.799	14.937	HE	$\mathcal{J}_0(\kappa a) \approx 0$
2	5,136	8,417	11,620	14.796	17.960	EH	$\mathcal{J}_2(\kappa a) = 0$
3	3.882	7.044	10.193	13.339	16.483	HE	$\mathcal{J}_1(\kappa a) \approx 0$
3	6.380	9.761	13.015	16.224	19.409	EH	$\mathcal{J}_3(\kappa a) = 0$

The use of this result in the simplified cut–off condition for $\mathrm{HE}_{\nu\mu}$ modes given by Eq. (4.194) or by Eq. (4.195) results in

$$\frac{2(\nu-1)}{\kappa a}\mathcal{J}_{\nu-1}(\kappa a) = \mathcal{J}_{\nu-2}(\kappa a) + \mathcal{J}_\nu(\kappa a) \quad \approx \quad \mathcal{J}_\nu(\kappa a) \tag{4.199}$$

The condition can only be satisfied at $\mathcal{J}_{\nu-2}(\kappa a) \approx 0$. The cut–off condition for $\mathrm{HE}_{\nu\mu}$ módů in the approximation of weak guiding where $(\mu + \varepsilon) \to 2$, is given by

$$\mathcal{J}_{\nu-2}(\kappa a) \quad \approx \quad 0 \tag{4.200}$$

The approximate condition for $\mathrm{HE}_{\nu\mu}$ modes coincides with the exact cut–off condition for $\mathrm{EH}_{\nu-2,\mu}$ modes. In special cases $\nu = 2$ and $\nu = 3$ this conclusion is illustrated in Table 4.4.[11]

4.7 Nomenclature of guided modes summarized

4.7.1 Fundamental mode HE_{11}

The fundamental HE_{11} modes display theoretically a zero cut–off frequency or thickness. As $a\omega/c$ increases, the fiber allows the propagation of TE_{01} and TM_{01} modes with the

[11] Dietrich Marcuse, *Light Transmission Optics*, Bell Laboratories Series, Van Nostrand Reinhold Company, New York 1972, p. 302.

common cut–off frequency, $(\kappa a)_c = 2,405$, corresponding to the first nodal point of the Bessel function of zero order given by $\mathcal{J}_0(\kappa a) = 0$. At the cut–off frequency, the argument $\kappa a = (N^2 - n_2^2)^{1/2} \frac{\omega}{c} a$ goes to $(\kappa a)_c$, where the effective guide index N $(\omega N/c = \beta)$ goes to n_2, i.e., $N \to n_2$. This means for the frequency f related to the angular frequency ω by $\omega = 2\pi f$,

$$(\kappa a)_c = \left(n_1^2 - n_2^2\right)^{1/2} \frac{\omega}{c} a = 2\pi \left(n_1^2 - n_2^2\right)^{1/2} \frac{a}{\lambda_{\text{vac}}} = 2\pi \left(n_1^2 - n_2^2\right)^{1/2} \frac{f}{c} a = 2.405 \,. \tag{4.201}$$

From this, we deduce the range where the fiber is monomode,

$$0 < f \leq \frac{2.405\ c}{2\pi a \left(n_1^2 - n_2^2\right)^{1/2}} \,. \tag{4.202}$$

The ratio of the vacuum wavelength to the core radius required for the monomode regime should not fall bellow the value given by,

$$\frac{\lambda_{\text{vac}}}{a} \geq \frac{2\pi}{2.405} \left(n_1^2 - n_2^2\right)^{1/2} , \tag{4.203}$$

or approximately below

$$\frac{\lambda_{\text{vac}}}{a} \geq 2.611 \left(n_1^2 - n_2^2\right)^{1/2} . \tag{4.204}$$

In terms of the vacuum wavelength, λ_{vac}, the range of monomode regime can be expressed as

$$\frac{2\pi a}{2.405} \left(n_1^2 - n_2^2\right)^{1/2} \leq \lambda_{\text{vac}} < \infty \,. \tag{4.205}$$

4.7.2 TE$_{0\mu}$ ("EH$_{0\mu}$") and TM$_{0\mu}$ ("HE$_{0\mu}$") modes ($\mu = 1, 2, 3, \ldots$)

TE$_{0\mu}$ modes (also EH$_{0\mu}$) and TM$_{0\mu}$ modes (also HE$_{0\mu}$) have common cut–off frequencies/thicknesses given by the nodes of the Bessel function of zero order, $\mathcal{J}_0(\kappa a)$, the solutions to $\mathcal{J}_0(\kappa a) = 0$.

4.7.3 EH$_{\nu\mu}$ modes ($\nu = 1, 2, 3, \ldots, \mu = 1, 2, 3, \ldots$)

The cut–off frequencies/thicknesses of EH$_{\nu\mu}$ modes are given by the nodal points of Bessel functions, $\mathcal{J}_\nu(\kappa a)$. Nodal points are the solutions of $\mathcal{J}_\nu(\kappa a) = 0$, $\kappa a \neq 0$.

4.7.4 HE$_{\nu\mu}$ modes ($\nu = 1, 2, 3, \ldots, \mu = 1, 2, 3, \ldots$)

$\nu = 1$

(a) HE$_{11}$, the cut–off frequency/thickness is zero,
(b) HE$_{1\mu}$ $(\mu \geq 2)$, the cut–off frequencies/thicknesses are given by $\mathcal{J}_1(\kappa a) = 0$, the nodal points of the Bessel function of the first order, $\mathcal{J}_1(\kappa a)$, $\kappa a \neq 0$.

$\nu > 1$

the cut–off frequencies/thicknesses are given by the condition,

$$(\mu + \varepsilon)\,\mathcal{J}_{\nu-1} - \left[\frac{\kappa a}{\nu - 1} - \frac{\nu\,(\epsilon - 1)\,(\mu - 1)}{\kappa a}\right]\mathcal{J}_{\nu} = 0$$

Appendix A

Acknowledgement

This work was inspired and supported by the late Professor Jaromír Pištora, director of Nanotechnology Center, Technical University of Ostrava, Czech Republic, a pioneer of Integrated Optics in Czechoslovakia in 1970s'.